THE FLOW BETWEEN ROTATING COAXIAL DISKS

Thesis by

Roque Kwok-Hung Szeto

In Partial Fulfillment of the Requirements

For the Degree of

Doctor of Philosophy

California Institute of Technology

Pasadena, California

1978

(Submitted MAY 2, 1978)

ACKNOWLEDGEMENT

I like to thank my advisor, Professor H. B. Keller, for suggesting the problem and his very helpful guidance in the preparation of this thesis. Without his 'infinite' patience this work would never have materialized. Also, I like to thank the Institute for the financial support in the form of Graduate Teaching Assistantship and Graduate Research Assistantship.

ABSTRACT

Numerical approximations of nonunique solutions of the Navier-Stokes equations are obtained for steady viscous incompressible axisymmetric flow between two infinite rotating coaxial disks. For example, nineteen solutions have been found for the case when the disks are rotating with the same speed but in opposite direction. Bifurcation and perturbed bifurcation phenomena are observed. An efficient method is used to compute solution branches. The stability of solutions is analyzed. The rate of convergence of Newton's method at singular points is discussed. In particular, recovery of quadratic convergence at "normal limit points" and bifurcation points is indicated. Analytical construction of some of the computed solutions using singular perturbation techniques is discussed.

TABLE OF CONTENTS

CHAPTER 1
THE PROBLEM

1.1 INTRODUCTION

The steady flow of a viscous fluid in a semi-infinite region bounded by a single infinite rotating disk was first studied by von Karman in 1921 [30]. He transformed the Navier-Stokes equations into nonlinear ordinary differential equations by introducing similarity variables. In 1951, Batchelor [1] furthered the study to the flow between two rotating coaxial disks, using the equations derived by von Karman.

For the rotating coaxial disks problem with no suction, many computations have been attempted. Among them: (i) Mellor, Chapple and Stokes in 1968 [22] computed three different solutions when one of the disks is stationary, that is $\gamma = 0$, where γ is defined as the ratio of the

angular velocity of upper disk to that of the lower disk; (ii) Pearson in 1965 [23] solved the time dependent problem and obtained two different steady-state solutions when $\gamma = -1$; and (iii) most recently Holodniok, Kubicek and Hlavacek in 1977 [8] obtained five different solutions for $\gamma = 0.8$. For large Reynolds number and $\gamma = -1$ there have been many theoretical investigations in recent years. This has been generated by the different conjectures of Batchelor [1] and Stewartson in 1952 [28]. The existence theorems of McLeod and Parter in 1974 [21] and the perturbation construction of Matkowsky and Siegmann in 1976 [18] showed convincingly the conjecture of Stewartson, which says the fluid is non-rotating in the interior inviscid region as the Reynolds number tends to infinity, is correct. However, the conjecture of Batchelor, which called for a transition layer midway between the two disks, is still an open question. In 1969, Tam [29] with similar perturbation techniques to that used later by Matkowsky et al., exhibited the computed solutions of Pearson.

In this thesis we systematically compute the many different solutions of the time-independent rotating coaxial disks problem with no suction. We report only a portion of the computed solutions for Reynolds number $R \leq 1000$. and

$-1 \leq \gamma \leq 1$, numbering eleven solutions for $\gamma = 1$ and nineteen for $\gamma = -1$. The results of Mellor et al., Holodniok et al. and the time dependent computations of Pearson are reproduced. The stability of the computed solutions are discussed. Asymptotic expansions of some of the solutions at $\gamma = -1$ are constructed.

In the next section, the formulation of the problem and an important lemma are given. In Chapter 2 the theory on which the computations are based is briefly discussed. This includes : simple bifurcation in Section 1, pseudo-arclength continuation in Section 2 and the notion of local exchange of linearized stability in Section 3 (Keller [12], Crandall and Rabinowitz [4]). A new result in exchange of stability is derived at the end of Section 3. Chapter 3 is divided into five sections. Section 1 discusses the numerical method of two-point boundary value problems (Keller [11]). Section 2 gives a brief description for computing a solution branch (Keller [13]). Section 3 provides a proof of rate of convergence of Newton's method at both regular and singular points; an extension to solution of general nonlinear systems in which the Jacobian is singular is indicated. Section 4 is concerned with the numerical treatment at singular points; an explicit method

for the computation of the coefficients of the algebraic bifurcation equation is given. The numerical implementation of local exchange of linearized stability (Keller [12]) will be treated in Section 5. In Chapter 4 the discussion of solution branches and their stablity is given. In the last Chapter of this thesis, we study different solutions for $\gamma = -1$ using singular perturbation techniques.

1.2 FORMULATION

We consider the axisymmetric time-dependent incompressible viscous flow between two infinite rotating disks. The lower disk occupies the plane $z = 0$ and the upper disk is at $z = L$. The upper and lower disks are allowed to rotate about the z-axis with angular velocities $\Omega_2(t)$, and $\Omega_1(t)$ respectively. Further, let $f_2(t)$ and $f_1(t)$ be the uniform suction through the surface of the upper and lower disks respectively. Using polar cylindrical coordinates (r, θ, z) with the corresponding fluid velocities denoted by (u, v, w), we write the governing equations of motion:

Continuity Equation

$$(1.2.1) \qquad (ru)_r + (rw)_z = 0$$

r-Momentum Equation

$$(1.2.2) \qquad u_t + u_r u - \frac{v^2}{r} + u_z w = -\frac{p_r}{\rho} + \nu\left(u_{rr} + \frac{u_r}{r} + u_{zz} - \frac{u}{r^2}\right)$$

θ-Momentum Equation

$$(1.2.3) \qquad v_t + v_r u + \frac{uv}{r} + v_z w = \nu\left(v_{rr} + \frac{v_r}{r} + v_{zz} - \frac{v}{r^2}\right)$$

z-Momentum Equation

$$(1.2.4) \qquad w_t + w_r u + w_z w = -\frac{p_z}{\rho} + \nu\left(w_{rr} + \frac{w_r}{r} + w_{zz}\right)$$

where p is pressure, ρ is density and ν is kinematic viscosity. We now introduce dimensionless variables, indicated by *. That is, $r=r^*L$; $z=z^*L$; $t=t^*/\Omega_0$; $u=u^*L\Omega_0$; $v=v^*L\Omega_0$; $w=w^*L\Omega_0$; $p/\rho=(p/\rho)^*L$; and $\Omega_i=\Omega_i^*\Omega_0$, $i=1,2$; where Ω_0 is a chosen reference value of angular velocity. Define the Reynolds number R:

$$(1.2.5) \qquad R = \frac{L^2\Omega_0}{\nu}$$

The dimensionless equations are identical to (1.2.1 - 1.2.4), with ν replaced by $1/R$ - and we drop the asterisk

from the equations.

Let the axial velocity w have the form (von Karman [30])

$$w = f(z,t) \tag{1.2.6}$$

The continuity equation then gives the radial velocity

$$u = -\frac{r}{2} f_z(z,t) \tag{1.2.7}$$

Differentiating the z-Momentum equation with respect to r and using (1.2.6) and (1.2.7):

$$p_r = A(r,t) \tag{1.2.8}$$

Substitution into the r-Momentum equation implies $(v^2/r^2 - A/r\rho)$ is a function of (z,t) alone, say B(z,t). Evaluating at z = 0 gives

$$\Omega_1^2(t) - \frac{A(r,t)}{r\rho} = B(0,t)$$

This implies that A/r must be independent of r. Hence the angular velocity must have the form

$$(1.2.9) \qquad v = rg(z) = r(\Omega_1^2(t) - B(0,t) + B(z,t)$$

Differentiation of the r-Momentum equation with respect to z once and using equations (1.2.6) - (1.2.9), we have

$$(1.2.10a) \qquad f_{zzt} = R^{-1} f_{zzzz} - (f f_{zzz} + 4 g g_z)$$

The θ-Momentum equation simplifies to

$$(1.2.10b) \qquad g_t = R^{-1} g_{zz} - (g_z f - g f_z)$$

The boundary conditions for (1.2.10a) and (1.2.10b) are

$$(1.2.11) \qquad \begin{aligned} f(0,t) &= f_1(t) \quad , \quad f(1,t) = f_2(t) \\ f_z(0,t) &= 0 \quad , \quad f_z(1,t) = 0 \\ g(0,t) &= \Omega_1(t) \quad , \quad g(1,t) = \Omega_2(t) \end{aligned}$$

For computational purpose, we write the above two nonlinear partial differential equations in (z,t) of (1.2.10a,b) as a first order system of partial differential equations.

$$(1.2.12) \qquad RB\, u_t = u_z - F(u,R)$$

where u, F, B are given by

$$u \equiv (f \quad f_z \quad f_{zz} \quad f_{zzz} \quad g \quad g_z)^T$$

$$(1.2.13) \qquad F \equiv \begin{bmatrix} u_2 \\ u_3 \\ u_4 \\ R(u_1u_4 + 4u_5u_6) \\ u_6 \\ R(u_1u_6 - u_2u_5) \end{bmatrix} \qquad B \equiv \begin{bmatrix} 0 & 0 & 0 & 0 & 0 & 0 \\ 0 & 0 & 0 & 0 & 0 & 0 \\ 0 & 0 & 0 & 0 & 0 & 0 \\ 0 & 0 & 1 & 0 & 0 & 0 \\ 0 & 0 & 0 & 0 & 0 & 0 \\ 0 & 0 & 0 & 0 & 1 & 0 \end{bmatrix}$$

The boundary conditions (1.2.11) become

$$(1.2.14) \qquad \begin{aligned} B_0\, u(0,t) &= \alpha_0(t) \\ B_1\, u(1,t) &= \alpha_1(t) \end{aligned}$$

where matrices B_0 and B_1 and vectors $\alpha_0(t)$ and $\alpha_1(t)$

$$(1.2.15a) \qquad B_0 \equiv B_1 = \begin{bmatrix} 1 & 0 & 0 & 0 & 0 & 0 \\ 0 & 1 & 0 & 0 & 0 & 0 \\ 0 & 0 & 0 & 0 & 1 & 0 \end{bmatrix}$$

$$(1.2.15b) \qquad \alpha_0(t) = \begin{bmatrix} f_1(t) \\ 0 \\ \Omega_1(t) \end{bmatrix}$$

$$\alpha_1(t) = \begin{bmatrix} f_2(t) \\ 0 \\ \Omega_2(t) \end{bmatrix}$$

For the time-independent problem with no suction at either disk, equations (1.2.12) and boundary conditions (1.2.14) become nonlinear two point boundary value problems for ordinary differential equations. Assuming Ω_1 is nonzero, we introduce γ as the ratio of angular velocity of the two disks:

$$\gamma = \frac{\Omega_2}{\Omega_1} \tag{1.2.16}$$

Taking $\Omega_1 = \Omega_0$, the equations and boundary conditions become

$$u_z = F(u, R) \tag{1.2.17a}$$

$$\begin{aligned} B_0\, u(0) &= e_3 \\ B_1\, u(1) &= \gamma e_3 \\ e_3 &= (0 \;\; 0 \;\; 1)^T \end{aligned} \tag{1.2.17b}$$

where u, F, B_0 and B_1 are same as above.

We note the time-independent problem has two parameters: R, the Reynolds number and γ, the ratio of the angular velocity of the two disks. We focus our studies on the following semi-infinite strip I

$$(1.2.18)\qquad \mathcal{I}(\gamma,R) \equiv \left\{ (\gamma,R) : |\gamma| \le 1,\ R > 0 \right\}$$

We can do this because solutions inside the strip are related to those outside : $|\gamma| > 1$, $R \ge 0$. For any nonzero γ and R, let $(f_1(z), g_1(z))$ satisfy the system (1.2.17). We seek a new pair (f_2, g_2) that are transformations of (f_1, g_1) such that the parameter γ in the boundary conditions (1.2.17b) is replaced by its reciprocal $1/\gamma$. This can easily be accomplished as follows:

$$(1.2.19a)\qquad f_2(z;\gamma,R) = (-1)^p \gamma^q f_1\left(1-z;\ \frac{1}{\gamma},\ \gamma^r(-1)^s R\right)$$

$$(1.2.19b)\qquad g_2(z;\gamma,R) = \frac{1}{\gamma}\ g_1\left(1-z;\ \frac{1}{\gamma},\ \gamma^r(-1)^s R\right)$$

where the constants p, q, r and s are to be determined from (1.2.17). The transformations (1.2.19) correspond to interchanging the role of the disks. That is, the bottom disk (z = 0) for g_1 becomes the top disk (z = 1) for g_2 and the top disk for g_1 becomes the bottom disk for g_2:

$$(1.2.20)\qquad g_2(1;\gamma,R) = \frac{1}{\gamma}\ g_1\left(0,\frac{1}{\gamma},\gamma^r(-1)^s R\right) = \frac{1}{\gamma}$$

Lemma 1.1 Let $(f_1(z;\gamma_0, R_0), g_1(z;\gamma_0, R_0))$ be a solution to (1.2.17) for the parameters $R = R_0$, $\gamma = \gamma_0 \neq 0$. Then $(-f_1(1-z;1/\gamma_0, |\gamma_0| R)/|\gamma_0|, g_1(1-z;1/\gamma_0, |\gamma_0|R)/\gamma_0)$ is a solution to (1.2.17) for the modified (or reduced) $R = |\gamma_0| R_0$, and $\gamma = 1/\gamma_0$.

Proof of Lemma 1.1: The no-slip boundary conditions for f_1 and f_{1z} are automatically satisfied. From (1.2.20) g_1 satisfies our desired boundary condition at $z = 1$. To determine the constants p, q, r and s we substitute (1.2.19) into the differential equations (1.2.17a). The r-Momentum equation gives $q = -1$ and $r = 1$. The θ-Momentum equation implies $p = s = 1$ for $\gamma > 0$ and $p = s = 2$ for $\gamma < 0$. This completes the proof.

For any Reynolds number R_0 let $U(\gamma) = (f_1(z;\gamma, R_0), g_1(z;\gamma, R_0))$ be a solution to (1.2.17). For $\gamma = 1$ applying Lemma 1.1 gives

$$U_+ = (-f_1(1-z;1,R_0), g_1(1-z;1,R_0)) \tag{1.2.21}$$

U_+ is a solution to (1.2.17) for the same Reynolds number

R_o and γ is unchanged.

In general U_+ is different from U(1). However we can have $U_+ = U(1)$ if and only if f_1 is anti-symmetric and g_1 is symmetric about z = 0.5. As a simple test we need only examine $f_1(0.5;\ 1,\ R)$ and $g_1(0.5;\ 1,\ R)$. Since if either

$$f_{1z}(0.5) \neq 0 \quad , \text{ or} \qquad g_{1z}(0.5) \neq 0 \tag{1.2.22}$$

is satisfied, then $U_+ \neq U(1)$.

Similarly for $\gamma = -1$ Lemma 1.1 gives

$$U_- = \left(-f_1(1-z;\ -1,\ R_o),\ -g_1(1-z;\ -1,\ R_o)\right) \tag{1.2.23}$$

U_- is different from U(-1) if either $f_1(z;\ -1,\ R_o)$ or $g_1(z;\ -1,\ R_o)$ is not antisymmetric about z = 0.5. We state this in

Corollary 1.2 (a) For any Reynolds number and $\gamma = 1$ let $U(1) = (f_1(z;\ 1,\ R),\ g_1(z;\ 1,\ R))$ be a solution to (1.2.17).

In general $U_+ \equiv (-f_1(1-z;\ 1,\ R),\ g_1(1-z;,\ 1,\ R))$ is different from $U(1)$. However, we can have $U_+ \equiv U(1)$ iff f_1 is anti-symmetric and g_1 is symmetric about $z = 0.5$.

(b) Correspondingly, for any Reynolds number and $\gamma = -1$ let $U(-1) \equiv (f_1(z;\ -1,\ R),\ g_1(z;\ -1,\ R))$ be a solution to (1.2.17). In general $U_- \equiv (-f_1(1-z;\ -1,\ R),\ -g_1(1-z;\ -1,\ R))$ is different from $U(-1)$. However, we can have $U_- \equiv U(-1)$ iff f_1 and g_1 are anti-symmetric about $z = 0.5$.

For any Reynolds number R and $\gamma = 1$ let $U(1)$ be a solution to (1.2.17). (Similar argument can be used for the case $\gamma = -1$.) We observe the boundary conditions for $U(1)$ at the upper disk are the same as those at the lower disk. For some small positive $\epsilon << 1$ we consider the following sets of boundary conditions

$$f_2(0) = f_{2z}(0) = f_2(1) = f_{2z}(1) = 0\ ; \quad g_2(0) = 1\ ;\ g_2(1) = 1-\epsilon\ . \tag{1.2.24}$$

$$f_3(0) = f_{3z}(0) = f_3(1) = f_{3z}(1) = 0\ ; \quad g_3(0) = 1-\epsilon\ ;\ g_3(1) = 1 \tag{1.2.25}$$

Here both $U_2 \equiv (f_2,\ g_2)$ and $U_3 \equiv (f_3,\ g_3)$ satisfy the differential equations (1.2.17a), and as ϵ tends to zero

they both tend to U(1). If g_1 is symmetric and f_1 is antisymmetric about $z = 0.5$ then solutions (f_2, g_2) and (f_3, g_3) satisfy

$$f_2(z) = f_3(1-z)$$
$$g_2(z) = g_3(1-z)$$

On the other hand if g_1 is asymmetric and/or f_1 is not antisymmetric about $z = 0.5$ then

$$f_2(z; 1-\epsilon, R_0) \neq f_3(1-z; 1-\epsilon, R_0) \tag{1.2.26}$$
$$g_2(z; 1-\epsilon, R_0) \neq g_3(1-z; 1-\epsilon, R_0)$$

CHAPTER 2
THE THEORY

In this chapter we describe the theory on which the numerical computations are based. In Section 1 we review simple bifurcation theory. Section 2 studies the continuation of solution branches by pseudo arc-length parametrization. In Section 3 we analyze the stability of solution branches.

2.1 SIMPLE BIFURCATION THEORY ON SMOOTH BRANCHES

We shall restrict ourselves to time-independent problems. Specifically let $\mathbb{B}$ be some Banach Space, we consider the nonlinear problem

$$G(u, \lambda) = 0 \tag{2.1.1}$$

where $u \in \mathbb{B}$, $\lambda \in \mathbb{R}$, and $G: \mathbb{B} \times \mathbb{R} \to \mathbb{B}$. The time-independent rotating coaxial disks problem is an example:

$$G(u,\lambda) \equiv \begin{Bmatrix} B_0 u(0) - e_3 \\ u_z - F(u,R) \\ B_1 u(1) - \gamma e_3 \end{Bmatrix} = 0$$

where F is given by (1.2.13) and B_0, B_1 and e_3 are given by (1.2.15a) and (1.2.17b). Here λ can be either the Reynolds number R or the ratio of the angular velocity of the two disks γ.

Let s be a parameter along a smooth solution branch Γ of (2.1.1). We see that s can be the parameter λ itself or it can be thought of as arc-length along Γ (Keller[13]). By a smooth branch we assume both the solution u and the parameter λ have all the derivatives with respect to s along Γ that will be required in this chapter.

Let $(u(s_0), \lambda(s_0))$ be a solution to (2.1.1).

Definition 2.0 $(u(s_0), \lambda(s_0))$ is said to be a regular point if the Frechet derivative

$$G_u^0 \equiv G_u(u(s_0), \lambda(s_0))$$

is nonsingular.

Definition 2.1 $(u(s_o),\lambda(s_o))$ is said to be a critical point if G_u^o is singular.

In this thesis, we deal with two different kinds of critical points: simple bifurcation points and normal limit points. We review some standard results on simple bifurcation points in this section. Normal limit points will be treated in the next section.

Definition 2.2 The critical point $(u(s_o),\lambda(s_o))$ is a simple bifurcation point if two smooth branches of (2.1.1) have non-tangential intersections. In particular, the following hold

$$\dim N(G_u^o) = \operatorname{codim} R(G_u^o) = 1 \tag{2.1.2}$$

$$G_\lambda^o \equiv G_\lambda(u(s_0),\lambda(s_0)) \in R(G_u^o) \tag{2.1.3}$$

At a simple bifurcation point $(u(s_o),\lambda(s_o))$ let the null space of G_u^o be spanned by φ_1, its adjoint by ψ_1. From (2.1.3), there exists $\varphi_o \in \mathbb{B}$ such that

$$G_u^o \varphi_o = - G_\lambda^o \tag{2.1.4}$$

We make φ_o unique by requiring

$$\psi_1^* \varphi_o = 0 \tag{2.1.5}$$

Repeated differentiations of (2.1.1) with respect to s yield

$$G_u u_s = - G_\lambda \lambda_s \tag{2.1.6}$$

$$G_u u_{ss} = - G_{uu} u_s u_s - 2 G_{u\lambda} u_s \lambda_s - G_\lambda \lambda_{ss} - G_{\lambda\lambda} \lambda_s \lambda_s \tag{2.1.7}$$

$$\begin{aligned} G_u u_{sss} = & - G_{uuu} u_s u_s u_s - 3(G_{uu\lambda} u_s \lambda_s + G_{u\lambda\lambda} \lambda_s \lambda_s - G_{u\lambda} \lambda_{ss}) u_s \\ & - 3 (G_{uu} u_s + G_{u\lambda} \lambda_s) u_{ss} - 3 G_{\lambda\lambda} \lambda_s \lambda_{ss} \\ & - G_\lambda \lambda_{sss} - G_{\lambda\lambda\lambda} \lambda_s \lambda_s \lambda_s \end{aligned} \tag{2.1.8}$$

Non-tangential intersection of branches of Definition 2.2 implies that the derivative $\lambda_s(s_o)$ cannot be zero on both

branches at the simple bifurcation point. Hence, evaluating (2.1.6) at $(u(s_o),\lambda(s_o))$ yields

$$\Psi_1^* G_\lambda^\circ = 0 \tag{2.1.9}$$

For (2.1.7) to have a solution at $(u(s_o),\lambda(s_o))$, its right hand side must lie in the range of G_u°, that is

$$\Psi_1^* \left\{ G_{uu}^\circ u_s^\circ u_s^\circ + 2 G_{u\lambda} u_s^\circ \lambda_s^\circ + G_{\lambda\lambda} \lambda_s^\circ \lambda_s^\circ \right\} = 0 \tag{2.1.10}$$

Because the null space is one dimensional, we can write $u_s(s_o)$ as a direct sum of φ_0 and φ_1. That is

$$u_s(s_0) = \alpha_0 \varphi_0 + \alpha_1 \varphi_1 \tag{2.1.11}$$

where α_0 is $\lambda_s(s_o)$.

Substituting (2.1.11) into (2.1.9) we obtain a quadratic equation for unknowns α_0 and α_1

$$a\alpha_1^2 + 2b\alpha_0\alpha_1 + c\alpha_0^2 = 0 \tag{2.1.12}$$

where coefficents a, b, c are given by

$$
\begin{aligned}
(2.1.13)\qquad a &= \psi_1^* G_{uu}^0 \varphi_1 \varphi_1 \\
b &= \psi_1^* \left\{ G_{uu}^0 \varphi_0 + G_{u\lambda}^0 \right\} \varphi_1 \\
c &= \psi_1^* \left\{ G_{uu}^0 \varphi_0 \varphi_0 + 2 G_{u\lambda}^0 \varphi_0 + G_{\lambda\lambda}^0 \right\}
\end{aligned}
$$

The unknowns α_0 and α_1 can be made unique by requiring

$$(2.1.14)\qquad \alpha_0^2 + \alpha_1^2 = 1$$

Equation (2.1.12) is the algebraic bifurcation equation. For nonlinear two point boundary value problems, an efficient computational method for the coefficients (2.1.13) will be given in the next chapter.

If a in (2.1.13) is non-zero, we form the quotient $q = \alpha_1/\alpha_0$. Let q_- be a nontrivial solution of (2.1.12), then we have another root $q = q_+$ of (2.1.12) if

$$(2.1.15)\qquad a q_- + b \neq 0$$

(2.1.15) is a condition for bifurcation. Thus, assuming roots are distinct, if q_- is the root corresponding to a known branch Γ_{q_-}, then q_+ is the root corresponding to the bifurcated branch.

Let Γ_{q-} be the smooth solution branch containing $(u(s_o),\lambda(s_o))$. A new branch Γ_{q+} is to be determined which emanates from $(u(s_o),\lambda(s_o))$. Now the roots $q_\pm$ of (2.1.12), if imaginary, have to occur in conjugate pairs. Along Γ_{q-} let u(s) be the real solution for the real parameter $\lambda(s)$. Hence at the simple bifurcation point the 'tangent vector' = $q_- = (\alpha_{o-}, \alpha_{1-})$ is real along Γ_{q-}. This proves the tangent vector at the bifurcation point along the new bifurcated branch, Γ_{q+}, is real. That is, the solution along Γ_{q+} is real.

Let $(\alpha_{o\pm}, \alpha_{1\pm})$ be the solutions of (2.1.12) satisfying (2.1.14). For sufficiently small δs, the approximate solutions near $(u(s_o),\lambda(s_o))$ are given by

$$u(s_o+\delta s) = u(s_o) + \delta s\, u_{s\pm}(s_o)$$
$$\lambda(s_o+\delta s) = \lambda(s_o) + \delta s\, \alpha_{o\pm} \qquad (2.1.16a)$$

where $u_{s\pm}(s_o)$ is given by

$$u_{s\pm}(s_o) = \alpha_{o\pm}\varphi_o + \alpha_{1\pm}\varphi_1 \qquad (2.1.16b)$$

2.2 NORMAL LIMIT POINTS AND PSEUDO ARC-LENGTH CONTINUATION

There are other types of critical points which are not bifurcation points. In this section we look into one special type at which the solution branch Γ_N 'turns back' on itself. We show (Keller [12]), by properly choosing the parameter s and solving an extended system, equation (2.1.1) has a unique isolated solution at the critical point in the s-parameter space.

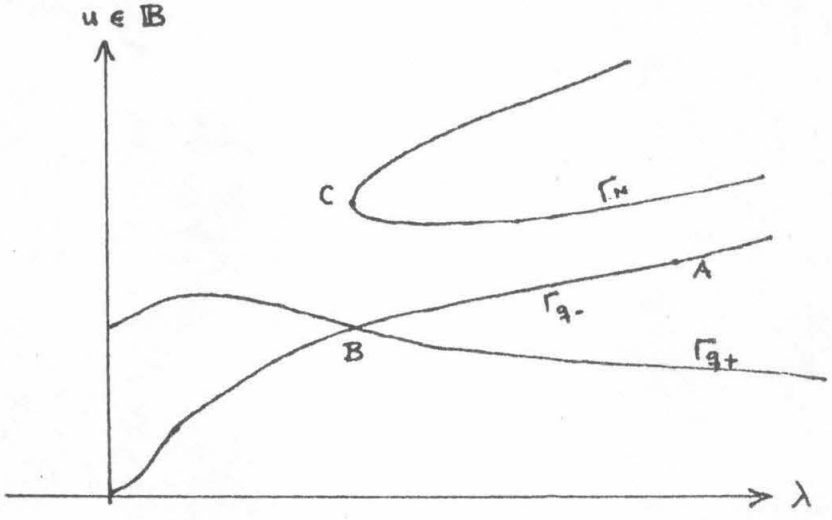

figure 2.1 : Bifurcation Diagram :-
A : regular solution point ; B : Bifurcation point ;
C : normal limit point.

We introduce the idea of pseudo-arclength parametrization of solution branches. Instead of solving equation (2.1.1) for a fixed λ, we let λ depend on a new parameter $s \in \mathbb{R}$. We then need an additional equation to determine λ - a normalization equation of the form

$$N_h(u,\lambda;s) = 0 \tag{2.2.1}$$

We now choose N_h such that s, the new introduced parameter, is an approximation to arc-length along Γ_N. In particular, we use

$$N_h \equiv \theta u_s(s_0)^*\left(u(s)-u(s_0)\right) + (1-\theta)\lambda_s(s_0)\left(\lambda(s)-\lambda(s_0)\right) - (s-s_0) = 0 \tag{2.2.2}$$

where $(u(s_0),\lambda(s_0))$ is a known solution of (2.1.1) and $\theta \in (0,1)$.

Definition 2.3 A critical point $(u(s_0),\lambda(s_0))$ of (2.1.1) is called a normal limit point if the operator

$$G_u(u(s_0),\lambda(s_0)) \equiv G_u^0$$

is singular and satisfies

$$\dim N(G_u^0) = \operatorname{codim} R(G_u^0) = 1 \tag{2.2.3}$$

$$G_\lambda^0 \notin R(G_u^0) \tag{2.2.4}$$

(We observe the difference between a normal limit point and a simple bifurcation point (Definition 2.2) is conditions

(2.1.3) and (2.2.4).)

At a normal limit point, (2.1.6) has a solution if and only if

$$\lambda_s(s_0) = 0 \tag{2.2.5}$$

In addition (2.2.4) implies

$$\psi_1^* G_\lambda \neq 0 \tag{2.2.6}$$

In the neighbourhood of a normal limit point, $\lambda(s)$ has a Taylor series in $(s-s_0)$

$$\lambda(s) = \lambda(s_0) + \sum_{j\geq 2} \frac{a_j}{j!}(s-s_0)^j \tag{2.2.7}$$

Indeed, simple calculations using (2.2.5)-(2.2.6) in (2.1.7) yield:

$$\lambda_{ss}(s_0) = a_2 = \frac{\psi_1^* G_{uu}^\circ \varphi_1 \varphi_1}{\psi_1^* G_\lambda^\circ} = \frac{a}{\psi_1^* G_\lambda^\circ} \tag{2.2.8}$$

If $a = 0$ $\lambda_{sss}(s_0)$ can easily be shown, using (2.1.8), to be

$$\lambda_{sss}(s_0) = a_3 = \frac{\psi_1^* \{ G_{uu}^\circ w\varphi_1 + G_{uuu}^\circ \varphi_1 \varphi_1 \varphi_1 \}}{\psi_1^* G_\lambda^\circ} \tag{2.2.9}$$

Here w is the solution to

$$(2.2.10) \qquad G_u^{\circ} w = G_{uu}^{\circ} \varphi_1 \varphi_1 \quad , \psi_1^* w = 0$$

If $a \neq 0$, in a small neighbourhood about s_o the solution branch 'turns back' on itself. In the following lemma and theorem of H.B. Keller [13], we see that, by solving the inflated system (2.1.1) together with (2.2.2), solution branches containing only normal limit points (especially those with $\lambda_{ss}(s_o)$ non-zero) possess only regular points in the pseudo-arclength s-space. That is, the extended Frechet derivative

$$(2.2.11) \qquad \mathcal{F}_{u\lambda} \equiv \frac{\partial [G\ N]}{\partial [u\ \lambda]} = \begin{bmatrix} G_u & G_\lambda \\ N_u & N_\lambda \end{bmatrix}$$

is nonsingular. Both the lemma and the theorem can be found in Keller [12].

Lemma 2.3 Let $\mathbb{B}$ be a Banach space and consider the linear operator $\mathcal{A} : \mathbb{B} \times \mathbb{R}^\nu \to \mathbb{B} \times \mathbb{R}^\nu$ of the form

$$\mathcal{A} \equiv \begin{bmatrix} A & B \\ C^* & D \end{bmatrix} \quad \text{where} \begin{cases} A : \mathbb{B} \to \mathbb{B}, & B : \mathbb{R}^\nu \to \mathbb{B} \\ C^* : \mathbb{B} \to \mathbb{R}^\nu & D : \mathbb{R}^\nu \to \mathbb{R}^\nu \end{cases}$$

(i) If A is nonsingular then $\mathcal{A}$ is nonsingular iff:

(2.2.12) $\left(D - C^* A^{-1} B\right)$ is nonsingular

(ii) If A is singular and

(2.2.13) $\dim N(A) = \operatorname{Codim} R(A) = \nu$

then $\mathcal{A}$ is nonsingular iff:

$$c_0)\ \dim R(B) = \nu\ ,\ c_1)\ R(B) \cap R(A) = 0$$

$$c_2)\ \dim R(C^*) = \nu\ ,\ c_3)\ N(A) \cap N(C^*) = 0$$

(iii) If A is singular and dim $N(A) > \nu$ then $\mathcal{A}$ is singular.

Using Lemma 2.3 with $\mathcal{A}$ being the Frechect derivative (2.2.11), the following can be proved easily.

Theorem 2.4 Let $(u(s_0), \lambda(s_0))$ be either a regular solution or a normal limit point solution. Let $G(u,\lambda)$ have two continuous derivatives in some sphere about $(u(s_0), \lambda(s_0))$. Then with $(u(s_0), \lambda(s_0)) \equiv (u_0, \lambda_0)$,

$(u_s(s_o), \lambda_s(s_o)) \equiv (u_{os}, \lambda_{os})$ and $u_s^*(s_o)$ as defined after (2.2.2) there exists a unique smooth arc of solutions $(u(s), \lambda(s))$ of (2.1.1) together with (2.2.2) on $|s - s_o| < \rho$ for some sufficiently small $\rho > 0$. On this solution arc the Frechet derivative $\mathcal{A}(s)$ of (2.2.11) is nonsingular.

2.3 STABILITY OF SOLUTION BRANCHES - LINEARIZED ANALYSIS

Having found the equilibrium solutions of (2.1.1) we like to know about their stability as solution of the corresponding time-dependent problem.

$$B u_t = G(u, \lambda) \tag{2.3.1}$$

In the rotating coaxial disk problem with no suction (2.3.1) becomes

$$B u_t = \frac{1}{R}\left(u_z - F(u, R)\right)$$

$$B_0 u(0) = e_3 \tag{2.3.2}$$

$$B_1 u(1) = \gamma e_3$$

where B, F, B_0, B_1 and e_3 are given by (1.2.13), (1.2.15) and (1.2.17b).

We perform a linearized stability analysis in a small neighbourhood of critical points. To be more precise, let $(u(s),\lambda(s))$ be the time-independent solution of (2.1.1) for $0<|s-s_0|<\rho$, where s_0 is a critical point and ρ is small. We then seek a solution to (2.3.1) in the form

$$u(s,t) = u(s) + \epsilon e^{\sigma t} w(s) \tag{2.3.3}$$

where ϵ is small compared to the norm of $u(s)$, and w is an unknown vector function. From (2.3.3) and (2.3.1), and neglecting $o(\epsilon)$ terms, we obtain the linear eigenvalue problem in σ:

$$\sigma B w = G_u(u(s),\lambda(s))\, w \tag{2.3.4}$$

Definition 2.5 The solution u of (2.3.3) is linearly stable if all the eigenvalues $\sigma=\sigma_R+i\sigma_I$ of (2.3.4) lie in the left half complex plane. It is linearly unstable if one or more eigenvalues of (2.3.4) lie in the right half complex plane.

At a simple bifurcation point or a normal limit point, the null space of the operator G_u^0 is one-dimensional.

Hence G_u° has a zero of multiplicity one. Clearly, for any nonzero K $\sigma(s_\circ) = 0$ and $w = K\varphi_1$ is a solution to (2.3.4) at the critical point. We assume $\sigma(s_\circ)$ is an isolated zero. And for s sufficiently close to $s_\circ$, the eigenpair $(\sigma(s), w(s))$ differs in magnitude from $(0, K\varphi_1)$ by a small amount. That is, the eigenvalue and eigenfunction has a Taylor series expansion

$$\sigma(s) = \sum_{j\geq 1} \frac{c_j}{j!}(s-s_0)^j \tag{2.3.5}$$

$$w(s) = K\varphi_1 + \sum_{j\geq 1} (s-s_\circ)^j \frac{w_j}{j!} \tag{2.3.6}$$

We observe there is a local exchange of linear stability with respect to the eigenpair $(0, K\varphi_1)$ if

$$\frac{d^{2K+1}}{ds^{2K+1}}\sigma(s_0) \neq 0 \tag{2.3.7}$$

$$\frac{d^{\ell}}{ds^{\ell}}\sigma(s_0) = 0$$

From Definition 2.5 we note that a solution branch Γ containing a critical point can be unstable even though (2.3.7) is true.

Repeated differentiations of (2.3.4) with respect to s yield

$$\sigma_s B w + \sigma B w_s = G_{uu} u_s w + G_{u\lambda} \lambda_s w + G_u w_s \tag{2.3.8}$$

$$\begin{aligned} \sigma_{ss} B w + 2\sigma_s B w_s + \sigma B w_{ss} &= G_{uu}\{u_{ss} w + 2u_s w_s\} + G_{uuu} u_s u_s w \\ &+ 2G_{uu\lambda} u_s w \lambda_s + G_{u\lambda}(\lambda_{ss} w + 2\lambda_s w_s) \\ &+ G_{u\lambda\lambda} \lambda_s \lambda_s w + G_u w_{ss} \end{aligned} \tag{2.3.9}$$

Evaluating at a critical point using the eigenpair $(0, K\varphi_1)$, we obtain

$$\sigma_s^\circ B \varphi_1 = G_{uu}^\circ u_s^\circ \varphi_1 + G_{u\lambda}^\circ \lambda_s^\circ \varphi_1 + G_u^\circ w(s_0)/K \tag{2.3.10}$$

$$\begin{aligned} \sigma_{ss}^\circ B \varphi_1 + 2\sigma_s^\circ B \frac{w_s(s_0)}{K} &= G_{uu}^\circ \{u_{ss}^\circ \varphi_1 + 2u_s^\circ w_s(s_0)/K\} \\ &+ G_{uuu}^\circ u_s^{\circ 2} \varphi_1 + 2G_{uu\lambda}^\circ u_s^\circ \varphi_1 \lambda_s^\circ \\ &+ G_{u\lambda\lambda}^\circ \lambda_s^\circ \varphi_1 + G_u^\circ w_{ss}(s_0)/K \end{aligned} \tag{2.3.11}$$

We now consider some special cases.

Theorem 2.5 Let $(u(s_\circ), \lambda(s_\circ)) \equiv (u_\circ, \lambda_\circ)$ be a solution to (2.1.1). Assume $G_u(u_\circ, \lambda_\circ) \equiv G_u^\circ$ is singular with $\dim N(G_u^\circ) = \operatorname{codim} R(G_u^\circ) = 1$. Let the null space of G_u° and its

adjoint be spanned by φ_1, Ψ_1 respectively. Further assume $\Psi_1^* B \varphi_1 \neq 0$. We have the following cases

(i) At a simple bifurcation point:

a) if $\lambda_s(s_0) \neq 0$ for one of the branches, Γ, then there is a local exchange of linear stability along Γ.

b) if $\lambda_s^\circ = 0$ for one of the branches, Γ, then there is no exchange of linear stability along Γ. The stability with respect to small perturbations of the eigenpair $(0, K\varphi_1)$ along Γ depends on the sign of $\sigma_{ss}(s_\circ)$ in (2.3.13).

(ii) At a normal limit point, we have a local exchange of linear stability about $s_\circ$ if

$$\frac{d^j}{ds^j}\lambda(s_0) \begin{cases} = 0 & j = 1, 2, \ldots, 2K-1. \\ \neq 0 & j = 2K \end{cases}$$

(2.3.12)

holds.

Part (ii) of Theorem 2.5 implies whenever Γ turns back on itself, we have a local exchange of linear stability; the proof follows immediately from the lemma below.

Lemma 2.6 Let (u_0, λ_0) be a normal limit point. With the notations of Theorem 2.5, we have for any integer $k \geq 2$, if

$$\frac{d^\ell}{ds^\ell}\lambda(s_0) \begin{cases} = 0 & K > \ell > 1 \\ \neq 0 & \ell = K \end{cases} \tag{2.3.13}$$

then

$$\begin{aligned} \frac{d^j}{ds^j}\sigma(s_0) &= 0 && j = 1, 2, \ldots, K-2 \\ \frac{d^{K-1}}{ds^{K-1}}\sigma(s_0) &= -\frac{d^K}{ds^K}\lambda(s_0)\left\{\frac{\Psi_1^* G_\lambda^0}{\Psi_1^* B \varphi_1}\right\} \end{aligned} \tag{2.3.14}$$

Remarks on Lemma 2.6: (1) By assumption, the eigenpair $(0, \varphi_1)$ is a solution to (2.3.4). Hence for some nonzero A_0 and B_0

$$\begin{aligned} u(s_0) &= A_0 \varphi_1 \\ w(s_0) &= B_0 \varphi_1 \end{aligned} \tag{2.3.15}$$

(2) For k = 2 Lemma 2.6 can easily be worked out. (2.1.7) gives

$$\lambda_{ss}(s_0) = A_0^2 \frac{\Psi_1^* G_{uu}^0 \varphi_1 \varphi_1}{\Psi_1^* G_\lambda^0} = \frac{A_0^2 a}{\Psi_1^* G_\lambda^0}$$

If $\lambda_{ss}(s_0) \neq 0$, then since $\Psi_1^* G_\lambda^0 \neq 0$ at a normal limit point, the coefficient a of (2.1.13) is nonzero. From (2.3.10) we have

$$\sigma_s(s_0) = -\frac{\Psi_1^* G^0_{uu} u_s(s_0) \varphi_1}{\Psi_1^* B \varphi_1} \tag{2.3.16}$$

But $u_s(s_0) = A_0 \varphi_1$ at a normal limit point. Hence

$$\sigma_s(s_0) = -\frac{\lambda_{ss}(s_0)\ \Psi_1^* G^0_\lambda}{A_0\ \Psi_1^* B \varphi_1} \tag{2.3.17}$$

From (2.3.7) we see that we have a local exchange of linear stability. The algebra gets more laborious and involved for k = 3, and it gets progressively worse as k increases. But Lemma 2.6 allows us to avoid this tedious work.

Proof of Lemma 2.6:

From (2.3.15) successive differentiations of (2.1.1) with respect to s yield

$$\begin{aligned}
&\frac{d}{ds}\left\{G_u u_s\right\}_{s=s_0} \equiv -\tilde{F}_2\left(u(s_0), u_s(s_0); \lambda(s_0)\right) + G^0_u u_{ss}(s_0) = 0 \\
&\frac{d^2}{ds^2}\left\{G_u u_s\right\}_{s=s_0} \equiv -\tilde{F}_3\left(u(s_0), u_s(s_0), u_{ss}(s_0); \lambda(s_0)\right) + G^0_u u_{sss}(s_0) = 0 \\
&\qquad\qquad \cdots\cdots\cdots \\
&\frac{d^{k-2}}{ds^{k-2}}\left\{G_u u_s\right\}_{s=s_0} \equiv -F_{k-1}\left[u(s_0), u_s(s_0), \ldots, \frac{d^{k-2}}{ds^{k-2}} u(s_0); \lambda(s_0)\right] \\
&\qquad\qquad + G^0_u \frac{d^{k-1}}{ds^{k-1}} u(s_0) = 0
\end{aligned} \tag{2.3.18}$$

and

$$\frac{d^{K-1}}{ds^{K-1}}\left(G_u u_s\right)_{s=s_0} \equiv -\tilde{F}_K\left(u(s_0), u_s(s_0), \ldots, \frac{d^{K+1}}{ds^{K+1}} u(s_0) ; \lambda(s_0)\right) + G_u^0\left(\frac{d^K}{ds^K} u(s_0)\right)$$

(2.3.19)

$$= \frac{d^K}{ds^K} \lambda(s_0)\, G_\lambda^0$$

Assume there exists a positive integer M such that

$$\text{(2.3.20a)} \qquad \frac{d^j}{ds^j}\, \sigma(s_0) = 0 \qquad j = 1, 2, \ldots, M$$

$$\text{(2.3.20b)} \qquad \frac{d^{M+1}}{ds^{M+1}}\, \sigma(s_0) \neq 0$$

We want to show that $M > (k - 3)$. We prove it by contradiction. Differentiating (2.3.4) (M + 1) times, we obtain

$$\text{(2.3.21)} \qquad \frac{d^j}{ds^j} G_u W\Big|_{s=s_0} \equiv -\tilde{D}_j\left(u(s_0), u_s(s_0), \ldots, \frac{d^j}{ds^j} u(s_0); W(s_0), W_s(s_0), \ldots, \frac{d^{j-1}}{ds^{j-1}} W(s_0) ; \lambda_0\right)$$

$$+ G_u^0\left(\frac{d^j}{ds^j} W(s_0)\right) = 0 \qquad j = 1, 2, \ldots, M$$

$$\text{(2.3.22)} \qquad \frac{d^{M+1}}{ds^{M+1}} G_u W\Big|_{s=s_0} \equiv -\tilde{D}_{M+1}\left(u(s_0), u_s(s_0), \ldots, \frac{d^{M+1}}{ds^{M+1}} u(s_0); W(s_0), W_s(s_0), \ldots, \frac{d^M}{ds^M} W(s_0) ; \lambda_0\right)$$

$$+ G_u^0\left(\frac{d^{M+1}}{ds^{M+1}} W(s_0)\right) = \frac{d^{M+1}}{ds^{M+1}} \sigma(s_0)\, \mathcal{B}\, W(s_0)$$

(Note that the terms involving derivatives of the parameter λ with respect to s in the functionals $\tilde{F}_j$ and $\tilde{D}_j$ in (2.3.18) and (2.3.21) respectively are identically zero by assumption (2.3.13).) From (2.3.15) we have at a normal

limit point

$$W(s_0) = C_0 u_s(s_0)$$

where $C_0 = B_0/A_0$. Next we show by induction that

$$\frac{d^{j-1}}{ds^{j-1}} W(s_0) = C_0 \frac{d^j}{ds^j} u(s_0) \tag{2.3.23}$$

for $j < (k-3)$. This is true for $j = 1$. Assume it is true for $j = (i-1)$. For the u-derivative equation we have from (2.3.18)

$$G_u^0\left(\frac{d^i}{ds^i} u(s_0)\right) = \tilde{F}_{i+1}\left(u(s_0), u_s(s_0), \ldots, \frac{d^{i-1}}{ds^{i-1}} u(s_0); \lambda_0\right) \; ; \; \psi_1^*\left(\frac{d^i}{ds^i} u(s_0)\right) = 0$$

Also for the w-derivative equation we have from (2.3.21)

$$G_u^0\left(\frac{d^{i-1}}{ds^{i-1}} W(s_0)\right) = \tilde{D}_{i-1}\left(u(s_0), u_s(s_0), \ldots, \frac{d^{i-1}}{ds^{i-1}} u(s_0); W(s_0), W_s(s_0), \ldots, \frac{d^{i-2}}{ds^{i-2}} W(s_0); \lambda_0\right),$$

$$\psi_1^*\left(\frac{d^{i-1}}{ds^{i-1}} W(s_0)\right) = 0$$

Higher order derivatives of $(G_u^0 w)$ are linear in $d^m w/ds^m$. By this we mean the right side $\tilde{D}_{i-1}$ has the form

$$\tilde{D}_{i-1} = \sum_{K=0}^{i-2} H_K\left(u(s_0), u_s(s_0), \ldots \frac{d^{i-1}}{ds^{i-1}} u(s_0)\right) \frac{d^K}{ds^K} W(s_0) \tag{2.3.24}$$

But we have for $j = 1,2,\ldots,(i-1)$

$$\frac{d^{j-1}}{ds^{j-1}} w(s_o) = C_o \frac{d^j}{ds^j} u(s_o) \tag{2.3.25}$$

This implies from (2.3.18) and (2.3.21)

$$\tilde{D}_{i-1} = C_o \tilde{F}_i \tag{2.3.26}$$

proving

$$\frac{d^{i-1}}{ds^{i-1}} w(s_o) = C_o \frac{d^i}{ds^i} u(s_o)$$

This concludes the induction process. We point out that higher derivatives of w and u with respect to s evaluated at s are made unique by requiring they have no component of φ_1.

Subtracting (2.3.18) from (2.3.22) with $M = (k-3)$ and using (2.3.25)-(2.3.26) give

$$\left(\frac{d^{k-2}}{ds^{k-2}} \sigma(s_o)\right) \mathcal{B}\, w(s_o) = G_u^o \left\{ \frac{d^{k-2}}{ds^{k-2}} \left[w(s_o) - u_s(s_o) \right] \right\} \tag{2.3.27}$$

Operating from the left with Ψ_1^* and noting $\Psi_1^* G_u^o = 0$:

$$\Psi_1^* \mathcal{B} \varphi_1 \left\{ \frac{d^{k-2}}{ds^{k-2}} \sigma(s_o) \right\} = 0$$

Because $\Psi_1^* B \varphi_1 \neq 0$, we have our contradiction that

$$\frac{d^{K-2}}{ds^{K-2}} \sigma(s_0) = \frac{d^{M+1}}{ds^{M+1}} \sigma(s_0) \neq 0$$

proving $M > (k - 3)$ in (2.3.20).

Operating Ψ_1^* from the left on equations (2.3.19) and (2.3.22) with $M = (k - 2)$, and observing the coefficients of both $(k - 1)$-st derivative of w and k-th derivative of u at the critical point s_0 are $\Psi_1^* G_u^0$, which is identically zero,

$$\Psi_1^* B \varphi_1 \frac{d^{K-1}}{ds^{K-1}} \sigma(s_0) = -\left(\frac{d^K}{ds^K} \lambda(s_0)\right) \Psi_1^* G_\lambda^0$$

At a normal limit point, $\Psi_1^* G_\lambda^0$ is nonzero; the right hand side of the equation above is nonzero by assumption (2.3.13). We have our desired result of (2.3.16), and the proof of Lemma 2.6 is completed.

The proof of Theorem 2.5 is very simple and it proceeds as follows.

Proof of Theorem 2.5

Operating (2.3.9) from the left with Ψ_1^* at the simple bifurcation point

$$\sigma_s(s_0) = \frac{\Psi_1^* \left(G^0_{uu} u_s(s_0) + G^0_{u\lambda} \lambda_s(s_0) \right) \varphi_1}{\Psi_1^* B \varphi_1}$$

Recall (2.1.10)

$$u(s_0) = \alpha_0 \varphi_0 + \alpha_1 \varphi_1$$

this gives

$$\sigma_s(s_0) = \frac{\alpha_1 a + \alpha_0 b}{\Psi_1^* B \varphi_1}$$

where a and b are the coefficients of the algebraic bifurcation equation (2.1.13).

If $\lambda_s(s_0) \neq 0$, the right hand side is nonzero because of the condition for bifurcation (2.1.15).

If $\lambda_s(s_0) = 0$, Ψ_1^* on (2.1.7) implies $a = \Psi_1^* G^0_{uu} \varphi_1 \varphi_1 = 0$. From (2.3.10) we have $\sigma_s(s_0) = 0$. To find out the stability of the branch we next determine the second derivative $\sigma_{ss}(s_0)$. Assume $\lambda_{ss}(s_0) \neq 0$. It is evident from the proof of Lemma 2.6 we can choose B_0 to be

equal to A_0 for $u_s(s_o)$ and $w(s_o)$. Thus, we have from (2.3.10)

$$w_s(s_o) = G_u^{o\,-1}\left\{ G_{uu}^{o}\, u_s(s_o)\, w(s_o)\right\}, \quad \psi_1^{*}\, w_s(s_o) = 0 \tag{2.3.28}$$

From (2.1.7) we have

$$\begin{aligned} u_{ss}(s_o) &= G_u^{o\,-1}\left\{ - G_{uu}^{o}\, u_s(s_o)\, u_s(s_o) - G_\lambda^{o}\, \lambda_{ss}(s_o)\right\} \\ &= w_s(s_o) - \lambda_{ss}\, \varphi_o \end{aligned} \tag{2.3.29}$$

where φ_o satisfies

$$G_u^{o}\, \varphi_o = - G_\lambda^{o}$$

Operating from the left with ψ_1^{*} on (2.1.8) and using the fact $\lambda_s(s_o) = 0$ yields

$$\psi_1^{*}\, G_{uuu}^{o}\, u_s(s_o)\, u_s(s_o)\, u_s(s_o) = -3\, \psi_1^{*}\left\{ G_{uu}\, u_{ss}(s_o) + G_{u\lambda}\, \lambda_{ss}(s_o)\right\} u_s(s_o) \tag{2.3.30}$$

Finally, operating from the left with ψ_1^{*} on (2.3.11) yields

$$\begin{aligned} \psi_1^{*} B\, w(s_o)\, \sigma_{ss}(s_o) &= 2\, \psi_1^{*}\, G_{uu}^{o}\, w_s(s_o)\, u_s(s_o) + \psi_1^{*}\, G_{uuu}^{o}\, u_s(s_o)\, u_s(s_o)\, u_s(s_o) \\ &\quad + \psi_1^{*}\left(G_{uu}^{o}\, u_{ss}(s_o) + G_{u\lambda}\, \lambda_{ss}(s_o)\right) u_s(s_o) \\ &= 2\, \psi_1^{*}\, G_{uu}^{o}\, w_s(s_o)\, u_s(s_o) + \frac{2}{3}\, G_{uuu}^{o}\, u_s^{3}(s_o) \end{aligned} \tag{2.3.31}$$

Since

$$u_s(s_0) = w(s_0) = A_0 \varphi_1$$

we have

$$\sigma_{ss}(s_0) = A_0^2 \left\{ \frac{\left[-2 \psi_1^* G^0_{uu} G_u^{0-1} G^0_{uu} \varphi_1 \varphi_1 + \tfrac{2}{3} \psi_1^* G^0_{uuu} \varphi_1 \varphi_1 \right] \varphi_1}{\psi_1^* B \varphi_1} \right\} \tag{2.3.32}$$

(2.3.32) implies the sign of $\sigma_{ss}(s_0)$ is independent of the sign of A_0.

CHAPTER 3

THE NUMERICAL METHODS

In this chapter we discuss the numerical methods in solving the rotating coaxial disks problem. These methods can be used to solve general nonlinear two point boundary value problems for ordinary differential equations with one or more parameters. The chapter is divided into five sections. Section 1 gives a brief account for numerical solutions of two point boundary value problems (Keller [11]). Section 2 discusses the numerical implementation of pseudo-arclength continuation and the computation of solution branches. Section 3 is concerned with the rate of convergence proof of Newton's method for solving the 'inflated' pseudo-arclength system of equations at both regular and critical points. Section 4 provides the treatment at simple bifurcation points. Lastly, Section 5 shows how the numerical computations of the local exchange of stability analysis is being handled.

3.1 NUMERICAL SOLUTIONS FOR NONLINEAR TWO POINT BOUNDARY VALUE PROBLEMS

The theory of difference schemes for solving nonlinear two point boundary value problems for ordinary differential equations is well known. Indeed, the basic convergence theorem can be found in Keller [11]. We only outline the scheme and discuss the solution procedures.

Let us consider the general first order system of ordinary differential equations:

$$u_x = f(x, u; \lambda) \qquad x \in [a, b] \tag{3.1.1}$$

$$\begin{aligned} g_1(u(a), \lambda) &= 0 \\ g_2(u(b), \lambda) &= 0 \end{aligned} \tag{3.1.2}$$

Here u, f both have dimension n; g_1, g_2 have dimension p, q = n - q respectively, with $p > 0$. λ is a parameter. We saw in Chapter 1 how the time-independent rotating coaxial disks problem was put into the form (3.1.1)-(3.1.2), with either the Reynolds number, R, or the ratio of the angular velocity of the two disks, γ, plays the role of λ.

The second order centered-Euler (or box) scheme is used to approximate (3.1.1). For any set of net points $\{x_j\}_{j=1}^{J}$ with

$$
\begin{aligned}
x_1 &= a \\
x_j &= x_{j-1} + h_{j-1} \\
x_J &= b
\end{aligned}
\tag{3.1.3}
$$

The scheme is

$$N_h u_j \equiv u_j - u_{j-1} - h_{j-1} f(x_{j-\frac{1}{2}}, \tfrac{1}{2}(u_j + u_{j-1}); \lambda) = 0 \qquad 2 \le j \le J$$

The boundary conditions (3.1.2) give

$$
\begin{aligned}
g_1(u_1, \lambda) &= 0 \\
g_2(u_J, \lambda) &= 0
\end{aligned}
$$

These difference equations can be written in the vector form:

$$G_h(u, \lambda) \equiv \begin{bmatrix} g_1(u_1, \lambda) \\ N_h u_2 \\ N_h u_3 \\ \vdots \\ N_h u_J \\ g_2(u_J, \lambda) \end{bmatrix} = 0 \tag{3.1.4}$$

To solve (3.1.4), we use Newton's method: let u^1 be an

initial guess

$$u^{\nu+1} = u^{\nu} + \delta u^{\nu} \tag{3.1.5}$$

$$\mathbb{A}^{\nu}\, \delta u^{\nu} = - G_h(u^{\nu}, \lambda) \tag{3.1.6a}$$

where

$$\mathbb{A}^{\nu} \equiv \begin{bmatrix} M_a^{\nu} & & & & \\ L_2^{\nu} & R_2^{\nu} & & & \\ & L_3^{\nu} & R_3^{\nu} & \ddots & \\ & & \ddots & \ddots & \\ & & & L_J^{\nu} & R_J^{\nu} \\ & & & & M_b^{\nu} \end{bmatrix} \tag{3.1.6b}$$

$$L_j^{\nu} \equiv -I - \frac{h_{j-1}}{2} f_u\left(x_{j-\frac{1}{2}}, \tfrac{1}{2}(u_j^{\nu} + u_{j-1}^{\nu}); \lambda\right) \tag{3.1.6c}$$

$$R_j^{\nu} \equiv I - \frac{h_{j-1}}{2} f_u\left(x_{j-\frac{1}{2}}, \tfrac{1}{2}(u_j^{\nu} + u_{j-1}^{\nu}); \lambda\right) \tag{3.1.6d}$$

$$M_a^{\nu} \equiv \frac{\partial g_1}{\partial u(a)}\left(u_1^{\nu}, \lambda\right) \tag{3.1.6e}$$

$$M_b^{\nu} \equiv \frac{\partial g_2}{\partial u(b)}\left(u_J^{\nu}, \lambda\right) \tag{3.1.6f}$$

The matrix $\mathbb{A}'$ can be put into a block tridiagonal form $\mathbb{A}' \equiv [B_i, A_i, C_i]$. All block submatrices are (n x n). The last (n - p) rows of B_i are zero, and the first p rows of C_i are zero. A fast block elimination algorithm which keeps the zeros' structure of B_i and C_i is used to solve (3.1.6):

$$[B_i, A_i, C_i] = [\beta_i \; I \; 0][0 \; \alpha_i \; C_i] \equiv \mathcal{L}\mathcal{U}$$

$$\begin{aligned} \alpha_1 &= A_1 \\ \beta_i &= B_i \alpha_{i-1}^{-1} \qquad i \geq 2 \\ \alpha_i &= A_i - \beta_i C_{i-1} \end{aligned} \tag{3.1.7}$$

A_1 is assumed to be nonsingular at the start of the algorithm. This can always be done by interchanging one or more rows of the last (n - p) rows of A_1 with the same number of rows from the first p rows of B_2. To justify the LU-factorization in (3.1.7), we need to show α_i is nonsingular, $i \geq 2$. (This, of course, is only true if the matrix $\mathbb{A}$ is non-singular. In our computations we have encountered no difficulty at bifurcation points or normal limit points, where $\mathbb{A}$ is singular. That is, α_i, $2 \leq i \leq (J - 1)$, are all nonsingular and only the last block α_J has determinant very close to zero.) We assume that A_1 can be written

$$A_1 \equiv P_1 (I + h Q_1)$$

here P_1 is a permutation matrix due to the boundary conditions and the switching of rows mentioned above. This assumption can, in general, be enforced by rescaling rows or columns of A_1. The norm of Q_1 is O(1).

All block submatrices A_i, $i \geq 2$, can also be written

$$A_i = P_2 (I + hQ_i)$$

where P_2 is a permutation matrix for all $i \geq 2$, and the norm of Q_i is O(1). This is true because we switch the k-th row of all A_i with the m-th row of all B_{i+1} if the k-th row of A_1 has to be switched with the m-th row of B_2 in order that A_1 is nonsingular. We proceed by induction. Assume κ_i is nonsingular and have a similar expansion as A_i

$$\kappa_i = P_2 (I + hR_{i1} + h^2 R_{i2} + O(h^3))$$

where the norm of matrices R_{i1} and R_{i2} is O(1). Then using the Banach Lemma (Issacson and Keller [9]), its inverse can be written as

$$\kappa_i^{-1} = (I - hR_{i1} - h^2 (R_{i2} - R_{i1}^2) + O(h^3)) P_2^{-1}$$

For clarity of presentation we drop the permutation matrix

P_2. At the (i + 1)-st stage of elimination we have

$$A_{i+1} = I + h Q_{i+1}$$

$$B_{i+1} = \begin{matrix} p \\ n-p \end{matrix}\begin{bmatrix} 1 & & \\ & \ddots & 1 \\ & & \end{bmatrix} + h\tilde{B}_{i+1} \text{ ; where } \tilde{B}_{i+1} = \begin{matrix} p \\ n-p \end{matrix}\begin{bmatrix} \times & \cdots & \times \\ \vdots & & \vdots \\ \circ & \cdots & \circ \end{bmatrix}$$

$$C_i = \begin{matrix} p \\ n-p \end{matrix}\begin{bmatrix} & & \\ & \ddots & 1 \\ 1 & & \end{bmatrix} + h\tilde{C}_i \text{ ; where } \tilde{C}_i = \begin{matrix} p \\ n-p \end{matrix}\begin{bmatrix} \circ & \cdots & \circ \\ \vdots & & \vdots \\ \times & \cdots & \times \end{bmatrix}$$

Here the norm of $\tilde{B}_{i+1}$ and $\tilde{C}_i$ is O(1). This very special structure of B_{i+1} and C_i implies

$$B_{i+1} C_i = h S_{i+1}$$

where the norm of S_{i+1} is O(1). Next we determine α_{i+1} from (3.1.7)

$$\begin{aligned} \alpha_{i+1} &= A_{i+1} - B_{i+1} \alpha_i^{-1} C_i \\ &= I + hQ_{i+1} - B_{i+1}\left(I - hR_{i,1} - O(h^2)\right) C_i \\ &= I + h(Q_{i+1} - S_{i+1}) + h^2(\tilde{B}_{i+1} R_{i,1} \tilde{C}_i) + O(h^3) \\ &= I + h R_{i+1,1} + h^2 R_{i+1,2} + O(h^3) \end{aligned}$$

Note that $R_{i+1,1}$ depends only on A_{i+1}, B_{i+1} and C_i. For

sufficiently small mesh size h, α_{i+1} is nonsingular. This completes the induction process.

α_i , $i \geq 1$, are decomposed into LU form using a new pivoting strategy. (Appendix 1)

$$\alpha_i = p_i \ell_i u_i q_i$$

where p_i , q_i are permutation matrices, l_i and u_i are lower and upper triangular matrices respectively.

The solution of (3.1.6) can easily be computed:

$$\mathcal{L} y = - G_h^\nu \tag{3.1.8}$$

$$U \delta u^\nu = y$$

Newton's method is said to have converged if for some prescribed error tolerance ϵ,

$$\frac{\| \delta u \|}{\| u \|} < \epsilon$$

For solutions exhibiting boundary layers or abrupt gradient changes, an adaptive mesh refinement is used. This is based on approximately equidistributing the first order

local truncation error, T_1, of the numerical scheme (Pereyra and Sewell [25]). For the centered-Euler method, T_1 is given by

$$(3.1.9) \qquad T_1(x_{j-1/2}) = \left(\frac{h_{j-1}}{2}\right)^2 \left\{ \frac{u'''(x_{j-1/2})}{3!} - \frac{f_u(x_{j-1/2}, u_{j-1/2}; \lambda)\, u''(x_{j-1/2})}{2!} \right\}$$

A fourth order method can be constructed by subtracting a second order approximation for T_1 from the difference equations. This can be done and yet still preserves the structure of the Jacobian matrix (3.1.6).

$$(3.1.9a) \qquad T_{1h}(x_{j-1/2}) = \frac{1}{3!}\left[f(x_j, u_j; \lambda) - 2f(x_{j-1/2}, \tfrac{1}{2}(u_j + u_{j-1}); \lambda) + f(x_{j-1}, u_{j-1}; \lambda) \right]$$
$$- \frac{h_{j-1}}{8} f_u(x_{j-1/2}; \tfrac{1}{2}(u_j + u_{j-1}); \lambda) \left[f(x_j, u_j; \lambda) - f(x_{j-1}, u_{j-1}; \lambda) \right]$$

To obtain higher order numerical solution to (3.1.1)-(3.1.2) we note the centered-Euler method has an asymptotic error expansion containing only even powers of h_j, provided the solution has sufficient derivatives

$$u_j = u(x_j) + \sum_{m>0} \left(\frac{h_j}{2}\right)^{2m} e_m(x_j)$$

We can eliminate these global error functions $e_m(x_j)$ successively by either (1) deferred correction (Pereyra [24]), or (2) Richardson extrapolation

(Keller [11]).

We now discuss the well-known notion of Euler-Newton continuation. Assume numerical solution has been found for the parameter $\lambda = \lambda_o$. Then for sufficiently small $\delta\lambda_o$, an improved initial guess for $u(\lambda_o + \delta\lambda_o)$ can be obtained by Euler's method

$$u'(\lambda_o + \delta\lambda_o) = u(\lambda_o) + \delta\lambda_o u_\lambda(\lambda_o) \tag{3.1.10}$$

Here the numerical solution for $u_\lambda(\lambda_o)$ can be computed using the Jacobian of the converged solution in (3.1.6), say A^∞ :

$$A^\infty u_\lambda(\lambda_o) = - G_\lambda(u(\lambda_o), \lambda_o) \tag{3.1.11}$$

The predictor $u'(\lambda_o + \delta\lambda_o)$ can now be used as an initial guess for Newton's method to solve the difference equations approximating (3.1.1)-(3.1.2) at $\lambda = \lambda_o + \delta\lambda_o$.

3.2 COMPUTATION OF SOLUTION BRANCHES CONTAINING LIMIT POINTS

The Euler-Newton continuation method discussed at the

end of last section can be used to compute most solution branches Γ. However, for branches Γ_n that contain normal limit points $\lambda(s_0)$ at which $\lambda_{ss}(s_0) \neq 0$ and $\lambda_s(s_0) = 0$, this straightforward Euler-Newton continuation fails to go past (or around) $\lambda(s_0)$, and special treatment at $\lambda(s_0)$ is needed. We saw in Chapter 2 that the difficulty with normal limit points can be circumvented by freeing the parameter and introducing an additional equation with a new parameter s, the pseudo-arclength parameter. That is, both the solution u and the parameter λ are functions of s. From Theorem 2.2 we saw that every solution along Γ_n is isolated in the parameter s-space. In this section we give a discussion on the numerical implementation of computing solution branches using pseudo-arclength Euler-Newton continuation.

We recall from Section 2 of Chapter 2 that λ is to be determined as part of the solution. The enlarged system consists of the set of finite difference equations (3.1.4) and the discrete normalization equation (2.2.2):

$$G_h(u,\lambda) = 0 \tag{3.2.1}$$

$$N_h(u,\lambda;s) \equiv \theta u_s^*(s_0)\left[u(s)-u(s_0)\right] + (1-\theta)\lambda_s(s_0)\left[\lambda(s)-\lambda(s_0)\right] - (s-s_0) = 0 \tag{3.2.2}$$

where $\theta \in (0,1)$ and $(u(s_o), \lambda(s_o)) \equiv (u_o, \lambda_o)$ is a known solution at $s = s_o$. (To start, say at $s = 0$, let $u_o(0)$ be the solution to only the system (3.2.1) for some fixed λ_o.)

We need to determine $u_s(s_o)$ and $\lambda_s(s_o)$. The derivative $u_\lambda(s_o)$ can be solved as in (3.1.11). Using the chain rule

$$u_s(s_o) = \lambda_s(s_o)\, u_\lambda(s_o) \tag{3.2.3}$$

We take the limit as $s \to s_o$ in (3.2.2)

$$\lambda_s^2(s_o) \left\{ \theta \| u_\lambda(s_o) \|_2^2 + (1-\theta) \right\} = 1$$

and solving for $\lambda_s(s_o)$

$$\lambda_s(s_o) = \frac{\pm 1}{\left[\theta \| u_\lambda(s_o) \|_2^2 + 1 - \theta \right]^{1/2}} \tag{3.2.4}$$

For $\theta \in (0,1)$, the denominator cannot be zero. We observe that the computation of the derivative $\lambda_s(s_o)$ in (3.2.4) is a function of (u_o, λ_o) at $s = s_o$ only and does not depend on solution (u, λ) at any other previously computed s-stations; also, at a normal limit point, s_1, we have, as $s \to s_1$

$$\| u_\lambda \|_2^2 \to \infty$$

Substituting (3.2.3) and (3.2.4) into (3.2.2)

$$(3.2.5)\qquad \frac{\pm 1}{\left(\theta \|u_\lambda(s_0)\|_2^2 + 1-\theta\right)^{1/2}}\left\{u_\lambda(s_0)^*\left[u(s)-u(s_0)\right]\theta + \left[\lambda(s)-\lambda(s_0)\right](1-\theta)\right\} = s - s_0$$

Choosing the positive sign in (3.2.4) implies $\lambda(s) \geq \lambda(s_0)$ if $\delta s \equiv s - s_0 \geq 0$, and $\lambda(s) \leq \lambda(s_0)$ if $\delta s \leq 0$. Correspondingly, choosing the negative sign in (3.2.4) implies the opposite.

The pseudo-arclength Euler one-step method can be used to otain the predictor for the solution at $(s_0 + \delta s)$

$$(3.2.6a)\qquad u'(s_0 + \delta s) = u(s_0) + \delta s\, u_s(s_0)$$

$$(3.2.6b)\qquad \lambda'(s_0 + \delta s) = \lambda(s_0) + \delta s\, \lambda_s(s_0)$$

These are then used as the initial guess for the pseudo-arclength Newton's method on (3.2.1)-(3.2.2) at $s = s_0 + \delta s$:

$$(3.2.7)\qquad \begin{bmatrix} G_{hu}^{\nu} & G_{h\lambda}^{\nu} \\ N_{hu}^{\nu} & N_{h\lambda}^{\nu} \end{bmatrix} \begin{bmatrix} \delta u^{\nu} \\ \delta\lambda^{\nu} \end{bmatrix} = -\begin{bmatrix} G_h^{\nu} \\ N_h^{\nu} \end{bmatrix}$$

$$(3.2.8)\qquad \begin{bmatrix} u^{\nu+1} \\ \lambda^{\nu+1} \end{bmatrix} = \begin{bmatrix} u^{\nu} \\ \lambda^{\nu} \end{bmatrix} + \begin{bmatrix} \delta u^{\nu} \\ \delta\lambda^{\nu} \end{bmatrix}$$

The following s-algorithm (Keller [13]) is used to solve (3.2.7):

$$G^{\nu}_{hu}\, y = G^{\nu}_{h\lambda} \tag{3.2.9}$$

$$G^{\nu}_{hu}\, z = -G^{\nu}_{h} \tag{3.2.10}$$

$$\delta\lambda^{\nu} = \frac{-(N^{\nu}_{h} + N^{\nu}_{hu}\, z)}{(N^{\nu}_{h\lambda} - N^{\nu}_{hu}\, y)} \tag{3.2.11}$$

$$\delta u^{\nu} = z - \delta\lambda^{\nu}\, y \tag{3.2.12}$$

The bulk of the computations for Newton's method is in the LU-factorization of the Jacobians G^{ν}_{hu}. The solution for the inflated system (3.2.7)-(3.2.8) only requires the additional evaluation of right hand side $G^{\nu}_{h\lambda}$ in (3.2.7), backward substitution in solving y in (3.2.9) and two inner products $N^{\nu}_{hu}\, z$ and $N^{\nu}_{hu}\, y$ in (3.2.11).

3.3 RATE OF CONVERGENCE OF NEWTON'S METHOD

For the inflated system (3.2.1)-(3.2.2) Lemma 2.3 and Theorem 2.4 implies Newton's method converges (i) quadratically for regular solution points and normal limit points, and (ii) linearly for simple bifurcation points. However, it is not clear that the s-algorithm

(3.2.9)-(3.2.12) without modification can be used at normal limit points where $G^{\circ}_{h\lambda} \notin R(G^{\circ}_{hu})$ (that is, there is no solution to (3.2.9)). In this section we show the s-algorithm need not be modified and we derive its rate of convergence. For completeness we also derive the rate of convergence for regular solution points and simple bifurcation points for the s-algorithm. An extension to Newton's method for general systems of equations in which the Jacobians are singular at the solution points is indicated. In particular we give a constructive proof of recovery of quadratic convergence for these singular problems. This result implies that we can actually obtain quadratic convergence at bifurcation points. Though the analysis below is done on critical points which have one-dimensional null space, the results go through for higher dimensional null spaces, provided the zeros of the Jacobian matrix all have Jordon block of size one, that is, they are simple zeros; Rall in 1966 [26] indicated how to recover quadratic convergence at singular points, but his numerical implementation was indirect.

We consider the general nonlinear system

(3.3.1) $F(x) = 0$

where $x \in \mathbb{R}^n$, $F: \mathbb{R}^n \to \mathbb{R}^n$. It is well known (see Issacson and Keller [9]) that Newton's method

$$F_x(x^\nu)\ \delta x^\nu = -F(x^\nu)$$

$$x^{\nu+1} = x^\nu + \delta x^\nu$$

will converge quadratically if the Jacobian $F_x^\nu(x^\nu)$ is non-singular, $F_{xx}(x^\nu)$ exists and the initial guess is sufficiently close to the solution.

For critical points with one-dimensional null space, sufficient conditions for convergence of Newton's method can be found in Reddien [27]:

Theorem 3.1 Let x be a solution to (3.3.1). Assume $N_1 \equiv$ null space $F_x(x^*)$ is one-dimensional. Let $B_\rho(x^*) \equiv \{ x \in \mathbb{R}^n : \| x - x^* \| \leq \rho \}$. Define the projector P_{X_1} from $\mathbb{R}^n$ onto X_1 to have null space N_1 and let $P_{N_1} = I - P_{X_1}$, where $\mathbb{R} = N_1 \oplus X_1$. Define $C_\theta(x^*) = \{ x \in \mathbb{R}^n : \| P_{X_1}(x - x^*) \| \leq \theta \| P_{N_1}(x - x^*) \| \}$. Assume $F_{xx}(x^*) N_1 N_1 \cap X_1 = \{ 0 \}$. Let $\| F_{xx}(x^*) \varphi\, x \| \geq c_1 \| \varphi \| \| x \|$ for all $\varphi \in N_1$, $x \in \mathbb{R}^n$ and with $c_1 > 0$. Then there exists $\rho > 0$ and $\theta > 0$ so that $F_x(x)$ has an inverse in $W_{\rho,\theta}(x^*) \equiv B_\rho(x^*) \cap C_\theta(x^*)$, $x \neq x^*$, satisfying $\| F_x(x)^{-1} \| \leq$

$c_2\|x - x^*\|$, the mapping $Gx \equiv x - F_x^{-1}(x)F(x)$ is a contraction on $W_{\rho,\theta}(x^*)$ mapping $W_{\rho,\theta}(x^*)$ into itself, and $F_x^{-1}(0) \cap B_\rho(x^*) = x^*$. Moreover, defining the sequence $x_i = Gx_{i-1}$ with $x_0 \in W_{\rho,\theta}(x^*)$, we have $x_i \to x^*$, $\|P_{X_1}(x_i - x^*)\| \le c\|x_{i-1} - x^*\|$ and $\|P_{N_1}(x_i - x^*)\| / \|P_{N_1}(x_{i-1} - x^*)\|$ tends to 0.5.

The proof can be found in Reddien [27]. We assume all the sufficient conditions of Theorem 3.1 are met.

Lemma 3.2 Assuming Newton's method (3.2.9)-(3.2.12) for solving (3.2.1)-(3.2.2) converges, we have

(1) Rate of convergence is quadratic (a) at regular points (that is, $G_{hu}(u_0, \lambda_0)$ is nonsingular), and (b) at normal limit points (that is, $G_{hu}(u_0, \lambda_0)$ is singular with one-dimensional null space and $G^0_{h\lambda} \notin R(G^0_{hu}(u_0, \lambda_0))$).

(2) Rate of convergence is linear at simple bifurcation point (that is, $G_{hu}(u_0, \lambda_0)$ is singular with one-dimensional null space and $G^0_{h\lambda} \in R(G^0_{hu}(u_0, \lambda_0))$).

Proof of Lemma 3.2 At regular solution points (u_0, λ_0), the Jacobian matrix $G_{hu}(u_0, \lambda_0)$ is non-singular. Define the error

at the ν-th iteration ε^ν, δ^ν:

$$\varepsilon^\nu = u^\nu - u_0 \tag{3.3.2a}$$

$$\delta^\nu = \lambda^\nu - \lambda_0 \tag{3.3.2b}$$

The difference between Newton iterates can then be written as

$$\begin{aligned} \delta u^\nu &= u^{\nu+1} - u^\nu \\ &= u^{\nu+1} - u_0 + u_0 - u^\nu \\ &= \varepsilon^{\nu+1} - \varepsilon^\nu \end{aligned} \tag{3.3.3}$$

$$\begin{aligned} \delta\lambda^\nu &= \lambda^{\nu+1} - \lambda^\nu \\ &= \delta^{\nu+1} - \delta^\nu \end{aligned} \tag{3.3.4}$$

Define μ^ν:

$$\mu^\nu = \left(\|\varepsilon^\nu\|_2^2 + \|\varepsilon^\nu\|_2 |\delta^\nu| + |\delta^\nu|^2 \right)^{1/2} \tag{3.3.5}$$

To show quadratic convergence, we need for any nonzero K,

$$\mu^{\nu+1} = K \mu^{\nu\,2}$$

Expanding G_h^ν, G_{hu}^ν, and $G_{h\lambda}^\nu$ in Taylor series about the solution (we drop the subscript h):

$$G^{\nu} = G^{\circ} + \left(G_u^{\circ}\varepsilon^{\nu} + G_\lambda^{\circ}\delta^{\nu} \right) + \frac{1}{2!}\left(G_{uu}^{\circ}\varepsilon^{\nu}\varepsilon^{\nu} + 2G_{u\lambda}^{\circ}\varepsilon^{\nu}\delta^{\nu} + G_{\lambda\lambda}^{\circ}\delta^{\nu}\delta^{\nu} \right)$$

(3.3.6)

$$+ \frac{1}{3!}\left(\varepsilon^{\nu}\frac{\partial}{\partial u} + \delta^{\nu}\frac{\partial}{\partial \lambda} \right)^3 G(u_\circ + \theta_1\varepsilon^{\nu}, \lambda_\circ + \zeta_1\delta^{\nu})$$

$$(3.3.7) \qquad G_u^{\nu} = G_u^{\circ} + \left(G_{uu}^{\circ}\varepsilon^{\nu} + G_{u\lambda}^{\circ}\delta^{\nu} \right) + \frac{1}{2!}\left(\varepsilon^{\nu}\frac{\partial}{\partial u} + \delta^{\nu}\frac{\partial}{\partial \lambda} \right)^2 G_u(u_\circ + \theta_2\varepsilon^{\nu}, \lambda_\circ + \zeta_2\delta^{\nu})$$

$$(3.3.8) \qquad G_\lambda^{\nu} = G_\lambda^{\circ} + \left(G_{u\lambda}^{\circ}\varepsilon^{\nu} + G_{\lambda\lambda}^{\circ}\delta^{\nu} \right) + \frac{1}{2!}\left(\varepsilon^{\nu}\frac{\partial}{\partial u} + \delta^{\nu}\frac{\partial}{\partial \lambda} \right)^2 G_\lambda(u_\circ + \theta_3\varepsilon^{\nu}, \lambda_\circ + \zeta_3\delta^{\nu})$$

for $0 < \theta_i, \zeta_i < 1$, $i = 1,2,3$. Substituting these expansions into (3.2.9)-(3.2.10) we obtain

$$(3.3.9) \qquad A^{\nu} y \equiv \left\{ G_u^{\circ} + \left[G_{uu}^{\circ}\varepsilon^{\nu} + G_{u\lambda}^{\circ}\delta^{\nu} \right] + \frac{1}{2!}\left(\varepsilon^{\nu}\frac{\partial}{\partial u} + \delta^{\nu}\frac{\partial}{\partial \lambda} \right)^2 G_u(u_\circ + \theta_2\varepsilon^{\nu}, \lambda_\circ + \zeta_2\delta^{\nu}) \right\} y$$

$$= G_\lambda^{\circ} + \left(G_{u\lambda}^{\circ}\varepsilon^{\nu} + G_{\lambda\lambda}^{\circ}\delta^{\nu} \right) + \frac{1}{2!}\left(\varepsilon^{\nu}\frac{\partial}{\partial u} + \delta^{\nu}\frac{\partial}{\partial \lambda} \right)^2 G_\lambda(u_\circ + \theta_3\varepsilon^{\nu}, \lambda_\circ + \zeta_3\delta^{\nu})$$

$$(3.3.10) \qquad A^{\nu} z = -\left\{ G^{\circ} + \left(G_u^{\circ}\varepsilon^{\nu} + G_\lambda^{\circ}\delta^{\nu} \right) + \frac{1}{2!}\left(G_{uu}^{\circ}\varepsilon^{\nu}\varepsilon^{\nu} + 2G_{u\lambda}^{\circ}\varepsilon^{\nu}\delta^{\nu} + G_{\lambda\lambda}^{\circ}\delta^{\nu}\delta^{\nu} \right) \right.$$

$$\left. + \frac{1}{3!}\left(\varepsilon^{\nu}\frac{\partial}{\partial u} + \delta^{\nu}\frac{\partial}{\partial \lambda} \right)^3 G(u_\circ + \theta_1\varepsilon^{\nu}, \lambda_\circ + \zeta_1\delta^{\nu}) \right\}$$

Assume y and z have expansions:

$$(3.3.11) \qquad y = y_\circ + \|\varepsilon^{\nu}\|_2 y_{1,1} + |\delta^{\nu}| y_{1,2} + O(\mu^{\nu 2})$$

$$(3.3.12) \qquad z = \|\varepsilon^{\nu}\|_2 z_{11} + |\delta^{\nu}| z_{1,2} + \|\varepsilon^{\nu}\|_2^2 z_{211} +$$

$$+ \|\varepsilon^{\nu}\|_2 |\delta^{\nu}| z_{212} + |\delta^{\nu}|^2 z_{222} + O(\mu^{\nu})^3$$

Here we have assumed the remainder terms are bounded. For example,

$$\| G_{uu}(u_0+\theta_2\varepsilon^\nu, \lambda_0+s_2\delta^\nu)\,\varepsilon^\nu\varepsilon^\nu \|_2 = O(\mu^{\nu 2})$$

$$\| G_{\lambda\lambda u}(u_0+\theta_3\varepsilon^\nu, \lambda_0+s_3\delta^\nu)\,\delta^\nu\varepsilon^\nu \|_2 = O(\mu^{\nu 2})$$

The solution to (3.3.9) can be obtained by solving successively for y_0, (y_{11}, y_{12}). At a regular point:

$$(3.3.13)\quad y = -u_\lambda + G_u^{\circ -1}\left\{G_{u\lambda}\varepsilon^\nu + G_{\lambda\lambda}\delta^\nu + G^\circ_{uu}\varepsilon^\nu u_\lambda + G^\circ_{u\lambda}\delta^\nu u_\lambda\right\} + O(\mu^{\nu 2})$$

Similarly the solution to (3.3.10) is given by

$$(3.3.14)\quad z = -(\varepsilon^\nu - u_\lambda\delta^\nu) + \frac{1}{2!}G_u^{\circ -1}\left\{G^\circ_{uu}\varepsilon^\nu\varepsilon^\nu + 2G^\circ_{u\lambda}\varepsilon^\nu\delta^\nu + G^\circ_{\lambda\lambda}\delta^\nu\delta^\nu\right\} + O(\mu^{\nu 3})$$

The normalization equation N of (3.2.2) and its partial derivatives with respect to u and λ can be written as

$$(3.3.15)\quad \begin{aligned} N^\nu &\equiv \theta\, u_s(s_0)^*\, u^\nu(s) + (1-\theta)\,\lambda_s(s_0)\,\lambda^\nu(s) - c_1 \\ &= \theta\, u_s(s_0)^*\,\varepsilon^\nu + (1-\theta)\,\lambda_s(s_0)\,\delta^\nu \\ &= 0 \end{aligned}$$

$$(3.3.16)\quad N_u^\nu = u_s(s_0)^*$$

$$N_\lambda^\nu = \lambda_s(s_0) \tag{3.3.17}$$

where c_1 is given by

$$c_1 = \theta u_s(s_0)^* u(s_0) + (1-\theta)\lambda_s(s_0)\lambda(s_0) + (s - s_0)$$

Using (3.3.13)-(3.3.17) the solutions $(\delta u^\nu, \delta\lambda^\nu)$ in the 'backward substitution' (3.2.11)-(3.2.12) can be written

$$\delta\lambda^\nu = \frac{-\left\{\theta u_s(s_0)^* \varepsilon^\nu + (1-\theta)\lambda_s(s_0)\delta^\nu\right\} + \theta u_s(s_0)^* \left\{\varepsilon^\nu - \delta^\nu u_\lambda - \frac{1}{2} G_{uu}^{\circ -1}\left[G_{uu}^\circ \varepsilon^\nu \varepsilon^\nu + 2G_{u\lambda}^\circ \varepsilon^\nu \delta^\nu + G_{\lambda\lambda}^\circ \delta^\nu \delta^\nu\right] + O(\mu^\nu)^3\right\}}{(1-\theta)\lambda_s(s_0) - \theta u_s(s_0)^* \left\{-u_\lambda + G_{uu}^{\circ -1}\left[G_{u\lambda}^\circ \varepsilon^\nu + G_{uu}^\circ \varepsilon^\nu u_\lambda + G_{\lambda\lambda}^\circ \delta^\nu + G_{u\lambda}^\circ \delta^\nu u_\lambda + O(\mu^\nu)^2\right]\right\}}$$

$$= \frac{-\delta^\nu\left\{(1-\theta)\lambda_s(s_0) + \theta u_s(s_0)^* u_\lambda(s)\right\} + K_1^\nu \mu^{\nu 2}}{(1-\theta)\lambda_s(s_0) + \theta u_s(s_0)^* u_\lambda(s) + K_2^\nu \mu^\nu}$$

where K_1^ν and K_2^ν are constants. For sufficiently small $\delta s \equiv (s - s_0)$, $(1-\theta)\lambda_s(s_0) + \theta\lambda_s(s_0)u_\lambda(s_0)u_\lambda(s)$ is nonzero. Hence

$$\delta\lambda^\nu = -\delta^\nu + K_3^\nu \mu^{\nu 2} \tag{3.3.18}$$

where K_3^ν is a constant. Substituting (3.3.18) into (3.2.12) and using the derived solutions for y and z, we obtain

$$\delta u^\nu = (-\varepsilon^\nu + \delta^\nu u_\lambda + f_1) - \left\{-\delta^\nu + K_3 \mu^{\nu 2}\right\}(-u_\lambda + f_2/\mu^\nu) \tag{3.3.19}$$

$$= -\varepsilon^\nu + f_3$$

where $\|f_j\| = O(\mu^\nu)^2$, for $j = 1,2,3$. This completes the proof for regular solution points.

We next consider normal limit points. Recall at a normal limit point $G_u^\circ \equiv G_u(u_\circ, \lambda_\circ)$ is singular, and

$$G_\lambda^\circ \notin R(G_u^\circ)$$

Because G_λ is not in the range, there is no solution to the linear system

$$G_u^\circ \, y = G_\lambda$$

However, we note that in algebraic eigenvalue problems inverse iteration is often used to compute the eigenvector corresponding to a simple eigenvalue. Specifically let σ be a simple eigenvalue of

$$(A - \sigma I)\, x = 0$$

To determine its eigenvector we solve iteratively

$$(A - \sigma I)\, x_\nu = x_{\nu-1}$$

with x_0 an initial guess not in the range of $(A - \sigma I)$ (Issacson and Keller [9]). We now proceed to show the solution of (3.3.9) at a normal limit point is equivalent to one step of inverse iteration. That is, $y = x_1$, for $\sigma = 0$, $A = G_u^0$ and $x_0 = G_\lambda$.

The assumption that Newton's method converges implies that at every iteration the Jacobian matrix G_u^ν is non-singular (Theorem 3.1). Using some form of pivoting strategy, the LU-decomposition of G_u^ν can be put into the form

$$P^\nu G_u^\nu Q^\nu \equiv L^\nu U^\nu = \begin{bmatrix} L_{n-1,n-1}^\nu & 0 \\ L_{1,n-1}^\nu & 1 \end{bmatrix} \begin{bmatrix} U_{n-1,n-1}^\nu & U_{n-1,1} \\ 0 & s^\nu \end{bmatrix} \tag{3.3.20}$$

where $L_{n-1,n-1}^\nu$ and $U_{n-1,n-1}^\nu$ are nonsingular lower and upper triangular matrices respectively, and s^ν is small in absolute value. As Newton's method converges, s^ν goes arbitrary close to zero: The Taylor series of G_u^ν is given by

$$\begin{aligned} G_u^\nu &= G_u^0 + G_{uu}^0 \varepsilon^\nu + G_{u\lambda}^0 \delta^\nu + O(\mu^\nu)^2 \\ &= P^{-1} L^0 U^0 Q^{-1} + \mu^\nu B \end{aligned}$$

where $\|B\| = O(1)$. For clarity of presentation, we only

consider U^ν and U°:

$$\begin{bmatrix} U^\nu_{n-1,n-1} & U^\nu_{n-1,1} \\ 0 & S^\nu \end{bmatrix} = \begin{bmatrix} U^\circ_{n-1,n-1} & U^\circ_{n-1,1} \\ 0 & 0 \end{bmatrix} + \mu^\nu \tilde{B}$$

where $\|\tilde{B}\| = O(1)$. The eigenvalues of U^ν are given by the solution of

$$\det\left(\lambda I_{n-1} - U^\nu_{n-1,n-1}\right)(\lambda - S^\nu) = 0$$

Since zero is a simple eigenvalue of U°, we have from analytic perturbation theory of simple eigenvalues (Lancaster [15]),

$$S^\nu = K\mu^\nu \tag{3.3.21}$$

for some positive constant K . This proves the determinant of the Jacobian matrix or the smallest eigenvalue goes to zero as $\mu^\nu \to 0$. The solution to (3.3.9) can be computed as follows

$$L^\nu_{n-1,n-1}\begin{bmatrix} z_{n-1} \\ d \end{bmatrix} = \begin{bmatrix} G_{\lambda,n-1} \\ G_{\lambda,1} \end{bmatrix} \tag{3.3.22}$$

$$U^\nu_{n-1,n-1}\begin{bmatrix} y_{o,n-1} \\ y_{o,1} \end{bmatrix} = \begin{bmatrix} z_{n-1} \\ d \end{bmatrix} \tag{3.3.23}$$

(3.3.22) has solution

$$z_{n-1} = (L^{\nu}_{n-1,n-1})^{-1} G_{\lambda,n-1}$$

$$d = G_{\lambda,1} - L^{\nu}_{1,n-1} z_{n-1}$$

Because G_{λ} is not in the range of G_{u}, d is different from zero. (3.3.23) has solution

$$y_0 = \frac{d}{s^{\nu}} \varphi_1^{\nu} + \begin{pmatrix} (U^{\nu}_{n-1,n-1})^{-1} z_{n-1} \\ 0 \end{pmatrix}$$

where we write

(3.3.24)
$$\varphi_1^{\nu} \equiv \begin{pmatrix} -(U^{\nu}_{n-1,n-1})^{-1} U_{n-1,1} \\ 1 \end{pmatrix}$$

φ_1^{ν} is the approximation to the right eigenvector φ_1 at the ν-th iteration, and it is the solution of

(3.3.25a)
$$\begin{bmatrix} U^{\nu}_{n-1,n-1} & U^{\nu}_{n-1,1} \\ 0 & s^{\nu} \end{bmatrix} \begin{pmatrix} \varphi^{\nu}_{1,n-1} \\ 1 \end{pmatrix} = \begin{pmatrix} 0 \\ s^{\nu} \end{pmatrix}$$

Define the error for the right eigenvector e^{ν}

$$e^{\nu} = \varphi_1^{\nu} - \varphi_1 = \begin{pmatrix} e^{\nu}_{n-1} \\ 0 \end{pmatrix}$$

where φ_1 satisfies

$$(3.3.25b)\qquad \begin{bmatrix} U^{\circ}_{n-1,n-1} & U^{\circ}_{n-1,1} \\ 0 & 0 \end{bmatrix} \begin{bmatrix} \varphi_{1,n-1} \\ 1 \end{bmatrix} = \begin{bmatrix} 0 \\ 0 \end{bmatrix}$$

Subtracting (3.3.25a) from (3.3.25b), we obtain the equation for e^{ν}:

$$U^{\circ}_{n-1,n-1}\, e^{\nu}_{n-1} = O(\mu^{\nu})$$

This gives $\|e^{\nu}\| = O(\mu^{\nu})$. We now can write down the solution y of (3.2.9) for a normal limit point

$$(3.3.26)\qquad y = \frac{d}{s^{\nu}} \varphi_1 + O(1)$$

Next we solve z of (3.2.10) for a normal limit point. We write

$$(3.3.27)\qquad z = u + w$$

where u, w are solutions of

$$(3.3.28a)\qquad G^{\nu}_{u}\, u = -G^{\circ}_{\lambda}\, \delta^{\nu}$$

$$(3.3.28b)\qquad G^{\nu}_{u}\, w = -G^{\circ}_{u}\varepsilon^{\nu} - \frac{1}{2!}\left\{ G^{\circ}_{uu}\varepsilon^{\nu}\varepsilon^{\nu} + 2G^{\circ}_{u\lambda}\varepsilon^{\nu}\delta^{\nu} + G^{\circ}_{\lambda\lambda}\delta^{\nu}\delta^{\nu} \right\} + O(\mu^{\nu})^{3}$$

Equation (3.3.28a) has been analysed above. That is, using the analysis for the equation (3.3.9) we have

$$u = -\delta^{\nu} y_0 + \text{smaller terms} \tag{3.3.29}$$

The solution of (3.3.28b) is a little more involved. Using the notations in Theorem 3.1, any vector $x \in \mathbb{R}^n$ can be written uniquely

$$x = x_R \oplus x_N \tag{3.3.30}$$

where $x_R \in X_1$, $x_N \in N_1$, $N_1 \oplus X_1 = \mathbb{R}^n$. In addition, if $v(= v_R \oplus v_N) \in \mathbb{R}^n$

$$\begin{aligned} & G_u^{\circ} x_R \in X_1 \\ & G_{uu}^{\circ} x_R v \in X_1 \\ & G_{uu}^{\circ} x_N v_N \in N_1 \end{aligned} \tag{3.3.31}$$

Thus w_N, w_R satisfy

$$\begin{aligned} &\left\{ G_u^{\circ} + G_{uu}\varepsilon_N^{\nu} + P_{N_1}\left(G_{u\lambda}^{\circ}\delta^{\nu} + \tfrac{1}{2}\left(\varepsilon^{\nu}\tfrac{\partial}{\partial u} + \delta^{\nu}\tfrac{\partial}{\partial\lambda}\right)^2 G_u(u_0+\theta_2\varepsilon^{\nu}, \lambda_0+s_2\delta^{\nu})\right)\right\} w_N \\ &= -\tfrac{1}{2} G_{uu}\varepsilon_N^{\nu}\varepsilon_N^{\nu} - \tfrac{1}{2} P_{N_1}\left(2 G_{u\lambda}^{\circ}\delta^{\nu}\varepsilon^{\nu} + G_{\lambda\lambda}^{\circ}\delta^{\nu}\delta^{\nu} + \tfrac{1}{3}\left(\varepsilon^{\nu}\tfrac{\partial}{\partial u} + \delta^{\nu}\tfrac{\partial}{\partial\lambda}\right)^3 G(u_0+\theta_1\varepsilon^{\nu}, \lambda_0+s_2\delta^{\nu})\right) \end{aligned} \tag{3.3.32}$$

$$\left\{G_u^\circ + G_{uu}\varepsilon^\nu + P_{X_1}\left(G_{u\lambda}^\circ\delta^\nu + \tfrac{1}{2}\left(\varepsilon^\nu\tfrac{\partial}{\partial u} + \delta^\nu\tfrac{\partial}{\partial\lambda}\right)^2 G_u(u_0+\theta_2\varepsilon^\nu, \lambda_0+s_2\delta^\nu)\right)\right\} w_R$$

(3.3.33)

$$= -G_u^\circ \varepsilon_R^\nu - \tfrac{1}{2!}P_{X_1}\left[2G_{u\lambda}^\circ\delta^\nu\varepsilon^\nu + G_{\lambda\lambda}^\circ\delta^\nu\delta^\nu + \tfrac{1}{3}\left(\varepsilon^\nu\tfrac{\partial}{\partial u} + \delta^\nu\tfrac{\partial}{\partial\lambda}\right)^3 G(u_0+\theta_1\varepsilon^\nu, \lambda_0+s_1\delta^\nu)\right)$$

$$- \tfrac{1}{2}G_{uu}\varepsilon^\nu\varepsilon_R^\nu$$

We now use expansions similar to (3.3.11) for w_R

(3.3.34) $$w_R = -\varepsilon_R^\nu + \|\varepsilon^\nu\|_2^2 w_{1,11} + \|\varepsilon^\nu\|_2|\delta^\nu| w_{1,12} + |\delta^\nu|^2 w + O(\mu^\nu)^3$$

where $\|w_{ijk}\| = O(1)$. The solution for w can be calculated

(3.3.35) $$w_R = -\varepsilon_R^\nu - \tfrac{1}{2}G_u^{\circ -1}\left[G_{uu}\varepsilon^\nu\varepsilon_R^\nu + 2P_{X_1}\left[2G_{u\lambda}^\circ\delta^\nu\varepsilon^\nu + G_{\lambda\lambda}\delta^\nu\delta^\nu\right]\right]$$

$$- G_{uu}\varepsilon^\nu\varepsilon_R^\nu + O(\mu^\nu)^3$$

(3.3.36) $$w_N = -\frac{\varepsilon_N^\nu}{2} + a_1^\nu\varphi_1\mu^\nu + O(\mu^\nu)^2$$

Knowing these solutions, we can now determine $\delta\lambda^\nu$ and δu^ν of (3.2.11)-(3.2.12) for a normal limit point

$$\delta\lambda^\nu = \frac{-\left[\theta u_s(s_0)^*\varepsilon^\nu + (1-\theta)\lambda_s(s_0)\delta^\nu\right] + \theta u_s^*(s_0)\left\{\varepsilon^\nu + \delta^\nu\frac{d\varphi_1}{s^\nu} - (a_1^\nu+\tfrac{1}{2})\varphi_1\mu^\nu + O(\mu^\nu)^2\right\}}{(1-\theta)\lambda_s(s_0) - \theta u_s(s_0)^*\left[\frac{d\varphi_1}{s^\nu} + O(1)\right]}$$

$$= -\delta^\nu + s^\nu\mu^\nu\left\{\frac{(a_1^\nu+\tfrac{1}{2})\theta u_s(s_0)^*\varphi_1 + O(\mu^\nu)}{d\theta u_s(s_0)^*\varphi_1 - (1-\theta)s^\nu\lambda_s(s_0) + O(s^\nu)}\right\}$$

Using (3.3.21) we have

$$\delta\lambda^\nu = -\delta^\nu + K_4^\nu\mu^{\nu 2}$$

and

$$\delta u^\nu = \left\{ -\varepsilon^\nu + f_7 + (a_1^\nu + \tfrac{1}{2})\varphi_1 \mu^\nu - \delta^\nu \frac{d\varphi_1}{s^\nu} \right\} - \left\{ \delta^\nu + s^\nu \mu^\nu \left[\frac{(a_1^\nu + \frac{1}{2})\theta u_s(s_0)^* \varphi_1 \mu^\nu + O(\mu^\nu)^2}{\theta u_s(s_0)^* d\varphi_1} \right] \right\} \frac{d\varphi_1}{s^\nu} + O(\mu^\nu)^3$$

$$= -\varepsilon^\nu + f_7 + O(\mu^\nu)^3$$

where $\|f_7\| = O(\mu^\nu)^2$. This proves quadratic convergence and part (1) of the lemma.

At a simple bifurcation point, $G_\lambda^\circ \in R(G_u^\circ)$. The solution to (3.2.9) becomes

$$y = -u_\lambda + f_8$$

where $\|f_8\| = O(\mu^\nu)$. The solution to (3.2.10) at a simple bifurcation point is similar to that for a normal limit point, except y in (3.3.28) is being replaced by $-u_\lambda$.

$\delta\lambda^\nu$, δu^ν of (3.2.11)-(3.2.12) at a simple bifurcation point become

$$\delta\lambda^\nu = \frac{-\theta u_s(s_0)^* \varepsilon^\nu - (1-\theta)\lambda_s(s_0)\delta^\nu - \theta u_s(s_0)^* [-\varepsilon^\nu + \delta^\nu u_\lambda + w_N + w_R]}{(1-\theta)\lambda_s(s_0) - \theta u_s(s_0)^* [-u_\lambda + f_8 + O(\mu^\nu)^2]}$$

$$= -\delta^\nu + \frac{\theta u_s(s_0)^* [-w_N - w_R]}{(1-\theta)\lambda_s(s_0) + \theta u_s(s_0)^* u_\lambda(s) + c_7}$$

$$= -\delta^\nu + \gamma^\nu$$

where c_7, γ^ν are $O(\mu^\nu)$.

$$\delta u^\nu = -\varepsilon^\nu + \delta^\nu u_\lambda + w_N + w_R - (\delta^\nu - \gamma^\nu) u_\lambda$$

$$= -\varepsilon^\nu + w_N + w_R + \gamma^\nu u_\lambda$$

here $(w_N + w_R - \eta^{\nu} u_{\lambda})$ is $O(\mu^{\nu})$. The proof of Lemma 3.2 is now completed.

Normal limit points and simple bifurcation points are both singular points at which the operator $G_u^{\bullet}$ is singular. Yet using the s-algorithm, we saw Newton's method converges quadratically for normal limit points and linearly for bifurcation points. However this should be no surprise because of the necessary and sufficient conditions of Lemma 2.3. By 'inflating' the system for normal limit points we have constructed a projection operator which projects to zero the part of the error between Newton iterations that only vanishes linearly. This recovers the quadratic convergence. This result can be extended to solutions of general nonlinear systems of equations with the Jacobian having nontrivial null spaces.

Theorem 3.3 Using the same notations as in Theorem 3.1 for a finite dimensional system, the following iteration procedure will recover quadratic convergence

$$F_x(x^\nu)\ z = -F(x^\nu)$$

$$F_x(x^\nu)\ \varphi_1^\nu = b^\nu \tag{3.3.37}$$

$$F_x^*(x^\nu)\ \psi_1^\nu = d^\nu$$

$$\delta x^\nu = z + \frac{\psi_1^{\nu *} z}{\psi_1^{\nu *} \varphi_1^\nu} \varphi^\nu \equiv z - c^\nu \tag{3.3.38}$$

$$x^{\nu+1} = x^\nu + \delta x^\nu$$

where b^ν, d^ν are to be constructed such that they do not lie in the range of F_x and F_x^* respectively. For example, let us consider b^ν. Assume the Jacobian F_x is factorized into LU-form

$$P F_x Q = LU$$

where P and Q are permutation matrices, L is a nonsingular lower triangular matrix and U is a upper triangular matrix with its diagonal elements satisfying the following

$$|u_{nn}| << 1$$

$$|u_{nn}| << |u_{kk}| \qquad n > k$$

then b^ν is given by

$$b^\nu = \left\{P^{-1}(0, \ldots\ldots, 0, 1)\right\}^T$$

(We note this is in agreement with (3.3.23) of Lemma 3.2.)

Remarks on Theorem 3.3

(1) The correction term c^{ν} is the projection of z of (3.3.37) onto the null space of $F_x(x^*)$. This in essence is equivalent to the corrected Newton process of Rall (1966, [26]). However in actual computations, he did not compute the projection operator.

(2) For simple bifurcation points, let Φ_1 and Ψ_1 be the null vector and its adjoint of the inflated matrix. The procedure defined in Theorem 3.3 implies quadratic convergence for the inflated system.

(4) For higher dimensional null spaces, Theorem 3.3 can be extended by computing all the independent null vectors and their adjoint, φ_1, φ_2, ...; and Ψ_1, Ψ_2, ... This is equivalent to inflating the original problem by additional M equations for M-dimensional parameter vector problems, that is, M-multiple normal limit points.

Proof of Theorem 3.3 Vectors b^{ν}, d^{ν} are to be constructed such that they do not lie in the range of $F_x(x^*)$ and $F_x^*(x^*)$ respectively. The solutions of equations (3.3.37) can be written down (using the equations (3.3.35)-(3.3.36) and (3.3.26) in Lemma 3.2)

$$(3.3.39) \qquad z = -\varepsilon_R^{\nu} - \frac{\varepsilon_N^{\nu}}{z} + \eta^{\nu}$$

$$\varphi_1^{\nu} = \varphi_1 + \delta^{\nu} f_1 \tag{3.3.40}$$

$$\psi_1^{\nu} = \psi_1 + \delta^{\nu} f_2 \tag{3.3.41}$$

where φ_1 and ψ_1 are normalized, that is $\psi_1^* \varphi_1 = 1$ and $\| x^{\nu} - x^* \| \equiv \| \epsilon^{\nu} \|_2 \equiv \delta^{\nu}$, $\delta^{\nu} = O(\delta^{\nu})$, $\| \eta^{\nu} \|_2 = O(\delta^{\nu 2})$, and $\| f_1 \|_2$ and $\| f_2 \|_2$ are $O(1)$. Substituting (3.3.39)-(3.3.41) into (3.3.38) we obtain

$$\delta x^{\nu} = \left(-\epsilon_R^{\nu} - \frac{\epsilon_N^{\nu}}{2} + \eta^{\nu} \right) + \frac{(\psi_1^* + \delta^{\nu} f_2^*)\left(-\epsilon_R^{\nu} - \frac{\epsilon_N^{\nu}}{2} + \eta^{\nu}\right)(\varphi_1 + \delta^{\nu} f_1)}{(\psi_1^* + \delta^{\nu} f_2^*)(\varphi_1 + \delta^{\nu} f_1)}$$

$$= -\epsilon^{\nu} + f_3 \delta^{\nu 2}$$

where $\| f_3 \|_2 = O(1)$. This completes the proof of Theorem 3.3.

3.4 NUMERICAL TREATMENT AT SIMPLE BIFURCATION POINT

In this section we give a treatment at simple bifurcation point and the switching of branches. An efficient method to compute the coefficients (2.1.13) of the algebraic bifurcation equation is provided. This is also applicable to multiple bifurcation points as well as general nonlinear two point boundary value problems for ordinary differential equations with one or more parameters.

If s is the pseudo-arclength parameter (see Section 2 of Chapter 2), let $Det_h(s)$ be the determinant of the converged discretized Jacobian along a smooth branch. (We drop the subscript h.) We assume there exists $s_b > s_a$ such that $Det(s_a)Det(s_b) < 0$. That is, the determinant has gone through a change in sign. The critical point $(u(s_o), \lambda(s_o))$ at which the converged discretized Jacobian is arbitrary close to zero can be located by 'modified' bisection or 'modified' regular falsi. That is, special treatment has to be taken because the normalization equation depends on the arc-length parameter s. To be more specific, let δs_{ab} be the increment we take to go from s_a to s_b. The derivatives (u_s , λ_s) in (3.2.2) are different at the two arclength stations $s = s_a$ and $s = s_b$. If we want to approximately go back to s_a from s_b, we need to determine δs_{ba}. Taylor series of $\lambda(s)$ about s_a and s_b:

$$\lambda(s_b) = \lambda(s_a) + \delta s_{ab}\,\lambda_s(s_a) + O(\delta s_{ab})^2$$

$$\lambda(s_a) = \lambda(s_b) + \delta s_{ba}\,\lambda_s(s_b) + O(\delta s_{ba})^2$$

Solving for δs_{ba}

$$\delta s_{ba} = -\delta s_{ab}\left(\frac{\lambda_s(s_a)}{\lambda_s(s_b)}\right)$$

Thus to $O(\delta s_{ab}^2)$, δs_{ab} is equal to δs_{ba} if and only if

$$\lambda_s(s_a) = \lambda_s(s_b).$$

The next step is to compute the null vector φ_1 and its adjoint ψ_1 of the approximate singular Jacobian G_u^o. This can easily be accomplished by inverse iteration discussed in last section. Keller [14] observed the computations of all the independent eigenvectors and their adjoint can be obtained trivially from the LU-factorization of the discretized Jacobian: Let Φ, Ψ be N x m matrices containing m columns of independent null vectors and their adjoint respectively. Then

$$\Phi = \begin{bmatrix} -(U_{N-m,N-m})^{-1} U_{N-m,m} \\ I_{m\times m} \end{bmatrix}$$

$$\Psi = \left[-L_{m,N-m} (L_{N-m,N-m})^{-1} \quad I_{m\times m} \right]^*$$

At the bifurcation point, $\lambda_s(s_o)$ cannot be zero for both branches (non-tangential intersection property of Definition 2.2), we look for bifurcation only if

$$\psi_1^* G_\lambda = 0 \tag{3.4.1}$$

If the test for bifurcation (3.4.1) is positive, we next solve the algebraic bifurcation equation and switch branches. At a simple bifurcation point $G_\lambda^\circ \in G_u^\circ$, let $\hat{\varphi}_o$ be a solution to

$$G_u^\circ \hat{\varphi}_o = - G_\lambda^\circ$$

But G_u° is singular, $\hat{\varphi}_o$ can be made unique by requiring it has no component in the null space of G_u°. This can easily be done

$$\varphi_o = \hat{\varphi}_o - \psi_1^* \hat{\varphi}_o \varphi_1$$

The vector φ_o so constructed satisfies

$$\psi_1^* \varphi_o = 0$$

(If the critical point is a simple bifurcation point the null space of G_u° is one dimensional. Using some form of pivoting strategy, G_u° has the LU-factorization that was discussed in Theorem 3.3. Thus, in our computations we can check the dimension of $N(G_u^\circ)$ by printing out the diagonal elements of U.)

In a small neighbourhood of the simple bifurcation point we have the expansions (2.1.16)

$$
\begin{aligned}
u_{\pm}(s_0+\delta s) &= u(s_0) + \delta s\, u_{s\pm}(s_0) + O(\delta s)^2 \\
\lambda_{\pm}(s_0+\delta s) &= u(s_0) + \delta s\, \alpha_{0\pm} + O(\delta s)^2
\end{aligned}
\tag{3.4.2}
$$

$$
u_{s\pm}(s_0) = \alpha_{0\pm}\varphi_0 + \alpha_{1\pm}\varphi_1 \tag{3.4.3}
$$

where $(\alpha_{0\pm}, \alpha_{1\pm})$ are the distinct roots of the algebraic bifurcation equation. To switch branches, we must solve for these roots.

For very general nonlinear eigenvalue problems (may it be algebraic equations, integral equations, ordinary differential equations or partial differential equations) Keller [13] has suggested four different approaches for the computation of bifurcated branches. In one of these, the first method, the coefficients of the algebraic bifurcation equation must be computed. These are, we recall:

$$
\begin{aligned}
a &= \psi_1^* G^0_{uu} \varphi_1 \varphi_1 \\
b &= \psi_1^* (G^0_{uu}\varphi_0 + G^0_{u\lambda})\varphi_1 \\
c &= \psi_1^* (G^0_{uu}\varphi_0\varphi_0 + G^0_{u\lambda}\varphi_0 + G^0_{\lambda\lambda})
\end{aligned}
\tag{3.4.4}
$$

We focus our attention on his first approach in application to nonlinear two-point boundary value problems for ordinary differential equations. Though all finite element and finite difference schemes give similar results, we derive our equations using the Jacobian matrix obtained from the centered-Euler scheme. We note the scalars a, b and c in (3.4.4) involve computations of vectors of the form (a) $G^{\circ}_{\lambda\lambda}$, (b) $G^{\circ}_{u\lambda}\, v$, and (c) $G^{\circ}_{uu}\, vw$, where v and w are vectors which are not functions of u or λ.

We have no problems with (a) and (b). The derivative u_x on the left hand side of (3.1.1) does not depend on λ, giving

$$(3.4.5)\qquad G^{\circ}_{\lambda\lambda} = \begin{bmatrix} \frac{\partial^2 g_1}{\partial\lambda^2}(u_1^{\circ},\lambda^{\circ}) \\ \frac{\partial^2 f}{\partial\lambda^2}(x_{1\frac{1}{2}},\frac{1}{2}(u_1^{\circ}+u_2^{\circ});\lambda^{\circ}) \\ \frac{\partial^2 f}{\partial\lambda^2}(x_{2\frac{1}{2}},\frac{1}{2}(u_2^{\circ}+u_3^{\circ});\lambda^{\circ}) \\ \vdots \\ \frac{\partial^2 f}{\partial\lambda^2}(x_{J-\frac{1}{2}},\frac{1}{2}(u_{J-1}^{\circ}+u_J^{\circ});\lambda^{\circ}) \\ \frac{\partial^2 g_2}{\partial\lambda^2}(u_J^{\circ},\lambda^{\circ}) \end{bmatrix} \quad ; \quad G^{\circ}_{u\lambda}\, v = \frac{\partial A^{\circ}}{\partial\lambda}\, v$$

To determine (c) we proceed in two steps:

$$(i)\qquad H = G^{\circ}_{u}\, v$$

(ii) $\alpha = H_u w$

From (3.1.6) H can be written

$$H = \mathbb{A}^{\circ} v$$

The vector v does not explicitly depend on the solution u of (3.1.4). The derivative u_x is linear in u and hence gives no contribution to G°_{uu}. Hence

$$\alpha \equiv (\alpha_j) = \begin{bmatrix} \frac{\partial^2 g_1}{\partial u(a)^2}(u_1^{\circ}, \lambda^{\circ})\, v_1 w_1 \\ -\frac{\partial^2 f}{\partial u^2}\left(x_{1/2}, \frac{1}{2}(u_1^{\circ}+u_2^{\circ}); \lambda^{\circ}\right)\left(\frac{v_1+v_2}{2}\right)\left(\frac{w_1+w_2}{2}\right) \\ \vdots \\ -\frac{\partial^2 f}{\partial u^2}\left(x_{J-1/2}, \frac{1}{2}(u_J^{\circ}+u_{J-1}^{\circ}); \lambda^{\circ}\right)\left(\frac{v_J+v_{J-1}}{2}\right)\left(\frac{w_J+w_{J-1}}{2}\right) \\ \frac{\partial^2 g_2}{\partial u(b)^2}(u_J^{\circ}, \lambda^{\circ})\, v_J w_J \end{bmatrix}$$

Component-wise, for any $x_j \in (a,b]$, the k-th component of α_j is

$$\alpha_{j,k} = \sum_{\ell,m} \frac{\partial^2 f_k}{\partial u_\ell \partial u_m}\left(x_{j-1/2}, \tfrac{1}{2}(u_j^{\circ}+u_{j-1}^{\circ}); \lambda^{\circ}\right)\left\{\frac{v_{j-1,\ell}+v_{j,\ell}}{2}\right\}\left\{\frac{w_{j-1,\ell}+w_{j,\ell}}{2}\right\}$$

where the second subscript of $v_{j-1,\ell}$ (or $w_{j-1,\ell}$) denotes the l-th component of the vector v_{j-1} (or w_{j-1}) at the net point x_{j-1} and the derivative

$$\frac{\partial f_k}{\partial u_\ell}$$

denotes the differentiation of the k-th component of f with respect to the l-th component of u. At the boundary points

$$\alpha_{a,K} = \sum_{\ell,m} \frac{\partial^2 g_{1,K}}{\partial u(a)_\ell \, \partial u(a)_m} v_{i,\ell} \, w_{i,m}$$

$$\alpha_{b,K} = \sum_{\ell,m} \frac{\partial^2 g_{2,K}}{\partial u(b)_\ell \, \partial u(b)_m} v_{J,\ell} \, w_{J,m}$$

To obtain the coefficients a, b and c in (3.4.4), we need to form the inner product Ψ_i^* with $G^{\circ}_{uu} vw$, say. Let p be the number of left boundary conditions of (3.1.1)-(3.1.2). We write

$$K = K_{B.C} + K_i$$

where $K_{B.C.}$ and K_i are contributions from boundary points and internal points respectively. They can easily be seen to be

$$K_{B.C} = \sum_{1}^{P} \Psi_{i,\ell} \alpha_{a,\ell} + \sum_{P+1}^{n} \Psi_{J,\ell} \alpha_{b,\ell-p}$$

$$K_i = \sum_{\ell=2}^{J} \left\{ \sum_{K=p+1}^{n} h_{\ell-1} \Psi_{\ell-1,K} \alpha_{\ell,K-p} + \sum_{k=1}^{P} h_{\ell-1} \Psi_{\ell,K} \alpha_{\ell,K+n-p} \right\}$$

As the mesh size $h \to 0$, K_i tends to

$$\sum_{K=1}^{P} \int_a^b \Psi_k \alpha_{k-p+n} \, dx + \sum_{k=p+1}^{n} \int_a^b \Psi_k \alpha_{k-p} \, dx$$

For the rotating coaxial disks problem the contribution from the boundary conditions is zero, and K is given by

$$K = \sum_{\ell=2}^{J} h_{\ell-1} \left\{ \begin{array}{l} \psi_{\ell,1}\left[\left(v_{\ell-\frac{1}{2},1} w_{\ell-\frac{1}{2},4} + v_{\ell-\frac{1}{2},4} w_{\ell-\frac{1}{2},1}\right) + 4\left(v_{\ell-\frac{1}{2},5} w_{\ell-\frac{1}{2},6} + v_{\ell-\frac{1}{2},6} w_{\ell-\frac{1}{2},5}\right)\right. \\ \left. + \psi_{\ell,3}\left[\left(v_{\ell-\frac{1}{2},1} w_{\ell-\frac{1}{2},6} + v_{\ell-\frac{1}{2},6} w_{\ell-\frac{1}{2},1}\right) - \left(v_{\ell-\frac{1}{2},2} w_{\ell-\frac{1}{2},5} + v_{\ell-\frac{1}{2},5} w_{\ell-\frac{1}{2},2}\right)\right]\right\} \end{array}$$

Thus the coefficients in (3.4.4) can be obtained by various combinations of v and w, where v and w are now φ_0 and φ_1.

To check our calculations, we observe one of the roots corresponds to the tangent along the known branch. The derivative λ_s^0 should be equal to either α_{0-} or α_{0+} of the solution of the algebraic bifurcation equation. Let $(\alpha_{0+}, \alpha_{1+})$ be the root for the new bifurcated branch. To switch branches, we must change our normalization to

$$N \equiv \theta\left(\alpha_{0+}\varphi_0 + \alpha_{1+}\varphi_1\right)^*\left[u(s) - u(s_0)\right] + (1-\theta)\,\alpha_{0+}\left[\lambda(s) - \lambda(s_0)\right] - (s - s_0) = 0$$

and use the initial guess along the new branch

$$u'(s_0 + \delta s) = u(s_0) + \delta s\left(\alpha_{0+}\varphi_0 + \alpha_{1+}\varphi_1\right)$$

$$\lambda'(s_0 + \delta s) = \lambda(s_0) + \delta s\,\alpha_{0+}$$

3.5 NUMERICAL IMPLEMENTATION OF STABILITY ANALYSIS

The computational aspects of exchange of linearized stability analysis is to be studied in this section. In a small neighbourhood of a critical point for the equilibrium problem, assume the time-dependent problem has solution of the form

$$U(t) = u(s) + \epsilon e^{\sigma t} w(s) \tag{3.5.1}$$

To determine if the eigenvalue $\sigma(s)$ has gone from positive to negative (or vice versa) as we tranverse through the critical point, there are two approaches:

(1) Computation at the critical point - determine the lowest nonzero derivative. For example, from Section 2.3

$$\sigma_s(s_0) = \frac{\alpha_1 a + \alpha_0 b}{\psi_1^* B \varphi_1} \tag{3.5.2}$$

Here a and b are the coefficients of the algebraic bifurcation equation, which can be computed effortlessly (see last section), and (α_0, α_1) is a solution to the algebraic bifurcation equation. (For normal limit points α_0 is identically zero and we set α_1 to be equal to one.) If $\sigma_s(s_0)$ is zero, the next derivative can be seen to be

$$\sigma_{ss}(s_0) = \frac{2\psi_1^*\left(G_{uu}^0 w\varphi_1 + \frac{2}{3}G_{uuu}^0\varphi_1\varphi_1\varphi_1\right)}{\psi_1^* B \varphi_1} \tag{3.5.3}$$

where w satisfies

$$G_u^0 w = -G_{uu}^0 \varphi_1\varphi_1 \tag{3.5.4}$$

(The solution for w can be computed without special treatment, w is made unique by requiring $\psi_1^* w$ to be equal to zero.)

(2) Computation near the critical point - Substituting (3.5.1) into the time-dependent problem gives a linear eigenvalue problem in σ:

$$\begin{aligned} \sigma B w &= G_u(u(s),\lambda(s))\, w \\ w^* w &= 1 \end{aligned} \tag{3.5.5}$$

for $|s - s_0| < \delta$, for some small $\delta > 0$. Newton's method is used to solve (3.5.2) for (σ, w), with the initial guess $(0, \varphi_1)$. A simple change of variable yields

$$\begin{aligned} w^{\nu+1} &= \delta\sigma^\nu v^{\nu+1} \\ \left(G_u(u(s),\lambda(s)) - \sigma^\nu B\right) v^{\nu+1} &= B w^\nu \\ \delta\sigma^\nu &= \frac{1}{2 w^{\nu *} v^{\nu+1}} \end{aligned}$$

CHAPTER 4

THE COMPUTATIONAL RESULTS

In this chapter we discuss the computations of the rotating coaxial disks problem. It is divided into two sections. Section 1 describes the solution branches. Section 2 gives a detailed treatment at critical points; local exchange of linearized stability calculations are discussed.

4.1 SOLUTION BRANCHES

In this section we describe the many computed solutions using the analysis and methods of the last two chapters. All the computed solutions are second order accurate in the mesh size h. Notions of cells (Batchelor [1]) and sub-cells are introduced. In some of the solution branches, the axial and radial velocities for some positive γ are approximately the same as those for negative γ , and we explain this γ - sign-independent phenomenon using standard

singular perturbation techniques.

Let us consider the general problem (3.1.1)-(3.1.2). Assume a solution is known for some λ. In Section 3.2 we described the numerical procedure of obtaining a solution for λ_1 using Euler-Newton pseudo-arclength s-continuation. Hence we can 'continue' to trace out a solution branch for $\lambda_0 \leq \lambda \leq \lambda_1$.

In the rotating coaxial disks problem we have at our disposal to continue in one of the two parameters: the Reynolds number R or the ratio of the angular velocity of the two disks γ. All the solution branches are computed using a systematic approach; no clever initial guesses are needed. In our calculations Euler-Newton pseudo-arclength s-continuation procedure is used. When a solution at a particular R and γ is desired we switch to straight-forward Euler-Newton continuation.

Let S(f, g) be a solution to the rotating coaxial disks problem with no suction.

Definition 4.1 S(f, g) is a large amplitude solution if the outer (inviscid) solution tends to infinity in magnitude in the limit Reynolds number R tending to infinity.

Definition 4.2 S(f, g) is a finite amplitude solution if the outer (inviscid) solution is finite in magnitude in the limit Reynolds number R tending to infinity.

For R = 0 and $|\gamma| \leq 1$ we have the unique solution of (1.2.17)

$$f = 0$$
$$g = 1 + (\gamma - 1)\,\bar{z} \tag{4.1.1}$$

It is easily shown that solutions (4.1.1) are stable (Definition 2.5). From these solutions we let the Reynolds number R be the continuation parameter and use our pseudo-arclength continuation for fixed $\gamma_k = -1 + k(0.1)$, $k = 0,1,\ldots,20$. For the purpose of this discussion we stop at R = 500, and we denote these solutions by $S(\gamma_k, R = 500)$. We have the following:

(a) The determinant of the converged discretized Jacobian G_{hu} has a change in sign for $\gamma = -1$ and R between 110 and 120. This will be followed up in next section.

(b) By inspecting the solution profiles for cases $\gamma = 0$ and $\gamma = -0.1$ we suspect these two solutions belong to different branches (or families), say $\Gamma(0)$ and $\Gamma(-0.1)$. Fixing $R = 500$ we continue in γ from $\gamma = 0$ to $\gamma = -0.1$ of $\Gamma(0)$ and from $\gamma = -0.1$ to $\gamma = 0$ of $\Gamma(-0.1)$. Our suspicion is confirmed. We obtain two distinct solutions for (i) $\gamma = 0$ and $R = 500$, and (ii) $\gamma = -0.1$ and $R = 500$. Similar phenomena occur for (1) $\gamma = -0.3$ and $\gamma = -0.4$, and (2) $\gamma = -0.9$ and $\gamma = -1$. Case (1) will be treated in detail in the next section. Case (2) will be discussed later in this section. For the missing gaps in γ, (that is, $\gamma \in [0,1]$, $\gamma \in [-0.1,-0.3]$ and $\gamma \in [-0.4,-1]$), there is no abrupt change in the solution profiles. This can be confirmed by fixing $R = 500$ and continuing from $\gamma = \gamma_\alpha$ to $\gamma = \gamma_\beta$ say, and the solution so obtained for $\gamma = \gamma_\beta$ is found to be identical to $S_o(\gamma_\beta, R = 500)$. In this way we obtain four different solution branches (or families) when we continue in γ for $R = 500$. In Figure 4.1 we show the intervals (γ_a, γ_b) in which these branches have solutions for $R = 500$. The '*'-sign indicates the points $(\gamma_*, R = 500)$ where we start to continue in γ from the

solutions $S_o(\gamma_*, R = 500)$. We note that the second and fourth branches do not extend the full interval $[-1,1]$. That is, these branches turn around at the limit points, γ_{*1} and γ_{*2}.

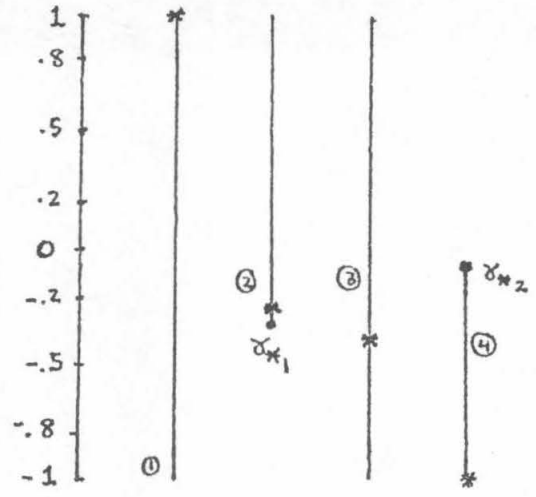

Figure 4.1

Because solutions at $R = 0$ are unique, the new branches obtained above cannot have solutions for $R(\gamma) < R_c(\gamma)$. These critical points $R_c(\gamma)$ are found to be normal limit points (Definition 2.3). Let Γ_{ab} be a solution branch for some fixed $\gamma = \gamma_o$.

$$\Gamma_{ab} = \left\{ (u(s), R(s); \gamma_o) : G(u(s), R(s); \gamma_o) = 0 \,,\; s_b \leq s \leq s_a \right\}$$

The Reynolds number is the parameter along Γ_{ab} - a similar convention is used when we fixed the Reynolds number.

We assume $s_b >> s_\alpha$. If Γ_{ab} cannot be extended to R = 0, then it must have at least one limit point. For branches (with γ = constant and which do not form closed loops) containing R = 0 have an <u>even</u> number of limit points and those <u>not</u> containing R = 0 have an <u>odd</u> number of limit points. Moreover for sufficiently large R, solution branches containing odd number of limit points have at least two distinct solutions.

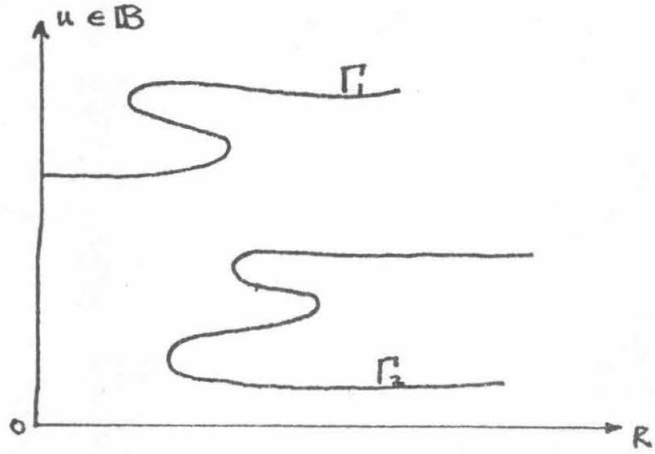

Figure 4.2: Γ_1 has two (even number) limit points
Γ_2 has three (odd number) limit points

For some $R = R_\alpha$, let the pair (f(z), g(z)) be a solution for $\gamma = 1$ of branch Γ_α satisfying: (The case for $\gamma = -1$ can be treated in a similar fashion.)

$$f(1/2) \neq 0 \quad , \text{ or}$$

$$g_z(1/2) \neq 0$$

Then Corollary 1.2 implies the solution

$$U_+ = (-f(1-z),\ g(1-z))$$

is different from (f, g). Fixing the Reynolds number at R_α we next continue in γ using the solution U_+. From Corollary 1.2 and using (1.2.26) the new computed branch $\Gamma_{U_+,\alpha}$ is different from Γ_α.

We comment on the solutions outside the strip I of (1.2.16), that is $|\gamma| > 1$, $R > 0$. For some fixed R, say $R = R_a = 1000$, we consider a solution branch Γ_a that excludes $\gamma = 0$. Assume Γ_a has a normal limit point at $\gamma = \gamma_N$. By Lemma 1.1 we see the branch for the 'reduced' Reynolds number $\mathcal{R} = R_a|\gamma_N|$ 'turns around' at $1/\gamma_N$. The computations of branches 7-10-11 is an example. (See description of branches for the numbering system.)

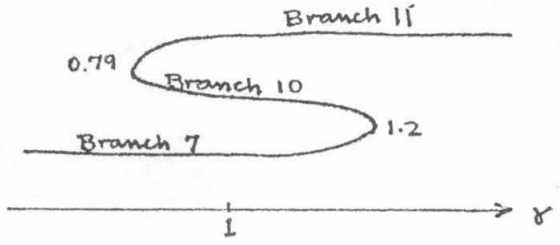

figure 4.3 : Schematic Drawing of Branch 7-10-11 at R = 1000

We observe that $0.79 \neq 1/1.2$. This is because using Lemma 1.1 the critical point $(R, \gamma) = (1000, 0.79)$ transforms

into (790, 1/0.79).

In figure 4.4 we show the loci of critical points with the number of solutions indicated. We point out these curves are only second order accurate in the mesh size h. That is, a critical point is one at which the linearized operator G_u is singular. The determinant of the discretized linearized operator has the asymptotic expansion (for the centered-Euler method)

$$\det(G_{u,h}) = \det(G_u) + h^2\alpha_1 + h^4\alpha_2 + \ldots.$$

We either gain two solutions or lose two solutions as we transverse these curves of critical points. We now give a few comments.

There is a unique solution in the region $0 \leq R \leq 55$. and $|\gamma| \leq 1$. Because the solution f at E is not antisymmetric, from Corollary 1.2 and using (1.2.26) we deduce there must be another fold meeting EβF at E. This fold turns out to be EαF. The normal limit point curve EβF is computed in the following sequence of calculations: (i) Let $\Gamma_+(\gamma)$ be a solution branch for some fixed non-negative γ and contain

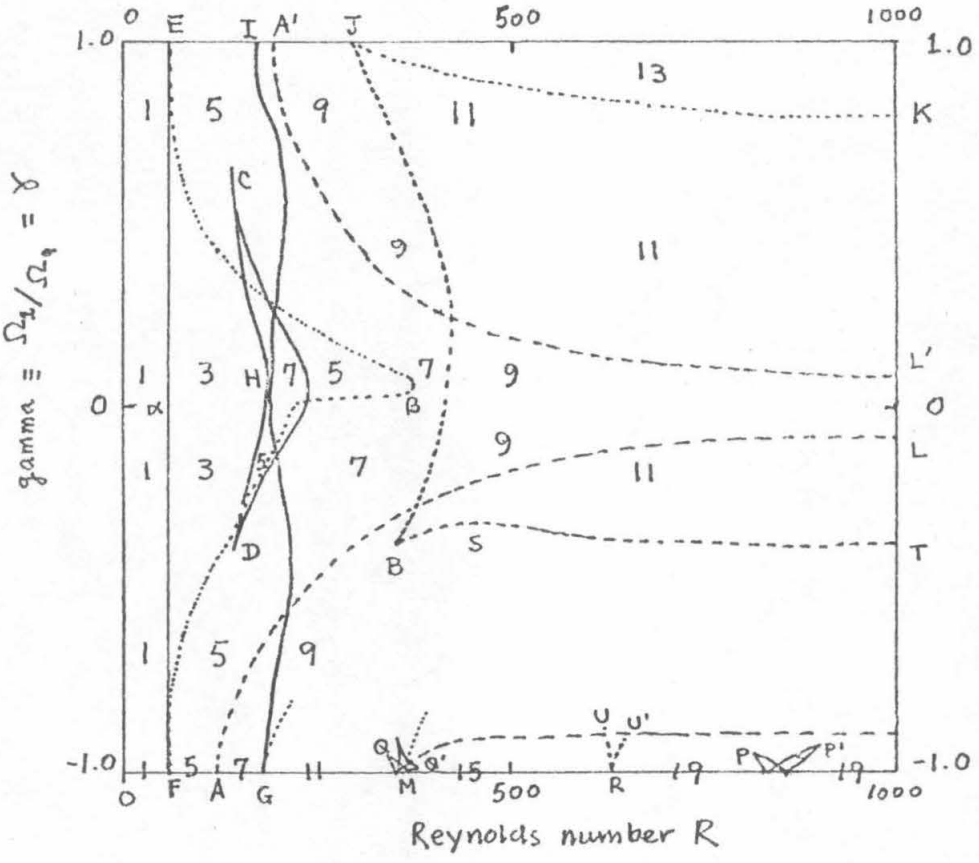

figure 4.4 Loci of Critical Points

solutions for $R \geq 0$. Let $S(\gamma = 0)$ be a solution on Γ_+ $(\gamma = 0)$ at $R = 500$. Now fix $R = 500$ and continue in γ until $\gamma = -1$. The solutions for negative γ obtained above give half of the curve $E\beta F$ when we use our pseudo arclength continuation procedure on the Reynolds number, keeping γ fixed. (ii) Let $S(\gamma = -0.1)$ be a solution on Γ_- $(\gamma = -0.1)$ at $R = 500$, where solution exists for $R \in [0, 1000]$ on Γ_-. We continue in γ until $\gamma = 1$. These new solutions give the other half of $E\beta F$ when we continue in R, keeping γ fixed. The lips CHD "belongs" to $E\alpha F$: for $\gamma \in (-0.4, 0.65)$ the solution branch Γ possesses three normal limit points (one is on $E\alpha F$ and two on the lips CHD). As we approach from the center of the lips towards the tips C, D the two normal limit points coalesce into one and then disappear as we pass the tips. The phenomenon of coalesence of normal limit points is quite common in this problem (A, B and the tips of lips P, P', Q, Q'; they are also called cusps). The normal limit point curve GHI touches the left side of the lips CHD at H. The half lips Q "belongs" to GHI, and Q "belongs" to GI' which is not shown. We have a similar phenomenon for the lips P and P' with RU and RU'. There is a little finger MN which touches the lips Q near $\gamma = -1$. Corollary 1.2 can be applied to $\gamma = -1$ solution of MN. Except for the branch that extends to $R = 0$, all the solutions discussed in this

paragraph are large amplitude solutions.

The critical point $A \equiv (R \approx 119., \gamma = -1)$ is a bifurcation point (Definition 2.2). For $\gamma = -1 + \epsilon$, $1 >> \epsilon > 0$ we obtain two solution branches b_1 and b_2. This is the classical example of bifurcation-perturbed-bifurcation, where ϵ is the "impurity". The locus of normal limit point of b_1 gives the hyperbola-shaped AL; for finite Reynolds number this perturbed-bifurcation sheet does not have a solution for $\gamma = 0$ (that is, the normal limit point $R_m(\gamma)$ tends to infinity as γ tends to zero). We next consider the branch b_2 of the perturbed-bifurcation sheet. For $-1/3 \leq \gamma < -1$, b_2 extends back to $R = 0$; there is a cusp at $B \equiv (R_c = 347.8, \gamma = -.3834)$ where b_2 begins to develop into an s-curve which extends back to $R = 0$ until $\gamma = -1/3$. For $-1/3 < \gamma \leq 1$, branch b_2 'turns around', giving the limit point curve BJ. (For future discussion, let S_{bif} denote the solution for $\gamma = 1$, $R = 1000$ by using pseudo-arclength continuation from the solution along b_2, and $S_{bif,m}$ be the solution for $\gamma = 1$, $R = 1000$ which is obtained by continuation in R of S_{bif} and it has a normal limit point at J.)

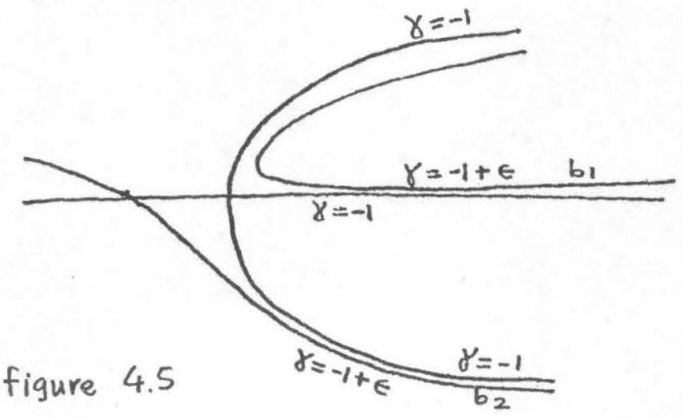

figure 4.5

For $\gamma = \gamma_r$ slightly larger than -1/3, let $\Gamma_{ridge}(\gamma_r)$ be the solution branch that extends back to R = 0. Let $S(R, \gamma)$ be a solution on Γ_{ridge}. For $R = R_r \geq 447.8$ we continue in γ and the result of the computation is amazing: this solution branch does not have solution for γ less than $\gamma_n(R)$; it 'turns back up' to join with the solution branch that contains S_{bif}. This accounts for the normal limit point curve (or ridge) ST. (The curve BST will be treated in detail in the next section.)

Corollary 1.2 is applied to $\gamma = 1$ solution at the normal limit point J and this gives the little finger JK and the hyperbola-shaped A'L'. This needs a little explanation to show how we obtain from four to six solutions for $R \gtrsim 290$ at $\gamma = 1$: Corollary 1.2 is applied to solutions S_{bif} and $S_{bif,n}$ (cf. last paragraph), yielding solutions S'_{bif} and $S'_{bif,n}$. We fixed R = 1000 and continue in γ. The branch

starting from the solution S'_{bif} does not have solution for $\gamma \leq 0.1$; it 'turns back up' to a symmetric solution $S'_{bif,s}$ at $\gamma = 1$. Similarly the branch starting from $S'_{bif,n}$ does not have solution for $\gamma \leq 0.79$ and it 'turns back up' to a symmetric solution at $\gamma = 1$. we now fix $\gamma = 1$ and continue in R for both symmetric solutions, and they meet at the normal limit point A'. Something must have happened in between - an exchange of solution branch has taken place at $(R_e, \gamma_e) = (292, .993)$. We now show schematically how this comes about. Let $\Gamma_{1,\gamma}(R)$ and $\Gamma_{2,\gamma}(R)$ be two solution branches for some $\gamma = \gamma_e - \epsilon$, $1 >> \epsilon > 0$. When $\gamma = \gamma_e$ Γ_{1,γ_e} meets Γ_{2,γ_e} at $R(s_e) = R_e$. For $\gamma = \gamma_e + \epsilon$ we have part of $\Gamma_{1,\gamma}$ joins part of $\Gamma_{2,\gamma}$, and the remaining part of $\Gamma_{1,\gamma}$ joins the remaining part of $\Gamma_{2,\gamma}$.

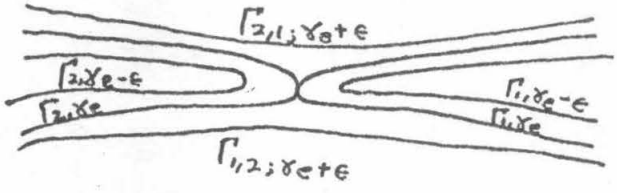

Figure 4.6 : Exchange of Solution Branches

In the remainder of this section we exhibit some of our computed solution branches. Figures 4.8-4.24 are the velocity profiles $(f(z), f_z(z), g(z)) = (w(z), -2u(z)/r, v(z)/r)$ for the indicated Reynolds number.

The third axis which "goes into and out of the paper" is the γ-axis. Each curve is a velocity profile for a particular γ. For example, in figure 4.8a the solution curves are the profiles for the angular velocity $v = rg(z)$ for $\gamma = -1$ to $\gamma = 1$, with the first curve 'out of the paper or closest to the viewer' at $\gamma = 1$ and the last curve at $\gamma = -1$.

Using both the axial and radial velocity profiles we can draw streamlines, (Batchelor [1]). The notion of cells can be introduced.

Definition 4.3 A cell is a region bounded by planes of constant z that includes only its own recirculating fluid. In other words, it is a region bounded by planes of constant z at which the axial velocity f(z) is zero.

Let z_a, z_b be two consecutive zeros of f(z). Assuming nontrivial solution, f(z) must attain at least one relative extremum at $z_e \in (z_a, z_b)$. If there is more than one relative extremum, we call it a cell-with-structure.

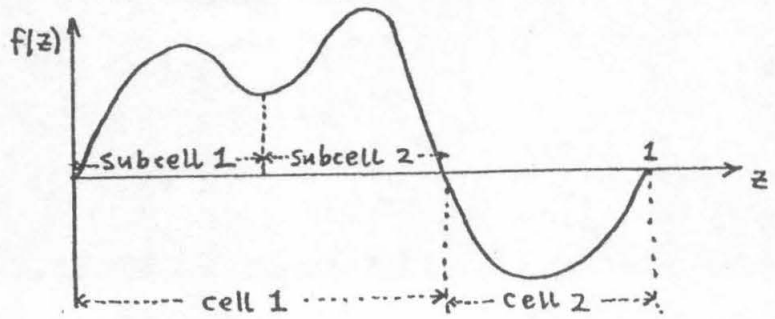

figure 4.5 cell-with-structure

Definition 4.4 Let $C_s[z_a, z_b]$ be a cell-with-structure. A subcell is a region bounded by planes of constant $z_1 < z_2$, $z_1, z_2 \in [z_a, z_b]$, satisfying (i) either the axial velocity $f(z)$ or the radial velocity $f_{\bar{z}}(z)$ is zero at z_1 and z_2, and (ii) there exists one $z_s \in (z_1, z_2)$ such that $f_{\bar{z}\bar{z}}(z_s) = 0$, $f_{\bar{z}\bar{z}\bar{z}}(z_s) \neq 0$.

The cell-with-structure in figure 4.5 has two subcells. Let N_{max} and N_{min} be the number of relative maxima and the number of relative minima of $f(z)$ in $C_s[z_a, z_b]$ respectively. The number of subcells is given by

$$N_s = \frac{N_{max} + N_{min} + 1}{2} \tag{4.1.2}$$

We must show N_s is an integer. Assume $f > 0$ in (z_a, z_b). In between two relative maxima there is a relative minimum. Furthermore between $f(z_a) = f(z_b) = 0$ there must be one more relative maximum than minimum. That is

$$N_{max} = N_{min} + 1$$

From Definition 2.4 a solution is linearly stable only if all its eigenvalues in the linearized stability analysis lie in the left half complex plane. The exchange of stability calculations only gives the information that one of its eigenvalues has changed sign. We can say a solution branch is linearly unstable from these calculations. For this reason, we can only classify some, but not all, the stable branches. The computations of exchange of stability analysis will be discussed in the next section. (For most solution branches we stopped our calculations at R = 1000. Hence when we we say solution branch exists for $R \geq 0$ we mean the solution branch exists for R in the computed range $[0, 1000]$ and we strongly believe it exists for all R. Most of the branches shown are at Reynolds number R = 1000. The exceptions are: (i) the cosine branch 9 is at R = 400, (ii) branches 12 and 13 are at R = 210, and (iii) branches 14 through 17 are at R = 190.) Following are the descriptions of some of the computed solution branches:

Branch 1: solid body branch $-1 \leq \gamma \leq 1$ figure 4.8

The entire branch is stable. For $\gamma \geq 0$ solution exists for $R \geq 0$. Some of these solutions are well known. For

instance the following have computed solutions on this branch:

Mellor et al. [22]; $\gamma = 0$, large R

Lance and Rogers [16]; $\gamma \geq 0$, various ranges of $R \leq 1000$

Greenspan [7]; $\gamma = 0$, $R = 1000$

Holodniok et al. [8]; $\gamma = 0.8$, $R \leq 1000$

The solutions for $\gamma < 0$ on this branch are unknown. As γ decreases from zero to -1 the number of cells increases from one to two, and the cells are cells-with-structure. At $\gamma = -1$ there is a region near the upper disk where both the axial and angular velocity profiles behave like a cosine function; the maximum angular velocity of fluid is about thirteen times that of the disks in absolute value - large amplitude solution (Definition 4.1).

Branch 2: bifurcation negative branch $-1 \leq \gamma \leq 1$ figure 4.9

The branch is stable. For $-1 < \gamma \leq -1/3$ solution exists for $R \geq 0$. Some of these solutions have also been computed by:

Pearson [23]; $\gamma = -1$, $R = 1000$

Holodniok [8]; $\gamma = 0.8$, $R \leq 1000$

The solution has two cells for all $|\gamma| \leq 1$. The parameter γ has very little effect on the velocity profiles in the inviscid region. The solution at $\gamma = -1$ comes from the

symmetric bifurcation from the Stewartson solution branch ($\gamma = -1$) at $R_{bif} = 119$.

Branch 3: bifurcation positive branch A $-1 \leq \gamma < 0$ figure 4.10

The branch is stable. For finite Reynolds number there is no solution on this branch for $\gamma = 0$. (Branches 3 - 6 have the same phenomenon.) Only Pearson has computed the solution at $\gamma = -1$. The solutions have two cells. In contrast to Branch 2, the effect of γ is more appreciable throughout the inviscid region.

Branch 4: bifurcation positive branch B $-1 \leq \gamma < 0$ figure 4.11

For large Reynolds number the branch is unstable. At $\gamma = -1$, the solution exists for all R and there is an exchange of stability at the bifurcation point R = 119. This is the second of the four branches that does not have a solution for $\gamma = 0$ at a finite R. This is a two-cell branch, a continuation of Branch 3 after normal limit points $R_n(\gamma)$. There have been many analytical studies of this branch for $\gamma = -1$ and large R.

Branch 5: symmetric positive γ branch A $0<\gamma\leq 1$ figure 4.12

The branch is stable, and solution exists for $0<\gamma\leq 1$. Only Holodniok et al. [8] computed the solution for $\gamma = 0.8$. This is a two-cell solution branch. The solution for $\gamma = 1$ is obtained by applying Corollary 1.2 to the $\gamma = 1$ solution of Branch 2. Then the whole solution branch at R = 1000 and $\gamma\in(0, 1]$ is then obtained by pseudo-arclength continuation in γ, keeping R fixed at R = 1000. The axial and radial velocities have the same form as those of Branch 3 even though the sign of γ is opposite. This γ-sign-independent phenomenon is also observed in Branch 5 (with Branch 6).

For large Reynolds number the rotating coaxial disks problem with no suction can be analysed using singular perturbation techniques. (A detailed description appears in Chapter 5.) Let $\epsilon^2 = 1/R$. Near the lower disk, assume the following asymptotic expansion in

$$z = \epsilon^a t$$

$$f = \epsilon^{\alpha_0} f_0 + \epsilon^{\alpha_1} f_1 + \cdots \qquad \alpha_K > \alpha_{K-1}$$

$$g = g_0 + \epsilon^{\beta_1} g_1 + \epsilon^{\beta_2} g_2 + \cdots \qquad \beta_K > \beta_{K-1}$$

Depending on (α_0 , a), the leading order equations can be written

$$
\begin{aligned}
f_{0tttt} &= f_0 f_{0ttt} + c\,4\, g_0 g_{0t} \\
g_{0tt} &= g_{0t} f_0 - g_0 f_{0t}
\end{aligned}
\tag{4.1.3}
$$

where c, depending on (α_0, a), is either zero or one. (4.1.3) is to be solved with conditions at t = 0:

$$
\begin{aligned}
f_0(0) &= f_{0t}(0) = 0 \\
g_0(0) &= \gamma
\end{aligned}
\tag{4.1.4}
$$

Let the solution be bounded as $t \to \infty$. Let (F, G) be such a solution when γ in (4.1.4) is equal to one. Then for arbitrary nonzero γ, we find we have the set of similar solutions to (4.1.3)-(4.1.4)

$$
\begin{aligned}
f(t,\gamma) &= |\gamma|^{1/2} F(|\gamma|^{1/2} t) \\
g(t,\gamma) &= \gamma\, G(|\gamma|^{1/2} t)
\end{aligned}
\qquad c = 1 \tag{4.1.5}
$$

$$
\begin{aligned}
f(t,\gamma) &= \gamma^p F(\gamma^p t) \\
g(t,\gamma) &= \gamma\, G(\gamma^p t)
\end{aligned}
\qquad p \neq 0,\ c = 0 \tag{4.1.6}
$$

The above similar solutions of (4.1.3)-(4.1.4) imply the axial and the radial velocities have the same solution to leading order irrespective of the sign of γ. As t tends to infinity $f(t, \gamma)$ tends to a constant independent of the sign of γ. That is

$$
\lim_{t\to\infty} f(t,\gamma) = \lim_{t\to\infty} f(t,-\gamma)
$$

Thus, for some $\gamma_o \neq 0$, $f(t, \gamma_o)$ and $f(t, -\gamma_o)$ can be matched to the same outer (inviscid) solution.

Branch 6: symmetric positive γ branch B $0 < \gamma \leq 1$ figure 4.13

The branch is unstable. Only Holodniok et al. computed the solution for $\gamma = 0.8$. The solutions have two cells. This branch is a continuation of Branch 5 after normal limit points $R_n(\gamma)$. Both the γ-sign-independent phenomenon and the non-existence of solutions at $\gamma = 0$ for finite Reynolds number are present.

Branch 7: $-0.3776 \leq \gamma \leq 1$ figure 4.14

The branch is unstable. Only Holodniok et al. computed the solution for $\gamma = 0.8$. This is a two-cell branch, obtained by the continuation of Branch 2 after normal limit point $R_n(\gamma)$. The solution for $\gamma = 1$ is not symmetric.

Branch 8: $-0.3776 \leq \gamma \leq 1$ figure 4.15

The branch is stable. For $\gamma \in [-1/3, 0)$ solutions exist for $R \geq 0$. Only Mellor et al. computed the solution for $\gamma = 0$. The number of cells varies between one to three as γ changes. The γ-sign-independent phenomenon is evident here for $\gamma > 0$ (with $\gamma < 0$ of Branch 1). The solution at $\gamma = 1$ is not symmetric about $z = 0.5$.

Branch 9: cosine branch $-1 \leq \gamma \leq 1$ ($R = 400$) figure 4.16

The branch is unstable. Only Mellor et al. computed the solution for $\gamma = 0$. This is a one-cell branch, with γ having tremendous effect on the magnitude of the velocities in the inviscid region. This is an another example of the γ-sign independent phenomenon (with itself).

Branch 10: finger branch A $0.79 \leq \gamma \leq 1$ figure 4.17

The stability of this branch is not known. By continuing the solution outside $\gamma = 1$, this solution branch 'turns around' at about $\gamma = 1.2$ ($R = 1000$). Solutions have two cells; the cell near the top disk has structures.

Branch 11: finger branch B $0.79 \leq \gamma \leq 1$ figure 4.18

Solutions are linearly unstable. This is a two-cell branch; the cell near the top disk has structures. Solution for $\gamma = 1$ is asymmetric about $z = 0.5$ and it is a mirror image of the solution of Branch 7.

Branch 12: $-1 \leq \gamma \leq 1$ ($R = 210$) figure 4.19

This is a one-cell large amplitude solution branch. This branch does not have solution for $R < 55$. For $\gamma = 1$ $f(z)$ is not anti-symmetric about $z = 0.5$ (even though g is symmetric about $z = 0.5$). Applying Corollary 1.2 gives the $\gamma = 1$ solution of cosine branch 9.

Branch 13: $-1 \leq \gamma \leq 1$ ($R = 210$) figure 4.20

This is a two-cell large amplitude solution branch. For $\gamma \leq -0.3$ the cell near the top disk has structures. Furthermore, there is an exchange of solution branches; solution branches for fixed $\gamma < 0.05$ turn around at $R_n(\gamma)$ lying on $E \propto F$ (cf. figure 4.4), and solution branches for fixed $\gamma > 0.05$ turn around at $R_n(\gamma)$ lying on GHI.

Branch 14: $-1 \leq \gamma \leq -0.7$, $-0.23 \leq \gamma \leq 1.0$ (R = 210) figure 4.21

This is a two-cell large amplitude solution branch. For $\gamma \geq 0.3$ the cell near the top disk has structures. This branch is the counterpart of branch 13: solution branches for fixed $\gamma < 0.05$ turn around at $R_n(\gamma)$ lying on GHI and solution branches for fixed $\gamma > 0.05$ turn around at $R_n(\gamma)$ lying on E∝F. We note that there is no solution for γ in (-0.25,-0.65) at R = 210 (see figure 4.4).

Branch 15: $-0.125 \leq \gamma \leq 0.05$ (R = 190) figure 4.22

This is a two-cell large amplitude solution branch, lying inside the lips CHD. There is an exchange of solution branches: solution branches for fixed $\gamma < 0.05$ turn around at $R_n(\gamma)$ lying on lips CHD and solution branches for fixed $\gamma > 0.05$ turn around at $R_n(\gamma)$ lying on GHI. (Solutions for $\gamma \geq 0.9$ and R = 190 are not shown in figure 4.22)

Branch 16: $0.025 \leq \gamma \leq 0.225$ (R = 190) figure 4.23

This is a two-cell large amplitude solution branch. This is the counterpart of branch 15 (as branch 14 is the

counterpart of branch 13). (Solutions for $\gamma \leq -0.9$ and $R = 190$ are not shown in figure 4.23.)

Branch 17: -0.125 0.2 (R = 190) figure 4.24

This is a two-cell large amplitude solution branch. This is the second of the two solutions which lie inside the lips CHD.

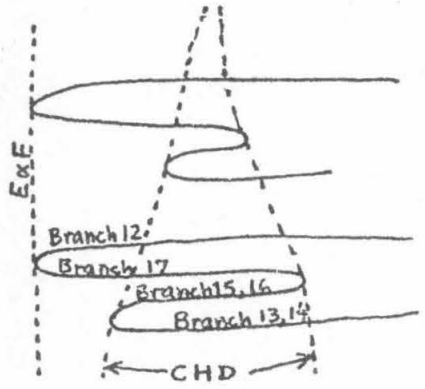

Figure 4.25

Figures 4.26 and 4.27 are $g(0.5; \gamma, R = 500)$ and $(g(0.5; \gamma, R = 1000)$ respectively. These are the 'bifurcation diagrams', where the parameter is γ. (Here we have shown only some of the computed solutions.) Correspondingly figures 4.28-4.33 show $g(0.5; \gamma_K, R)$ as a function of R for fixed $\gamma_K = 1, 0.8, 0, -0.2, -0.8$ and -1 respectively. (Note that $g(0.5; -1, R) = 0$ on the Stewartson's solution branch.) The numbers indicated are the

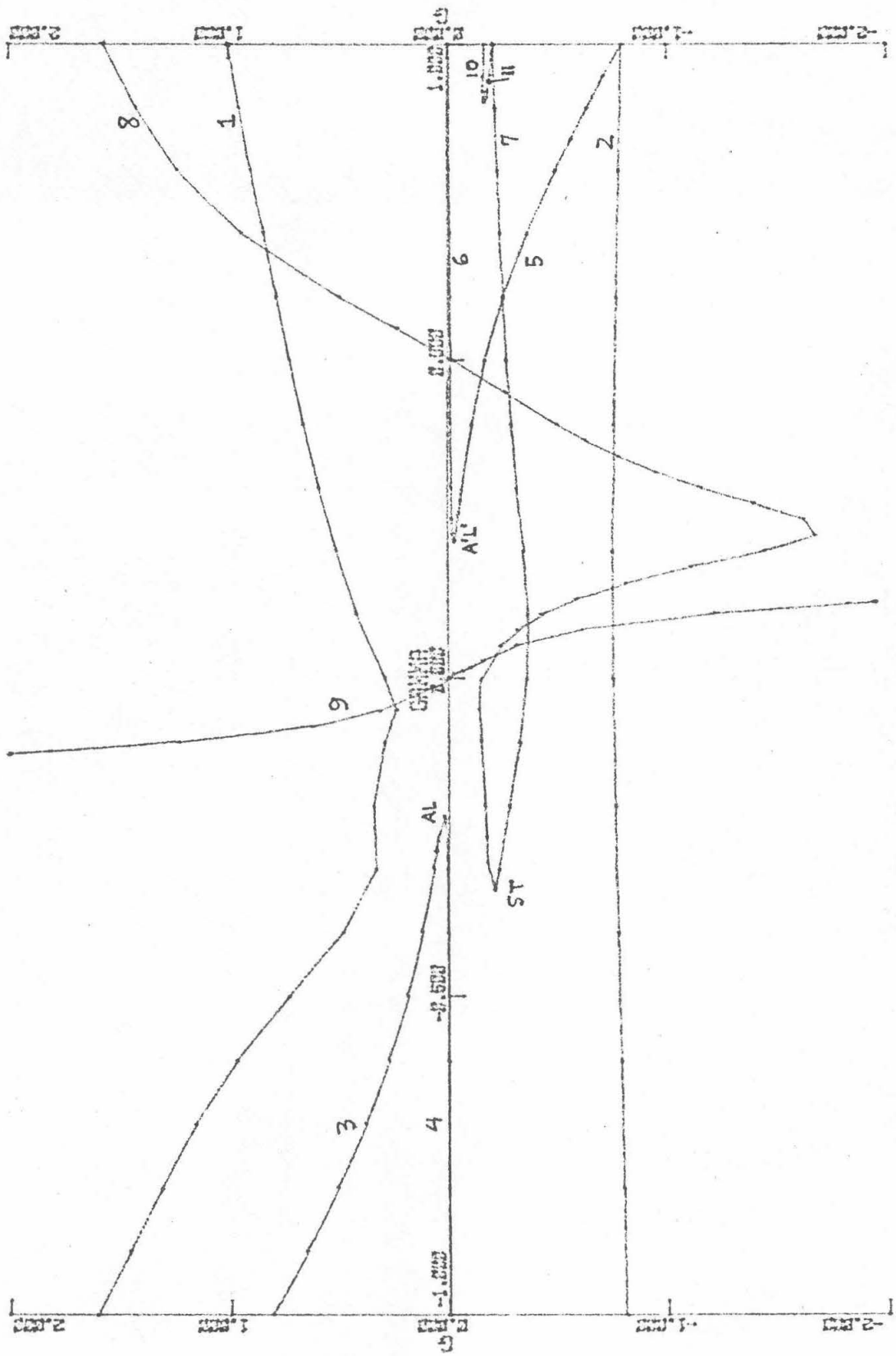

Figure 4.2.6 $q(\frac{1}{2}; \gamma, R=500)$

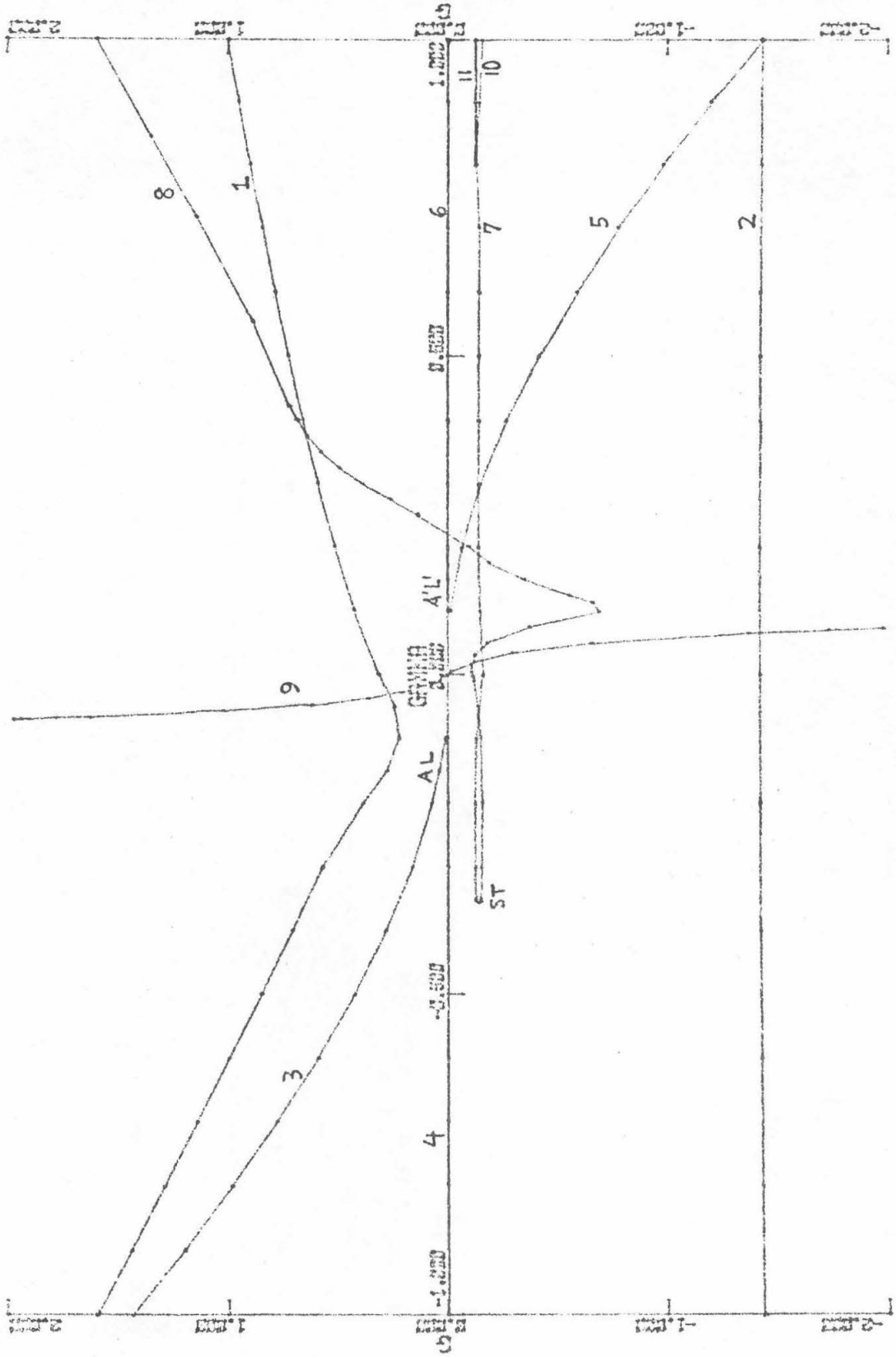

Figure 4.27 $g(0.5; \gamma, R=1000)$

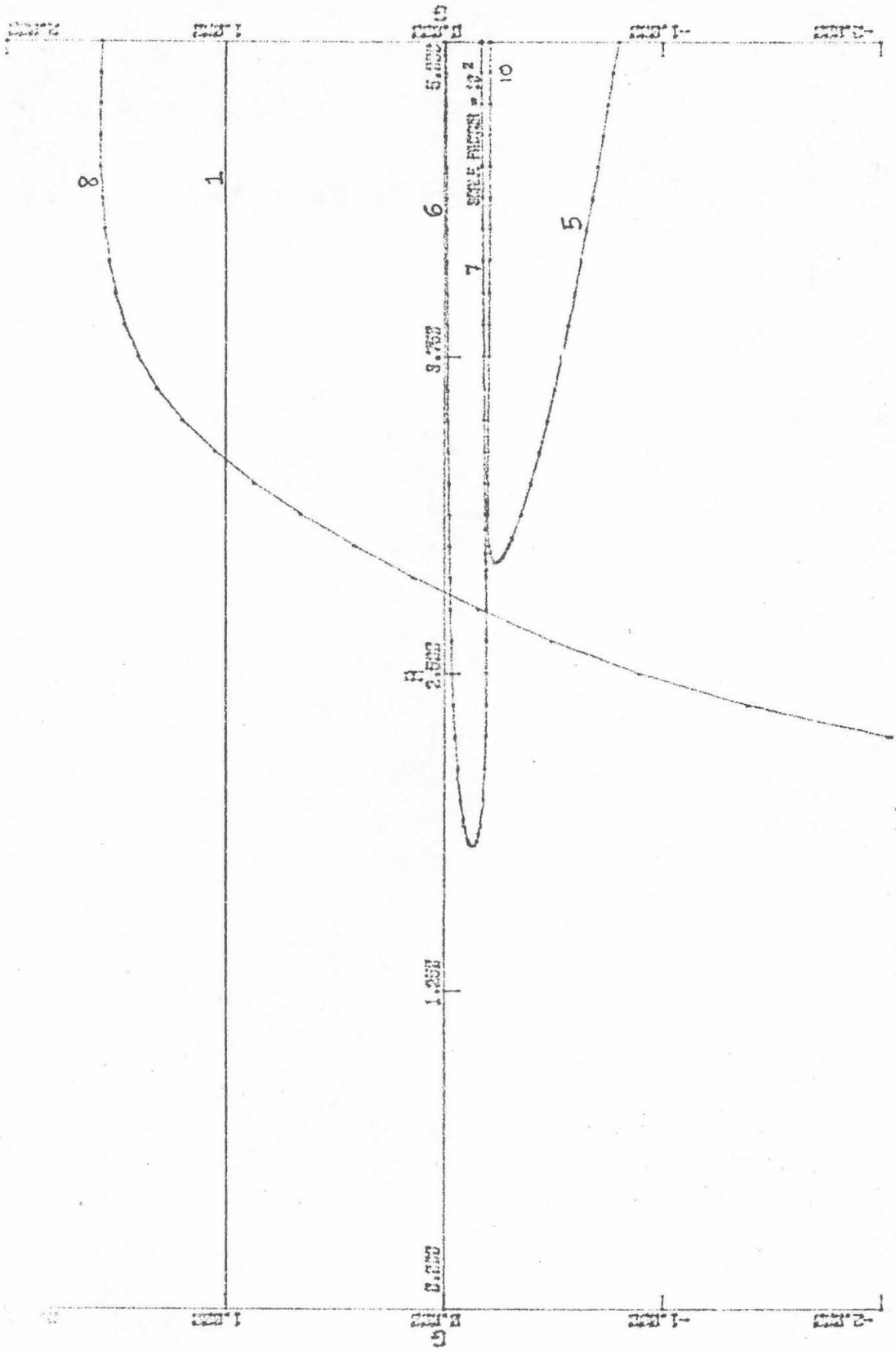

Figure 4.28 $g(0.5; \gamma=1., R)$

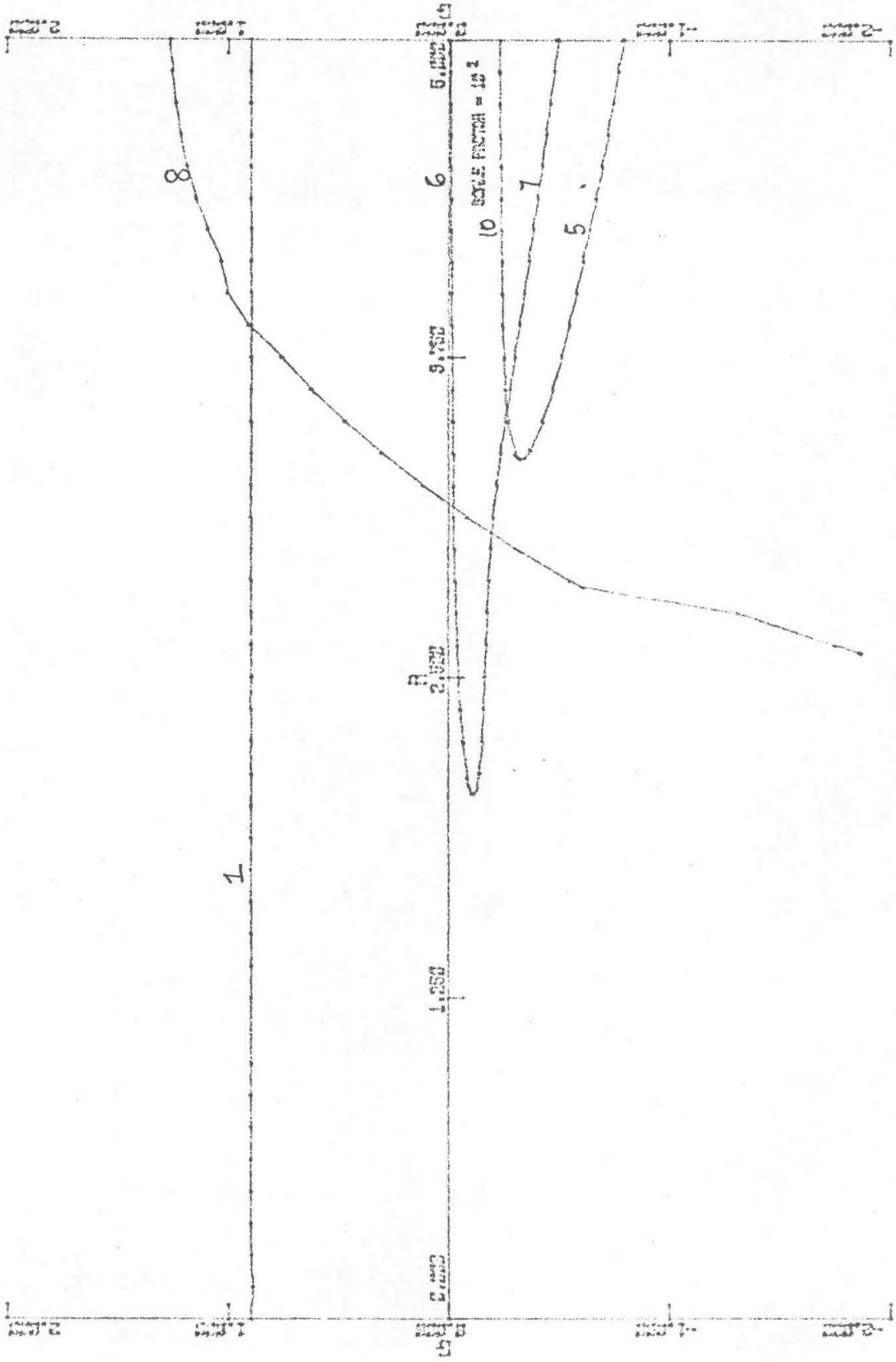

Figure 4.29 $\rho(\chi; \delta=0.8, R)$

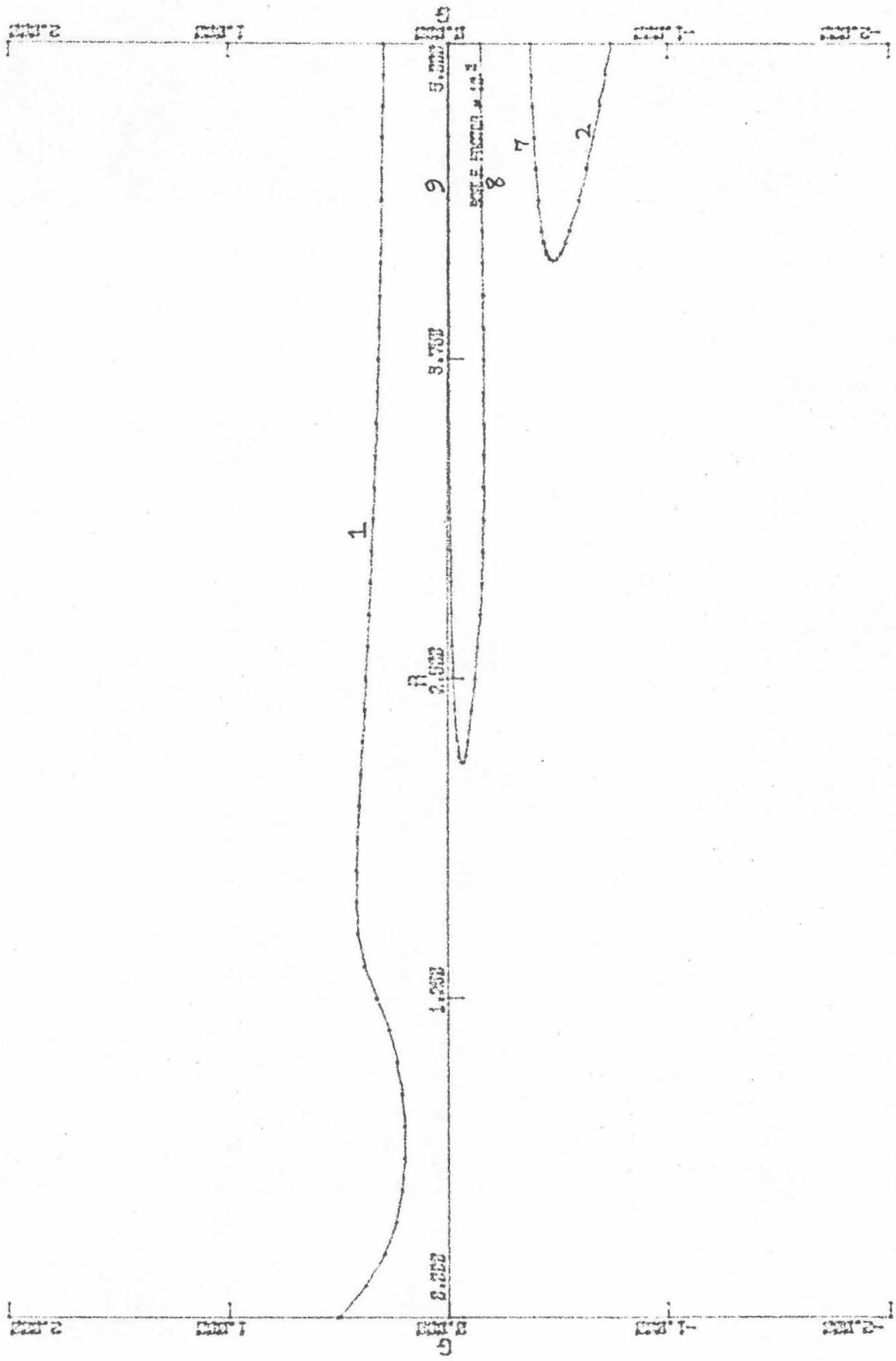

Figure 4.30 $g(\frac{1}{2}; \gamma = 0, R)$

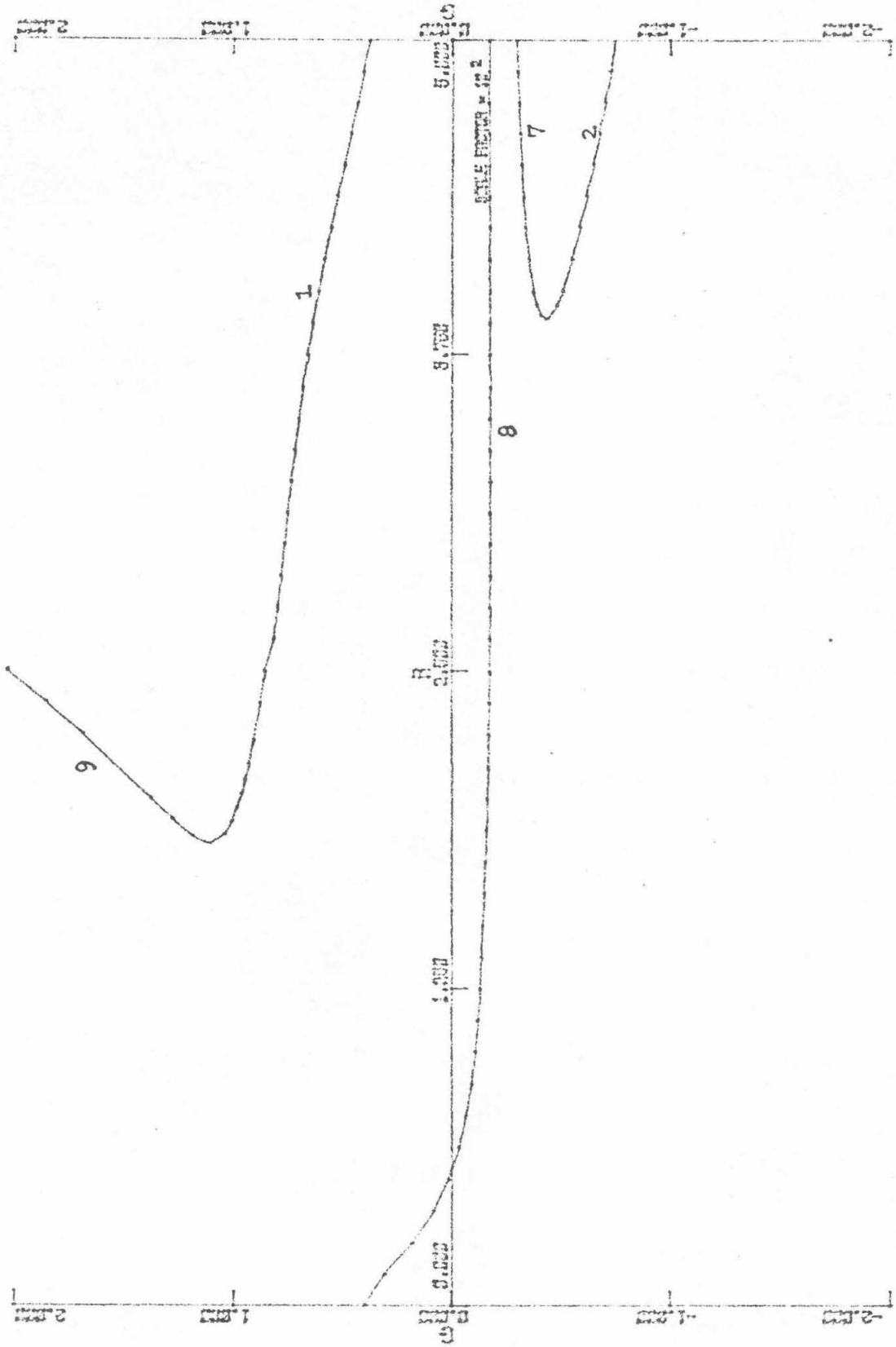

Figure 4.31 $\phi(\nu_z; \delta=-0.2, R)$

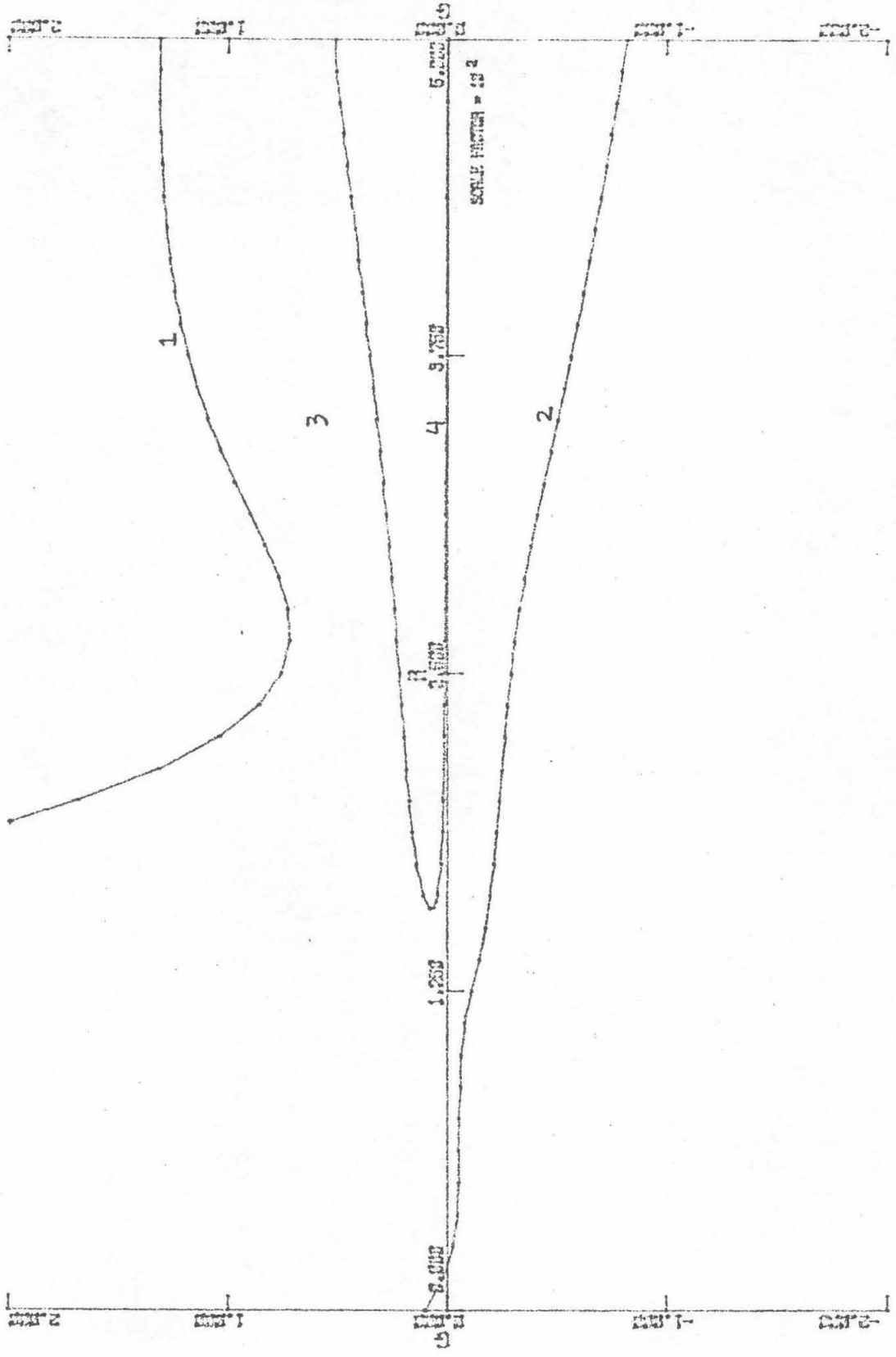

Figure 4.32 $g(\frac{1}{2}, \gamma=-0.8, R)$

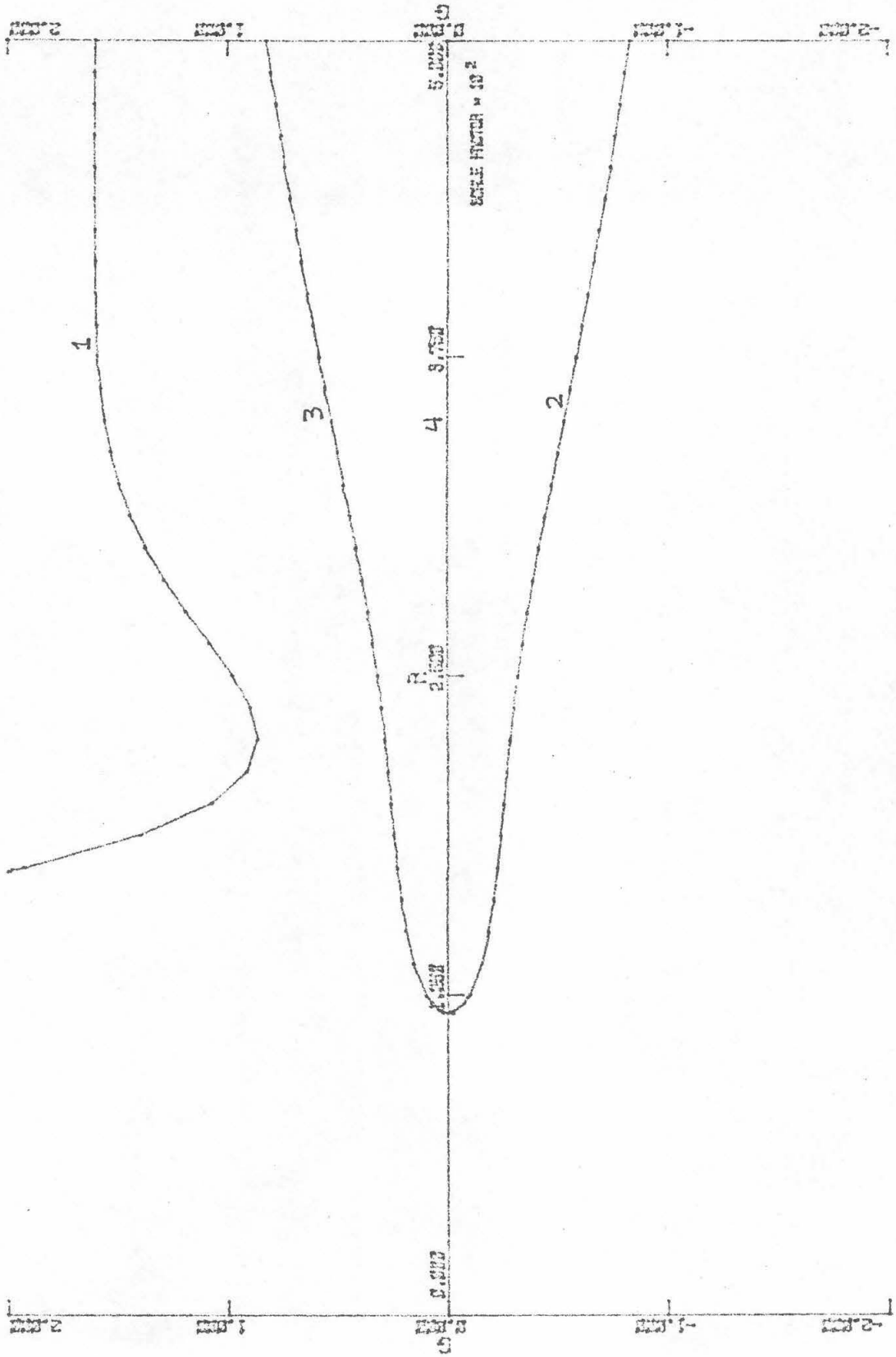

Figure 4.33 $g(\frac{1}{2}; \chi=-1, R)$

branch numbering system used above. Lastly, the unmarked intersections in figure 4.25-4.26 are not bifurcation points. That is, these intersections will probably go away if we plot functions other than g(0.5).

4.2 CRITICAL POINTS AND STABILITY CALCULATIONS

In this section we give an account of the computations at and near critical points: (1) Bifurcation points, (2) Normal limit points and (3) Coalesence of normal limit points. Local exchange of linearized stability computations are given.

(1) Bifurcation points -

(a) Switching of Branches: For $\gamma = -1$ the determinant of the converged discretized Jacobian has a sign change between R = 110 and R = 120. Using interval bisection, the critical point R_c is located, with the determinant of the discretized Jacobian very small.

$$\det\left(G_{hu}^{\circ}\right) = -5.78 \times 10^{-5}$$

The quadratic convergence of Newton's method is lost at the critical point. (From Lemma 3.3 and Theorem 3.4 we know the critical point cannot be a normal limit point.) Dimension of the null space is found to be one by checking the last block of diagonal elements of the LU-factorization of the discretized Jacobian. φ_1 and ψ_1^*, the null vector and its adjoint respectively, are computed using inverse iteration. Simple bifurcation is confirmed by forming the inner product $\psi_1^* G_\lambda$.

$$\psi_{1h}^* G_{\lambda h}^0 = 5.68 \times 10^{-7}$$

The coefficients (a_h, b_h, c_h) of the simple bifurcation equation are computed and the tangent vectors (α_0, α_1) solved.

$$a_h = -1.82 \times 10^{-6}$$

$$b_h = -8.0 \times 10^{-3}$$

$$c_h = 9.57 \times 10^{-5}$$

$$(\alpha_{01}, \alpha_{11})_h = (1, 6.0 \times 10^{-3})$$

$$(\alpha_{02}, \alpha_{12})_h = (1.14 \times 10^{-4}, 1)$$

The solution of the algebraic bifurcation equation has the property that any constant multiplying (α_0, α_1) is also a solution. This gives symmetric bifurcation:

$$(\alpha_{03}, \alpha_{13})_h = (1.14 \times 10^{-4}, -1)$$

From these solutions, we form the initial guesses for $k = 1,2,3$:

$$
\begin{aligned}
u_{h,K}(\delta s) &= u_h(R_c) + \delta s \left(\frac{\partial u}{\partial s}\right)_{h,K} \qquad 0 < \delta s << 1 \\
R_{h,K}(\delta s) &= R_c + \delta s\, \alpha_{o,K} \qquad (4.2.1) \\
\left(\frac{\partial u}{\partial s}\right)_{h,K} &= \left[\alpha_{oK}\varphi_o + \alpha_{1K}\varphi_1\right]_h
\end{aligned}
$$

The normalization equation (3.1.2) is now a function of the tangent vector at the simple bifurcation point:

$$
\begin{aligned}
N_{h,K} \equiv \theta\left[\alpha_{oK}\varphi_o + \alpha_{1K}\varphi_1\right]_h^* \left(u_{h,K}(\delta s) - u_h(R_c)\right) \qquad (4.2.2) \\
+ (1-\theta)\,\alpha_{oK}\left(R_{h,K}(\delta s) - R_c\right) - \delta s = 0
\end{aligned}
$$

The s-algorithm is applied with the normalization equation and initial guess $(u_{h,K}, R_{h,K}, N_{h,K})$ of (4.2.1)-(4.2.2). Quadratic convergence of Newton's method is recovered once we step away from the bifurcation point.

For k = 1 the computed solution is a continuation of the old branch we started on. For k = 2,3 the bifurcated branches are obtained and we continue the solution to $R = 1000$. They are found to be the solutions at $\gamma = -1$ on Branches 2 and 3. These are also the solutions obtained by Pearson [23] using the time-dependent approach.

For $\gamma = -1 + \gamma_{imp}$, $0 < \gamma_{imp} << 1$, using the above three solutions in our arc-length continuations, the phenomenon of perturbed bifurcation is observed. (Keener and Keller [10], Matkowsky and Reiss [19])

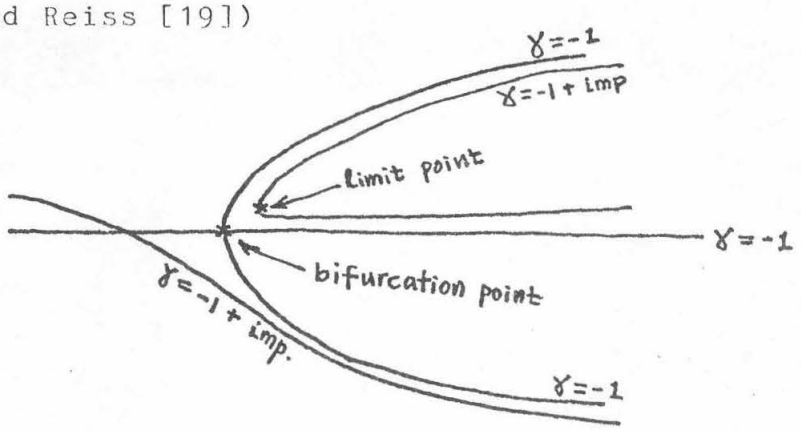

figure 4.34 : bifurcation - perturbed - bifurcation

(b) Local exchange of linearized stability computations:

Method (1) - Eigenvalue problem close to bifurcation point-

Newton's method is used to solve the eigenvalue problem (3.5.5) for $\sigma_k(\delta s)$ near a bifurcation point. $(0, \varphi_1)$ is used as the initial guess for $k = 1,2,3$. Quadratic convergence is observed. (This is no surprise because the normalization equation

$$\| w \|_2^2 = 1$$

is $N = 0$ with $\theta = 1$.)

For k = 1 and with $\delta R = 0.03$ we obtain eigenvalues

$$\sigma_1 (R_c - \delta R) = -.732 \times 10^{-4}$$
$$\sigma_1 (R_c + \delta R) = .482 \times 10^{-3} \qquad (4.2.3)$$

This implies solution is stable for $R < R_c$, and unstable for $R > R_c$.

For k = 2,3 and $\delta R = .30$ we obtain

$$\sigma_2 (R_c + \delta R) = -.225 \times 10^{-2}$$
$$\sigma_3 (R_c + \delta R) = -.223 \times 10^{-2} \qquad (4.2.4)$$

This implies the bifurcated branch is stable, in agreement with the steady solution of time-dependent computations of Pearson.

Method (2) - σ -derivative at the bifurcation point:

For k = 1, we obtain

$$\sigma_s (s_0) = \frac{\alpha_1 a + \alpha_0 b}{\psi_1^* B \varphi_1} \qquad (4.2.5)$$
$$= 0.08$$

Along the Stewartson's solution branch there is an exchange of linearized stability at the bifurcation point. Because solution is stable at $R = 0$ this branch becomes unstable for $R > R_c$. This agrees with the eigenvalue problem results (4.2.3). For $k = 2,3$ we have $\lambda_s(R_c)$ $(\equiv \alpha_o) = 0$. Because the coefficient a of the algebraic bifurcation equation is also zero, we have $\sigma_s(R_c)$ identically equal to zero along the bifurcated branch. To compute the second derivative $\sigma_{ss}(R_c)$ we need to solve an additional equation:

$$G_u^o \, w = - G_{uu}^o \varphi_1 \varphi_1 \quad , \quad \psi_1^* w = 0$$

Because G is at most quadratic in the dependent variables, the third Frechet derivative G_{uuu}^o is identically zero.

$$\sigma_{ss}(R_c) = \frac{2 \psi_1^* G_{uu}^o \varphi_1 w}{\psi_1^* B \varphi_1} \tag{4.2.6}$$

$$= -2.0$$

Along the bifurcated solution branch, for δs sufficiently small, the eigenvalue $\sigma(s)$ near the bifurcation point has a Taylor series expansion

$$\sigma(s) = \sum_{j \geq 2} \frac{\sigma_j}{j!} (\delta s)^j \quad , \qquad s - s_o \equiv \delta s$$

Thus the bifurcated solution branch is linearly stable because $\sigma_{ss}(s_o)$ is negative. This agrees with the eigenvalue problem results (4.2.4).

(2) Normal limit points:

(a) Computations around limit points - There are many normal limit points in the rotating coaxial disks problem. The powerful pseudo-arclength continuation allows us to zip in and out of this type of critical points.

'Modified' bisection is used to locate the critical point. The arc-length step-size has to be decreased near normal limit points. We use two different approaches:

(1) We let θ in the normalization equation be a function of the derivative of parameter with respect to s. Specificially

$$N_h \equiv \theta\, u_s(s_o)^* \left(u(s)-u(s_o)\right) + (1-\theta)\,\lambda_s(s_o)\left(\lambda(s)-\lambda(s_o)-(s-s_o)\right)=0$$

Using the 'exact' arclength normalization equation

$$\|u_s(s_o)\|_2^2 + |\lambda_s(s_o)|^2 = 1$$

the derivative λ_s can be computed

$$\lambda_s(s_o) = \frac{\pm 1}{[\|u_\lambda(s_o)\|_2^2 + 1]^{1/2}}$$

Now consider the pseudo-arclength normalization equation $N_h = 0$. If $\lambda_s(s_o)$ is small we want $\theta u_s(s_o)^*(u(s) - u(s_o))$ to be 'dominant' over $(1 - \theta)\lambda_s(s_o)(\lambda(s) - \lambda(s_o))$. That is, when we are near a limit point ($|\lambda_s| << 1$) we want to choose θ to slow down the increment in λ for a given arclength increment δs. This can easily be accomplished by requiring

$$\frac{\theta}{1-\theta} = \frac{\| u_s(s_o) \|_2^2}{|\lambda_s^2(s_o)|} \equiv \|u_\lambda(s_o)\|_2^2$$

Solving for θ:

$$\theta = \frac{\| u_\lambda(s_o) \|_2^2}{1 + \|u_\lambda(s_o)\|_2^2}$$

(2) Newton's method converges if the initial guess is sufficiently close to the solution. Let $x = (u, \lambda)^T$. Keller [13] indicates the radius of curvature $|x_{ss}(s)|$ is some measure of how good the initial guess is. For computational purpose we consider an easier and more practical approach to estimate the curvature. Let $g(0.5, \lambda)$ be a function of λ. (Here λ can be the Reynolds number,

keeping γ fixed, or vice versa.) Then κ of $g(0.5, \lambda)$ along Γ is

$$\kappa = \frac{g_{\lambda\lambda}(\tfrac{1}{2}; \lambda)}{\left(1 + g_{\lambda}^2(\tfrac{1}{2}; \lambda)\right)^{3/2}}$$

We see $\kappa(\lambda_o)$ can be approximately determined using backward differences on $g_\lambda(0.5; \lambda_o)$ and $g_\lambda(0.5; \lambda_o - \delta\lambda_o)$, where g_λ is obtained in the predictor one step Euler continuation. A very rough criterion for the arclength increment δs_{new} can be determined by the ratio of $\kappa(\lambda_o)$ and $\kappa(\lambda_o - \delta\lambda_o)$:

$$\delta s_{new} = \begin{cases} \delta s_{old} & \text{if } \tfrac{1}{3} \leq \left|\dfrac{\kappa(\lambda_o)}{\kappa(\lambda_o - \delta\lambda_o)}\right| \leq 3 \\ 2\,\delta s_{old} & \text{if } \left|\dfrac{\kappa(\lambda_o)}{\kappa(\lambda_o - \delta\lambda_o)}\right| < \tfrac{1}{3} \\ \delta s_{old}/2 & \text{if } \left|\dfrac{\kappa(\lambda_o)}{\kappa(\lambda_o - \delta\lambda_o)}\right| > 3 \end{cases}$$

At the normal limit point Newton's method converges quadratically. Thus, the rate of convergence proof in Section 3.3 is verified computationally.

(b) Local exchange of linearized stability computations:

Method (1) Eigenvalue problem near limit points -

We follow the same procedure described for the case of simple bifurcation point. The results agree with the theory of Section 2.3. For $\gamma = -0.9$ of Branches 3 and 4 we have

$$\begin{aligned} \sigma\ (\text{Branch } 3\ ,\ R = 138.34) &= -0.652 \times 10^{-4} \\ \sigma\ (\text{Branch } 4,\ R = 138.34) &= 0.804 \times 10^{-4} \end{aligned} \tag{4.2.7}$$

That is, Branch 3 is linearly stable and Branch 4 is linearly unstable.

Method (2) σ -derivative at a normal limit point -

This poses no difficulty. For the same case as in method (1), we have

$$\begin{aligned} \sigma_s\ (s_o) &= -\ \frac{\psi_1^*\ G_{uu}^o\ \varphi_1 \varphi_1}{\psi_1^*\ B\ \varphi_1} \\ &= 4.0 \end{aligned} \tag{4.2.8}$$

In a small neighborhood of the limit point $\sigma\ (s)$ has the Taylor series expansion

$$\sigma(s) = \sigma_s(s_o)\ (s - s_o) + O(s - s_o)^2$$

From (4.2.8) we conclude there is an exchange of linearized stability. This is in agreement with the eigenvalue problem results (4.2.7).

There are a few interesting phenomena near critical points where (1) coalesence of normal limit points and development of s-curve(or cusp), (2) exchange of solution branches. We conclude this section by locally studying one of these phenomena.

(3) Coalesence of normal limit point and development of s-curve-

In the process of sweeping the solution sheet for Branch 2, it is found that for $\gamma > -1/3$ the solution branch $\Gamma_c(R)$ does not extend back to R = 0. A careful and tedious pseudo-arclength continuation is performed. For $\gamma \leq -.384$, the branch Γ_c goes back to R = 0. Slighly increasing γ to -.3839 we obtain a normal limit point with $R_{ss}(R=347.78) = 0$. (Here we have $\lambda = R$.) When we increase γ further to -.3834 this normal limit point splits into two normal limit points, forming an s-curve which still goes back to R = 0. The second normal limit point disappears at $\gamma = -1/3$. The limit points $l_{1,i}$, $l_{2,i}$ and $l_{3,i}$ in figure 4.35 correspond to the limit points on BJ, BS and ST respectively in figure 4.4. Furthermore, for $\gamma = -1/3$ the two limit points from BS and TS meet together at R = 447.8. That is, BST has a relative maximum at R = 447.8 and

$\gamma = -1/3.$

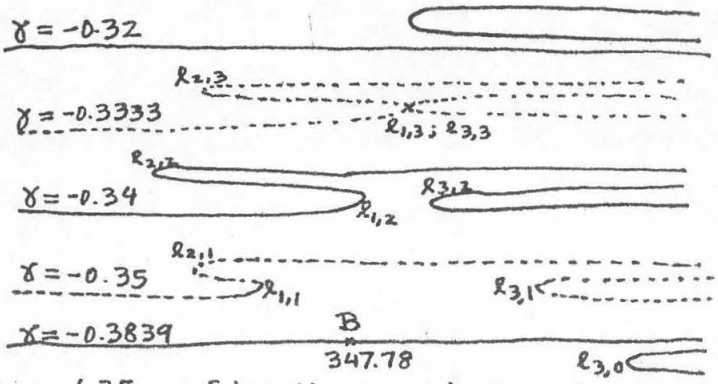

figure 4.35 : Schematic cusp development of critical point B

Next we perform an exchange of linear stability computations and obtain (1) the 'mid-section' of the s-curve is unstable, (2) the 'head' and 'tail' of the s-curve are stable. (This is an example in which the eigenvalue $\sigma(s)$ of the linearized problem (2.3.6) goes from negative to positive and then back to negative while the rest of the spectrum stays in the left half complex plane.)

CHAPTER 5

THE PERTURBATION ANALYSIS

5.1 PRELIMINARIES

In Chapter 4 we saw the many computed solutions of the rotating coaxial disks problem with no suction. These calculations open up many theoretical questions. Foremost ones are: (1) Is Batechelor's conjecture correct? (2) Is there an infinite number of solutions? In this short chapter we do not attempt to address to these questions, nor do we try to launch an extensive systematic investigation. Rather, we give a flavor of the different kinds of solutions that can be constructed using singular perturbation techniques (Cole [3]). Some work has been done in the last few years. A lot as yet has to be accomplished before we can close the topic. Indeed for the flow of a viscous fluid in a semi-infinite region bounded by a single infinite rotating disk, Dijkstra and Zandbergen [5] recently computed nonunique solutions. (Lentini-Gil [17] furthered their calculations and conjectured an infinite number of

solutions for the case when the fluid is nonrotating at infinity.) These solutions, we shall see in this chapter, are the boundary layer solutions in our perturbation construction. Which of their computed solutions shall we use to match with the inviscid solution(s)?

We restrict ourselves to the case $R >> 1$ and $\gamma = -1$. In Section 2 we study the perturbation construction of Stewartson's solution. In Section 3 we review Tam's expansion for our bifurcated solutions (see Chapter 4). His results are extended to higher order terms. In the last section we indicate some new perturbation constructions for large amplitude solutions (see Chapter 4).

For $\gamma = -1$ and large Reynolds number we let $\epsilon^2 = R^{-1}$ and rewrite our governing equations:

$$\epsilon^2 f_{zzzz} = f f_{zzz} + 4 g g_z$$
$$\epsilon^2 g_{zz} = g_z f - g f_z \qquad (5.1.1)$$

The boundary conditions for (5.1.1) are

$$f(0) = 0 \; ; \qquad f(1) = 0$$

$$f_z(0) = 0 \; ; \qquad f_z(1) = 0$$

$$g(0) = 1 \; ; \qquad g(1) = -1$$

In its most general form, assume the following expansion

$$z = \epsilon^a t$$

$$f = \epsilon^{\alpha_0} f_0 + \epsilon^{\alpha_1} f_1 + \epsilon^{\alpha_2} f_2 + \ldots \qquad \alpha_K > \alpha_{K-1}$$

$$g = \epsilon^{\beta_0} g_0 + \epsilon^{\beta_1} g_1 + \epsilon^{\beta_2} g_2 + \ldots \qquad \beta_K > \beta_{K-1}$$

Substituting into (5.1.1) we obtain

$$\epsilon^{2-4a}\left\{\epsilon^{\alpha_0} f_{0tttt} + \epsilon^{\alpha_1} f_{1tttt} + \ldots\right\}$$

$$= \epsilon^{-3a}\left\{\epsilon^{2\alpha_0} f_0 f_{0ttt} + \epsilon^{\alpha_0+\alpha_1}(f_0 f_{1ttt} + f_1 f_{0ttt}) + \ldots\right\}$$

$$+4\epsilon^{-a}\left\{\epsilon^{2\beta_0} g_0 g_{0t} + \epsilon^{\beta_0+\beta_1}(g_0 g_{1t} + g_1 g_{0t}) + \ldots\right\}$$

$$\epsilon^{2-2a}\left\{\epsilon^{\beta_0} g_{0tt} + \epsilon^{\beta_1} g_{1tt} + \ldots\right\}$$

$$= \epsilon^{-a}\left[\epsilon^{\alpha_0+\beta_0}(g_{0t} f_0 - g_0 f_{0t}) + \epsilon^{\alpha_0+\beta_1}(g_{1t} f_0 - g_1 f_{0t})\right.$$

$$\left. + \epsilon^{\alpha_1+\beta_0}(g_{0t} f_1 - g_0 f_{1t}) + \ldots\right]$$

The leading order equations depend on $(\alpha_0, \beta_0; a)$. For nonzero a, we have either boundary layer region or transition layer region. The following is a list of leading order equations:

(1) von Karman single disk boundary layer equation:

$(\alpha_o, \beta_o; a) = (1, 0; 1)$

(5.1.3)
$$f_{ottttt} = f_o f_{ottt} + 4 g_o g_{ot}$$
$$g_{ott} = g_{ot} f_o - g_o f_{ot}$$

(2) radial momentum uncoupled boundary layer equation:

$(\alpha_o, \beta_o; a) = (0, 0; 2)$

(5.1.4)
$$f_{otttt} = f_o f_{ottt}$$
$$g_{ott} = g_{ot} f_o - g_o f_{ot}$$

(3) angular momentum uncoupled boundary layer equation:

$(\alpha_o, \beta_o; a) = (2 - a + k, 2 - 2a + k/2, a)$, k, $a > 0$

(5.1.5) $a = 1$
$$f_{otttt} = 4 g_o g_{ot}$$
$$g_{ott} = 0$$

(5.1.6) $a > 1$
$$f_{otttt} = 0$$
$$g_{ott} = 0$$

(4) cosine inviscid equation: $(\alpha_o, \beta_o ; a) = (k, k, 0)$ $k < 2$

$$f_o f_{ottt} + 4 g_o g_{ot} = 0$$
$$g_{ot} f_o - g_o f_{ot} = 0 \qquad (5.1.7)$$

(5) cubic polynomial inviscid equation: $(\alpha_o, \beta_o; a) = (k_f, k_g, 0)$, $k_f < 2$, $k_g > k_f$

$$f_o f_{ottt} = 0$$
$$g_{ot} f_o - g_o f_{ot} = 0 \qquad (5.1.8)$$

(6) non-rotating inviscid equation: $(\alpha_o, \beta_o; a) = (k_f, k_g, 0)$, $k_f < 2$, $k_g < k_f$

$$g_o g_{ot} = 0$$
$$g_{ot} f_o - g_o f_{ot} = 0 \qquad (5.1.9)$$

Some of the above leading order equations will be used to construct some of our computed solutions. We note the boundary layer equations (5.1.3)-(5.1.4) are nonlinear and as yet no closed form solution has been found. However the inviscid equations (5.1.7)-(5.1.9) can be solved explicitly. In the following sections we confine our studies on the close z-interval [0, 0.5]. We thus restrict ourselves to

solutions for large R and $\gamma = -1$ having one of the following properties: (1) odd solution about z = 0.5, that is

$$f(\tfrac{1}{2}) = f_{zz}(\tfrac{1}{2}) = g(\tfrac{1}{2}) = 0 \tag{5.1.10}$$

and (2) even solution about z = 0.5, that is

$$f_z(\tfrac{1}{2}) = f_{zzz}(\tfrac{1}{2}) = g_z(\tfrac{1}{2}) = 0 \tag{5.1.11}$$

5.2 SOLUTION OF STEWARTSON - REVIEW

The solution of Stewartson has been analyzed by many workers. Among them are Tam [29], McLeod and Parter [21], and Matkowsky and Siegmann [18]. In this section we shall construct the solution using standard singular perturbation techniques.

We assume solution is odd about z = 0.5 (5.1.10). In the interval [0, 0.5] we use a two-layer model. That is, a boundary layer whose leading order equation is the von Karman single-disk equation (5.1.3), and a non-rotating inviscid outer layer whose leading order equation is given

by (5.1.9). To be more precise, near the bottom disk z = 0 we introduce the following expansions:

$$
\begin{aligned}
t &= z/\epsilon \\
f &= \epsilon f_0 + \epsilon^2 f_1 + \cdots \\
g &= g_0 + \epsilon^1 g_1 + \cdots
\end{aligned}
\tag{5.2.1}
$$

The equations for f_0 and g_0 are given by (5.1.3). The equations for f_1 and g_1 are

$$
\begin{aligned}
f_{1tttt} &= f_0 f_{1ttt} + f_{0ttt} f_1 + 4 (g_0 g_{1t} + g_{0t} g_1) \\
g_{1tt} &= (g_{1t} f_0 - g_1 f_{0t}) + (g_{0t} f_1 - g_0 f_{1t})
\end{aligned}
\tag{5.2.2}
$$

The boundary conditions are: (1) at the disk

$$
\begin{aligned}
f_0(0) &= f_{0z}(0) = 0 \\
g_0(0) &= 1
\end{aligned}
\tag{5.2.3}
$$

and (2) as $t \to \infty$

$$
\begin{aligned}
f_{0z}(\infty), f_{0zz}(\infty) &\to 0 \\
g_0(\infty) &= 0
\end{aligned}
\tag{5.2.4}
$$

The nonlinear equations (5.1.3) with boundary conditions (5.2.3)-(5.2.4) do not have closed form

solutions. From the analysis of McLeod and Parter [21] we can assume solution I of Dijkstra and Zandbergen [5] is to be used to match with the outer inviscid solution. As t tends to infinity, we have

$$
\begin{aligned}
f_0 &= -0.884 + O(e^{-0.884t}) \\
g_0 &= O(e^{-0.884t})
\end{aligned}
\tag{5.2.5}
$$

Next we consider the inviscid region. Assume expansions:

$$
\begin{aligned}
f &= \epsilon F_0(z) + \epsilon^2 F_1(z) + \cdots \\
g &= G_0(z) + \epsilon G_1(z) + \cdots
\end{aligned}
\tag{5.2.6}
$$

The leading order equations are given by (5.1.9). The higher order equations are:

$$
\begin{aligned}
& 4(G_0 G_{1z} + G_{0z} G_1) = 0 \\
& G_{0z} F_1 - G_0 F_{1z} + G_{1z} F_0 - G_1 F_{0z} = G_{0zz} \\
& F_0 F_{0zzz} + 4(G_0 G_{2z} + G_{0z} G_2 + G_1 G_{1z}) = 0 \\
& G_{0z} F_2 - G_0 F_{2z} + G_{2z} F_0 - G_2 F_{0z} + G_{1z} F_1 - G_1 F_{1z} = G_{1zz} \\
& \sum_{\ell \le K-1} F_\ell F_{K-\ell,zzz} + 4 \sum_{\ell \le K+1} G_\ell G_{K-\ell+1,z} = F_{K-2,zzzz} \qquad K \ge 2 \\
& \sum_{\ell \le K+1} (G_{\ell z} F_{K-\ell-1} - G_\ell F_{K-\ell+1,z}) = G_{K,zz}
\end{aligned}
\tag{5.2.7}
$$

From the boundary conditions (5.1.10) we obtain the solutions in the inviscid region:

$$G_K(z) = 0 \qquad K \geq 0$$

(5.2.8)

$$F_K(z) = C_K\left(z - \tfrac{1}{2}\right)$$

The constant C_0 is found by matching with the leading order solution ϵf_0 of (5.2.5)

$$C_0 = 1.768$$

The linear term $C_0 z$ is to be matched with $\epsilon^2 f_1$. Thus for large Reynolds number Stewartson's solution is non-rotating in the interior. It is a two-cell (Definition 4.3) solution. The streamlines of the flow are given in figure 5.1.

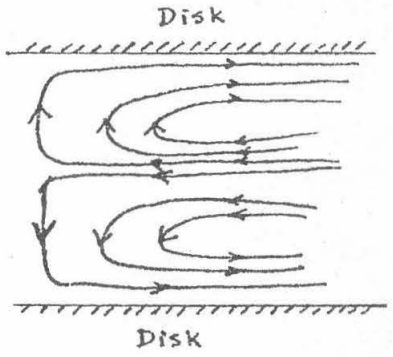

Figure 5.1 : Stewartson's solution

5.3 SOLUTION OF PEARSON (BIFURCATED)

For $\gamma = -1$ Pearson [23] using the time-dependent approach computed two steady state solutions at R = 1000. These are found to be our bifurcated solutions (see Chapter

4); these solution branches exist for $R > 119$. Further, our local exchange of linearized stability analysis confirmed Pearson's computed stable solutions. Tam [29], using singular perturbation techniques, constructed Pearson's solutions. In this section we review and extend Tam's work.

As in the construction of Stewartson's solution, we use a two-layer model and confine our studies to the closed interval [0, 0.5]. Even solution about $z = 0.5$ is assumed (5.1.11). The inviscid region has solution which is $O(1)$ as $R \to \infty$. The leading order equations in the boundary layer region is the same as in Section 5.2.

For the inviscid region we use the following expansions

$$f = F_0(z) + \epsilon F_1(z) + \epsilon^2 F_2(z) + \cdots$$
$$g = G_0(z) + \epsilon G_1(z) + \epsilon^2 G_2(z) + \cdots \tag{5.3.1}$$

These expansions are substituted into (5.1.1). The first three sets of equations for (F_0, G_0), (F_1, G_1) and (F_2, G_2) can be obtained by equating powers of ϵ :

$$F_0 F_{0zzz} + 4 G_0 G_{0z} = 0$$
$$G_{0z} F_0 - G_0 F_{0z} = 0 \tag{5.3.2}$$

$$F_0 F_{1zzz} + F_{0zzz} F_1 + 4(G_0 G_{1z} + G_{0z} G_1) = 0$$

(5.3.3) $$G_{0z} F_1 - G_0 F_{1z} + G_{1z} F_0 - G_1 F_{0z} = 0$$

$$F_0 F_{zzzz} + F_{0zzz} F_z + 4(G_0 G_{zz} + G_{0z} G_z) = F_{0zzzz} - F_1 F_{1zzz} - 4 G_1 G_{1z}$$

(5.3.4)

$$G_{0z} F_z - G_0 F_{zz} + G_{zz} F_0 - G_z F_{0z} = G_{0zz} - G_{1z} F_1 - G_1 F_{1z}$$

Even (or symmetric) boundary conditions (5.1.11) are imposed for both f and g in the inviscid region:

(5.3.5) $$F_{kz}(\tfrac{1}{2}) = F_{kzzz}(\tfrac{1}{2}) = G_{kz}(\tfrac{1}{2}) = 0 \qquad k \geq 0$$

Next we proceed to solve (5.3.2)-(5.3.5). In (5.3.2) the inviscid angular momentum equation can be satisfied by

(5.3.6) $$G_0(z) = \frac{\lambda_0}{2} F_0(z)$$

where λ_0 is a constant to be determined. Substituting (5.3.6) into the inviscid radial momentum equation of (5.3.2) we obtain

(5.3.7) $$F_0 \left(F_{0zzz} + \lambda_0^2 F_{0z} \right) = 0$$

For nontrivial solution we obtain

$$F_o = \tilde{A}_o + \tilde{B}_o \cos \lambda_o(z-1/2) + \tilde{C}_o \sin \lambda_o(z-1/2)$$

The boundary condition (5.3.5) implies $\tilde{C}_o = 0$. The solution for the pair (F_o, G_o) is given by

$$F_o = A_o (B_o + \cos \lambda_o(z-1/2)) \tag{5.3.8}$$

$$G_o = \frac{\lambda_o}{2} A_o (B_o + \cos \lambda_o(z-1/2))$$

Both equations in (5.3.3) and (5.3.4) have the form

$$\mathcal{L}\begin{pmatrix} F_K \\ G_K \end{pmatrix} \equiv \begin{pmatrix} F_o F_{Kzzz} + F_{ozzz} F_K + 4[G_o G_{Kz} + G_{oz} G_K] \\ G_{oz} F_K - G_o F_{Kz} + F_o G_{Kz} - F_{oz} G_K \end{pmatrix} = \begin{pmatrix} T_K \\ S_K \end{pmatrix} \tag{5.3.9}$$

$$k = 1, 2$$

where $T_1 = S_1 = 0$, and T_2 and S_2 are given by

$$T_2 = F_{0zzzz} - (F_1 F_{1zzz} - 4 G_1 G_{1z})$$

$$S_2 = G_{0zz} - G_{1z} F_1 - G_1 F_{1z}$$

(Matkowsky et al. [18] in 1976 performed a laborious calculation to show as $\epsilon \to 0$ rotating odd solution cannot exist. We observe this is the consequence of the fact that the coefficients multiplying the highest derivatives in (5.3.9) vanish at z = 0.5 if we admit rotating odd solution and the linear operator $\mathcal{L}$ become singular.)

Next, the requirement that $F_K(0.5)$ be nonzero implies

$$B_0 + 1 \neq 0 \tag{5.3.10}$$

Bearing in mind that this inviscid solution is to be matched with the numerical solution of the von Karman boundary-layer equations (5.1.3)

$$\begin{aligned} f &= -0.884\,\epsilon + O(\epsilon^2) \\ g &= O(\epsilon^2) \end{aligned} \tag{5.3.11}$$

Because $F_0(z)$ is $O(1)$, we must have

$$B_0 + \cos\frac{\lambda_0}{2} = 0 \tag{5.3.12}$$

From (5.3.10) and (5.3.12) we have

$$\cos\frac{\lambda_0}{2} \neq 1 \tag{5.3.13}$$

This proves the following lemma:

Lemma 5.1 Consider the problem (5.1.1)-(5.1.2). For small ϵ assume the outer (inviscid) solution:

$$\begin{aligned} f &= A_0\left(B_0 + \cos\lambda_0(z-\tfrac{1}{2})\right) + O(\epsilon) \\ g &= \frac{\lambda_0}{2} A_0\left(B_0 + \cos\lambda_0(z-\tfrac{1}{2})\right) + O(\epsilon) \end{aligned}$$

Further, let the boundary layer region have the limiting solution ($z = \epsilon t$)

$$\lim_{t\to\infty} \begin{pmatrix} f(t) \\ g(t) \end{pmatrix} = \begin{pmatrix} -0.884\,\epsilon \\ 0 \end{pmatrix} + O(\epsilon^2)$$

Then

$$\frac{\lambda_0}{2} \neq 2n\pi \quad , \quad n \text{ an integer}$$

Substituting (5.3.8) into (5.3.9) and using (5.3.6)-(5.3.7) we obtain

$$(5.3.13a) \quad -\lambda_0^2 F_{0z} F_K + F_0 F_{Kzzz} + 2\lambda_0 (F_{0z} G_K + F_0 G_{Kz}) = T_K$$

$$(5.3.13b) \quad \frac{\lambda_0}{2}(F_{0z} F_K - F_0 F_{Kz}) + F_0 G_{Kz} - F_{0z} G_K = S_K$$

Equation (5.3.13b) can be brought into the form

$$F_0^2 \left\{ \left(\frac{G_K}{F_0}\right)_z - \frac{\lambda_0}{2}\left(\frac{F_K}{F_0}\right)_z \right\} = S_K$$

Integrating, we get

$$(5.3.14) \quad G_K = \frac{\lambda_0}{2} F_K + F_0 \int_{1/2}^{z} \frac{S_K(\tilde{z})}{F_0^2(\tilde{z})}\, d\tilde{z}$$

We next use (5.3.13b) and (5.3.14) in (5.3.13a) to obtain

the following equation involving only the unknown F_k

$$-\lambda_0^2 F_{0z} F_k + F_0 F_{kzzz} + 2\lambda_0 \left\{ 2F_{0z}\left[\frac{\lambda_0}{2} F_k + F_0 \int_{1/2}^{z} \frac{S_k}{F_0^2}\, d\tilde{z} \right] + S_k - \frac{\lambda_0}{2}\left(F_{0z} F_k - F_0 F_{kz} \right) \right\} = T_k$$

This can be simplified:

$$(5.3.15) \qquad F_0\left(F_{kzzz} + \lambda_0^2 F_{kz} \right) = \left\{ T_k - S_k + 2F_{0z} F_0 \int_{1/2}^{z} \frac{S_k}{F_0^2}\, d\tilde{z} \right\} \equiv R_k$$

Solutions for (F_k, G_k), $k \geq 1$, are then given by the solutions of (5.3.15) and the equation (5.3.14).

For k = 1, we have

$$(5.3.16) \qquad \begin{aligned} F_1 &= A_1 \left(B_1 + \cos \lambda_0 (z - 1/2) \right) \\ G_1 &= \frac{\lambda_0}{2} A_1 \left(B_1 + \cos \lambda_0 (z - 1/2) \right) \end{aligned}$$

For k = 2, the non-homogeneous equation (5.3.15) can be written as a first order system

$$v_z = A_0(z)\, v + f$$

This has solution

$$v = \Phi(z)\, v(1/2) + \int_{1/2}^{z} \Phi(z-s)\, f(s)\, ds$$

where $\Phi(z)$ is the fundamental matrix (see Coddington and Levinson [2]), and for our equation (5.3.15), the fundamental matrix of its equivalent first order system can easily be seen to be

$$\Phi(z) = \begin{bmatrix} 1 & \frac{1}{\lambda_0}\sin\lambda_0(z-\frac{1}{2}) & \frac{1}{\lambda_0^2}\left(1-\cos\lambda_0(z-\frac{1}{2})\right) \\ 0 & \cos\lambda_0(z-\frac{1}{2}) & \frac{1}{\lambda_0}\sin\lambda_0(z-\frac{1}{2}) \\ 0 & -\lambda_0\sin\lambda_0(z-\frac{1}{2}) & \cos\lambda_0(z-\frac{1}{2}) \end{bmatrix}$$

Thus (F_2, G_2) is given by

$$(5.3.17a)\quad F_2(z) = A_2\left(B_2+\cos\lambda_0(z-\tfrac{1}{2})\right) - \frac{1}{\lambda_0^2}\int_{\frac{1}{2}}^{z}\frac{\left(1-\cos\lambda_0(z-\tau)\right)R_2(\tau)\,d\tau}{F_0(\tau)}$$

$$(5.3.17b)\quad G_2(z) = \frac{\lambda_0}{2}\left\{A_2\left(B_2+\cos\lambda_0(z-\tfrac{1}{2})\right) - \frac{1}{\lambda_0^2}\int_{\frac{1}{2}}^{z}\frac{\left(1-\cos\lambda_0(z-\tau)\right)R_2(\tau)\,d\tau}{F_0(\tau)}\right\} + F_0\int_{\frac{1}{2}}^{z}\frac{S_2(\bar{z})\,d\bar{z}}{F_0^2(\bar{z})}$$

In direct contrast to the analysis of Matkowsky et al.[18] we observe $F_0(s)$ tends to a nonzero constant A_0B_0 as z tends to 0.5. That is, the integrand of

$$\int_{\frac{1}{2}}^{z}\frac{\left(1-\cos\lambda_0(z-\tau)\right)R_2(\tau)\,d\tau}{F_0(\tau)}$$

is regular if $R_k(s)$ is regular. From (5.3.10) and (5.3.12) F_0 has the form

$$(5.3.19) \qquad F_0 = A_0 \left(1 + \cos \lambda_0 (z - \tfrac{1}{2}) \right)$$

For our bifurcated solutions Tam [29] observed, by forming the quotient $G_0(0.5)/F_0(0.5)$,

$$\frac{G_0(\frac{1}{2})}{F_0(\frac{1}{2})} = \frac{\lambda_0}{2} = \pm \pi$$

The solution for F_2 can be written down

$$F_2 = A_2 \left[B_2 + \cos \lambda_0 (z - \tfrac{1}{2}) \right] + \lambda_0 \int_{\frac{1}{2}}^{z} \left[1 - \cos \lambda_0 (z - \tau) \right] \left\{ \frac{(\lambda_0 + \frac{1}{2}) \cos \lambda_0 (\tau - \frac{1}{2})}{1 + \cos \lambda_0 (\tau - \frac{1}{2})} - \lambda_0 \sin \lambda_0 (z - \tau) \int_{\frac{1}{2}}^{\tau} \frac{\cos \lambda_0 (\mu - \frac{1}{2}) \, d\mu}{(1 + \cos \lambda_0 (\mu - \frac{1}{2}))^2} \right\} d\tau$$

Using the trigonometric half-angle identities the integral can be easily obtained

$$(5.3.20) \qquad F_2 = A_2 (B_2 + \cos \lambda_0 (z - \tfrac{1}{2})) + \frac{1}{\lambda_0} \left\{ \frac{-z}{3\lambda_0} \tan \frac{\lambda_0}{2} (z - \tfrac{1}{2}) \right\}$$

$$+ \text{well-behaved terms as } z \to 0 \text{ or } 1/2$$

Thus the inviscid solution for f is given by

$$(5.3.21) \qquad f = A_0 (1 + \cos \lambda_0 (z - \tfrac{1}{2})) + \epsilon A_1 (B_1 + \cos \lambda_0 (z - \tfrac{1}{2}))$$

$$+ \epsilon^2 F_2 + O(\epsilon^3)$$

Evaluating at z = 0, $\tan\{2\pi(z - 0.5)/2\}$ becomes $\tan\{\pi/2\}$.

The major difference between an even solution and an odd solution is that the singularity for the even solution is at $z = 0$, and the singularity for the odd solution is at $z = 0.5$ (see Matkowsky et al. [18]).

We next consider the boundary layer equations and indicate how to match its solutions with those from the inviscid region (0, 0.5). The boundary layer region has expansions

$$t = \frac{z}{\epsilon}$$

$$f = \epsilon f_0 + \epsilon^2 f_1 + \cdots$$

$$g = g_0 + \epsilon g_1 + \cdots$$

The equations for (f_0, g_0) and (f_1, g_1) are

(5.3.22)
$$f_{0tttt} = f_0 f_{0ttt} + 4 g_0 g_{0t}$$
$$g_{0tt} = g_{0t} f_0 - g_0 f_{0t}$$

(5.3.23)
$$f_{1tttt} = f_0 f_{1ttt} + f_{0ttt} f_1 + 4 (g_0 g_{1t} + g_{0t} g_1)$$
$$g_{1tt} = g_{1t} f_0 - g_1 f_{0t} + g_{0t} f_1 - g_0 f_{1t}$$

The boundary layer equations for (f_0, g_0) are the full nonlinear equations (5.1.1) with $R = 1$. There is no closed form solution. As in Section 5.2 we assume solution I of

Dijkstra and Zandbergen [5] is used to match with the solution (5.3.21) in the inviscid region (0, 0.5). For our matching purpose, we need to know the behavior of (f_0, g_0) as $t \to \infty$. We have (see Golstein [6])

$$(5.3.26)\qquad f_0 = f_{0\infty} + \sum_{n>0} \frac{a_{0n}}{n!} e^{n f_{0\infty} t}$$

$$g_0 = \sum_{n>0} \frac{b_{0n}}{n!} e^{n f_{0\infty} t}$$

$f_{0\infty}$ is found to be equal to -0.884 numerically. The first order term (f_1, g_1) has similar expansions for large t

$$(5.3.27)\qquad f_1 = f_{1\infty,0} + f_{1\infty,1} t + f_{1\infty,2} t^2 + \sum_{n>0} \frac{a_{1n}}{n!} e^{n f_{0\infty} t}$$

$$g_1 = g_{1\infty,0} + g_{1\infty,1} t + \sum_{n>0} \frac{b_{1n}}{n!} e^{n f_{0\infty} t}$$

The matching of the zeroth and first order terms gives

$$(5.3.28)\qquad A_1 (B_1 - 1) = -0.884$$

$$-A_0 \lambda_0^2/2 = f_{1\infty,2}$$

$$\lambda_0 A_1 (B_1 - 1)/2 = g_{1\infty,0}$$

For the matching of the function f, Tam [29] observed that the zeroth order term of the inviscid expansion is matched with the first order term of the boundary layer expansion, and that the first order term of the inviscid expansion is matched with the zeroth order term of the boundary layer

expansion. The singlular terms $\tan\{\pi(z - 0.5)\}$ etc. as z tends to zero can be matched with the inner solution if the expansion in $\exp(f_{\infty}t)$ can be written as an expansion in 1/t. This can be done because of the Burmann-Teixeira Theorem in complex variable theory (see Whittaker and Watson [31]). Indeed, exercises in complex variables give

$$\operatorname{sech} x = \frac{2}{e^{x} + e^{-x}} = 4\pi \sum_{k \geq 0}{}' \frac{(1+2k)(-1)^{k}}{(1+2k)^{2}\pi^{2} + 4x^{2}}$$

$$\operatorname{cosech} x = \frac{2}{e^{x} - e^{-x}} = \frac{1}{x} - 2x \sum{}' \frac{(-1)^{k}}{(1+2k)^{2}\pi^{2} + 4x^{2}}$$

$$\sum_{k \geq 0}{}' \frac{1}{k!}\left\{\frac{1}{1+a^{2k}x^{2}}\right\} = \sum_{k \geq 1} e^{\frac{1}{a^{2k}}} x^{-2k} (-1)^{k+1}$$

Lastly we observe the solution g(z) of our bifurcated solution branches are not symmetric about z = 0.5. Consider the bifurcated solution branch with $g(0.5) > 0$. Then there exists $z_{\alpha} \in (0.5, 1)$ such that $g(z_{\alpha}) = 0$. Furthermore, solution II ($\gamma = 0$) of Dijkstra et al.[5] has the property that there also exists $z_{\beta} \in (0, \infty)$ such that $g(z_{\beta}) = 0$. Thus it seems solution II should be matched with the inviscid solution in (0.5, 1).

5.4 SOME LARGE AMPLITUDE SOLUTION EXPANSIONS

In this section we look for other possible inner-outer (or boundary layer - inviscid) expansions for large Reynolds

number and $\gamma = -1$.

Let the inviscid region have expansions

$$f = \epsilon^{a_0} F_0 + \epsilon^{a_1} F_1 + \ldots\ldots$$

(5.4.1)

$$g = \epsilon^{b_0} G_0 + \epsilon^{b_1} G_1 + \ldots\ldots$$

Substituting into (5.1.1) we obtain

$$\epsilon^2\left(\epsilon^{a_0} F_{0zzzz} + \epsilon^{a_1} F_{1zzzz} + \ldots\right) = \epsilon^{2a_0} F_0 F_{0zzzz} + \epsilon^{a_0+a_1} F_0 F_{1zzzz}$$

(5.4.2a)

$$+ \epsilon^{a_0+a_1} F_{0zzzz} F_1 + \ldots + \epsilon^{2b_0} 4 G_0 G_{0z} + \epsilon^{b_0+b_1} 4(G_0 G_{1z} + G_{0z} G_1)$$

$$+ \ldots\ldots$$

$$\epsilon^2\left(\epsilon^{b_0} G_{0zz} + \epsilon^{b_1} G_{1zz} + \ldots\right) = \epsilon^{a_0+b_0}\left(G_{0z} F_0 - G_0 F_{0z}\right)$$

(5.4.2b)

$$+ \epsilon^{a_0+b_1}\left(G_{1z} F_0 - G_1 F_{0z}\right) + \epsilon^{a_1+b_0}\left(G_{0z} F_1 - G_0 F_{1z}\right)$$

$$+ \ldots\ldots$$

If $a_0 = b_0$ and $a_0 < 2$ we obtain the cosine inviscid equations (5.1.7). From the analysis of Section 5.3 and the results of Matkowsky et al. [18] we impose that the solution be even about $z = 0.5$

$$F(\tfrac{1}{2}) \neq 0 \,, \quad G(\tfrac{1}{2}) \neq 0$$

(5.4.3)

$$F_z(\tfrac{1}{2}) = F_{zzz}(\tfrac{1}{2}) = G_z(\tfrac{1}{2}) = 0$$

This gives the leading order solution:

$$f = \epsilon^{a_0} A_0 (B_0 + \cos \lambda_0 (z - 1/2)) + o(\epsilon^{a_0})$$

(5.4.4)

$$g = \epsilon^{a_0} \frac{\lambda_0}{2} A_0 (B_0 + \cos \lambda_0 (z - 1/2)) + o(\epsilon^{a_0})$$

We next seek boundary layer expansions that can match with (5.4.4)

$$t = z \epsilon^{-\gamma_0}$$

(5.4.5)

$$f = \epsilon^{\alpha_0} f_0 + \epsilon^{\alpha_1} f_1 + \cdots$$

$$g = g_0 + \epsilon^{\beta_1} g_1 + \epsilon^{\beta_2} g_2 + \cdots$$

where the thickness of boundary layer γ_0 and the leading order coefficient α_0 are to be determined. Substituting into (5.1.1),

$$\epsilon^{2-4\gamma_0} (\epsilon^{\alpha_0} f_{0tttt} + \epsilon^{\alpha_1} f_{1tttt} + \cdots) =$$

(5.4.6a)

$$\epsilon^{-3\gamma_0} (\epsilon^{2\alpha_0} f_0 f_{0ttt} + \epsilon^{\alpha_0 + \alpha_1} [f_0 f_{1ttt} + f_{0ttt} f_1] + \cdots)$$

$$+ \epsilon^{-\gamma_0} (4 g_0 g_{0t} + 4 \epsilon^{+\beta_1} (g_0 g_{1t} + g_{0t} g_1) + \cdots)$$

$$\epsilon^{2-2\gamma_0} (g_{0tt} + \epsilon^{\beta_1} g_{1tt} + \cdots) =$$

(5.4.6b)

$$\epsilon^{-\gamma_0 + \alpha_0} (g_{0t} f_0 - g_0 f_{0t}) + \epsilon^{-\gamma_0 + \alpha_1} (g_{0t} f_1 - g_0 f_{1t}) +$$

$$\epsilon^{-\gamma_0 + \alpha_0 + \beta_1} (g_{1t} f_0 - g_1 f_{0t}) + \cdots$$

For nontrivial equation for g_0, (that is, $g_{0zz} \neq 0$,) we have

(5.4.7) $$\alpha_0 + \gamma_0 = 2$$

The radial momentum equation then gives

(5.4.8a) $f_{0ttttt} = f_0 f_{0ttt} + 4 g_0 g_{0t}$ $\qquad \alpha_0 = \gamma_0 = 1$

(5.4.8b) $f_{0ttttt} = f_0 f_{0ttt}$ $\qquad \gamma_0 > 1$

Equations (5.4.8) have solution for large t:

(5.4.9a) $f \sim \epsilon^{\alpha_0} \left(f_{0\infty} + O(e^{f_{0\infty} t}) \right) + o(\epsilon^{\alpha_0})$ $\qquad f_{0\infty} < 0$

(5.4.9b) $g \sim O(e^{f_{0\infty} t})$ $\qquad f_{0\infty} < 0$

From (5.4.9b) we observe B_0 in (5.4.4) must satisfy

(5.4.10) $B_0 = 1$

The matching of the zeroth and first order terms of f implies

(5.4.11) $a_0 + 2\gamma_0 = \alpha_1$

(5.4.12) $a_1 = \alpha_0$

Higher order coefficients a_K, α_K, β_K can in this way be determined.

For example $(a_o, \alpha_o; \gamma_o) = (0, 1; 1)$ gives the singular perturbation construction for our bifurcated solutions. The $\gamma = -1$ solution of Branch 9 is another example. Indeed it seems many large amplitude solution branches can be constructed. That is, $(a_o, \alpha_o; \gamma_o)$ can be $(-1, 0; 2)$, $(-2, 0; 2)$, etc..

To end this chapter, we like to comment on what we have learnt and what we can expect in future endeavor. Our computational experiments and the solution constructions in this chapter seem to indicate the problem has an infinite number of solutions, with the number of cells tending to infinity. Secondly, the analysis of McLeod on the flow in an semi-infinite region bounded by a rotating disk [20] and our results of Chapters 4 and 5 lead us to strongly suspect Batchelor's conjecture is not possible, though we believe transition-layer type solutions may exist. Thirdly, the many different boundary-layer - inviscid expansions, some of which are listed in Section 5.1, and the removal of the properties of odd solutions and even solutions about $z = 0.5$ (5.1.10)-(5.1.11) lead us to believe other forms of solutions may exist. Fourthly, the γ -sign-independent behaviour in Chapter 4 may give us further insight in the construction analysis. Lastly, we ask are there more

bifurcation points on the Stewartson's solution branch?

APPENDIX: A NOTE ON MIXED PIVOTING STRATEGY FOR GAUSSIAN ELIMINATION

Let us consider the linear system of equations

$$Ax = b \tag{A.1.1}$$

where A is a (n x n) matrix, x is the solution and b is the given right hand side. In this appendix we give a new pivoting strategy for the solution of (A.1.1) by Gaussian elimination.

The matrix A is decomposed into lower and upper triangular matrices L and U. The decomposition consists of computing sequences of matrices $A^{(k)}$, $k = 1,2,.....,n$, where $A^{(1)} = A$. For $k \geq 2$, the matrix $A^{(k)}$ has zeros below the diagonal in the first $(k - 1)$ columns; $A^{(k+1)}$ is obtained from $A^{(k)}$ by subtracting a multiple of the k-th row from each

of the rows below it, (The 'multipliers' $a_{ik}^{(K)}/a_{kk}^{(K)}$ in general are different for each of the (n - k - 1) rows.) and the rest of $A^{(K)}$ is left unchanged. Thus assuming $a_{kk}^{(K)}$ is nonzero, we have

$$(A.1.2) \qquad L \equiv \begin{pmatrix} 1 & & & \\ m_{21} & 1 & & 0 \\ m_{31} & m_{32} & \ddots & \\ \vdots & \vdots & \ddots & \ddots \\ m_{n1} & m_{n,2} & \cdots & m_{n,n-1} \end{pmatrix} \quad U \equiv A^{(n)} = \begin{pmatrix} a_{1,1}^{(1)} & a_{1,2}^{(1)} & \cdots & a_{1,n}^{(1)} \\ & a_{2,2}^{(2)} & \cdots & a_{2,n}^{(2)} \\ & & \ddots & \vdots \\ & 0 & & a_{n,n}^{(n)} \end{pmatrix}$$

$$(A.1.3) \qquad m_{ik} = \frac{a_{i,k}^{(k)}}{a_{k,k}^{(k)}} \qquad i \geq (k+1)$$

$$(A.1.4) \qquad a_{ij}^{(K)} = \begin{cases} 0 & i \geq (k+1) \ , \ j = k \\ a_{ij}^{(K)} - m_{ik} a_{kj}^{(K)} & i \geq (k+1) \ , \ j \geq (k+1) \\ a_{ij}^{(K)} & \text{otherwise} \end{cases}$$

In the course of Gaussian elimination round-off error will, in general, be present. This error is inherent in computations because machines can only retain a finite number of digits. Let E be the round-off error matrix, that is

$$(A.1.5) \qquad LU = A + E$$

To determine E let us consider any real number x. When x is stored in the machine, it has been rounded-off to x_R, and can be represented

(A.1.6) $$x_R = x(1+\delta) \qquad |\delta| << 1$$

Using (A.1.6) the computation of the multiplers m_{ik} in the machine gives

$$m_{ik} = \frac{a_{ik}^{(k)}}{a_{kk}^{(k)}} (1+\delta_{ik})$$

Simplifying,

$$m_{ik} a_{kk}^{(k)} - a_{ik}^{(k)} = a_{ik}^{(k)} \delta_{ik}$$

This gives

(A.1.7) $$\epsilon_{ik}^{(k)} = a_{ik}^{(k)} \delta_{ik} \qquad i \geq k+1$$

which is the round-off error made by setting $a_{ik}^{(k+1)}$ equal to zero. Similarly for computations in (A.1.5) we obtain

$$a_{ij}^{(k+1)} = \left(a_{ij}^{(k)} - m_{ik} a_{kj}^{(k)} (1+\delta_{ik}) \right) \Big/ (1+\tilde{\delta}_{ij})$$

Hence

(A.1.8) $$\epsilon_{ij}^{(k+1)} = -m_{ik} a_{kj}^{(k)} \delta_{ik} - a_{ij}^{(k+1)} \tilde{\delta}_{ij} \qquad i,j \geq k+1$$

is the round-off error in the computation of $a_{ij}^{(k+1)}$.

Define matrices $E^{(k)} \equiv (\epsilon_{ij}^{(k)})$ and $L^{(k)} \equiv (\ell_{ij}^{(k)})$:

$$\text{(A.1.9a)} \qquad \ell_{ij}^{(k)} = \begin{cases} m_{ik} & i > k \ , \ j = k \\ 0 & \text{otherwise} \end{cases}$$

$$\text{(A.1.9b)} \qquad \epsilon_{ij}^{(k)} = \begin{cases} a_{ik}^{(k)} \delta_{ik} & i \geq k+1 \ , \ j = k \\ -m_{ik} a_{kj}^{(k)} \delta_{ij} - a_{ij}^{(k+1)} \tilde{\delta}_{ij} & i,j \geq k+1 \\ 0 & \text{otherwise} \end{cases}$$

Then the k-th stage of elimination can be written as

$$\text{(A.1.10)} \qquad A^{(k+1)} = A^{(k)} - L^{(k)} A^{(k)} + E^{(k)} \ , \qquad k = 1, 2, \ldots, n-1$$

But $L^{(k)} A^{(k)}$ depends only on the k-th row of $A^{(k)}$ which is the same as the k-th row of $A^{(n)}$. Adding (A.1.10) for $k = 1,2,\ldots..(n-1)$ yields

$$(L^{(1)} + L^{(2)} + \ldots.) A^{(n)} = A^{(1)} + E^{(1)} + E^{(2)} + \ldots. + E^{(n-1)}$$

$$LU = A + E$$

where

$$\text{(A.1.11)} \qquad E = \sum_{k=1}^{n-1} E^{(k)}$$

From equations (A.1.9) and (A.1.11) Wilkinson [32] observed that it is advisable to keep the multiplers less than or equal to one in absolute value. That is, the pivot $a_{kk}^{(k)}$ should satisfy

$$|a_{kk}^{(k)}| \geq |a_{j,k}^{(k)}| \qquad j \geq k$$

Taking the pivot to be the element of largest absolute value in a column (row) is called partial row (column) pivoting; and taking the pivot to be the element of largest absolute value in the whole matrix A at the k-th step of Gaussian elimination is called complete pivoting. It is evidently clear from (A.1.9) that complete pivoting gives the smallest possible round-off error. However, it takes machine time to search for pivots. At the k-th stage of Gaussian elimination, partial column or partial row pivoting takes (n - k + 1) searches while full pivoting takes (n - k + 1) searches. For a complete LU-factorization of a (n x n) matrix partial pivoting takes (n(n + 1) - 2)/2 searches, and full pivoting takes (n(n + 1)(2n + 1) - 6)/6 searches. For very large matrix it may not be practical to use full pivoting.

We introduce a new pivoting strategy called mixed pivoting: At the k-th stage of Gaussian elimination, $a_{kk}^{(k)}$ is chosen to be the largest element in absolute value along the k-th row and the k-th column of A :

$$|a_{kk}^{(k)}| \geq |a_{j,k}^{(k)}|, |a_{k,j}^{(k)}| \qquad j > k \tag{A.1.12}$$

That is, we do row (column) pivoting if the largest element lies on a column (row). In terms of round-off error, we observe that

$$\begin{aligned} |a_{ik}^{(k)}|_{\text{mixed}} &\leq |a_{ik}^{(k)}|_{\text{partial}} \\ |m_{ik} a_{kj}^{(k)}|_{\text{mixed}} &\leq |m_{ik} a_{kj}^{(k)}|_{\text{partial}} \end{aligned} \tag{A.1.13}$$

Evidently from (A.1.9) and (A.1.11) we have

$$\|E\|_{\text{full}} \leq \|E\|_{\text{mixed}} \leq \|E\|_{\text{partial}} \tag{A.1.14}$$

Of course, complete pivoting will in general gives the least round-off. However the price is high in that the operation count for the searches of pivots is $O(n^3)$, compared to $O(n^2)$ for mixed pivoting which, in turn, is approximately twice that of partial pivoting.

The following example (Wilkinson) shows the potential of this new mixed pivoting strategy.

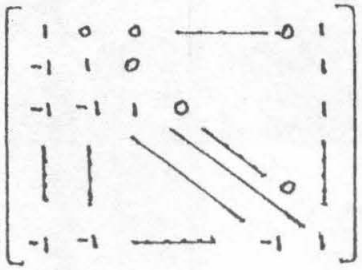

Using partial column pivoting strategy, we obtain

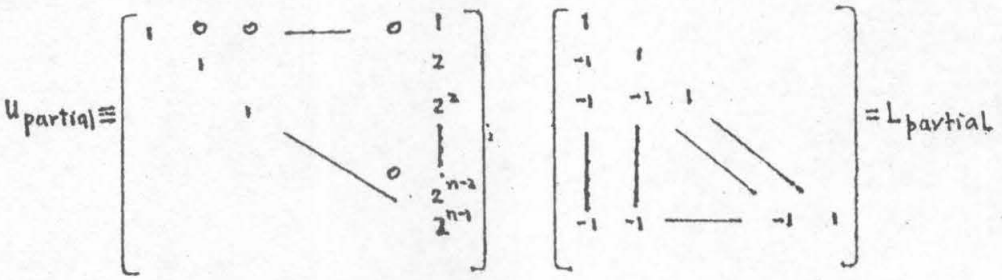

Using mixed pivoting strategy, we get (neglecting the permutation matrices)

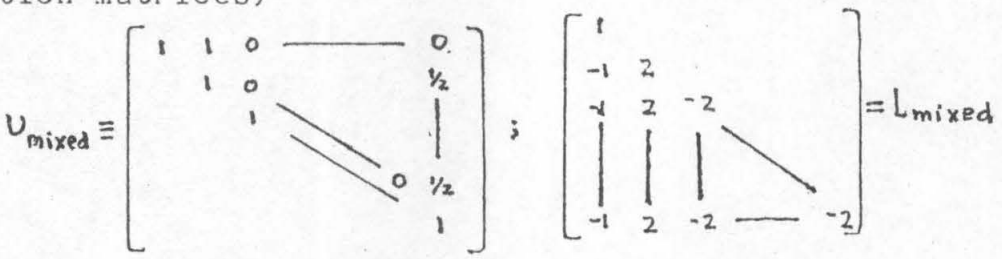

We observe in this example mixed pivoting strategy has the same desired result as when complete pivoting strategy is used.

For singular matrices, partial column (row) pivoting at the k-th stage of Gaussian elimination fails if $a_{\ell,k}^{(k)}$ ($a_{k,\ell}^{(k)}$), $l \geq k$, are all zero. We observe the new mixed pivoting allows the elimination process to continue unless all elements along both the k-th row and k-th column of $A^{(k)}$ are zero.

Although there are examples in which the largest element in absolute value always lies outside the searched column-row for mixed pivoting strategy, we see that it can cope with a larger class of matrix equations than partial pivoting can and yet the number of searches for pivots is kept within very reasonable limits. Indeed the probability of finding the largest element in absolute value in a searched area increases as we increase the number of row and column searches. But unfortunately the amount of work (searches) increases also approximately at the same rate. Hence to alleviate the problem that the largest element always lies inside (n - 1) of the submatrix (n + 1 - 1) at the k-th stage of elimination we can search one more row-column cyclically. That is, in addition to the leading row-column we search (n - (k - 1)mod(n/j)) row-column, for some j. Because we are interested in 'catching' the largest element in the submatrix, we see that this cyclic search is

better in general than searching two adjacent row-columns. To clarify our cyclic pivoting strategy let us consider a (10 x 10) matrix and let j be equal to 2. Then the row-column searches for the first five stages of Gaussian elimination are: (1,20), (2,19), (3,18), (4,17) and (5,16).

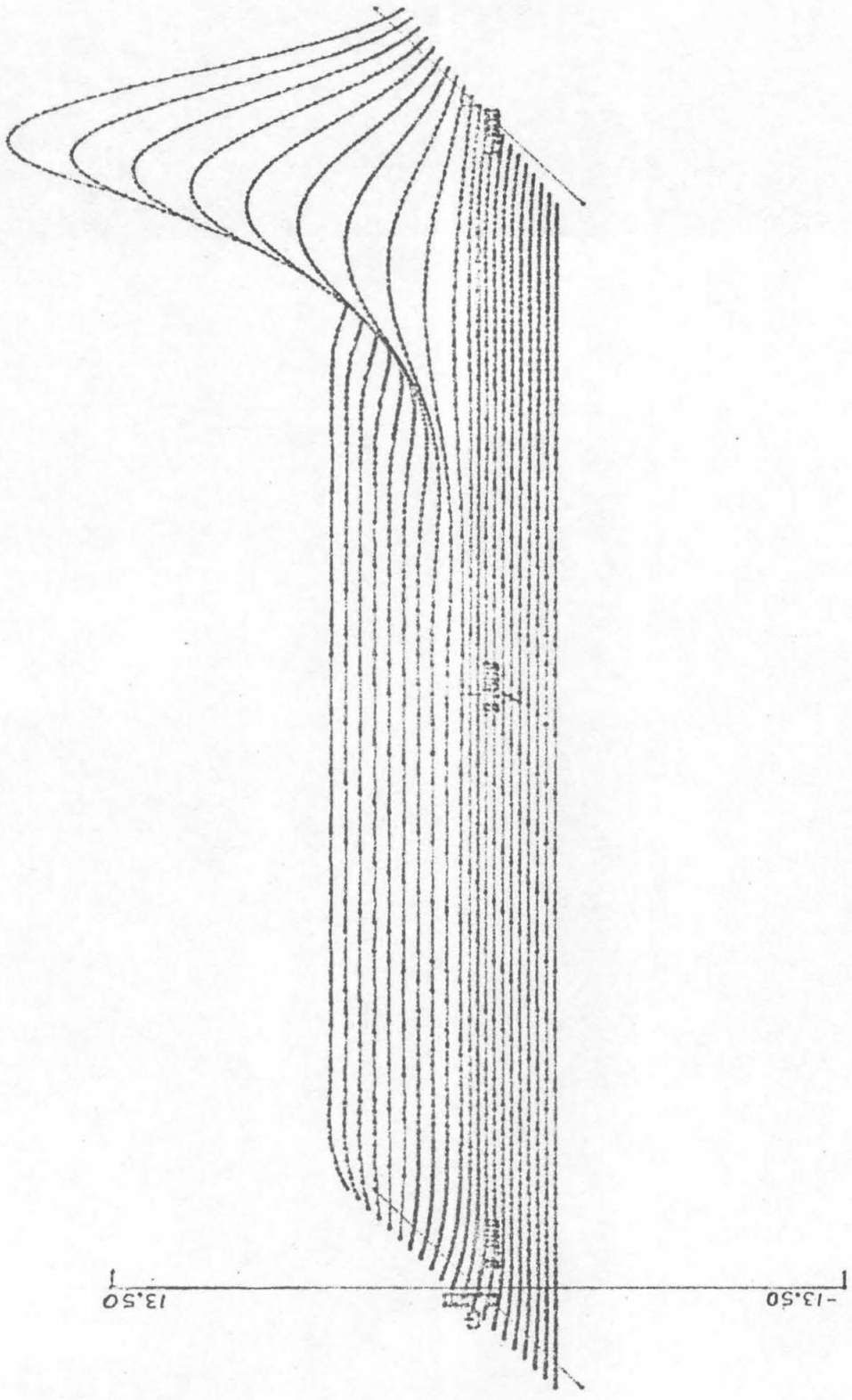

Figure 4.8 a :- Branch 1 - Solid Body Branch — Angular velocity

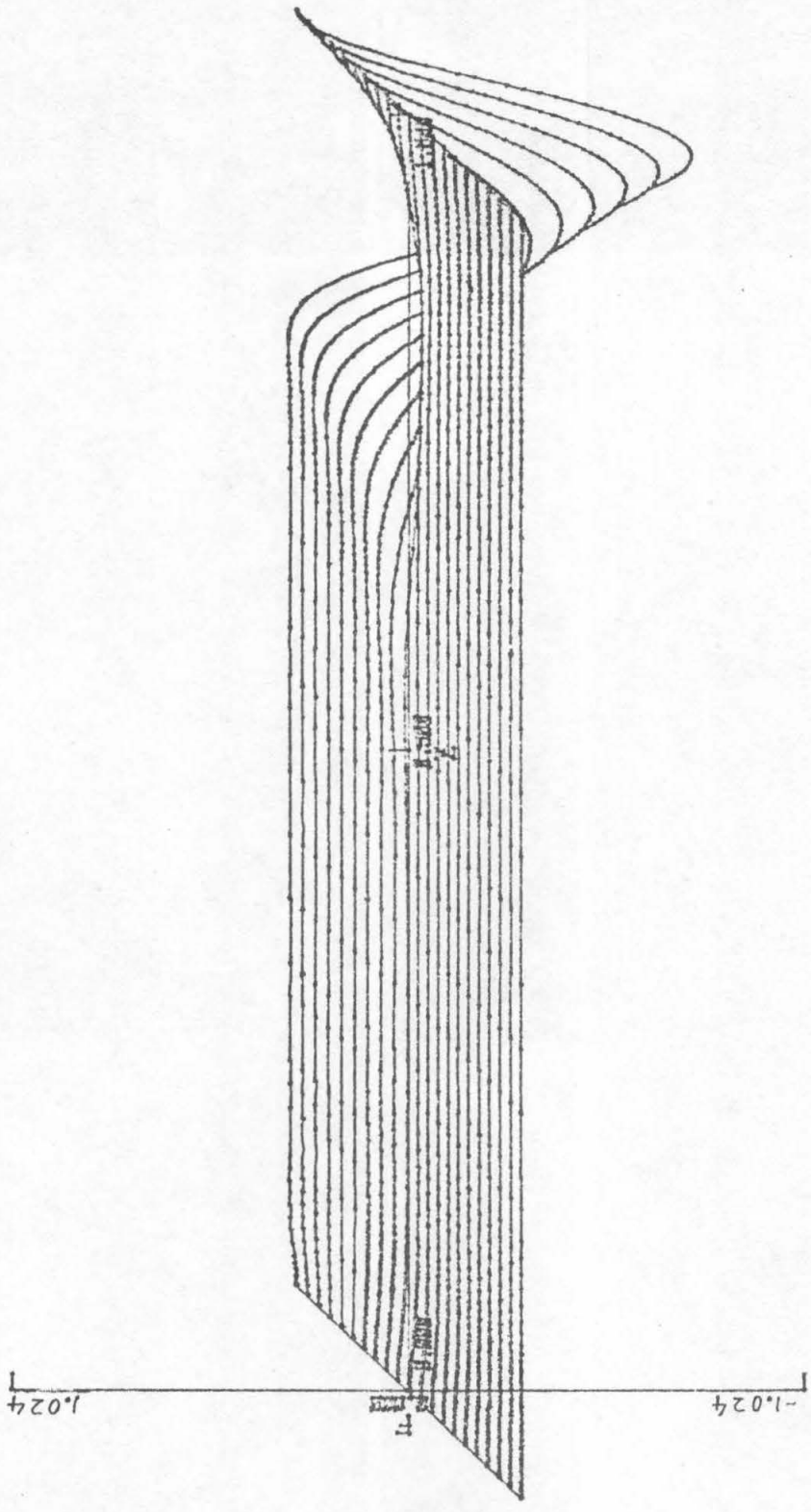

figure 4.8b :- Branch 1 - Solid Body Branch - Axial Velocity

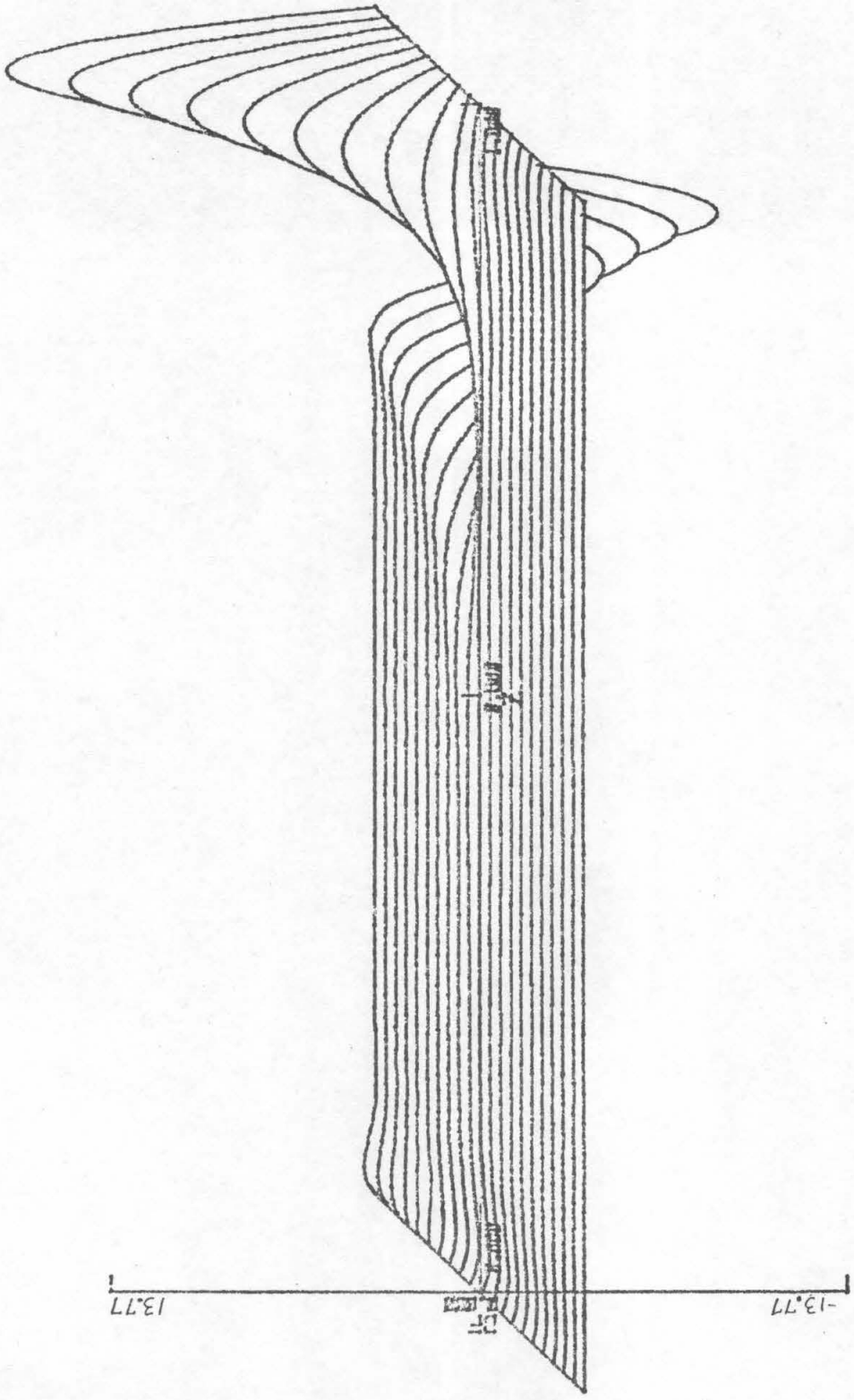

Figure 4.8 c :- Branch 1 - Solid Body Branch - Radial Velocity

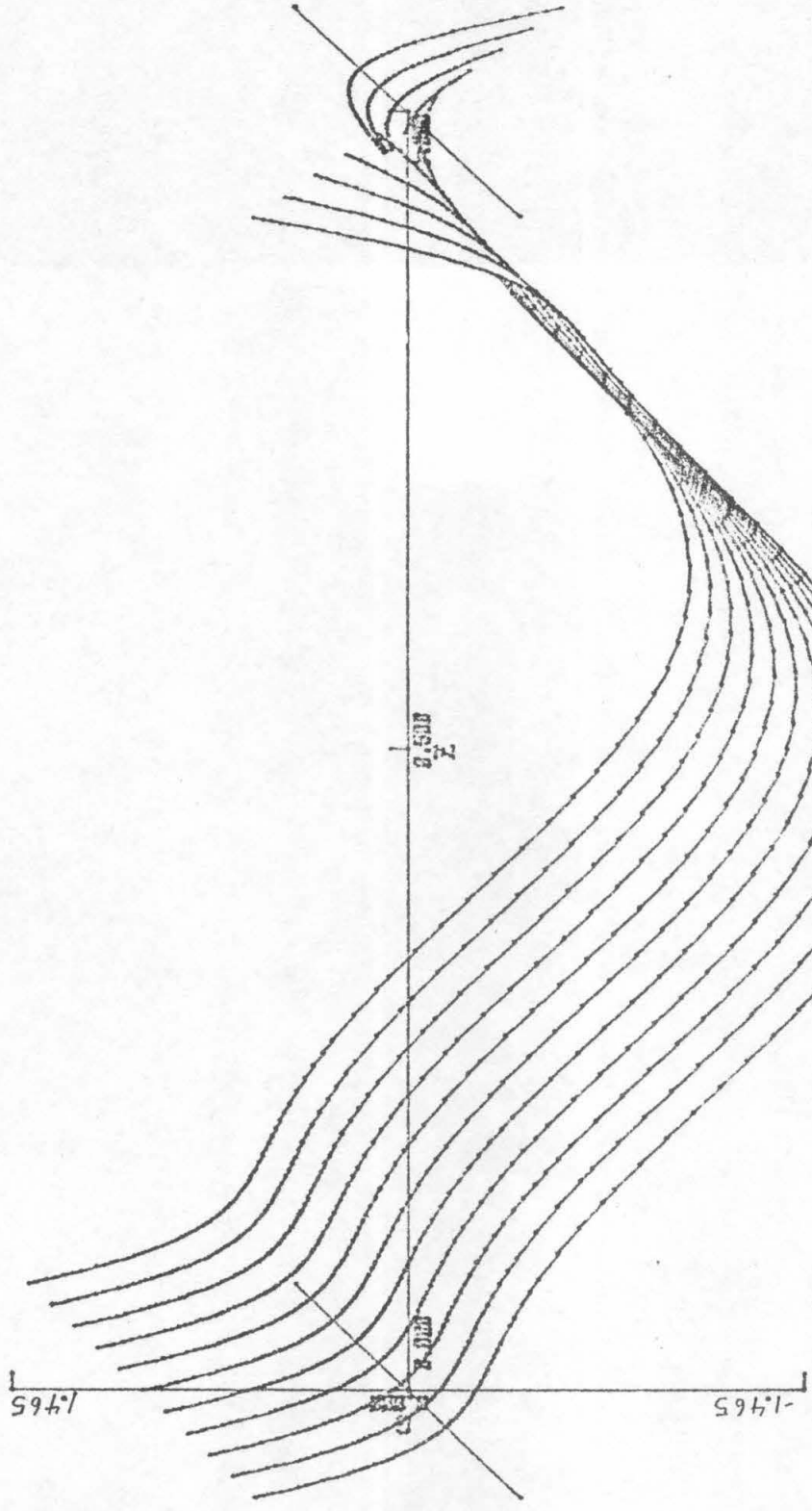

Figure 4.9 a : Branch 2 - Bifurcation Negative Branch — Angular velocity

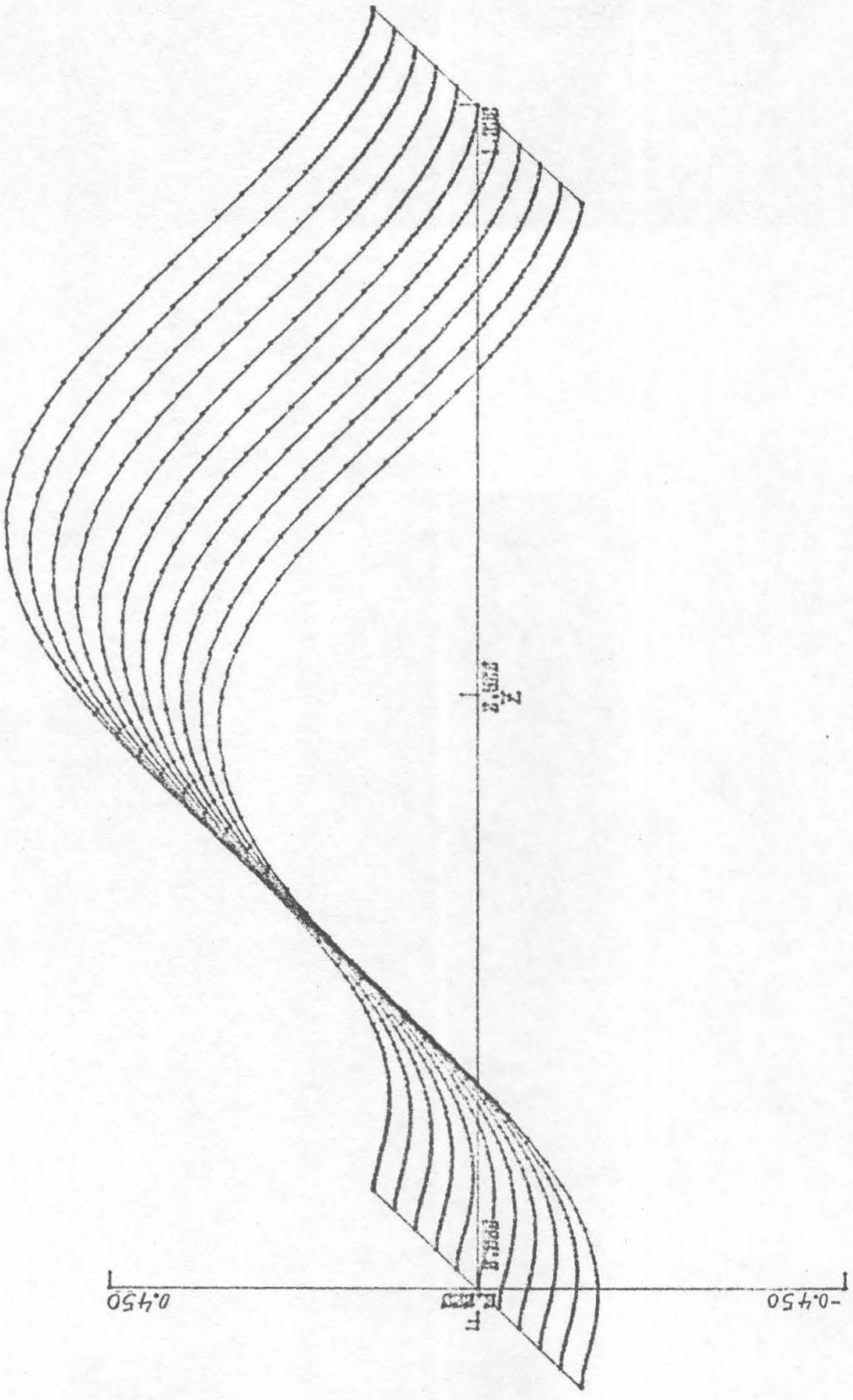

Figure 4.9 b :- Branch 2 - Bifurcation Negative Branch — Axial Velocity

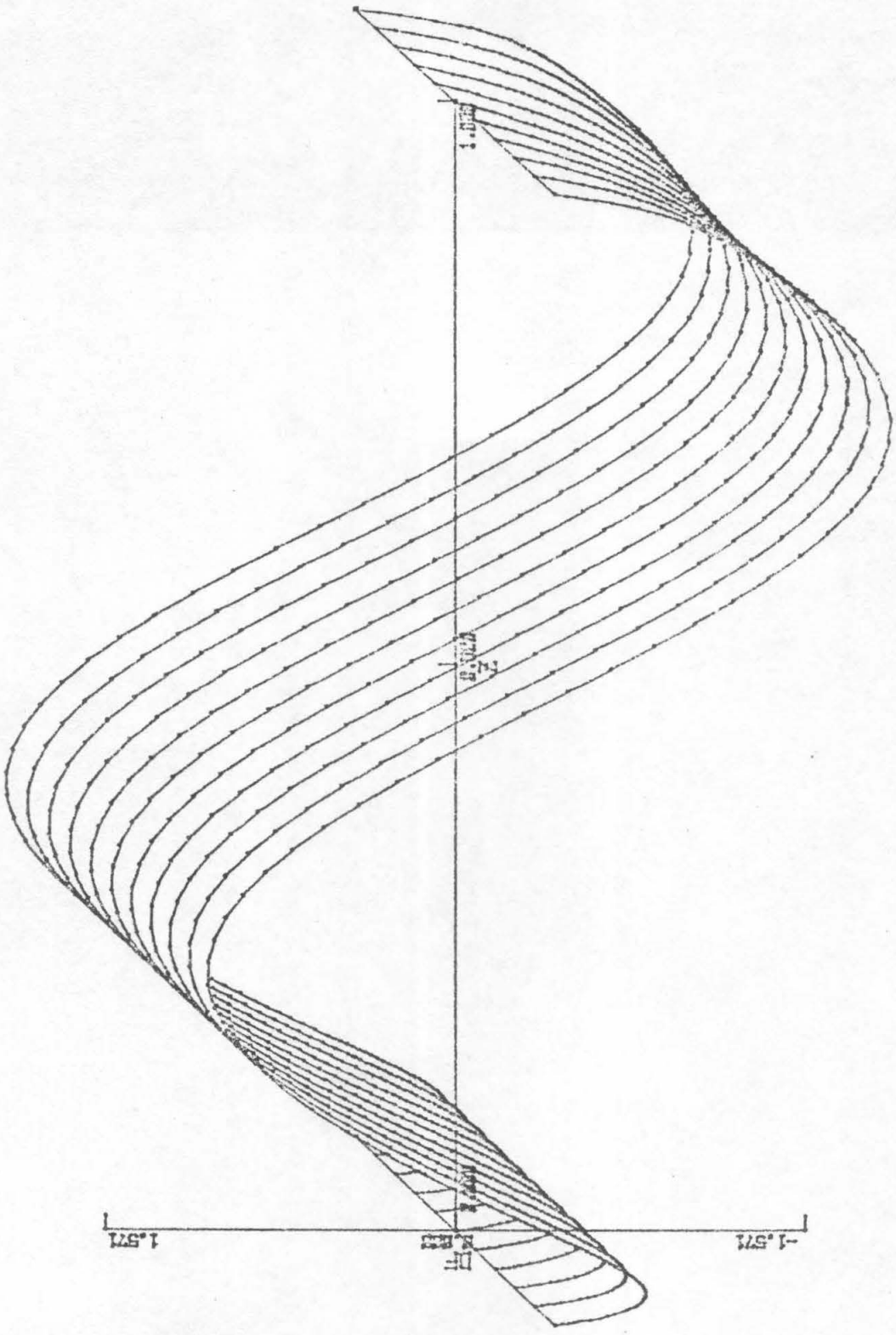

Figure 4.9c :- Branch 2 — Bifurcation Negative Branch — Radial Velocity

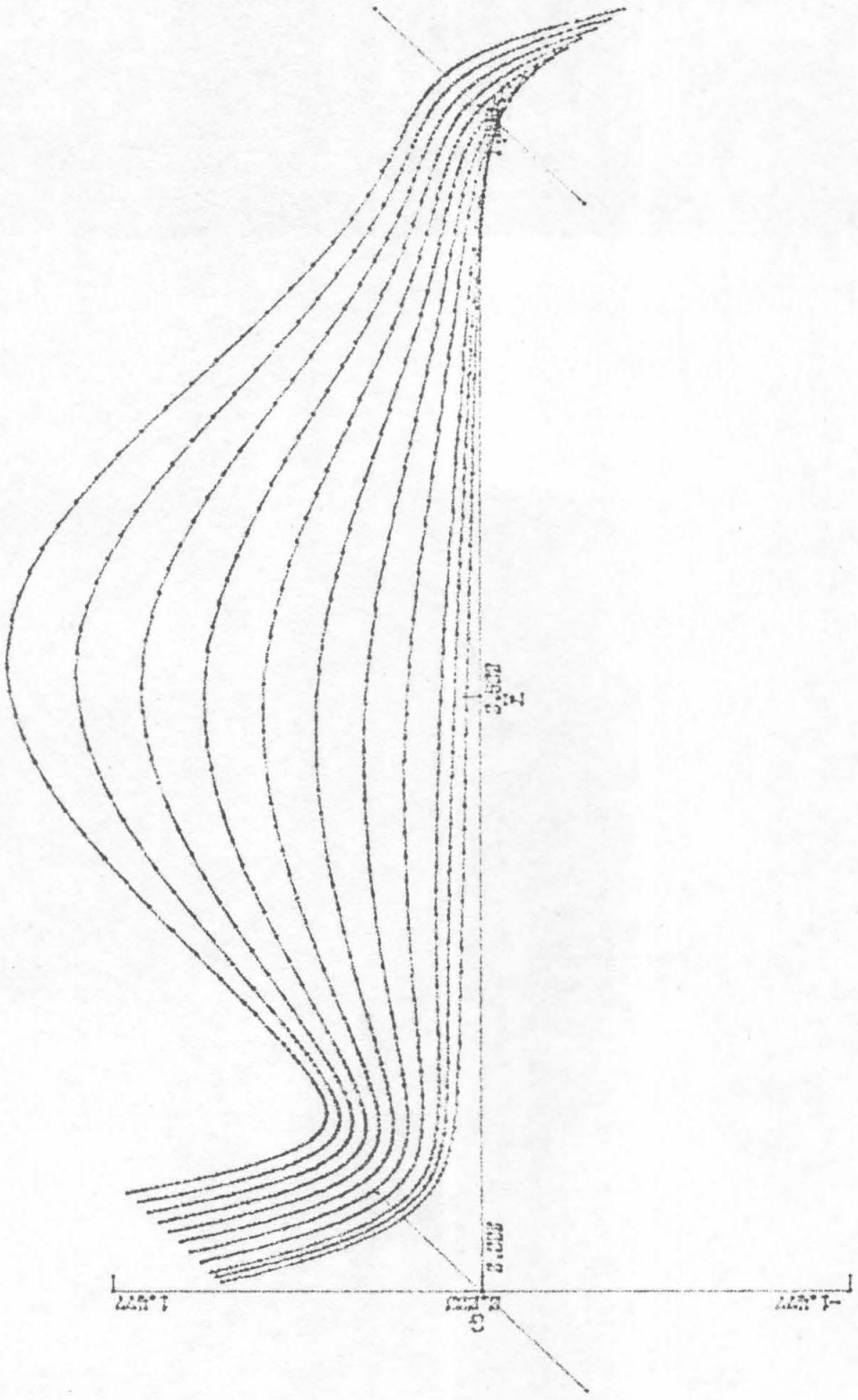

Figure 4.10 a :- Branch 3 — Bifurcation Positive Branch A - Angular Velocity

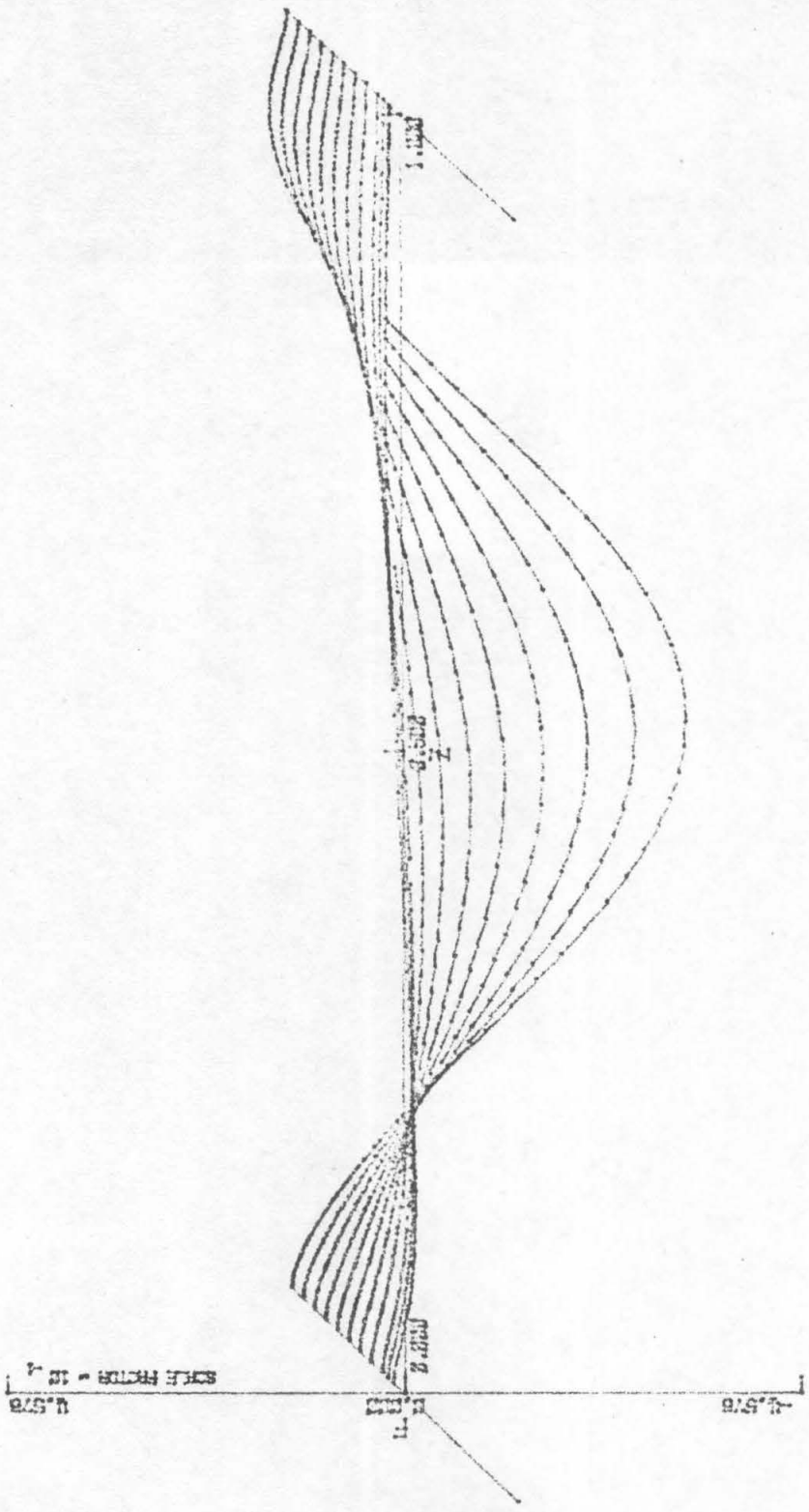

Figure 4.10 b : Branch 3 — Bifurcation positive Branch A — Axial Velocity

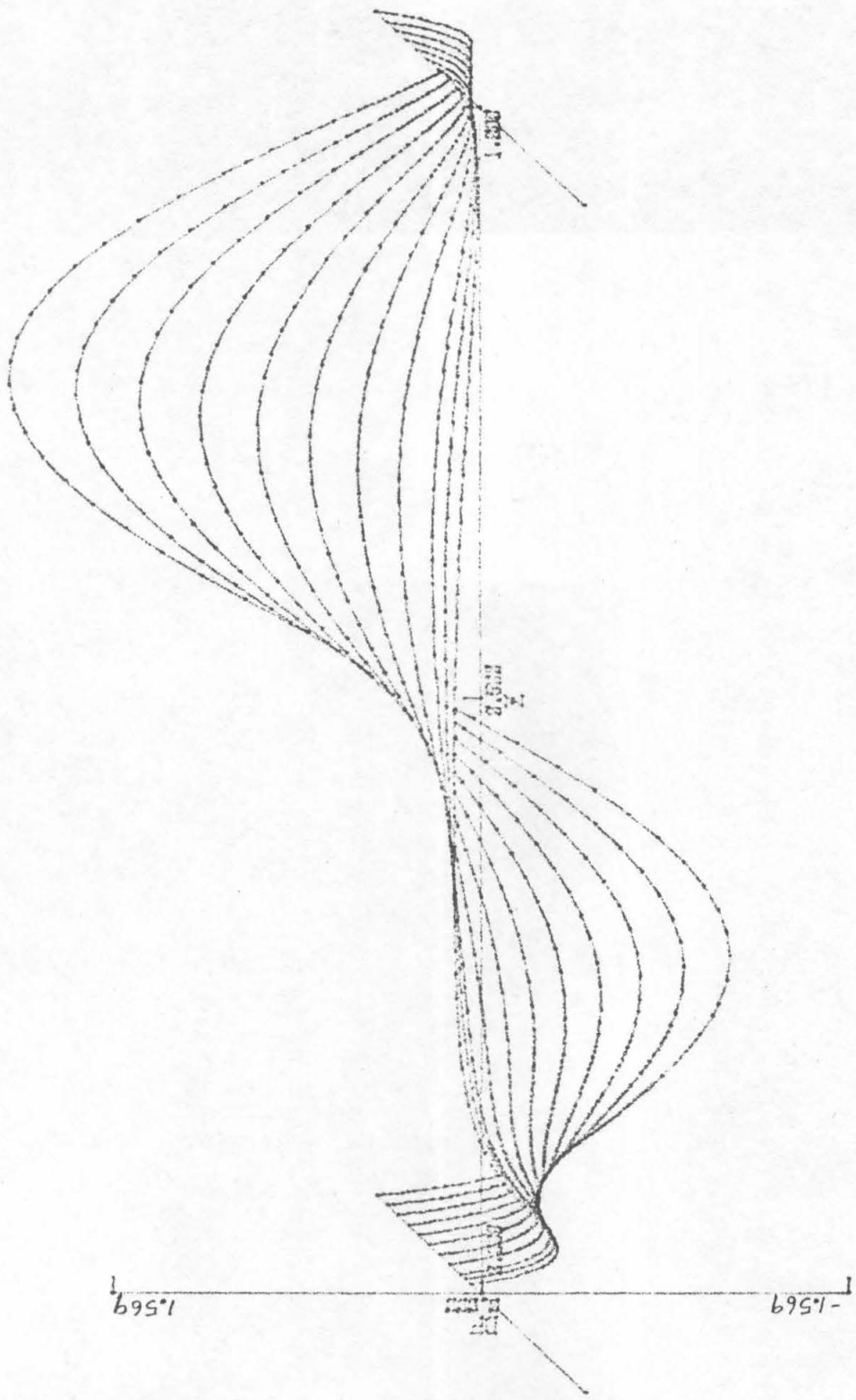

Figure 4.10c:- Branch 3 — Bifurcation Positive Branch A: Radial Velocity

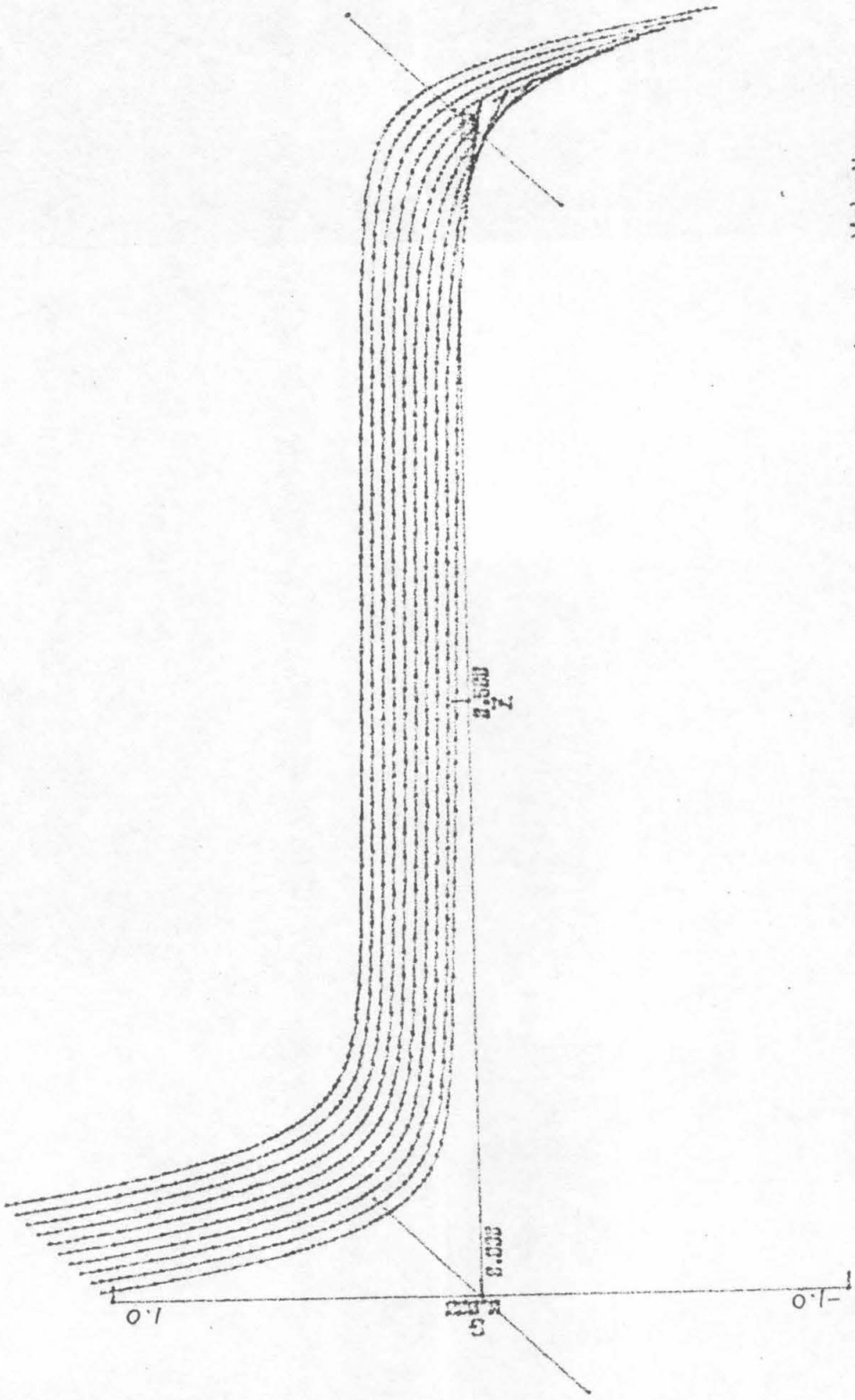

Figure 4.11 a:: Branch 4 - Bifurcation Positive Branch B - Angular Velocity

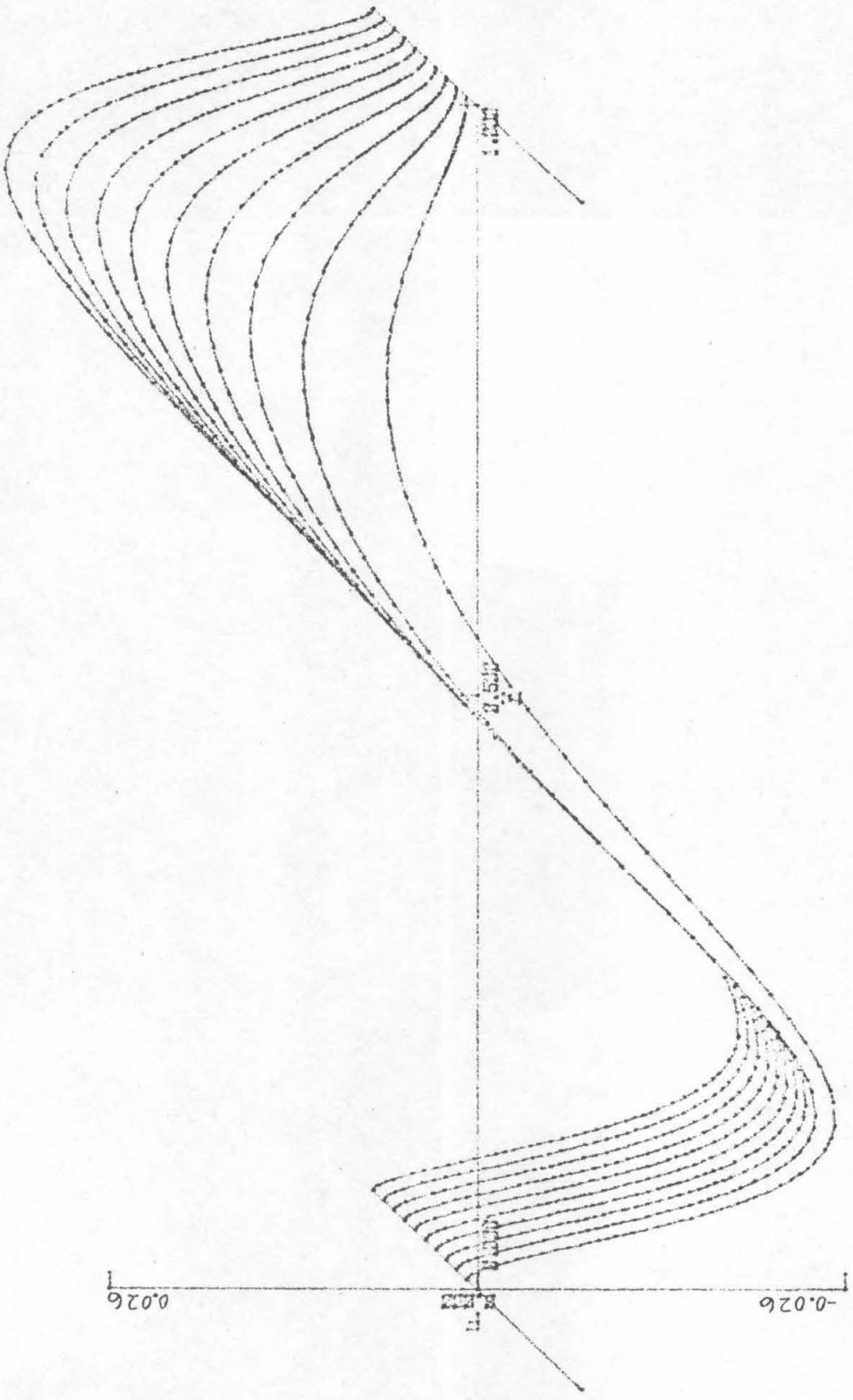

Figure 4.11b:- Branch 4 - Bifurcation Positive Branch B - Axial Velocity

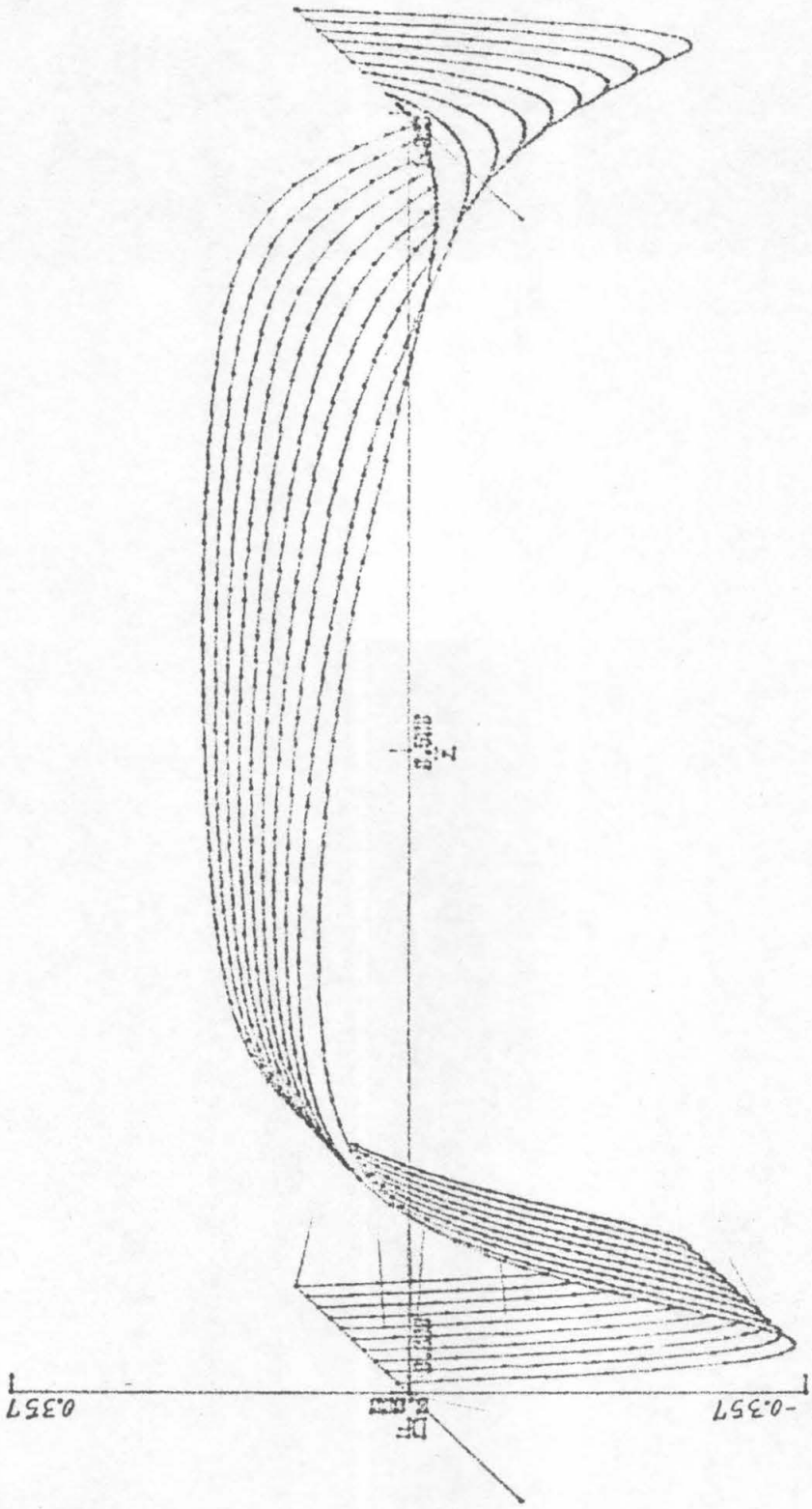

Figure 4.11c : Branch 4 – Bifurcation Positive Branch B – Radial Velocity

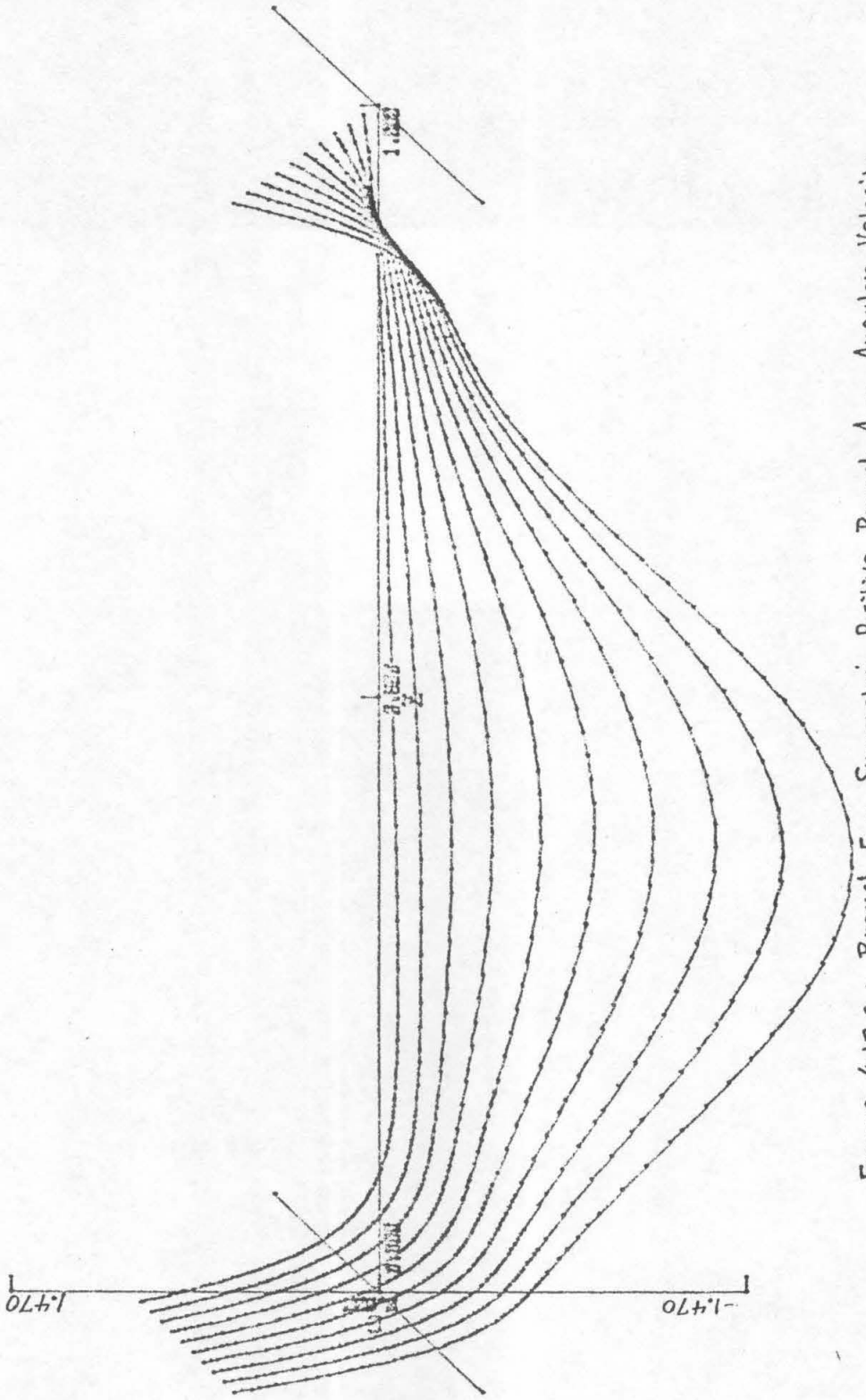

Figure 4.12a :- Branch 5 - Symmetric Positive Branch A - Angular Velocity

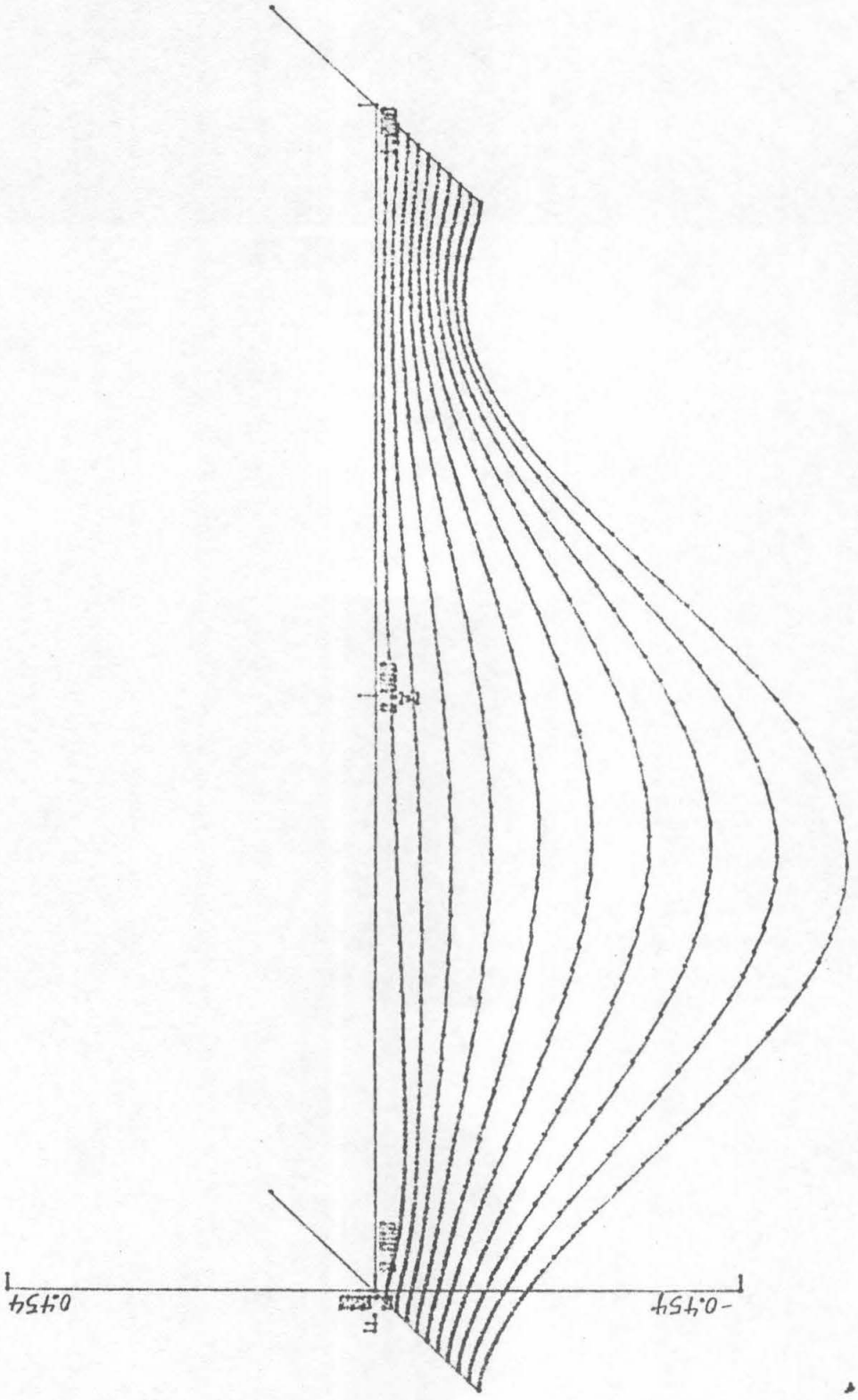

Figure 4.12 b: Branch 5 — Symmetric Positive Y Branch A — Axial Velocity

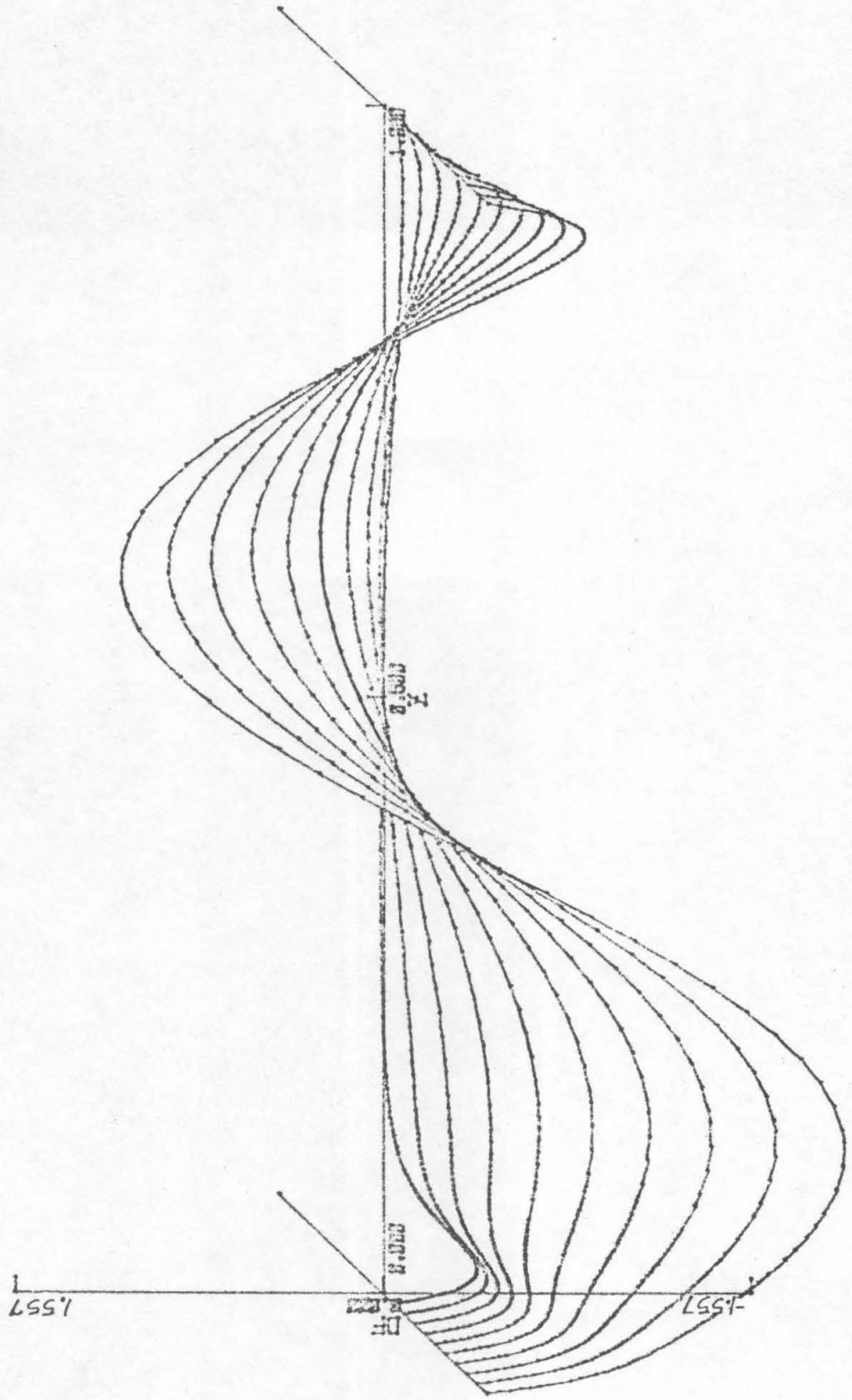

Figure 4.12c :- Branch 5 — Symmetric Positive γ Branch A — Radial Velocity

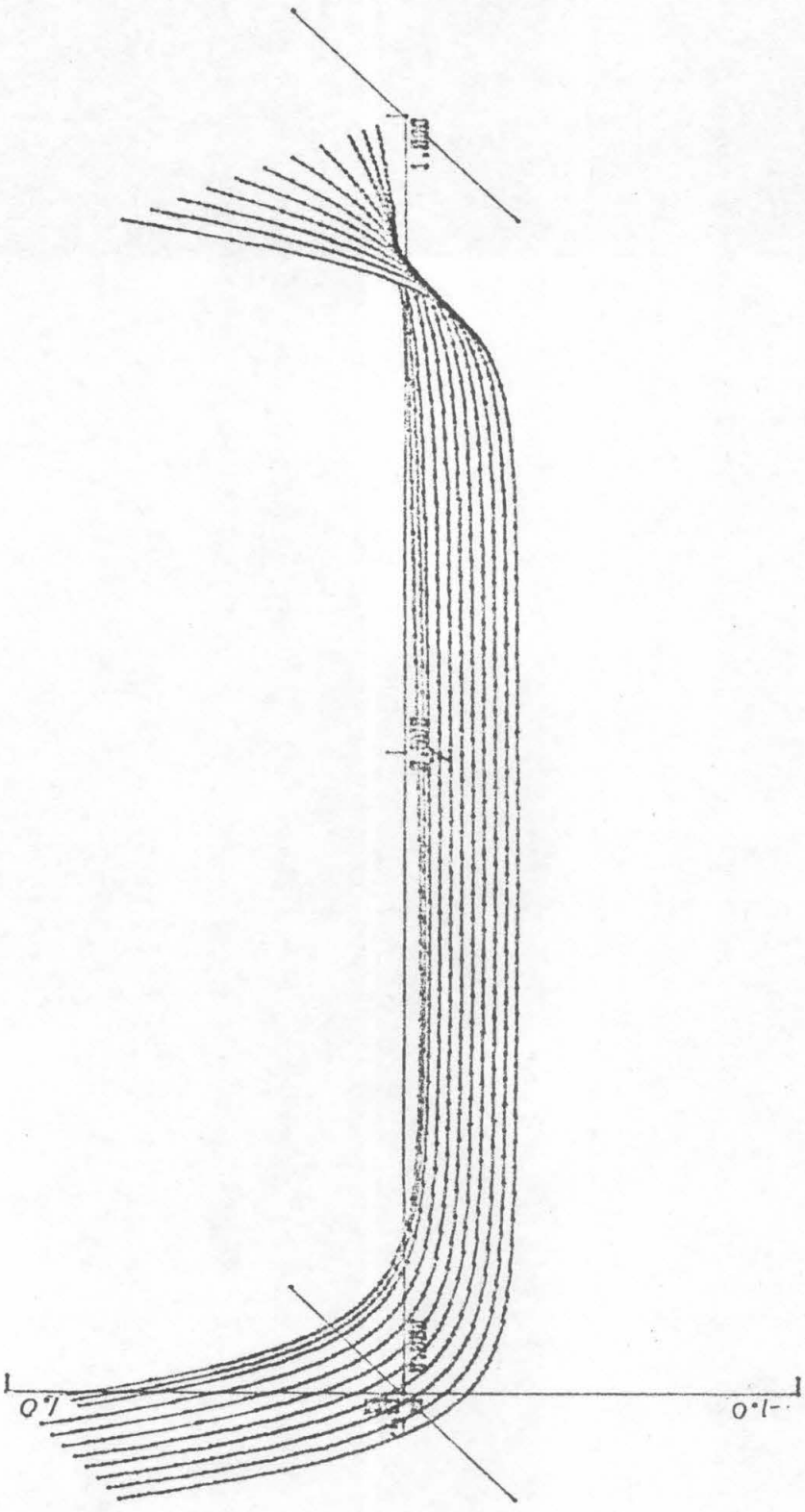

Figure 4.13a : Branch 6 — Symmetric Positive & Branch 8 — Angular Velocity

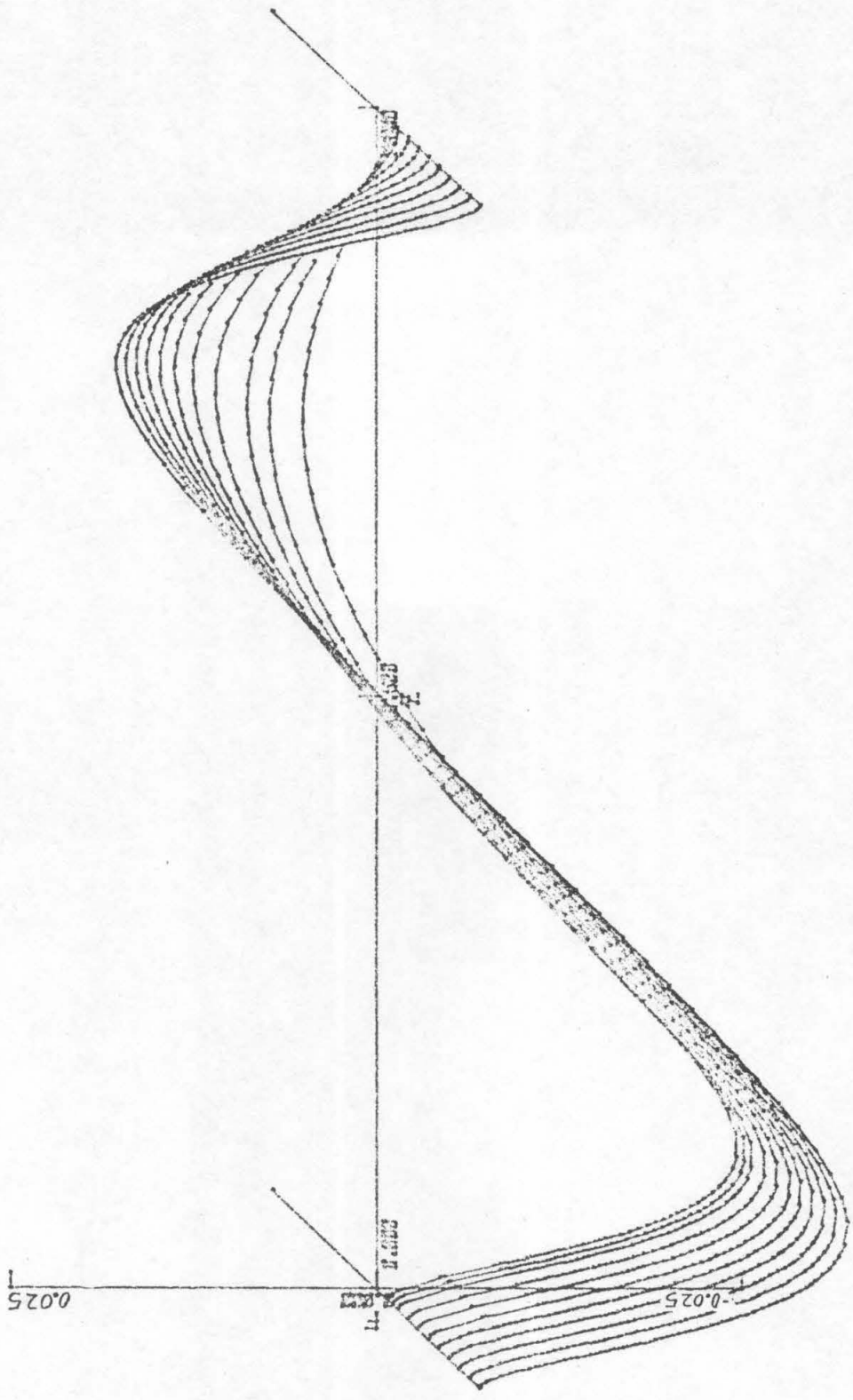

Figure 4.13b:- Branch 6 — Symmetric Positive γ Branch B — Axial Velocity

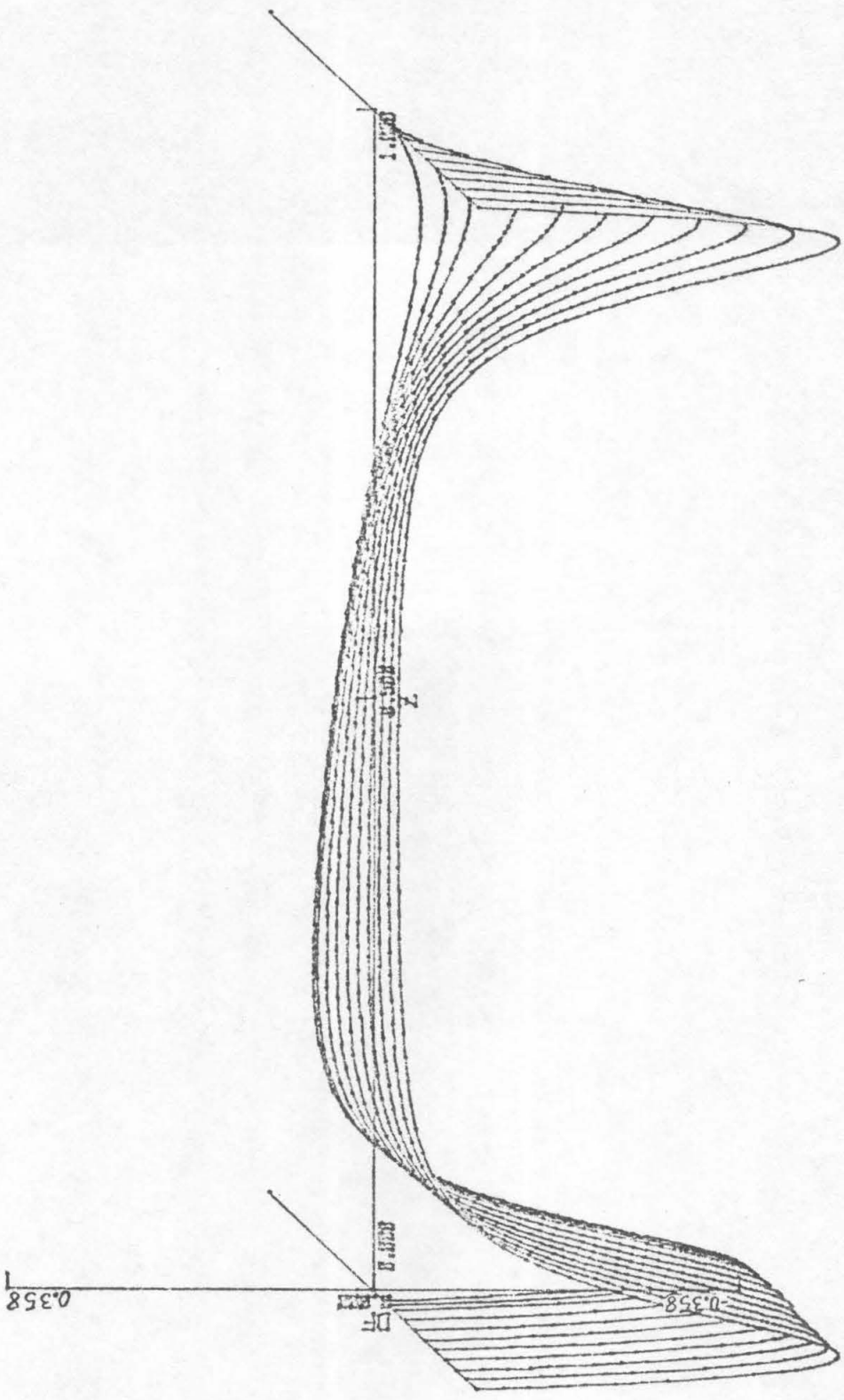

Figure 4.13 C :- Branch 6 — Symmetric Positive Y Branch — Radial Velocity

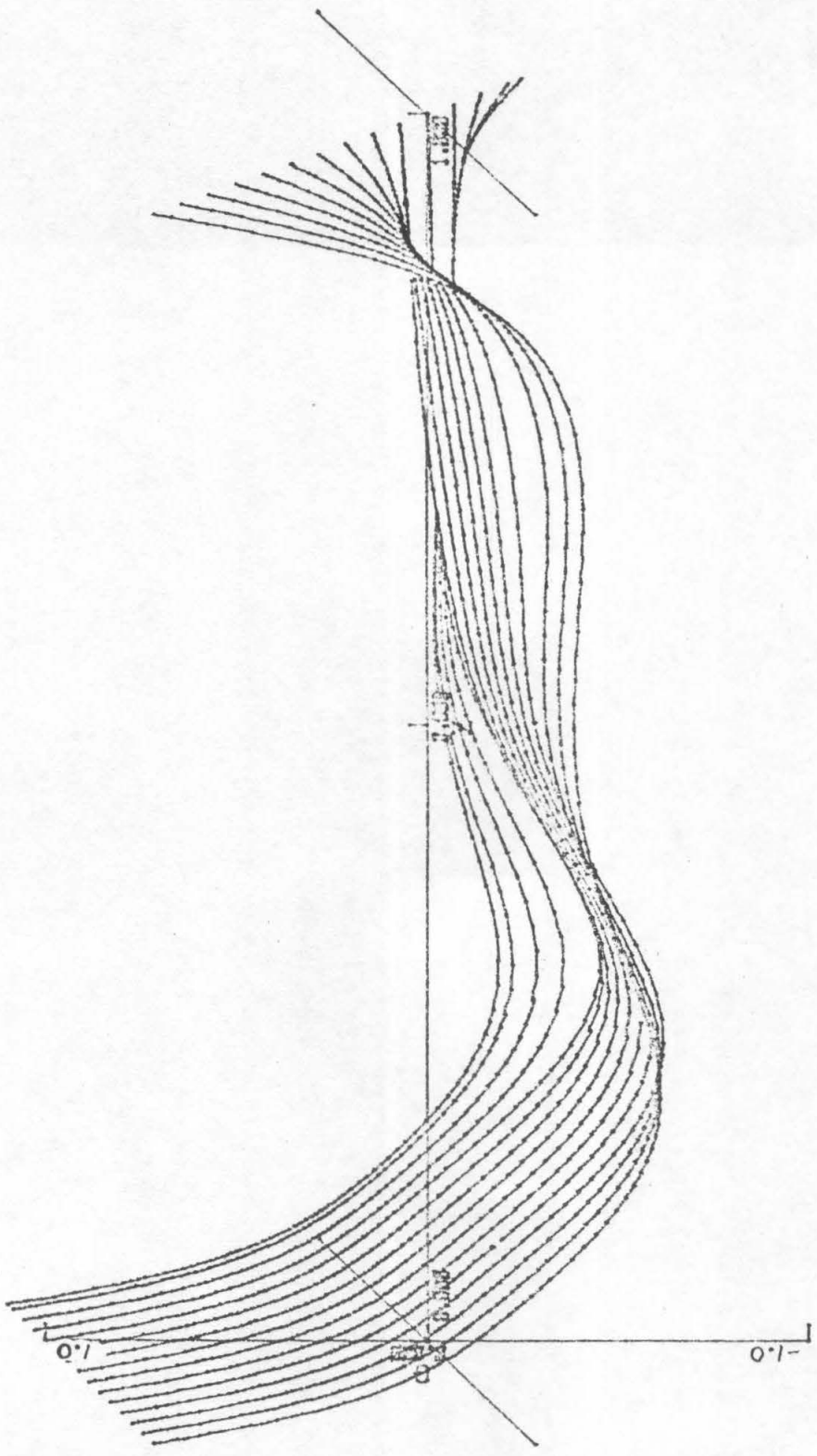

Figure 4.14 a :- Branch 7 - Angular Velocity

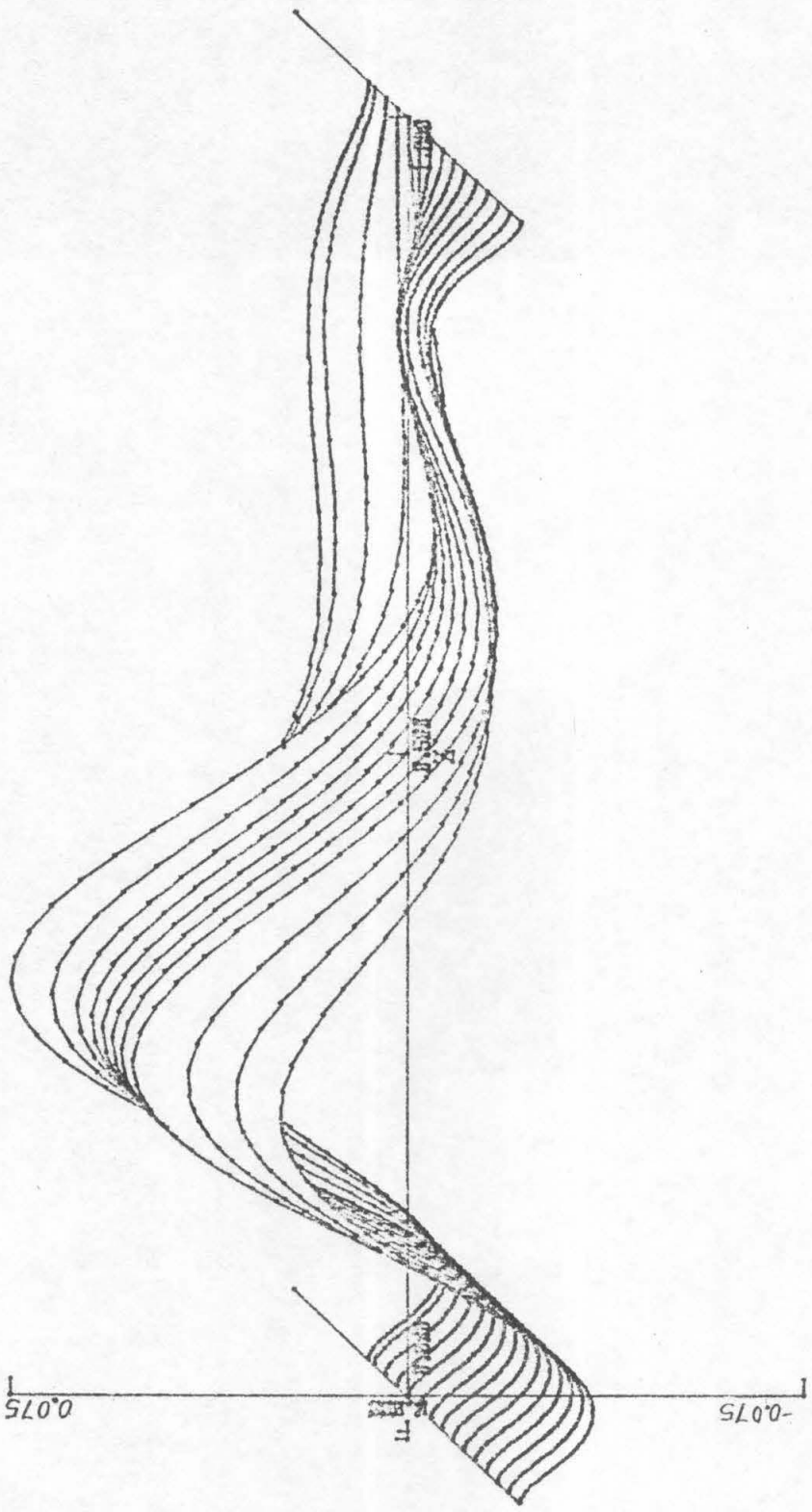

Figure 4.14 b :- Branch 7 - Axial Velocity

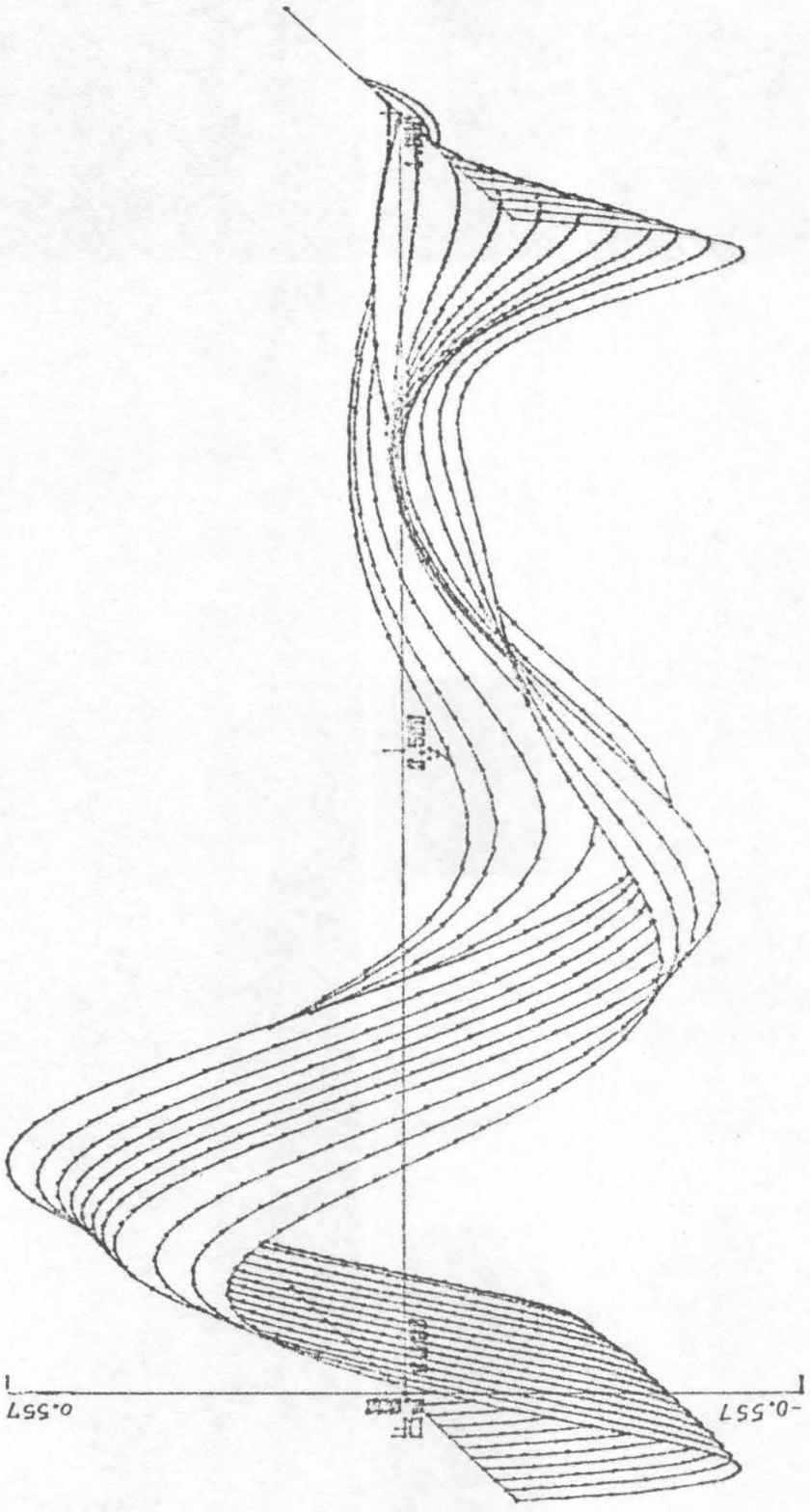

Figure 4.14 c :: Branch 7 - Radial Velocity

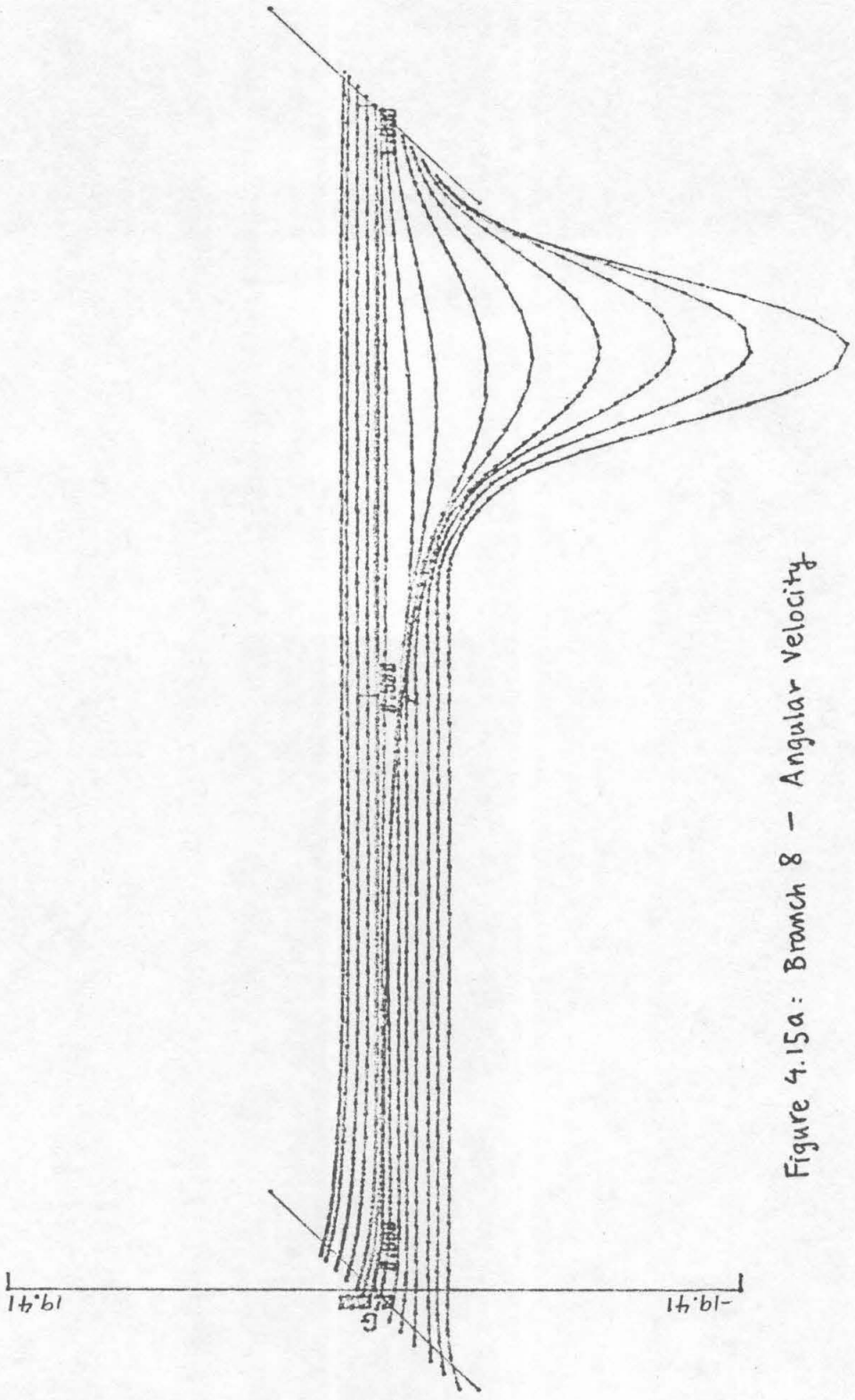

Figure 4.15a: Branch 8 - Angular Velocity

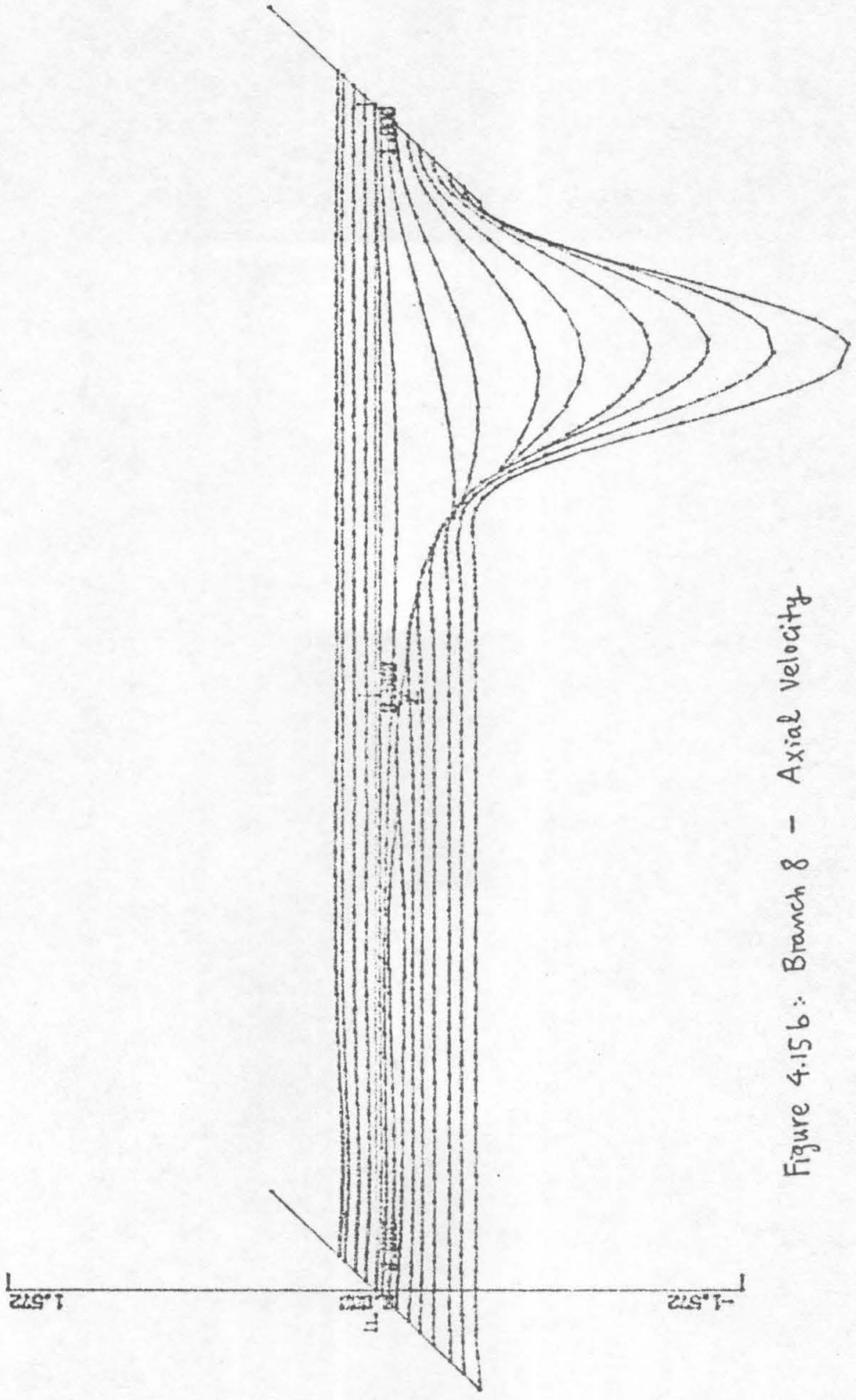

Figure 4.15b: Branch 8 - Axial Velocity

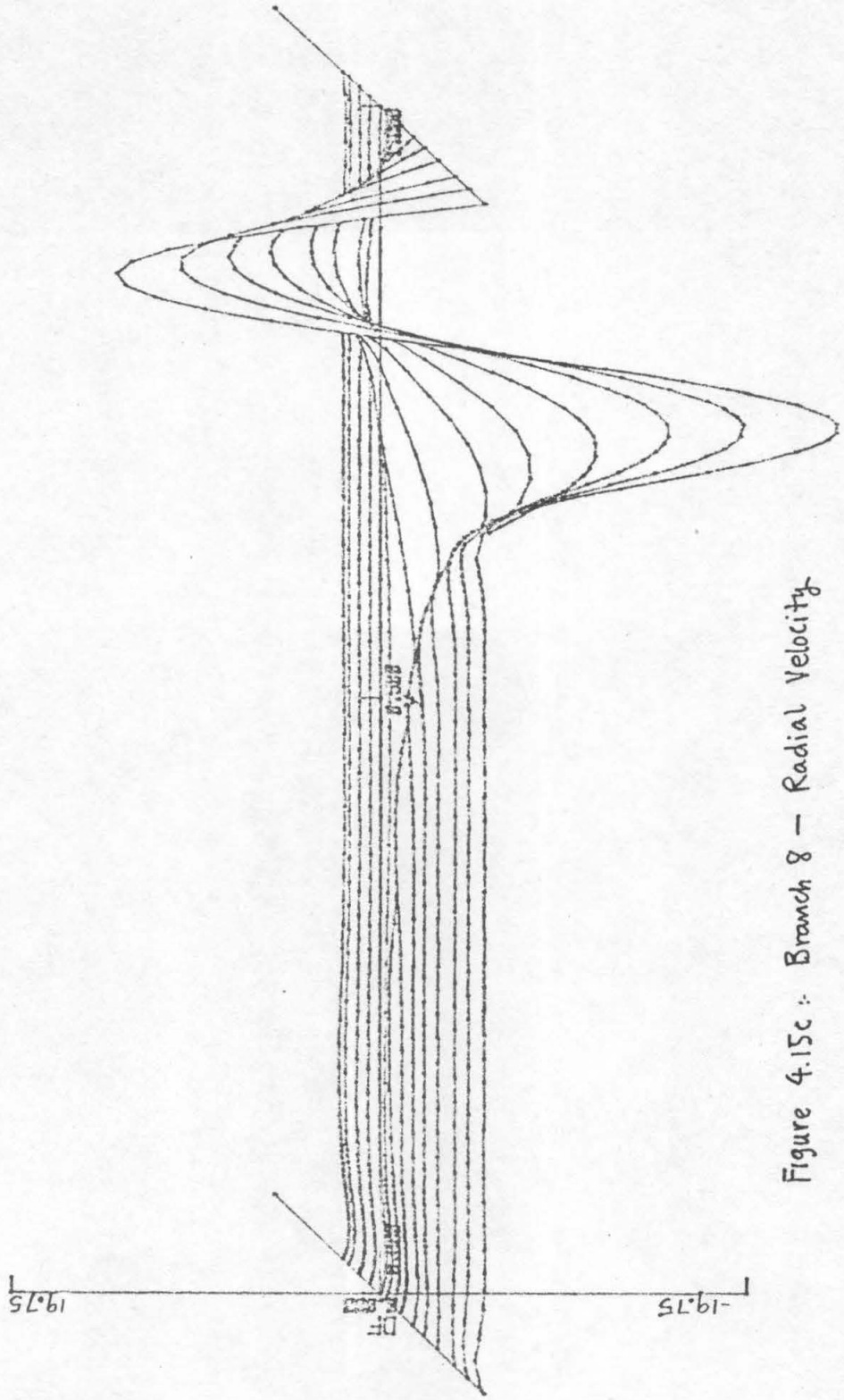

Figure 4.15c : Branch 8 — Radial Velocity

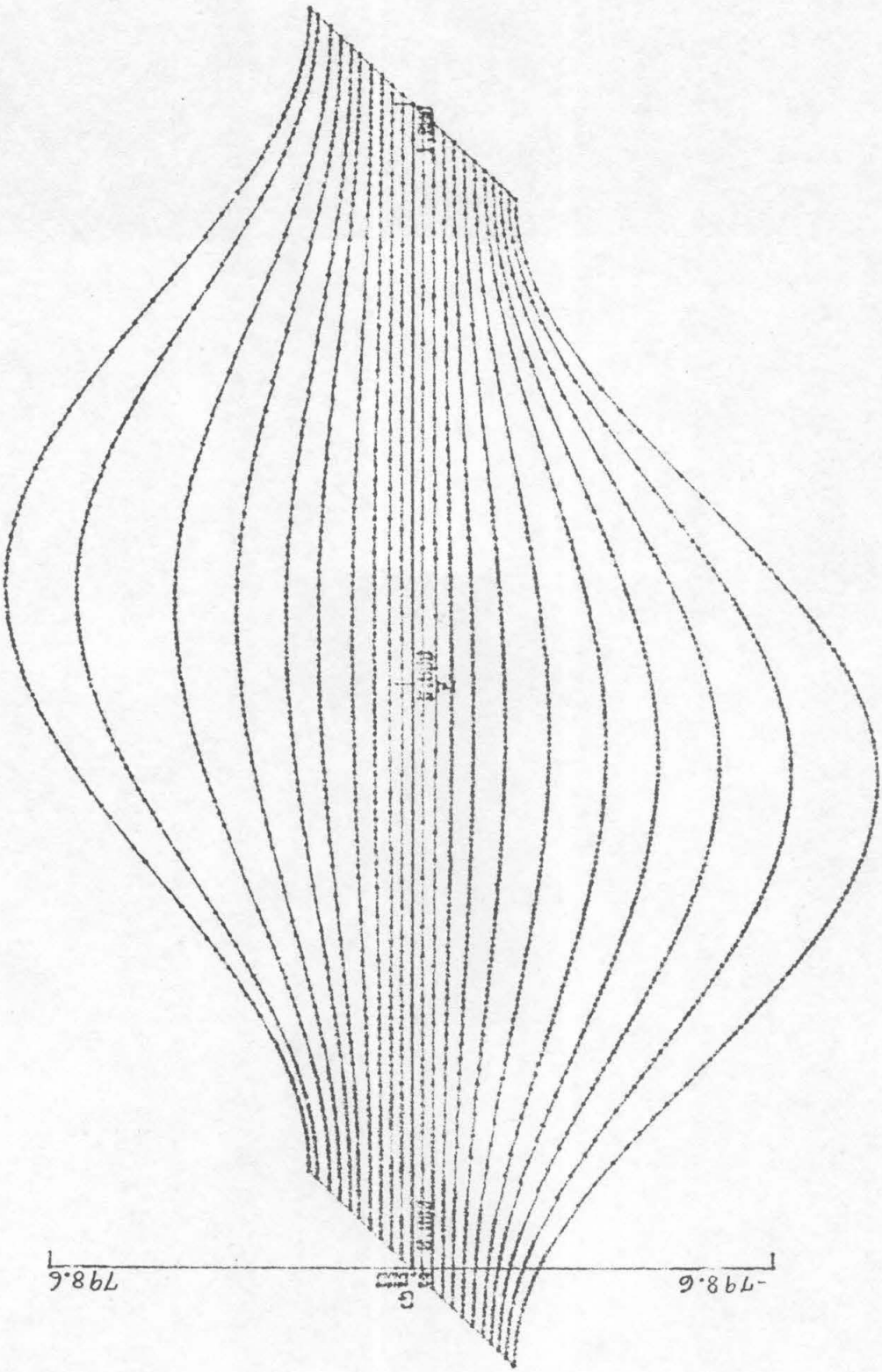

Figure 4.16 a : Branch 9 — Cosine Branch — Angular Velocity

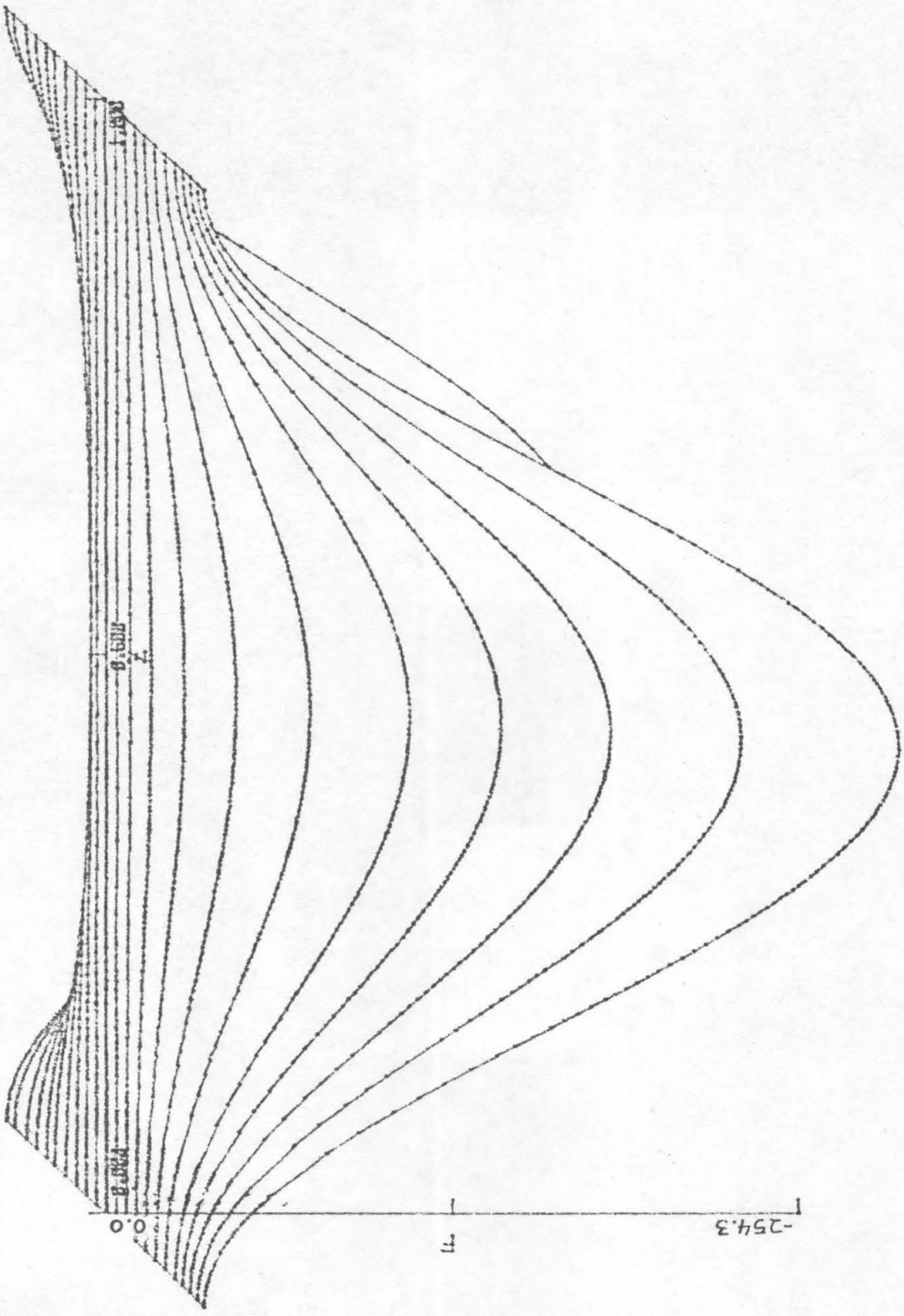

Figure 4.16 b : Branch 9 — Cosine branch — Axial Velocity

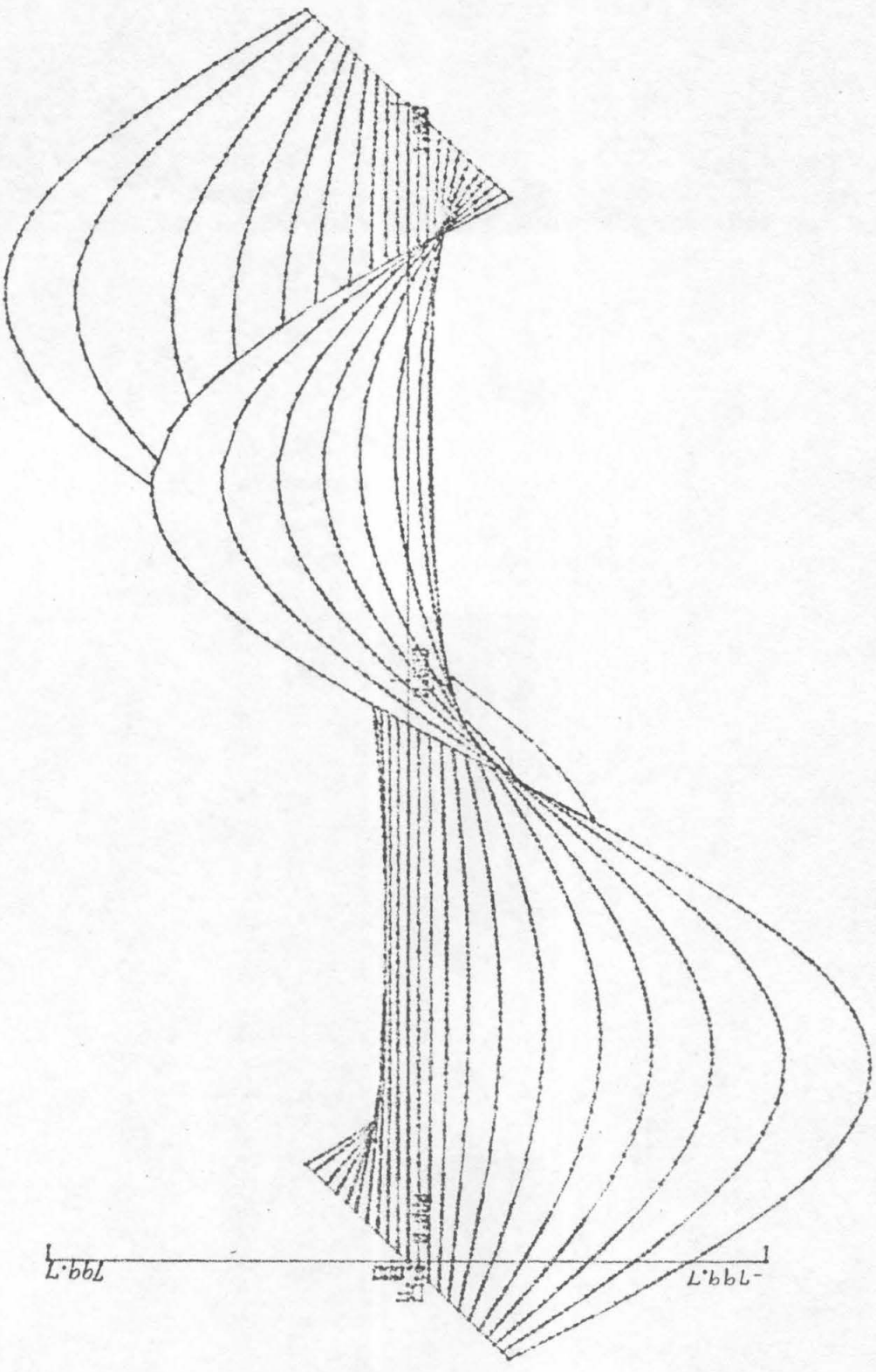

Figure 4.16c: Branch 9 – Cosine Branch – Radial Velocity

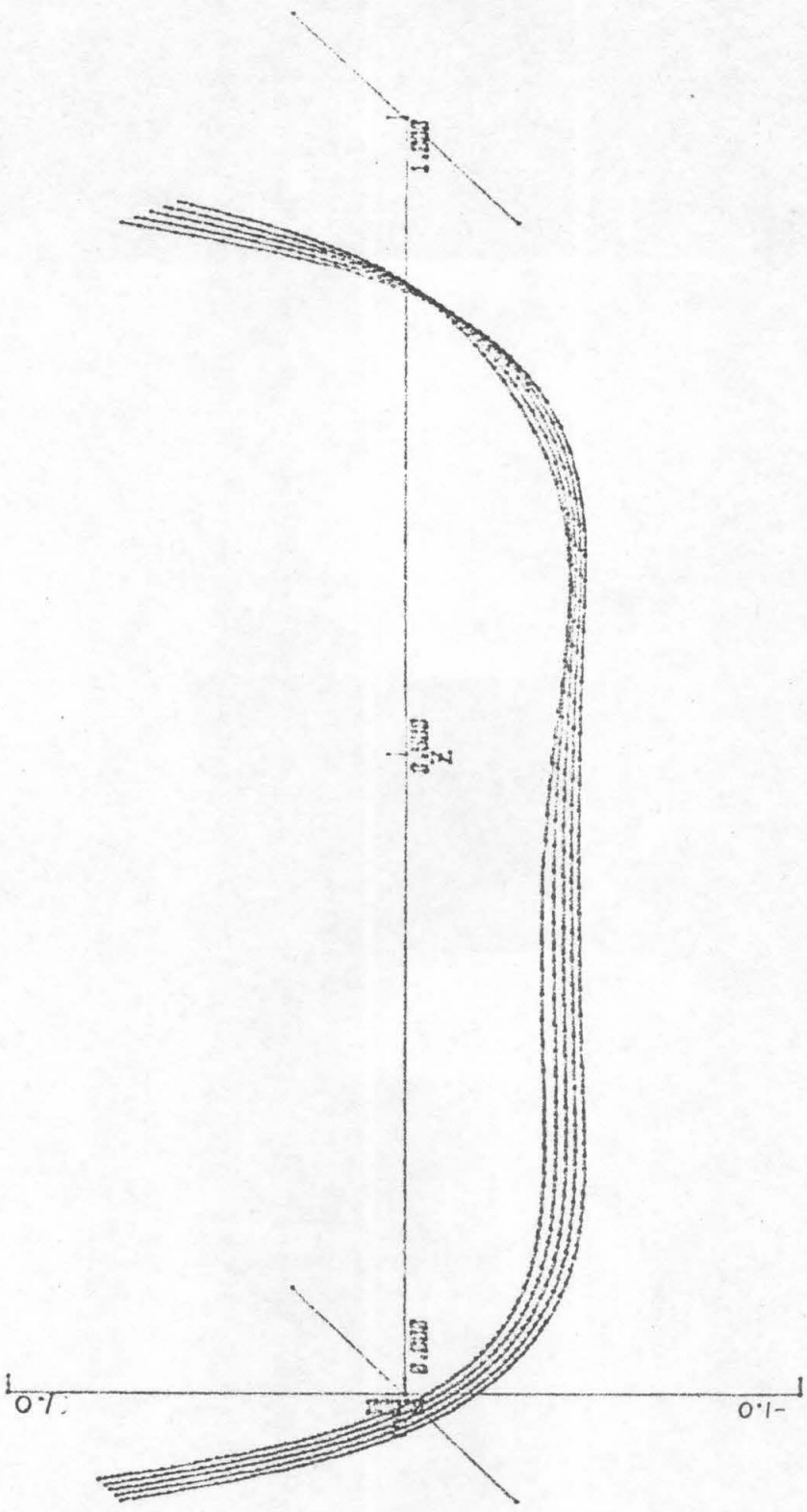

Figure 4.17a :- Branch 10 - Finger Branch A - Angular Velocity

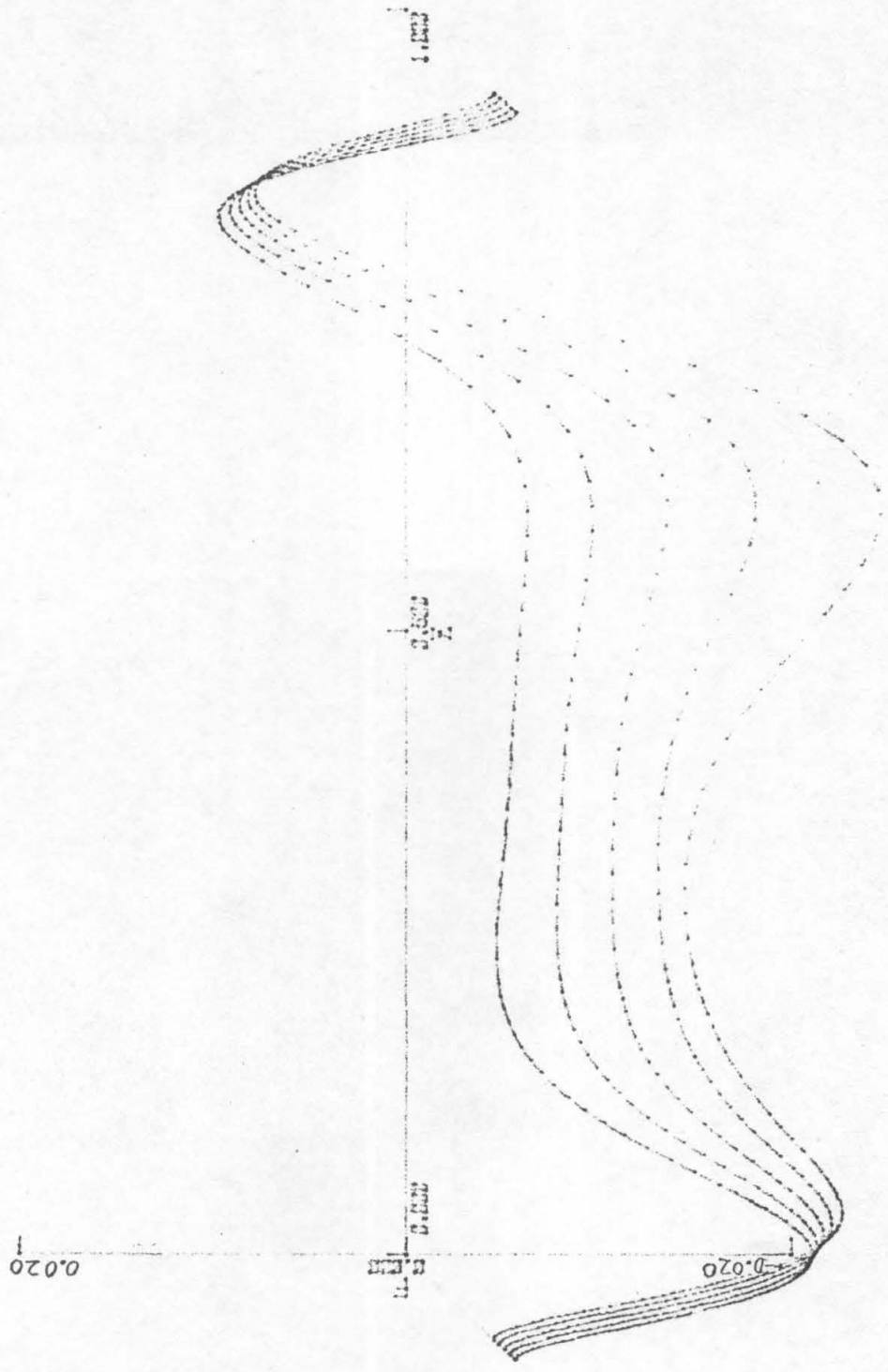

Figure 4.17b : Branch 10 – Finger Branch A – Axial Velocity

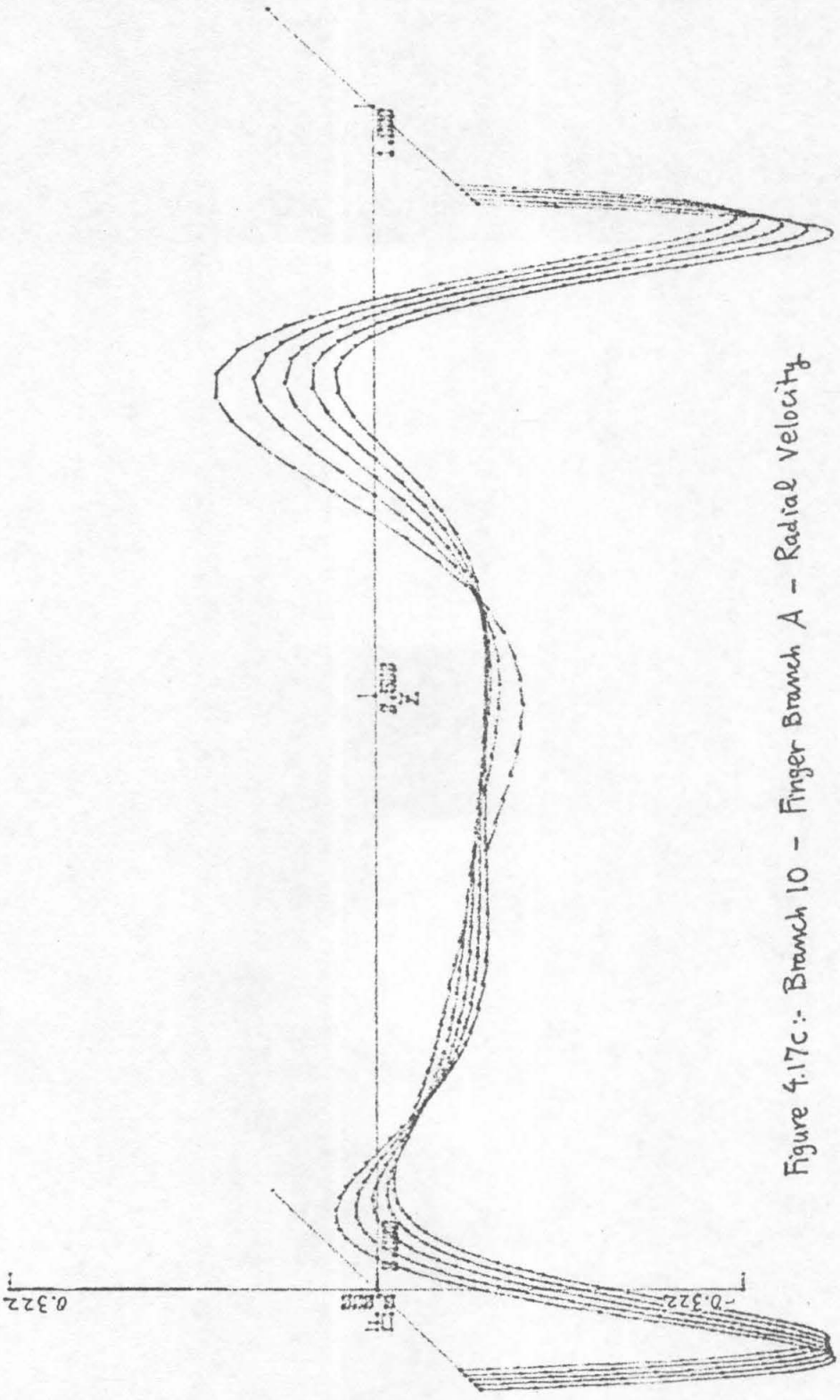

Figure 4.17c :- Branch 10 - Finger Branch A - Radial Velocity

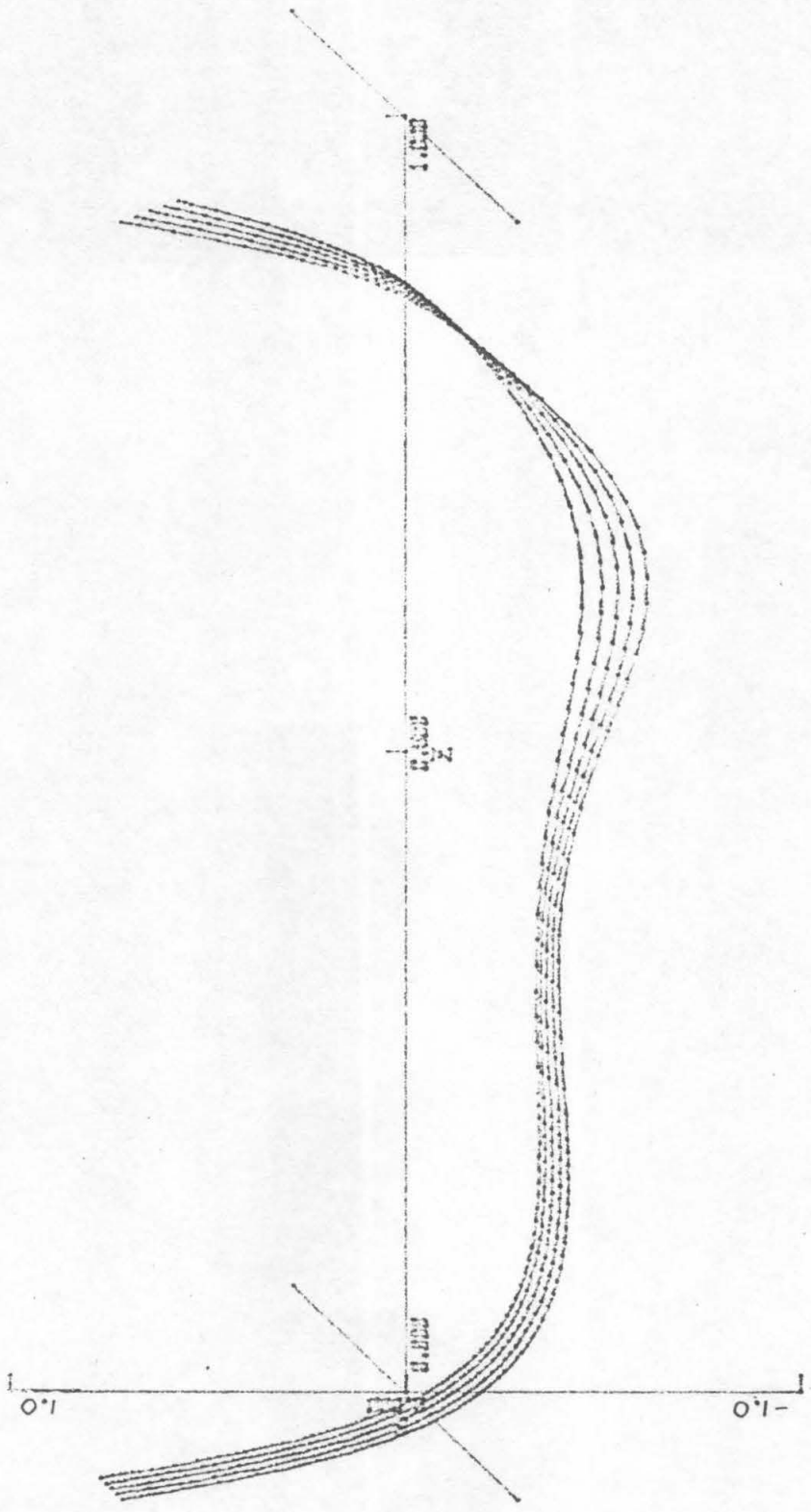

Figure 4.18 a :- Branch 11 - Finger Branch 8 - Angular velocity

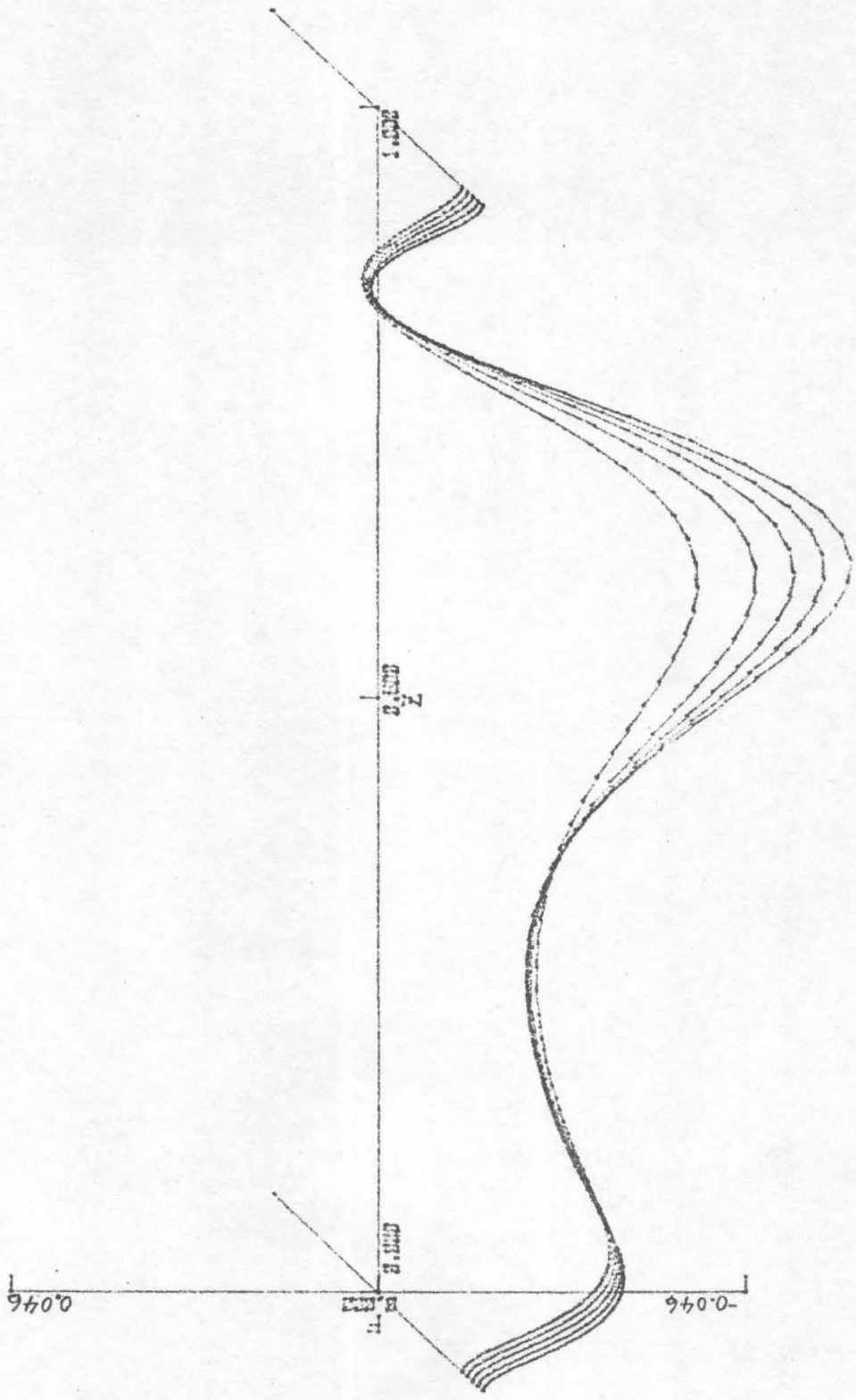

Figure 4.18 b: Branch 11 - Finger Branch B - Axial Velocity

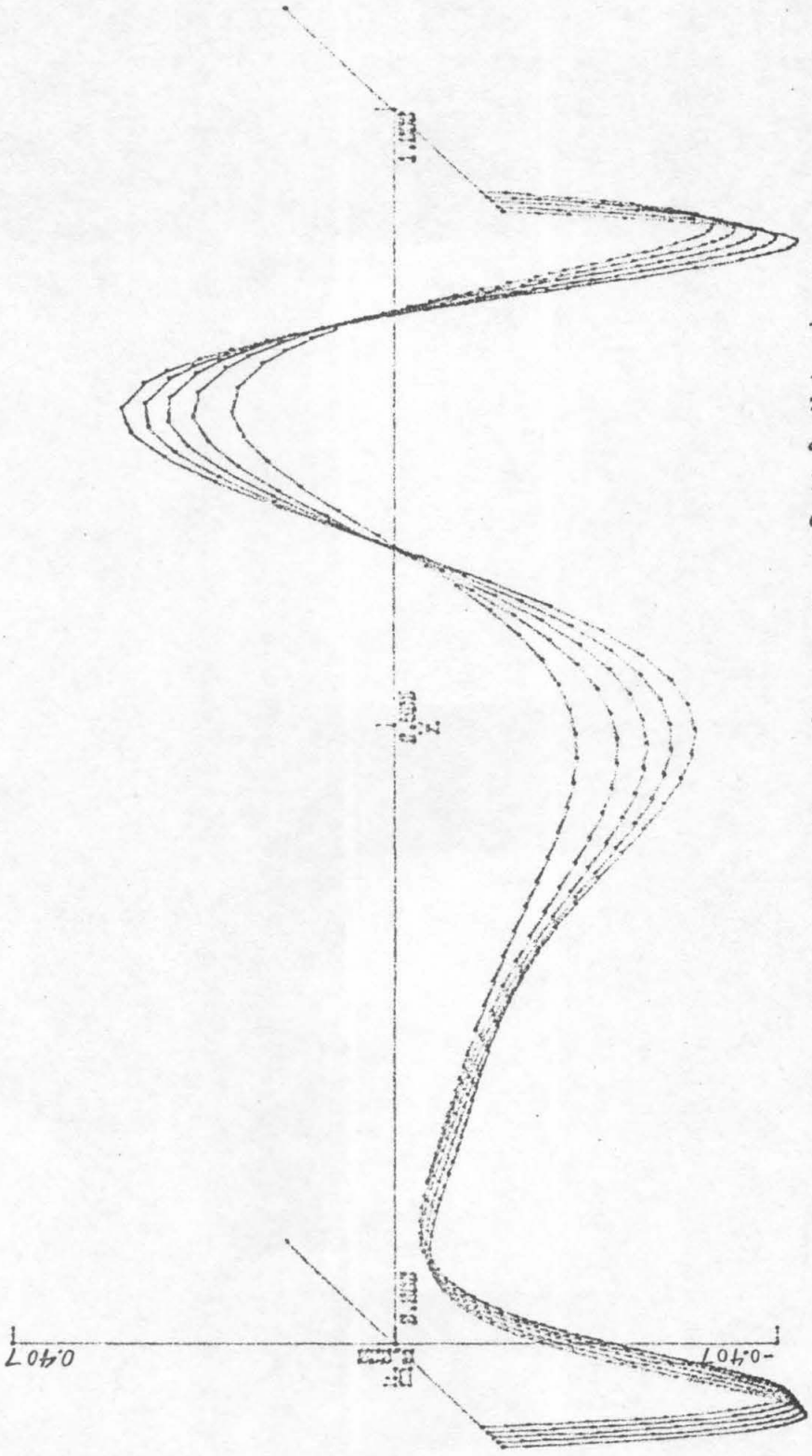

Figure 4.18c : Branch 11 – Finger Branch B – Radial Velocity

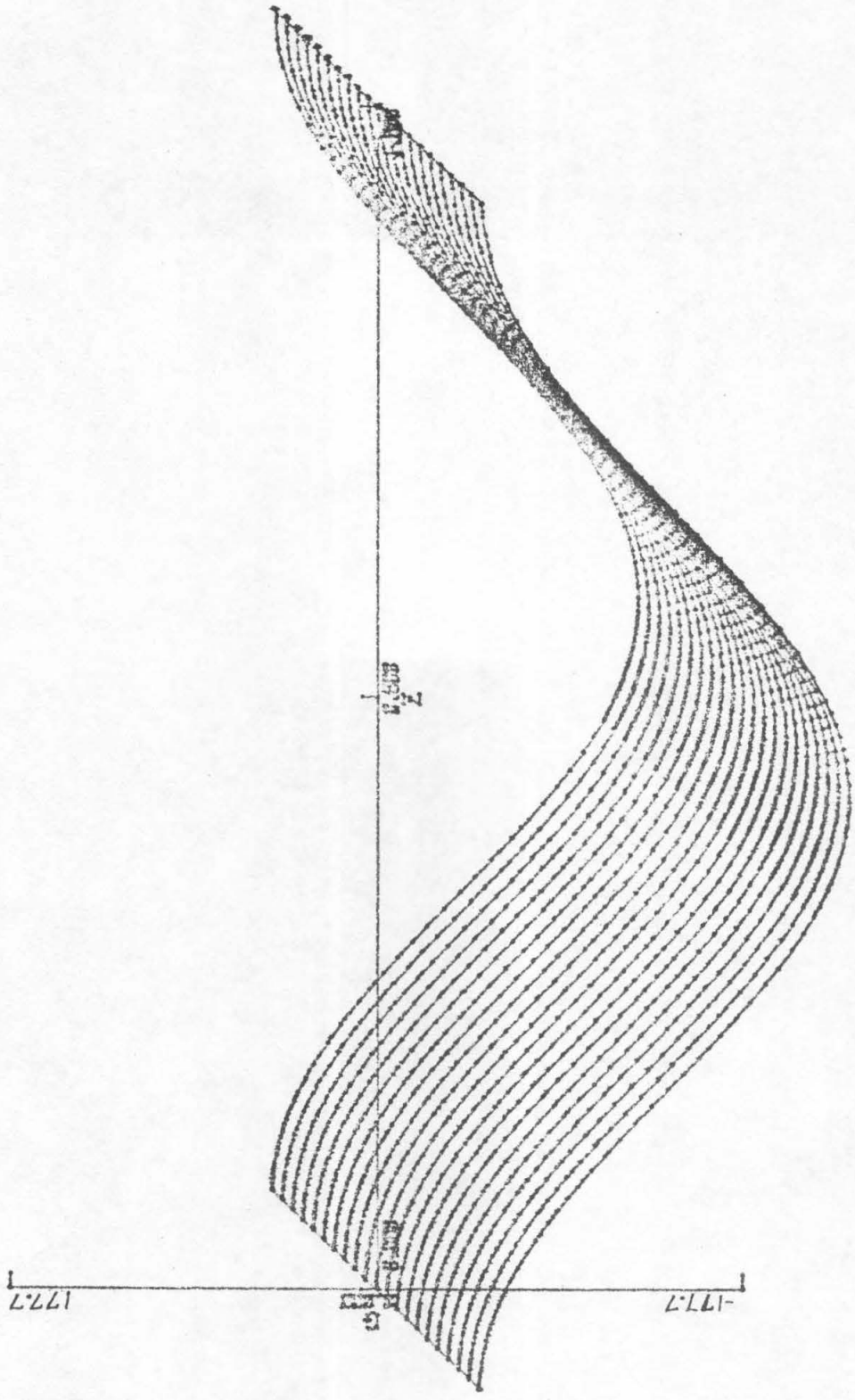

Figure 4.19a Branch 12 (R=210) — Angular Velocity

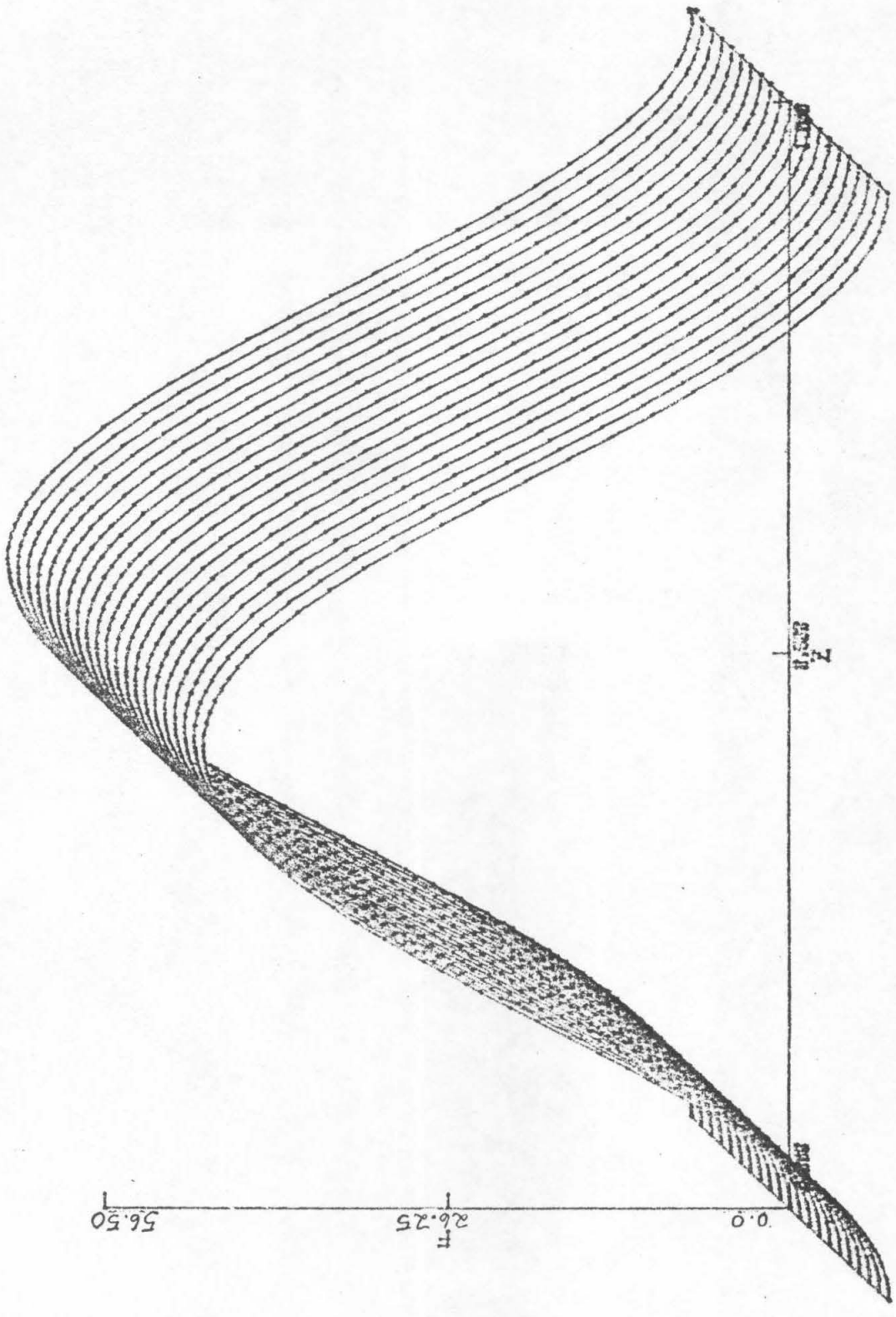

Figure 4.19b :- Branch 12 (R=210) - Axial Velocity

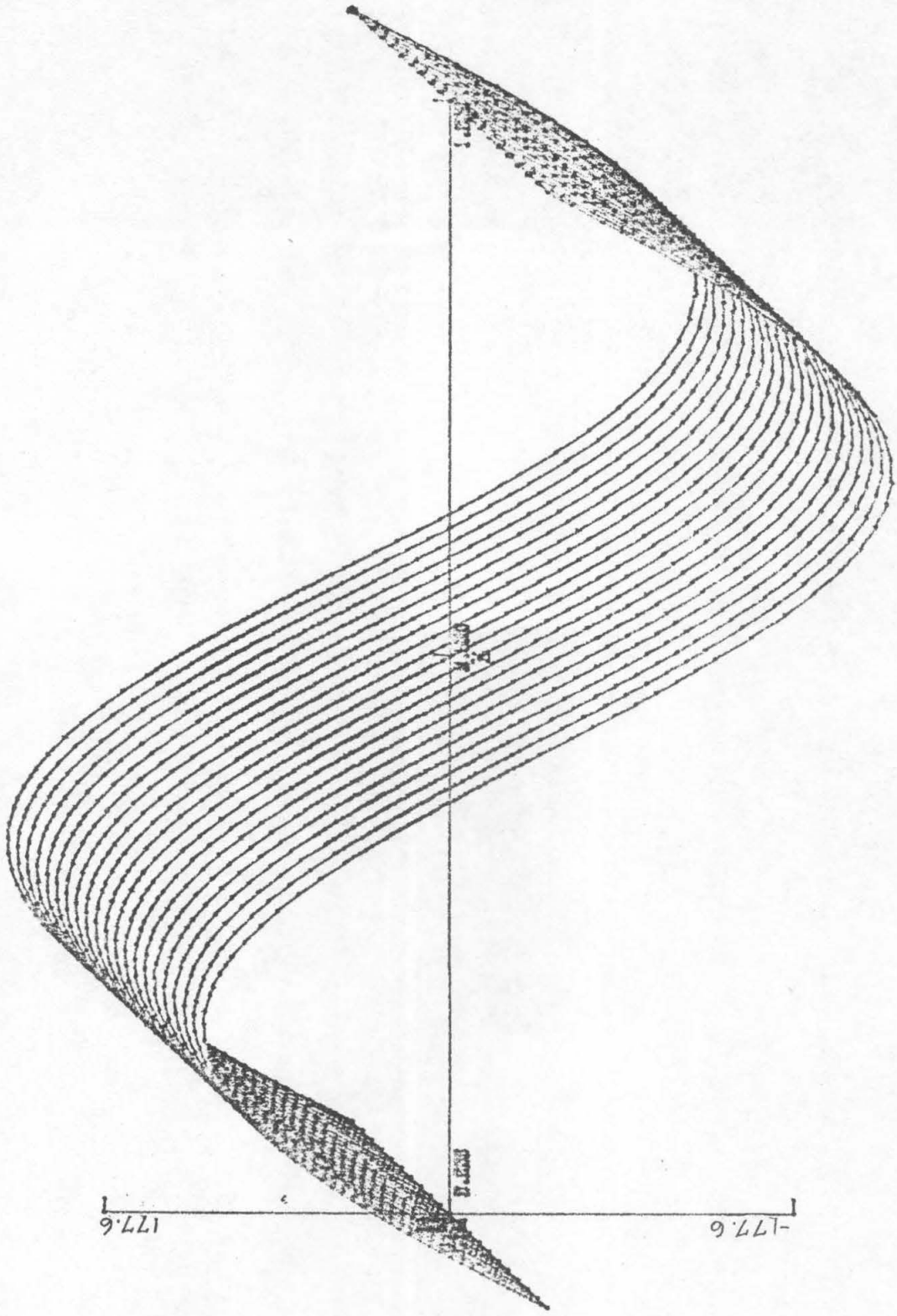

Figure 4.19c :- Branch 12 (R = 210) — Radial Velocity

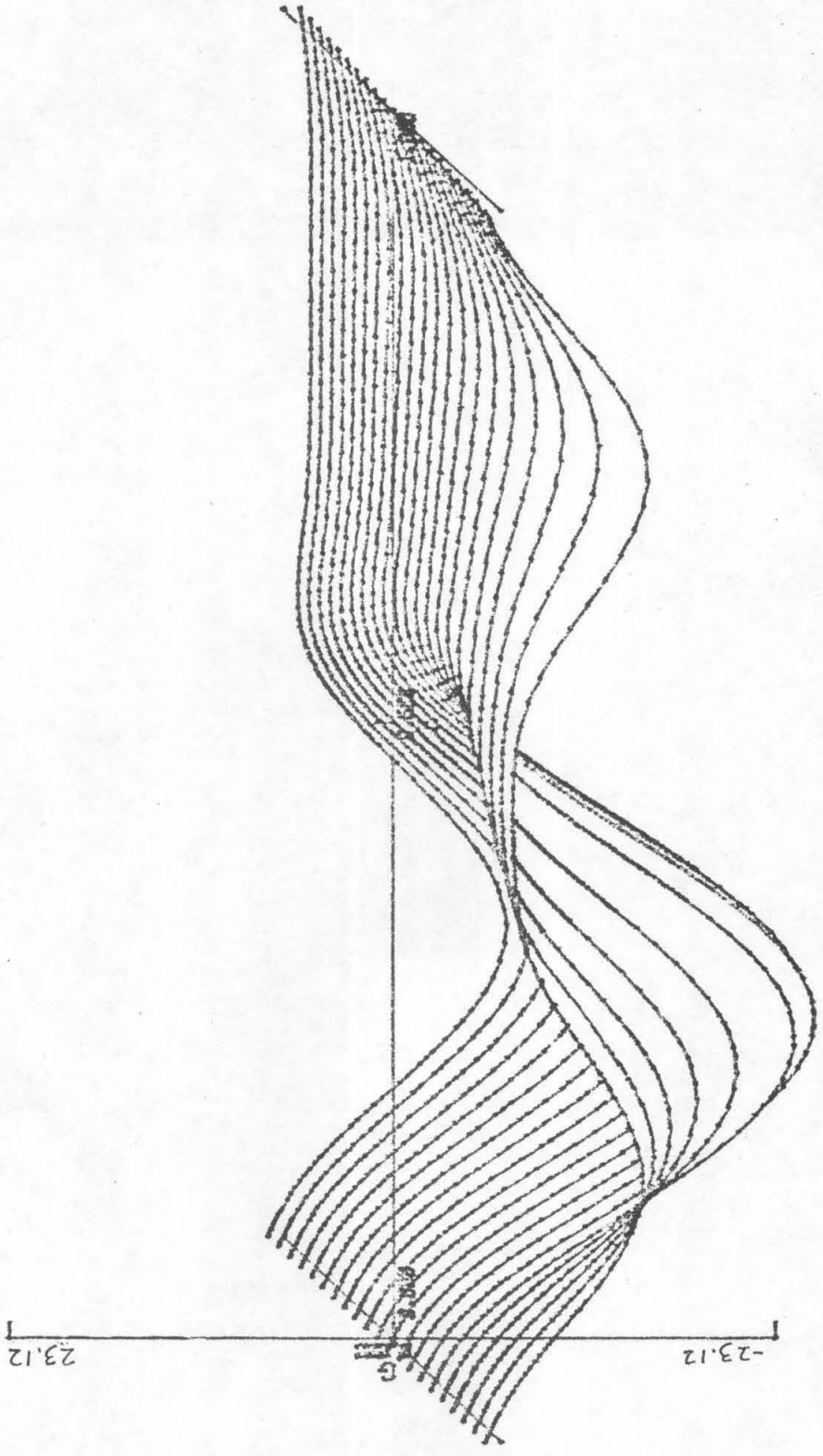

Figure 4.20a : Branch 13 (R=210) — Angular Velocity

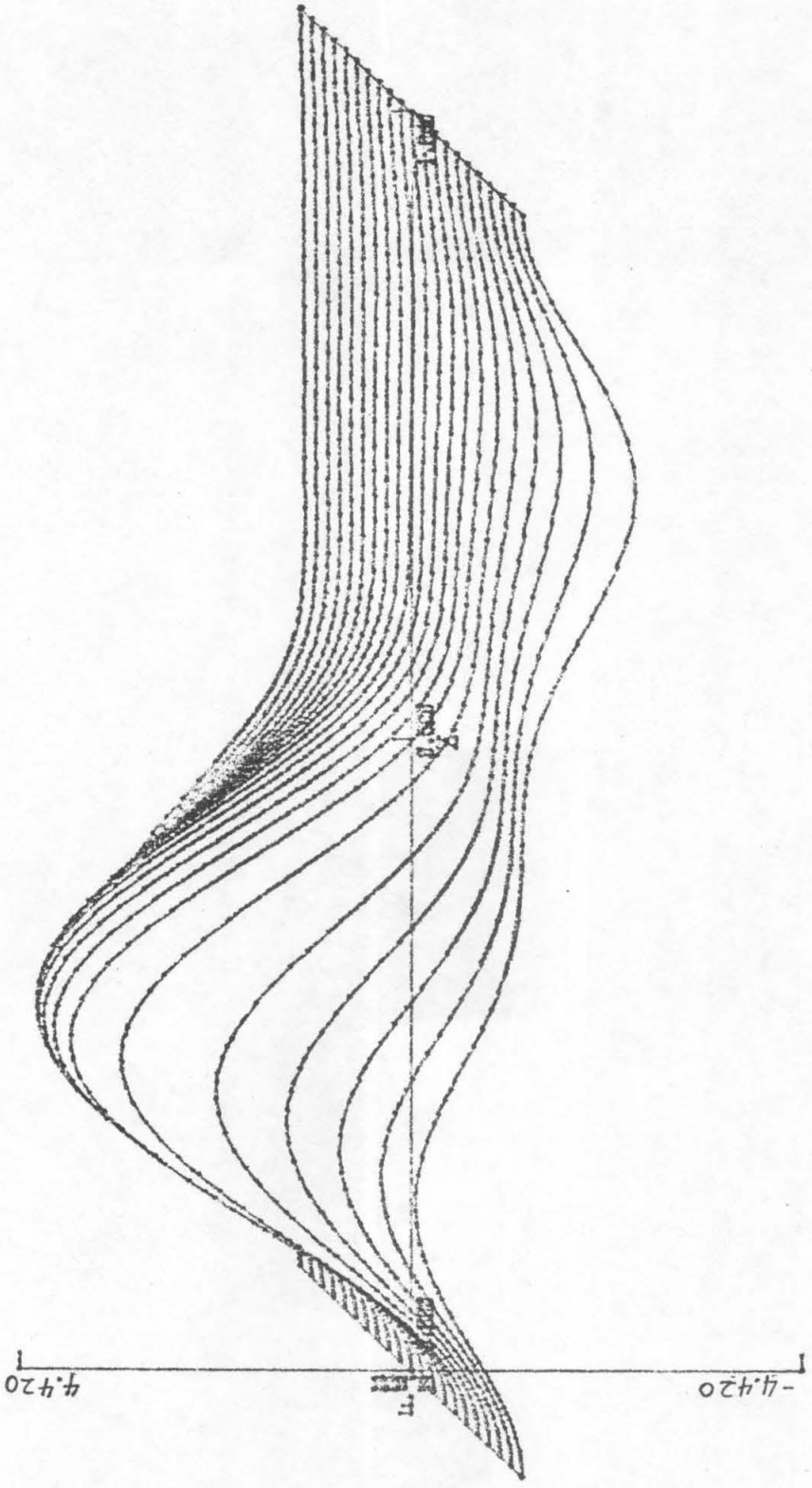

Figure 4.20 b : Branch 13 (R=210) — Axial Velocity.

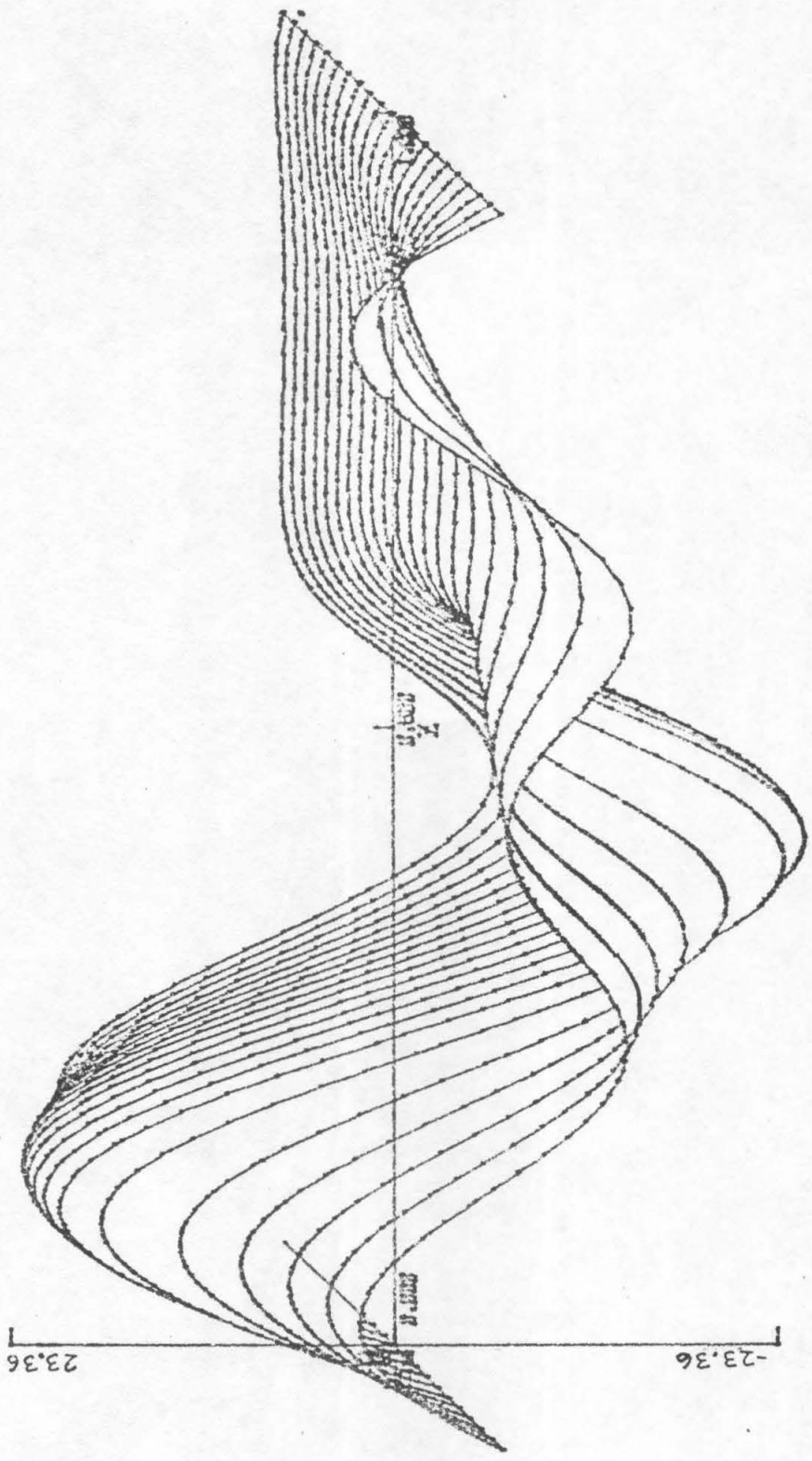

Figure 4.20c: Branch 13 (R = 210) — Radial Velocity

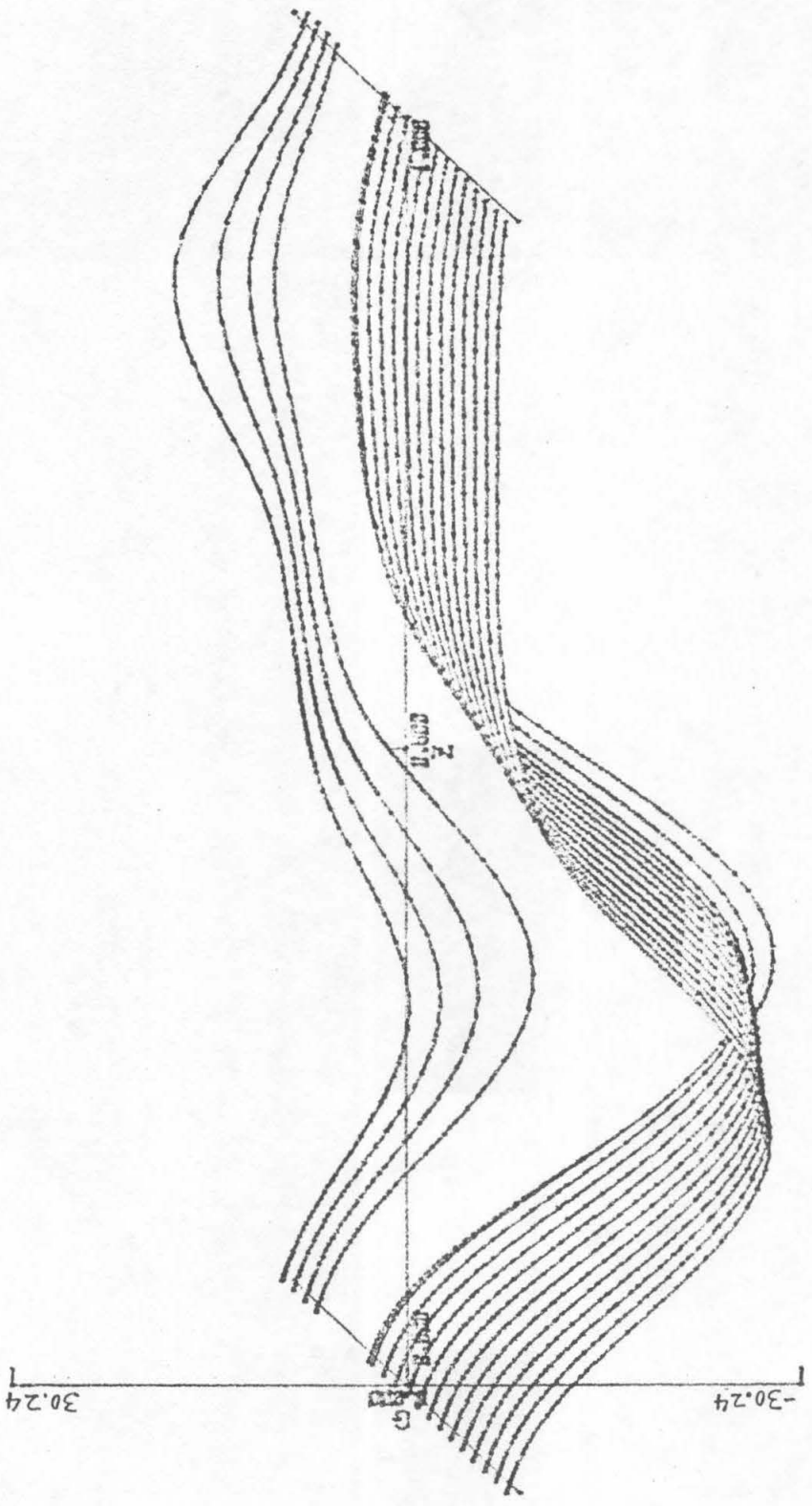

Figure 4.21a: Branch 14 (R=210) — Angular Velocity

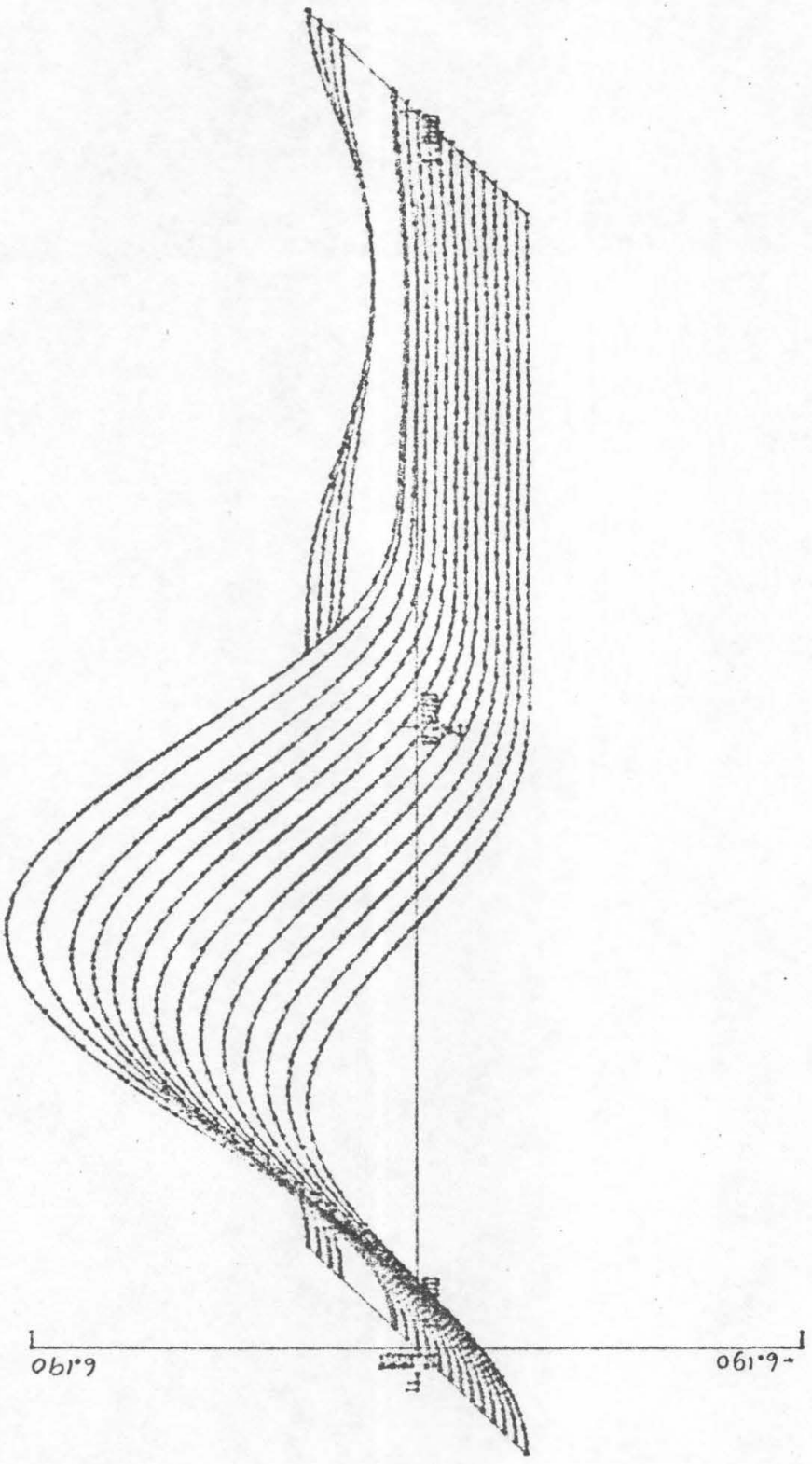

Figure 4.21b: Branch 14 (R=210) — Axial Velocity

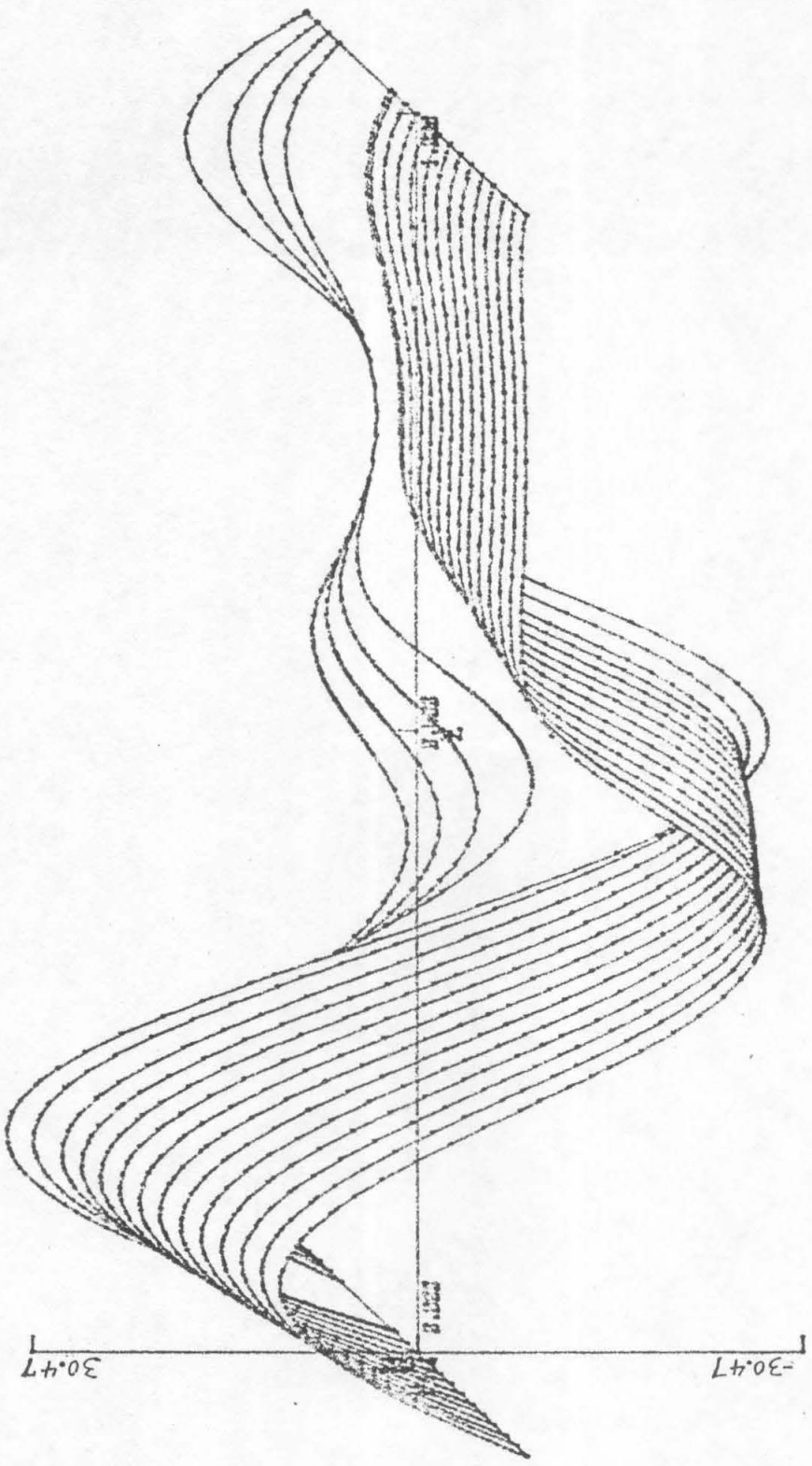

Figure 4.21c : Branch 14 (R= 210) — Radial Velocity

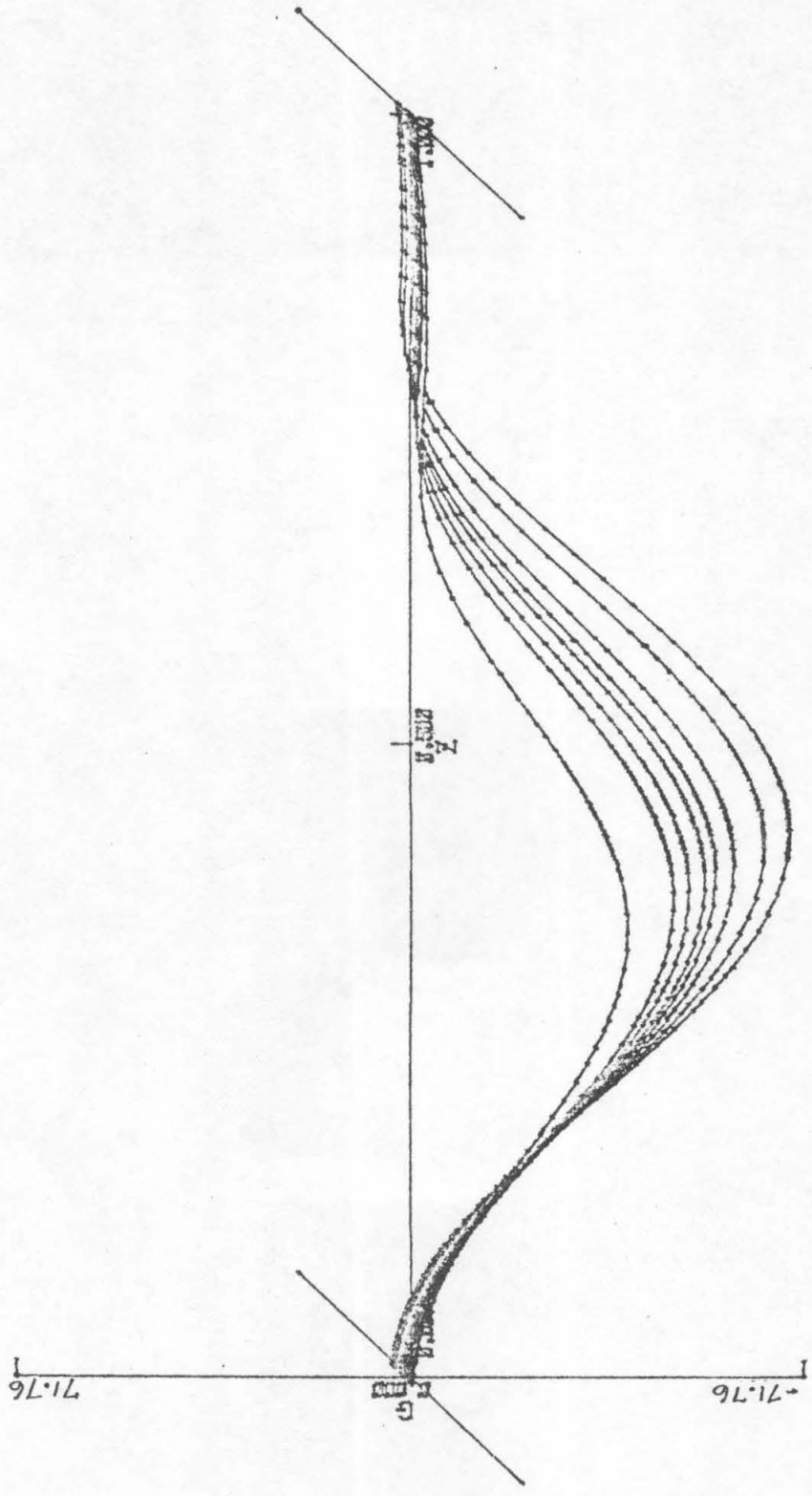

Figure 4.22a : Branch 15 (R=190) — Angular Velocity

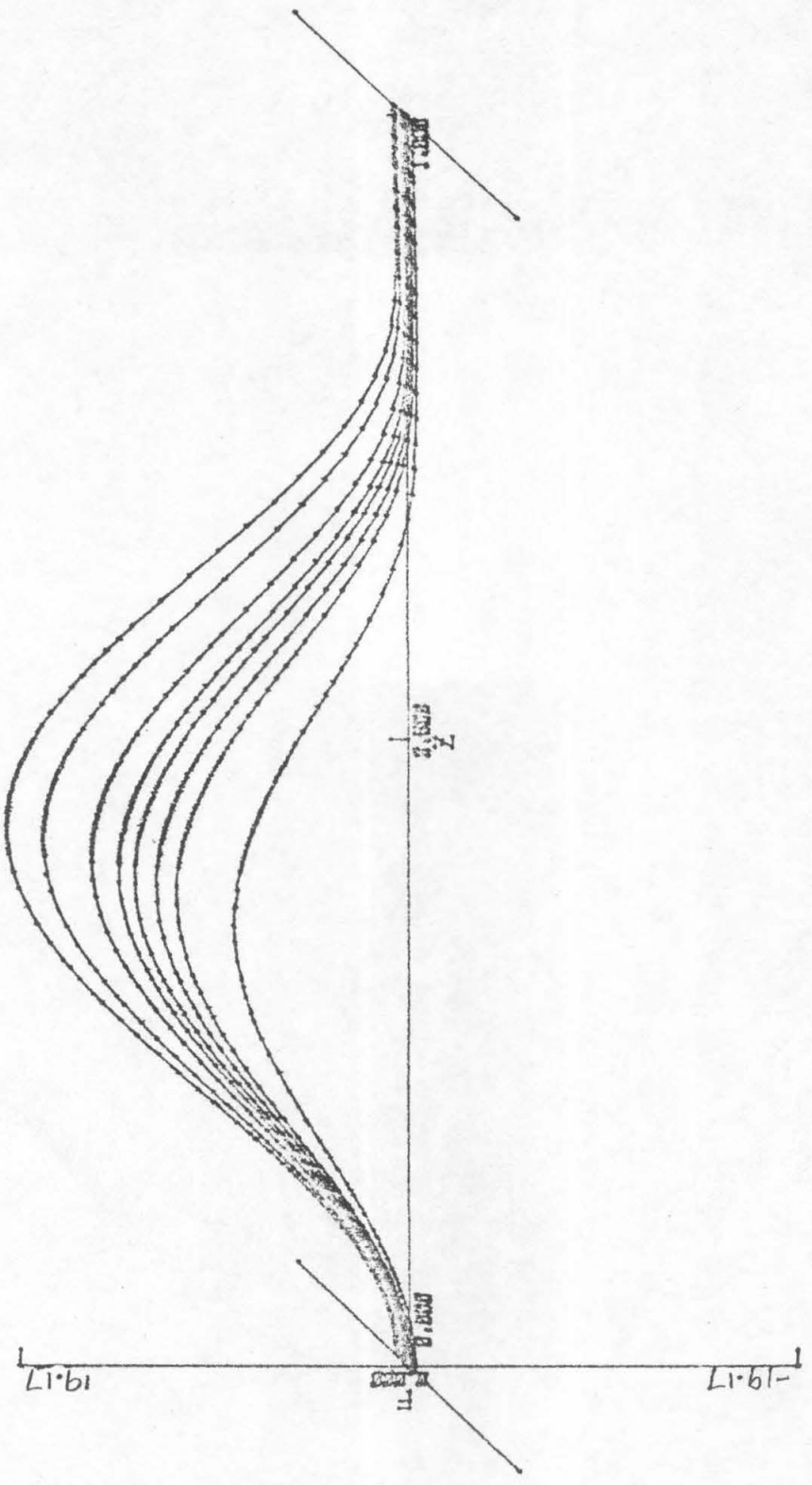

Figure 4.22b: Branch 15 (R=190) — Axial Velocity

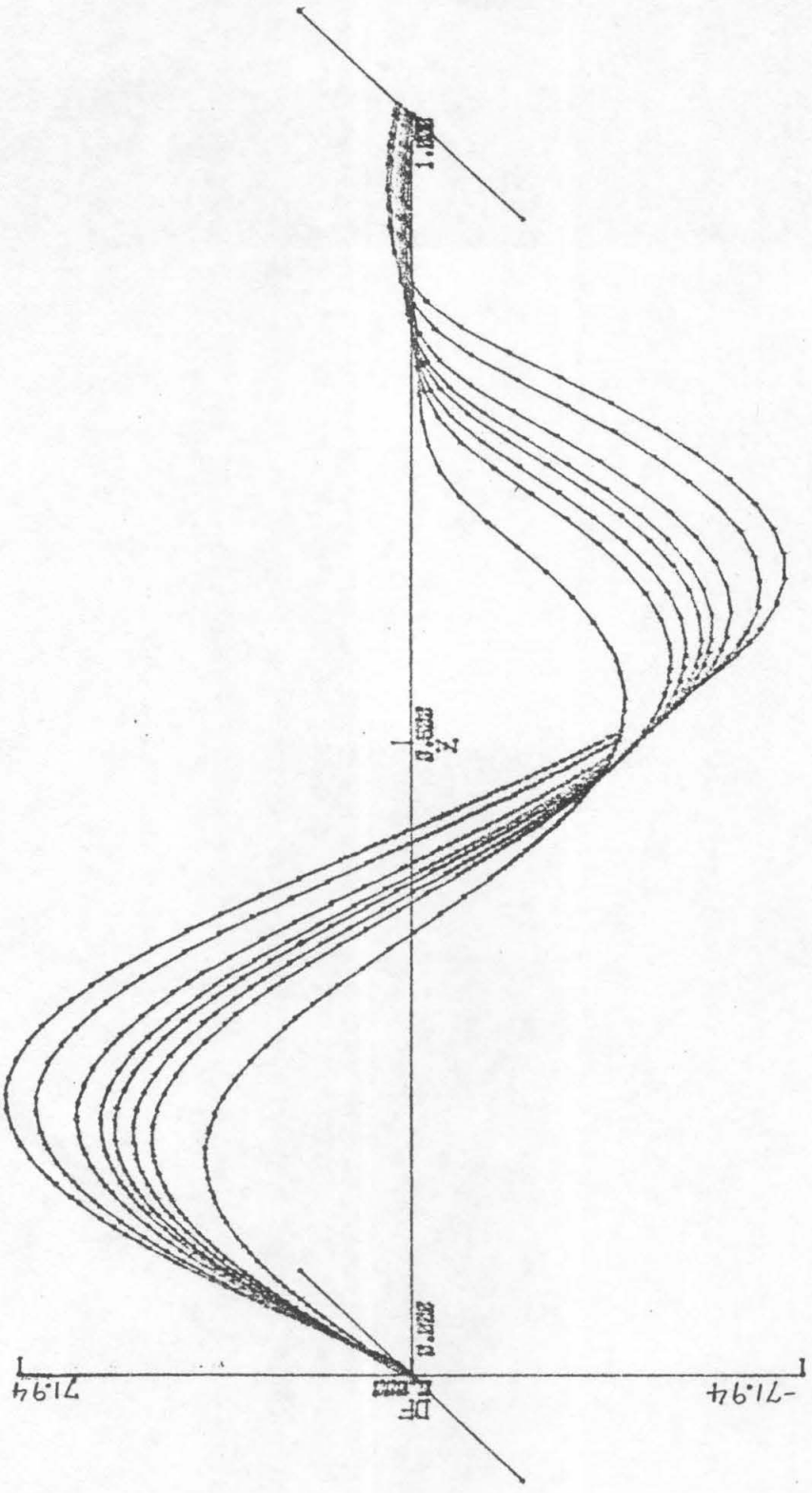

Figure 4.22c : Branch 15 (R=190) — Radial Velocity

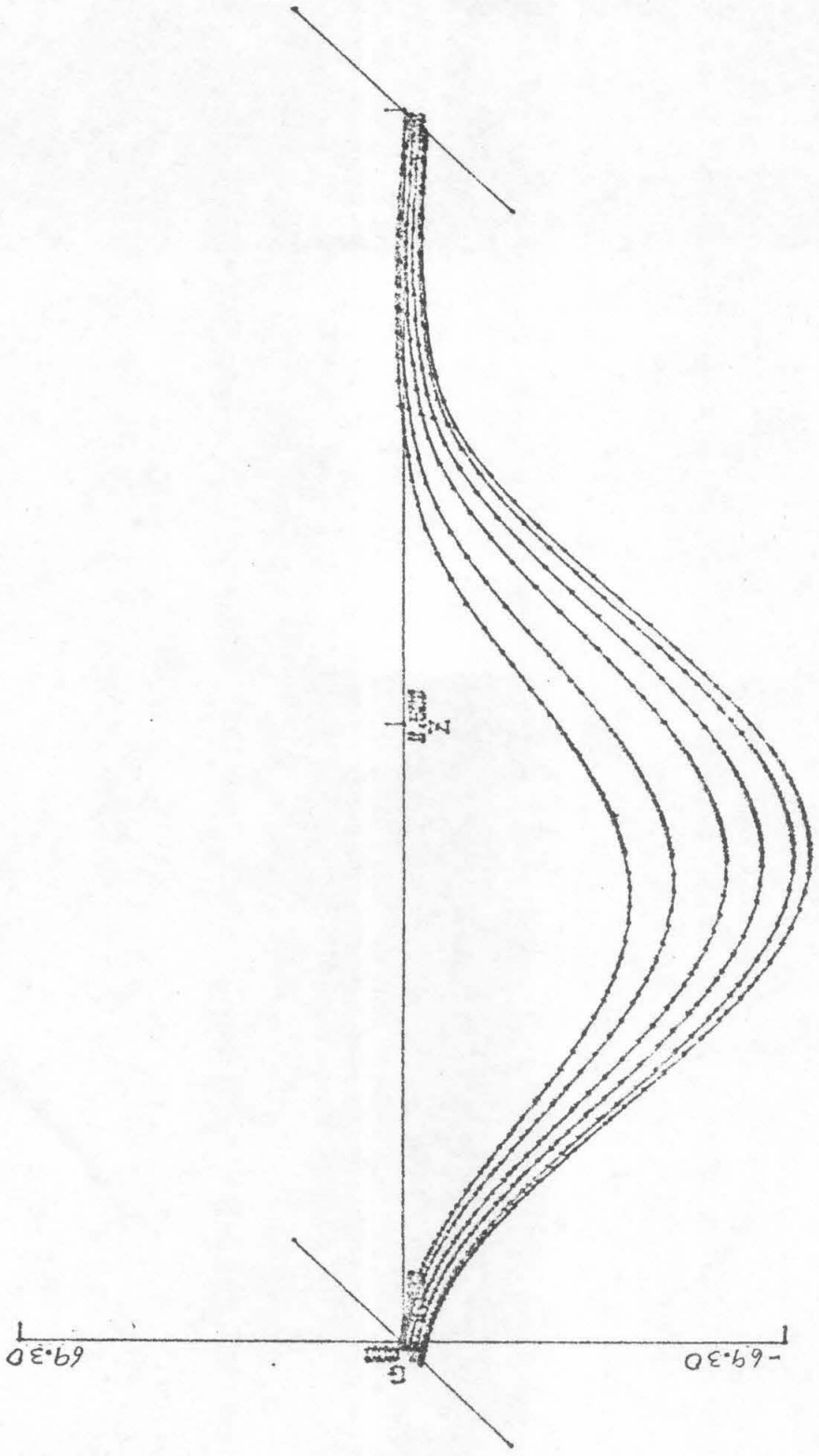

Figure 4.23a : Branch 16 (R=190) — Angular velocity

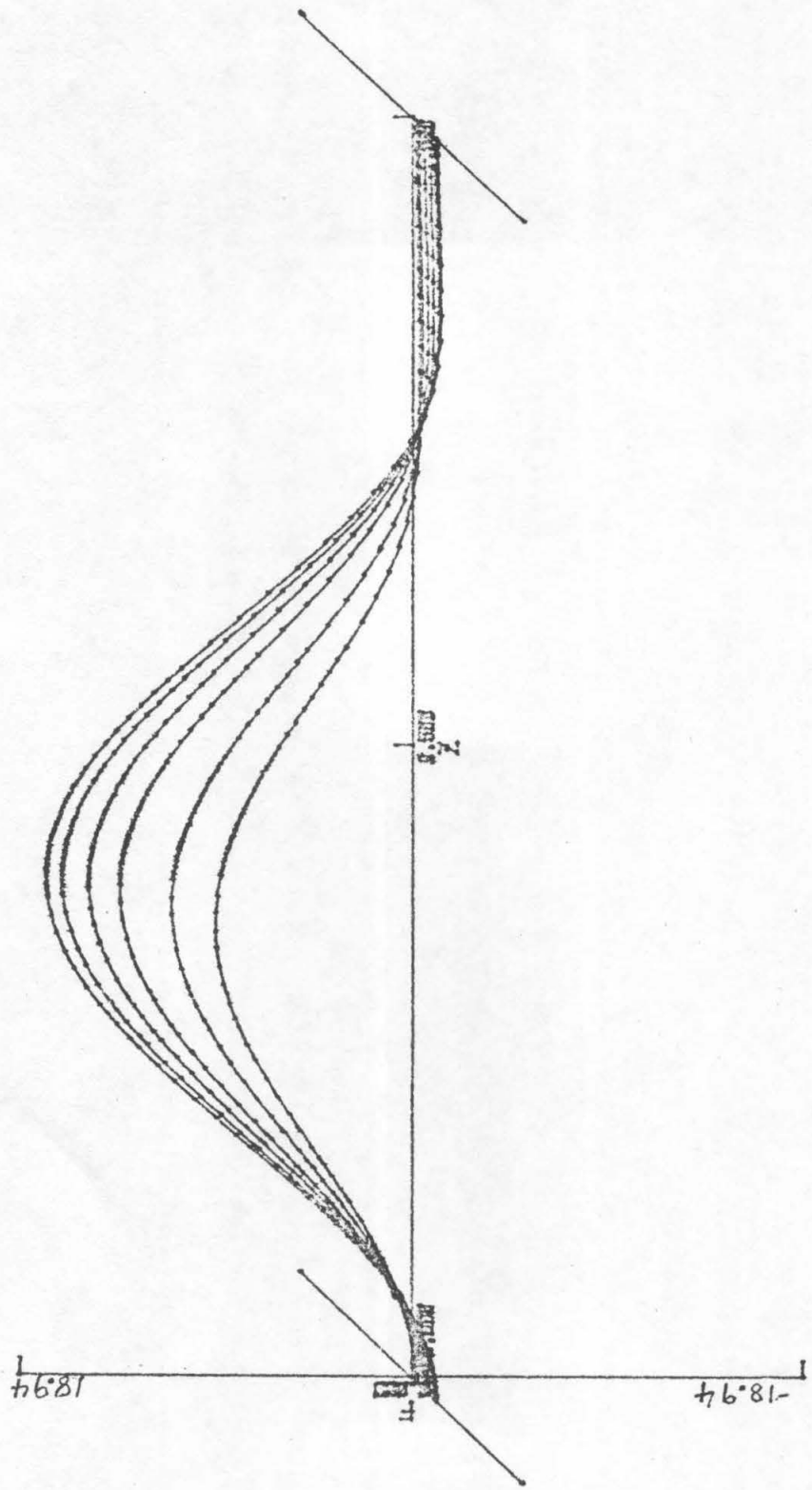

Figure 4.23 b: Branch 16 (R=190) - Axial Velocity

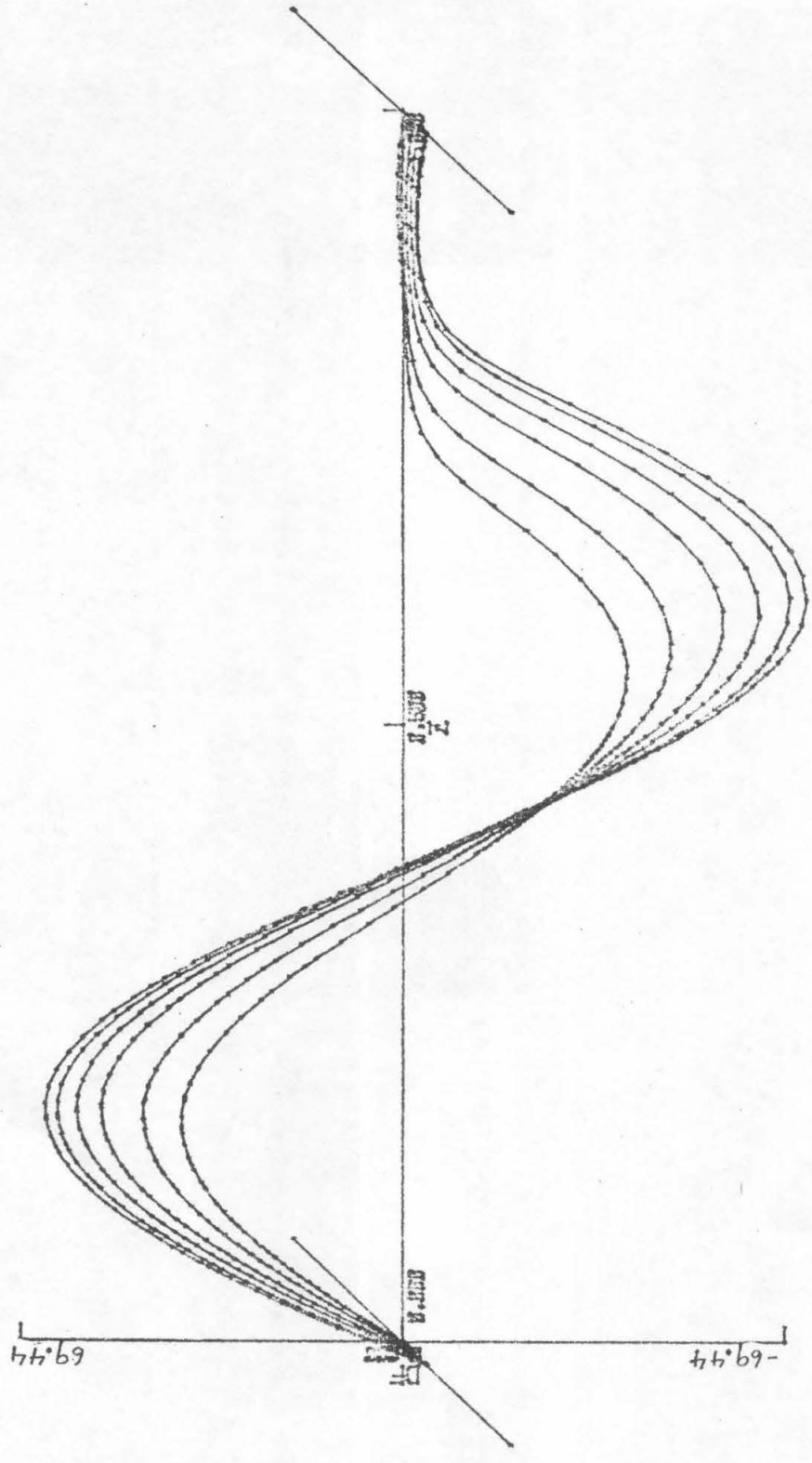

Figure 4.23c: Branch 16 (R=190) - Radial Velocity

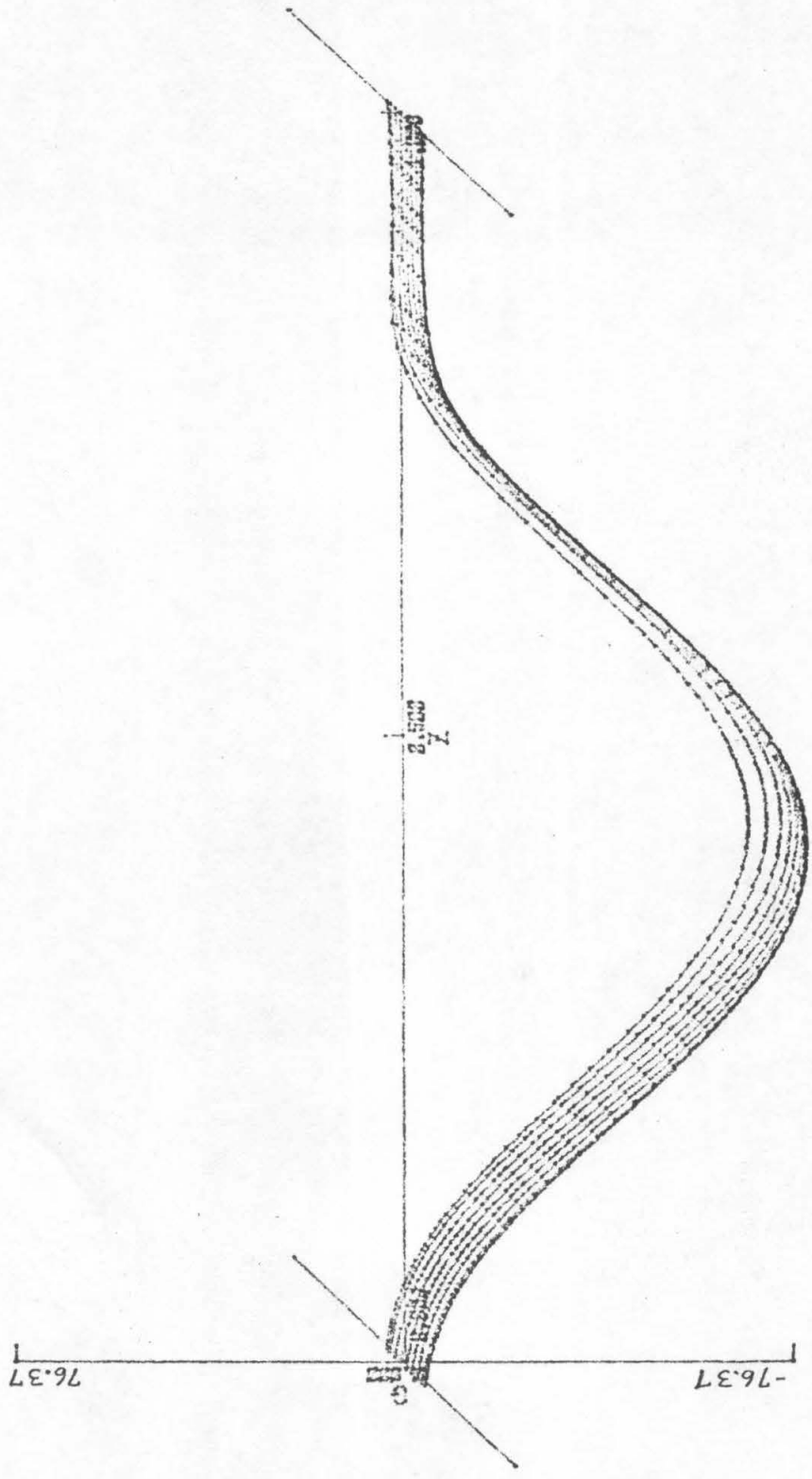

Figure 4.24 a : Branch 17 (R=190) - Angular Velocity

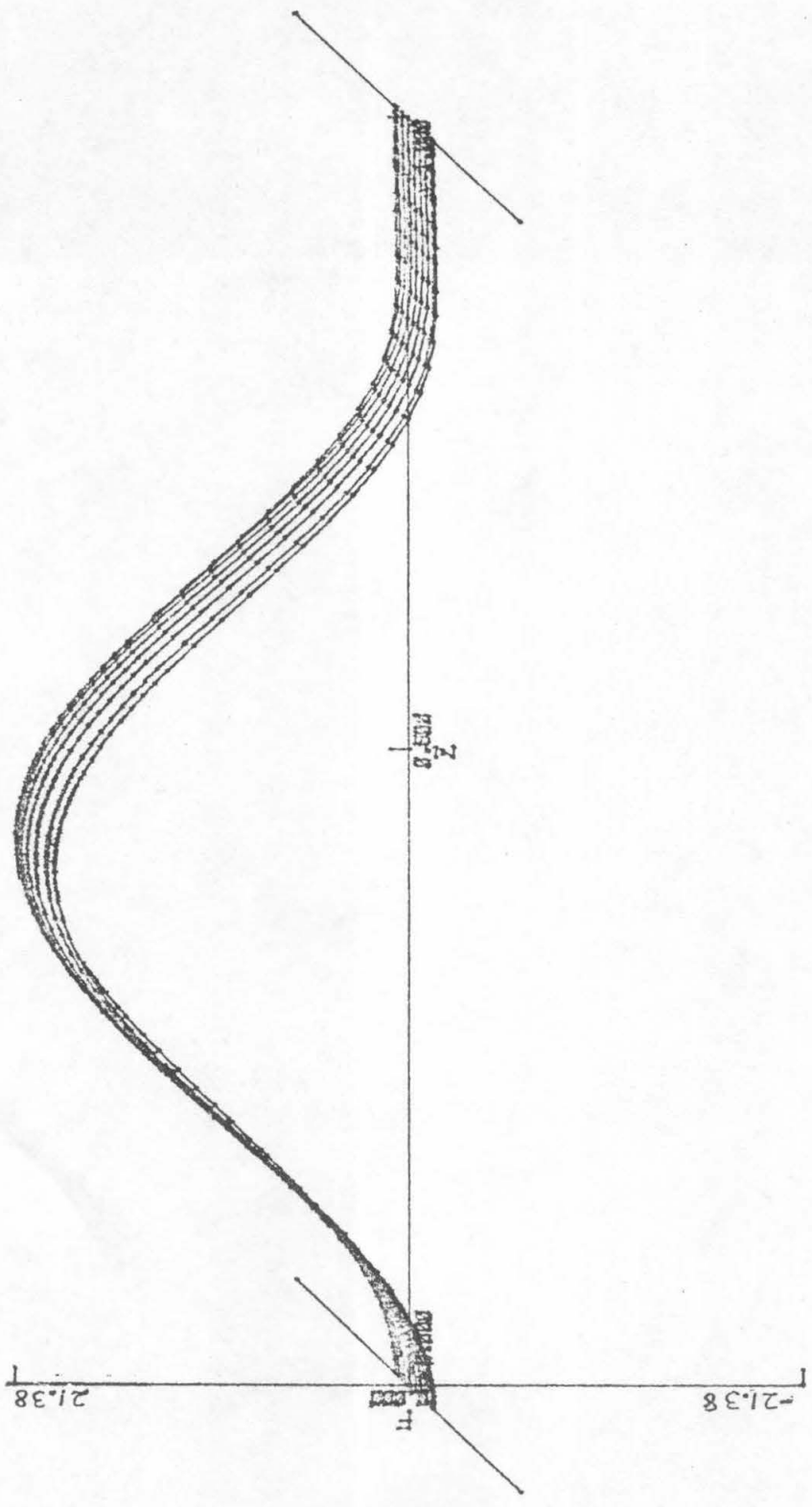

Figure 4.24 b: Branch 17 (R=190) — Axial Velocity

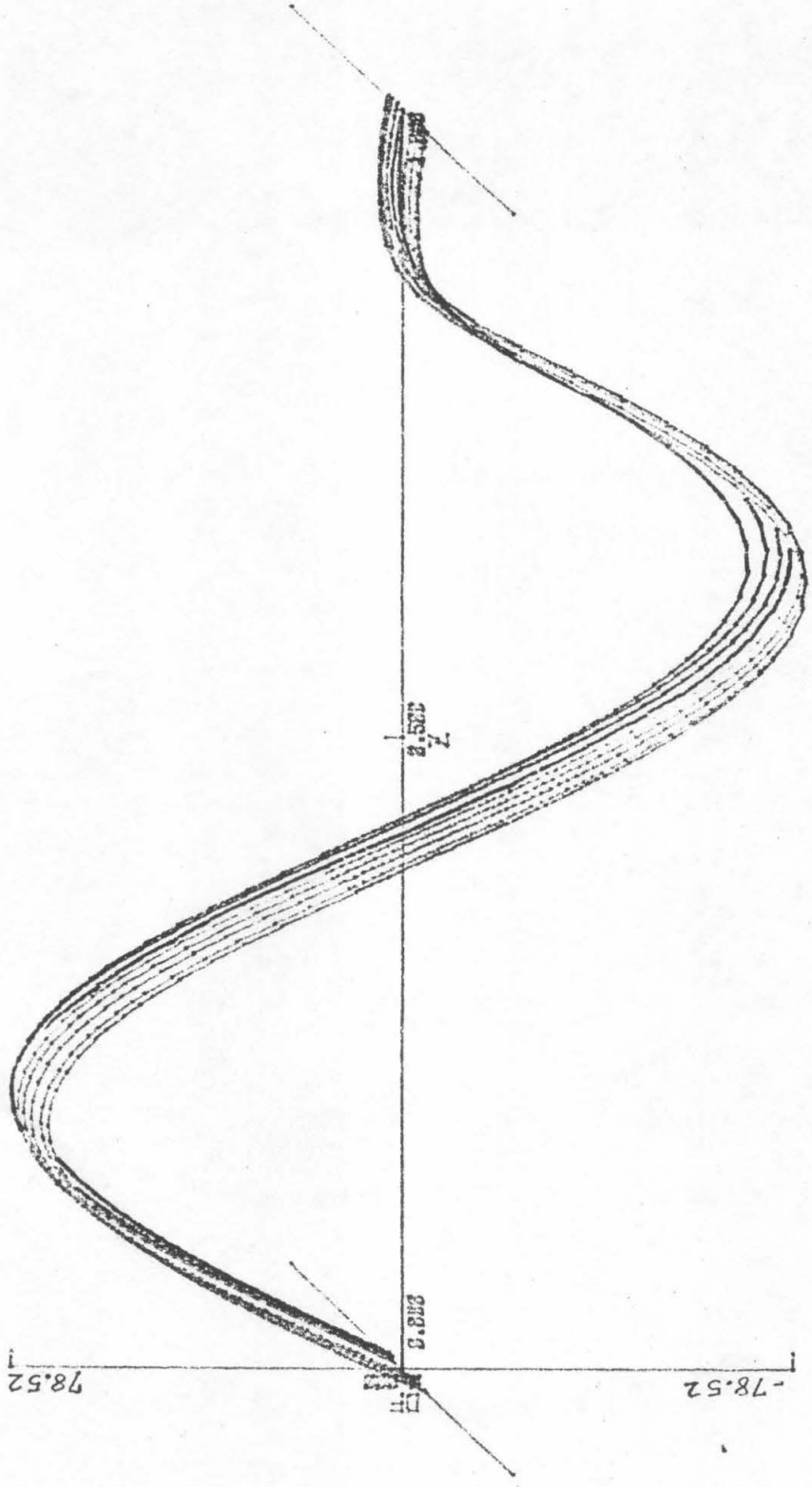

Figure 4.24c: Branch 17 (R=190) - Radial Velocity

REFERENCES

[1] Batchelor, G. K., "Note on a class of solutions of the Navier-Stokes equations representing steady rotationally-symmetric flow", Quart. J. Mech. Appl. Math. 4 (1951) 29-41

[2] Coddington, E. and Levinson, N., "Theory of ordinary differential equations", McGraw-Hill (1955)

[3] Cole, J., "Perturbation methods in applied mathematics", Blaisdell (1968)

[4] Crandall, M. G. and Rabinowitz P. H., "Bifurcation, perturbation of simple eigenvalues and linearized stability", M.R.C. Tech. Report No. 1295, Madison (1972)

[5] Dijkstra, D. and Zandbergen, P. J., "Nonunique solutions of the Navier-Stokes equations for the Karman swirling flow", Memorandum No. 155 (1976), Dept. of Appl. Math., Twente Univ. of Tech, Netherlands

[6] Goldstein, S., "Modern developments in fluid dynamics.

volume I", Dover (1965)

[7] Greenspan, D., " Numerical studies of flow between rotating coaxial disks", J. Inst. Math. Appl. 9 (1972) 370-377

[8] Holodniok, M., Kubicek, M. and Hlavacek V., "Computation of the flow between two rotating coaxial disks", J. F. M. 81 (1977) 689-699

[9] Issacson, E. and Keller, H. B., "Analysis of numerical methods", Wiley (1966)

[10] Keener, J. P. and Keller, H. B., "Perturbed bifurcation theory", Arch. Rational Mech. Anal. 50 (1973) 159-175

[11] Keller, H. B., "Accurate difference methods for nonlinear two point boundary value problems", SIAM J. Numer. Anal. 11 (1974) 305-320

[12] Keller, H. B., "Bifurcation theory and nonlinear eigenvalue problems , unpublished lecture notes, Caltech (1976)

[13] Keller, H. B., "Numerical solution of bifurcation and nonlinear eigenvalue problems", in Application of Bifurcation Theory (Rabinowitz, P. ed.), Academic Press (1977) 359-384

[14] Keller, H. B., "Singular systems, inverse iteration and least squares", submitted for publication

[15] Lancaster, P., "Theory of Matrices", Academic Press (1969)

[16] Lance, G. N. and Rogers, M. H., "The axially symmetric flow of a viscous fluid between two infinite rotating disks", Proc. Royal Soc. (A) 266 (1962) 109-121

[17] Lentini-Gil, M., "Boundary value problems in semi-infinite intervals", Ph. D. thesis, Caltech 1978

[18] Matkowsky, B. J. and Siegmann, W. L., "The flow between counter-rotating disks at high Reynolds number", SIAM J. Appl. Math. 30 (1976) 720-727

[19] Matkwosky, B. J. and Reiss, E. L., "Singular perturbations of bifurcations", SIAM J. Appl. Math. 33 (1977) 232-255

[20] McLeod, J., "Von Karman's swirling flow problem", Arch. Rational Mech. Anal. 33 (1969) 91-102

[21] McLeod, J. and Parter, S. V., "On the flow between two counter-rotating infinite plane disks", Arch. Rational Mech. Anal. 54 (1974) 301-327

[22] Mellor, C. E., Chapple, P. J. and Stokes, V. K., "On the flow between a rotating and a stationary disk", J. F. M. 31 (1968) 95-112

[23] Pearson, C. E., "Numerical solutions for the time-dependent viscous flow between two rotating coaxial disks", J. F. M. 21 (1965) 623-633

[24] Pereyra, V., "Iterated deferred corrections for nonlinear operator equations", Numer. Math. 10 (1967) 316-323

[25] Pereyra, V. and Sewell, E. G., "Mesh selection for discrete solution of boundary problem in ordinary differential equations", Numer. Math. 23 (1975) 261-268

[26] Rall, L., "Convergence of the Newton process to multiple solutions", Numer. Math. 9 (1966) 23-37

[27] Reddien, G., "On Newton's method in Banach space", submitted for publication

[28] Stewartson, K., "On the flow between two rotating coaxial disks", Proc. Camb. Phil. Soc. 49 (1953) 333-341

[29] Tam, K. K., "A note on the asymptotic solution of the flow between oppositely rotating infinite plane disks", SIAM J. Appl. Math. 17 (1969) 1305-1310

[30] von Karman, T.,"Uber laminare und turbulente reibung", Z. Angew. Math. Mech. 1 (1921) 232-252

[31] Whittaker, E. J. and Watson, G. N., "A course of modern analysis", Camb. Univ. Press (1902)

[32] Wilkinson, J. H., "Error analysis of direct methods of matrix inversion", ACM 8 (1961) 281-330